THE ROLE OF P450 EPOXYEICOSANOIDS IN CEREBRAL EXTRINSIC PERIVASCULAR VASODILATOR NERVE FUNCTION

By

Jeffrey J. Iliff

A DISSERTATION

Presented to the Department of Physiology & Pharmacology
and the Oregon Health & Science University
School of Medicine
in partial fulfillment of
the requirements for the degree of

Doctor of Philosophy

April 2010

School of Medicine

Oregon Health & Science University

CERTIFICATE OF APPROVAL

This is certify that the Ph.D. dissertation of

Jeffrey J. Iliff

has been approved

_____
Mentor/Advisor

_____
Member

_____
Member

_____
Member

_____
Member

_____
Member

Table of Contents

Index of Tables

Index of Figures

Index of Abbreviations

14,15-EEZE	14,15-Epoxyeicosa-5(Z)-enoic acid
ANOVA	Analysis of variance
AUDA	12-[[(tricyclo[3.3.1.13,7]dec-1-ylamino)carbonyl]amino]-dodecanoic acid
CGRP	Calcitonin gene-related peptide
CYP	Cytochrome P450
DHETs	Dihydroxyeicosatrienoic acids
EDHF	Endothelium-derived hyperpolarizing factor
EETs	Epoxyeicosatrienoic acids
ELISA	Enzyme-linked immunosorbent assay
HETEs	Hydroxyeicosatetraenoic acids
LC-MS/MS	Liquid chromatography-tandem mass spectrometry
MS-PPOH	N-(methylsulfonyl)-2-(2-propynyloxy)-benzenehexanamide
NMDA	N-methyl-D-aspartate
nNOS	Neuronal nitric oxide synthase
PPAR	Peroxisome proliferator-activated receptor
sEH	Soluble epoxide hydrolase
SEM	Standard error of the mean
TRPV1	Transient receptor potential vanilloid-1
TRPV4	Transient receptor potential vanilloid-4
VIP	Vasoactive intestinal peptide

Acknowledgements

I would first like to acknowledge the unceasing support of my wife Lisa, and children Anne, Charlie and Sam in the production of this work. They bore the weight of four years of graduate school as much as or more than I did, and as such they made this work possible.

I would like to acknowledge the help that I received from numerous researchers in the Departments of Anesthesiology and Perioperative Medicine, Neurological Surgery, Biomedical Engineering and Physiology and Pharmacology. Without their expertise and training, much of this work would not have been possible. Specificially, the contributions of Drs. Paco Herson, Ricky Wang, Ines Koerner and Justin Cetas have been particularly important.

I thank my dissertation committee, Drs. Mary Heinricher, Allison Fryer, Dennis Koop, Agnieszca Balkowiec and Patricia Hurn for their committed help through the last four years. Each of them has put in much time and effort, for no material benefit, to shaping my thinking and my work. I have learned a great deal from each of them.

I am most indebted to my mentor Dr. Nabil Alkayed. As I entered his lab, I could little have known just how gifted a scientist and a teacher he is. In that I have been exceedingly fortunate. His skill, intelligence, creativity, professionalism and integrity have been a constant example to me of the best that science has to offer. He has left an indelible impression on me and for that I thank him.

This work was supported in part by the Oregon Brain Institute Graduate Student Fellowship for the Neurobiology of Disease, funded by Vertex Pharmaceuticals; and by an NRSA F31 predoctoral fellowship (F31 NS060498-01; Iliff JJ, PI) from NINDS.

Author Publications

Peer-Reviewed Research Articles

Iliff JJ, Close LN, Selden NR, Alkayed NJ. A novel role for P450 eicosanoids in the neurogenic control of cerebral blood flow. Exp Physiol. 92(4):653-8, 2007.

Iliff JJ, Wang R, Zeldin DC, Alkayed NJ. Epoxyeicosanoids as mediators of neurogenic vasodilation in cerebral vessels. Am J Physiol: Heart Circ Phsyiol May; 296(5):H1352-63, 2009.

Iliff JJ, Balkowiec A, Alkayed NJ. The regulation of trigeminal ganglion neuroeffector function by epoxyeicosanoid signaling. J Neurochem (under review) 2010.

Reviews

Iliff JJ, Alkayed NJ. Soluble epoxide hydrolase inhibition: Targeting multiple mechanisms of ischemic brain injury with a single agent. Future Neurology. 4(2) 2009.

Iliff JJ, Jia J, Nelson J, Goyagi T, Klaus J, Alkayed NJ. Epoxyeicosanoid signaling in CNS function and disease. Prostaglandins and Other Lipid Mediators. (Epub ahead of print) 2009.

Published Abstracts

Iliff JJ, Close LN, Selden NR, Alkayed NJ. A novel role for P450 eicosanoids in the neurogenic control of cerebral blood flow. The FASEB Journal 21:748.3, 2007.

Iliff JJ, Wang R, Baumann TK, Alkayed NJ. Neurogenic control of cerebral vasculature: potential role of P450 epoxygenase. The FASEB Journal 2008.

Iliff JJ, Alkayed NJ. Evaluating crosstalk between epoxyeicosatrienoic acids (EETs) and neuropeptide signaling in neurogenic vasodilation. J Cereb Blood Flow Metab; 29, S206, 2009.

Dissertation Abstract

Chapter1: Introduction. Cerebral blood flow is controlled through three levels of regulation: intrinsic vasomotor regulation, neurovascular coupling, and regulation by perivascular vasomotor nerves. Epoxyeicosatrienoic acids (EETs) are arachidonic acid metabolites of cytochrome P450 (CYP). In the cerebral vasculature, EETs are vasodilators that contribute to intrinsic vasomotor regulation and to neurovascular coupling. In the present series of studies, I tested the overall hypothesis that EETs contribute to the regulation of the cerebral vasculature by perivascular vasodilator nerves.

Chapter 2. The hypothesis that parasympathetic and trigeminal vasodilator nerves surrounding the cerebral vasculature express EETs-synthetic CYP epoxygenase and EETs-regulatory sEH enzymes was tested. RT-PCR and Western blot revealed the expression of CYP-2J3 and CYP-2J4 epoxygenases and sEH in the rat sphenopalatine and trigeminal ganglia. Immunofluorescence double-labeling indicated that CYP-2J and sEH localize to neurons within both ganglia. These findings demonstrate that parasympathetic and trigeminal perivascular neurons possess the biochemical machinery for the synthesis and regulation of vasodilator EETs.

Chapter 3. The hypothesis that CYP-2J epoxygenases are constitutively active in primary rat trigeminal ganglion neurons was tested. LC-MS/MS detected the presence of 5,6-DHET, 8,9-, 11,12-, and 14,15-EETs regio-isomers within whole-cell extract from primary trigeminal ganglion neurons. These findings demonstrate the CYP-2J3 is functional and EETs are endogenously present in primary trigeminal ganglion neurons.

Chapter 4. The hypothesis that EETs are released from rat primary trigeminal ganglion

neurons was tested. EETs release from trigeminal neurons following stimulation with depolarizing K^+ or capsaicin was assayed by LC-MS/MS. No evidence for EETs release was observed. The regulation of neuropeptide release from trigeminal ganglion neurons by endogenous EETs was then evaluated. Capsaicin stimulation resulted in a ~5-fold increase in CGRP release measured by ELISA. Pre-treatment with the EETs antagonist 14,15-EEZE (10 μmol/L) and the CYP epoxygenase inhibitor MS-PPOH (10 μmol/L) significantly attenuated neuropeptide release. Similar findings were observed for K^+-stimulated CGRP release. These results demonstrate that endogenous EETs regulate neuropeptide release from primary trigeminal ganglion neurons.

Chapter 5. The hypothesis that EETs contribute to the regulation of cerebral blood flow by perivascular vasodilator nerves was tested *in vivo*. Electrical ethmoidal nerve stimulation increased cerebral blood flow measured by laser Doppler flowmetry via a closed cranial window. This effect was inhibited by the EETs antagonist 14,15-EEZE (10 μmol/L) from a baseline of 23±4% with 20 Hz stimulation to 7±1% following 14,15-EEZE treatment. Chemical stimulation of oral trigeminal fibers with capsaicin increased cerebral blood flow, and this effect was also inhibited by 14,15-EEZE. These findings demonstrate that EETs contribute to the regulation of cerebral blood flow by perivascular vasodilator nerves.

Chapter 6: Summary and Conclusions. In the present study, the expression and constitutive activity of EETs-synthetic CYP-2J epoxygenase is demonstrated in parasympathetic sphenopalatine and trigeminal ganglia neurons. The release of vasodilator EETs from primary trigeminal ganglion neurons could not be detected, however, endogenous EETs were demonstrated to regulate the release of vasoactive

neuropeptides from these neurons. This provides a mechanistic basis for the functional role of EETs in the regulation of cerebral blood flow by perivascular vasodilator nerves *in vivo*.

Chapter 1. Introduction

Cerebral blood flow is regulated with exquisite precision, being maintained at near-constant levels across a wide range of physiological conditions. This control is exerted at three broad mechanistic levels: the intrinsic regulation of cerebral vascular tone, neurovascular coupling, and the regulation of the cerebral vasculature by perivascular vasomotor neurons. These overlapping modes of regulation integrate to match changes in physiological state and cerebral metabolic demand with the supply of nutritive blood flow. Breakdown of this regulation can have catastrophic consequences, and contributes to many central nervous system pathologies, including most prominently, cerebral ischemia [1,2].

Epoxyeicosatrienoic acids (EETs) are fatty acid signaling molecules produced from arachidonic acid through the action of cytochrome P450 (CYP) epoxygenase enzymes (Figure 1). Known chiefly as potent vasodilators, including in the cerebral circulation, EETs are key regulators of cerebrovascular function under both physiological and pathophysiological conditions [3]. Among their many vasoregulatory actions in the cerebral circulation, EETs contribute both to intrinsic vasomotor regulation [4,5] as well as neurovascular coupling [6,7]. Additionally, emerging research in the epoxyeicosanoid field suggests that beyond these well-established vasoregulatory roles, EETs may participate in central or peripheral neuronal function [8,9]. In this context, an intriguing possibility is that EETs contribute to the regulation of cerebral blood flow at each of these three broad levels of integration: intrinsic vasomotor regulation, neurovascular coupling, and neurogenic

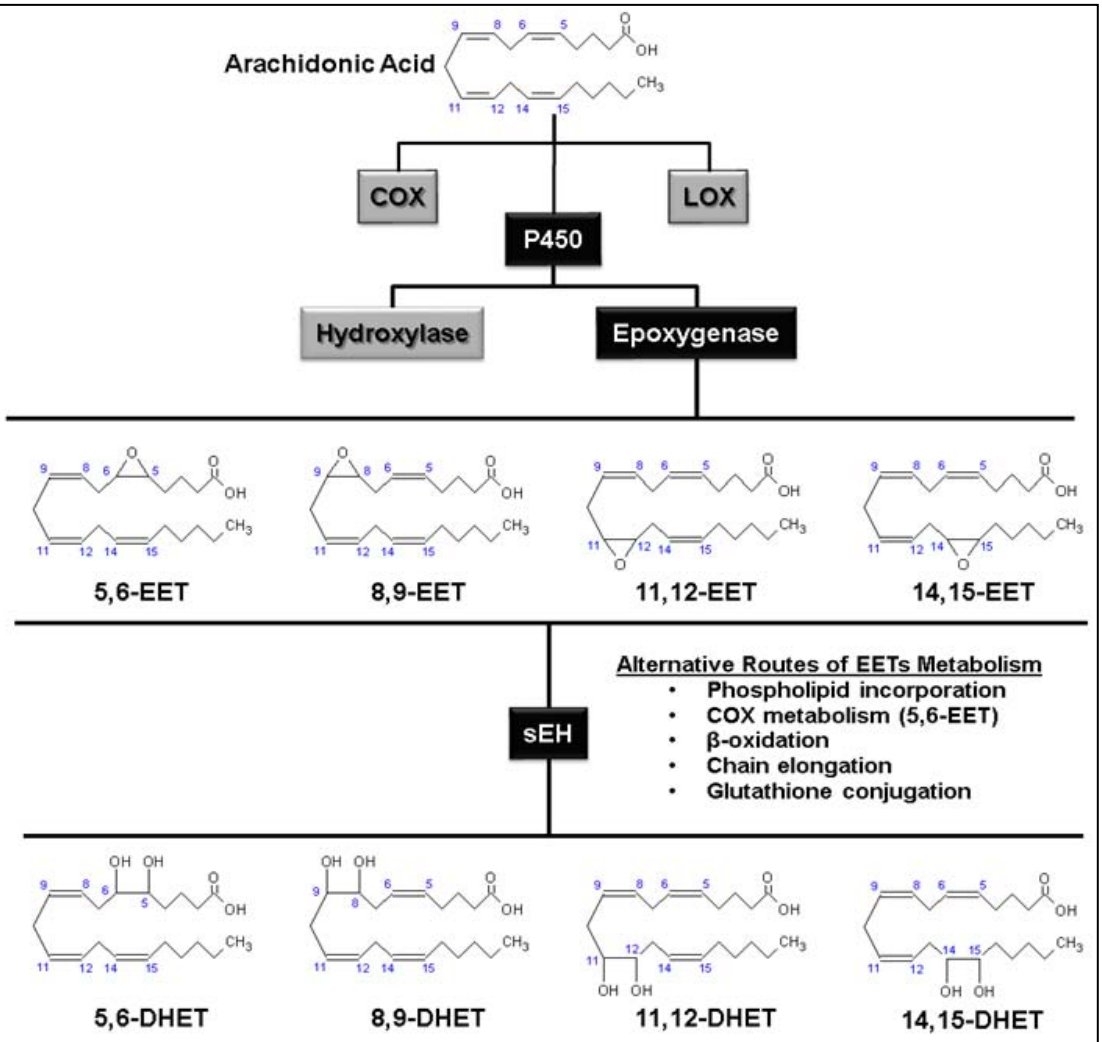

Figure 1. Pathways of epoxyeicosatrienoic acid (EETs) synthesis and metabolism. EETs are synthesized from arachidonic acid by cytochrome P450 epoxygenase enzymes, producing four distinct regio-isomers. EETs are metabolized predominantly through the activity of soluble epoxide hydrolase (sEH) which catalyzes their hydrolysis to corresponding dihydroxyeicosatrienoic acids (DHETs). COX: cyclooxygenase; LOX: lipoxygenase.

cerebral blood flow regulation. However, whether EETs contribute to the regulation of the cerebral vasculature by perivascular vasomotor nerves remains unexplored.

Cerebral Blood Flow Regulation

Because the brain exerts regulatory control over nearly every facet of physiological function, maintaining an adequate and uninterrupted blood supply to this organ is of paramount importance to survival. However, the maintenance of sufficient blood supply to the brain is hampered by the high oxygen extraction ratio of this tissue. Owing to the metabolic demands associated with maintaining neuronal membrane potentials, venous outflow blood from the brain has very little residual oxygen content to supply changes in metabolic demand. Thus, any change in tissue metabolic demand, such as occurs during neuronal activation, must be matched directly by a corresponding increase in blood supply, lest tissue hypoxia ensue resulting in compromise of neuronal function. However, the closed volume of the skull and the vulnerability of brain tissue to elevations in intracranial pressure require such changes in blood supply to be carefully offset to maintain nearly constant overall brain blood volume [1,2].

For this reason, cerebral blood flow is under robust regulatory control that is exerted at three general mechanistic levels: the intrinsic regulation of cerebral vasomotor tone [10], neurovascular coupling [1], and regulation by perivascular nerve populations [11]. These three overlapping levels of regulation work in concert to ensure that regional cerebral blood flow is held constant, local blood supply is modulated to ensure proper matching of blood flow to local changes in metabolic demand, and flow is coordinated along the vascular tree. In general, at each of these three regulatory levels, mechanisms are present that subserve each of these functions.

Intrinsic Regulation of Cerebrovascular Tone

As in most vascular beds, cerebral arteries and arterioles possess an intrinsic capacity to regulate their own vasomotor tone in response to changes in their physical or chemical environment [10]. Autoregulation is the process by which increases in intraluminal pressure are offset by intrinsic vasoconstriction. Through this mechanism, cerebral blood flow is maintained constant while a strong vasomotor tone is established against which other vasomotor stimuli act [12]. Metabolic coupling includes the direct effects of tissue pH, PaO_2 and $PaCO_2$, reflecting changes in local metabolic conditions, upon vasomotor tone. This mechanism participates is coupling local changes in metabolic demand with local blood supply [13,14]. Flow-mediated dilation is the process whereby alterations in endothelial shear stress resulting from downstream changes in blood flow, are transduced by the vascular endothelium into vasomotor stimuli. Through this mechanism, downstream alterations in blood flow are propagated upstream, thus coordinating flow along the cerebrovascular tree [15]. Each of these three mechanisms are observed to one extent or another in peripheral vascular beds, however, the cerebral vasculature is distinct in the relative strength of these intrinsic regulatory mechanisms compared to those in other circulations [2,10].

Autoregulation

Cerebral arteries and arterioles are subject to autoregulatory control whereby elevations in intraluminal pressure are actively opposed by vasoconstriction of the vessel. This intrinsic process maintains cerebral blood flow nearly constant across a

wide range of pressures, from 60 mmHg to 150 mmHg, and constitutes the vasomotor background upon which virtually all other vasoregulatory processes act. The cellular basis of cerebral autoregulation is thought to reside in the vascular smooth muscle, as ablation of the cerebrovascular endothelium does not alter autoregulatory responses in experimental animals [12]. The molecular mechanisms underpinning autoregulation, however, are less well defined. Early work demonstrated that in cerebral arteries, elevations in intraluminal pressure were associated with vascular smooth muscle depolarization, mobilization of intracellular calcium, and vasoconstriction. More recent work has implicated CYP hydroxylase metabolites of arachidonic acid, 20-hydroxyeicosatetrenoic acids (HETEs), as upstream mediators of the myogenic response in cerebral arteries [16,17].

20-HETE is a potent vasoconstrictor in the cerebral circulation that acts by negatively modulating calcium-sensitive K^+ channel activity, resulting vascular smooth muscle depolarization and calcium entry via voltage-gated calcium channels [17]. In isolated rat middle cerebral arteries, step elevations in intraluminal pressure from 20-140 mmHg resulted in a 6-fold increase in vascular 20-HETE concentrations. Furthermore, myogenic constrictions in response to elevations in intraluminal pressure were blocked with the inhibition of CYP hydroxylase activity, or by blocking the actions of 20-HETE with a putative antagonist [16]. These findings suggest that 20-HETE is a key mediator of the myogenic response in cerebral arteries.

Metabolic Coupling

In addition to reacting to changes in intraluminal pressure, cerebral vessels are capable of ‘sensing’ and responding to the metabolic conditions within the tissue surrounding

them. Such intrinsic metabolic coupling constitutes the first layer of regulation whereby local blood flow is tuned to meet local energetic demands. Cerebral arteries and arterioles react to tissue hypoxia and hypercapnia, conditions typically reflecting increased metabolic demand versus supply, with vasodilation [2,10].

In experimental animals including rats [13,18,19], rabbits [20] and cats, moderate to severe hypoxia (PaO_2 = 45 to 25 mmHg, respectively) results in profound dilation of pial arterioles ranging between of 20-60%. In isolated middle cerebral arteries, ablation of the endothelium blocks hypoxic vasodilation, demonstrating that this phenomenon is endothelium-dependent [19]. Hypoxic cerebral vasodilation is sensitive to both adenosine receptor antagonists, inhibitors of nitric oxide synthase, and the ATP-sensitive K^+ channel blocker glibenclamide [13,21]. Given that the effects of glibenclamide were not additive with either adenosine receptor blockade or nitric oxide synthase inhibition, it is thought that these two upstream vasomotor pathways are activated under hypoxic conditions, then converge downstream to activate ATP-sensitive K^+ channels to hyperpolarize and relax cerebral arteries and arterioles.

Cerebral arteries and arterioles also respond to hypercapnia with vasodilation. In rats, elevation of $PaCO_2$ from a physiological value of 40 mmHg to 80 mmHg increases cerebral blood flow by more than 100% [22]. In general, the cerebral vasodilation resulting from mild hypercapnia ($PaCO_2$ = 40 – 60 mmHg) can be fully inhibited by inhibitors of nitric oxide synthase, suggesting that nitric oxide is the key mediator of these responses [23,24,25]. Under conditions of severe hypercapnia (>60 mmHg) it has been reported that a residual hypercapnic cerebral blood flow response

persists in the presence of nitric oxide synthase inhibition [24]. These findings suggest that one or more additional mediators, such as free radicals or protons, are recruited under conditions of severe hypercapnia to contribute to these vasomotor responses. As was the case with hypoxic cerebral vasodilation, hypercapnic vasodilation is sensitive to the drug glibenclamide, demonstrating that the ATP-sensitive K^+ channel is the downstream effector of hypercapnic nitric oxide signaling and the associated vasomotor responses [14].

Flow Mediated Vasodilation

The vascular endothelium responds to changes in the frictional force of fluid movement along its surface with the release of vasoactive mediators that regulate vasomotor tone. These endothelium-derived factors include nitric oxide, the cyclooxygenase metabolite prostacyclin, and a putative endothelium-derived hyperpolarizing factor (EDHF). Thus, when flow velocity increases, arteries and arterioles respond with what is termed ‘flow-mediated vasodilation’ [10,15]. In the cerebral vasculature, flow-mediated vasodilation has been demonstrated in both arteries [26,27] as well as pial and penetrating arterioles [28]. One major function of flow-mediated vasodilation is the coordination of blood flow along the cerebrovascular tree. Many vasomotor stimuli, such as those stemming from neurovascular coupling detailed below, originate distally within intraparenchymal arterioles. Changes in flow in these distal vessels are propagated upstream to supply vessels in part through the resulting changes in shear stress experienced by the upstream vascular endothelium as flow downstream is increased. In this way, upstream vessel diameter is coupled to that of the downstream vessels.

Flow-mediated vasodilation is inhibited by the ablation of the cerebrovascular endothelium [27], and appears to be primarily mediated at lower levels of flow by endothelial nitric oxide production. At flow rates below 20 μL/min, elevations in flow produce vasodilation in rat and rabbit cerebral arterioles of between 10-20%. In several studies, these flow-mediated vasomotor responses were sensitive to inhibition of nitric oxide synthase, demonstrating that endothelial nitric oxide is a major mediator of these effects [28]. However, in the presence of nitric oxide synthase inhibition, a residual flow-mediated vasodilator response has been observed in cerebral arterioles. These residual responses are insensitive to cyclooxygenase inhibition, which indicates that the endothelium-derived vasodilator prostacyclin does not account for these effects [28]. Rather, they have been attributed to the so called EDHF. Although the molecular identity of this factor in the cerebral vasculature remains unknown, in peripheral vascular beds EDHF has been variously identified as H_2O_2, epoxyeicosatrienoic acids (EETs), atrial natriuretic peptide, as well as the electrotonic spread of endothelial hyperpolarization to the vascular smooth muscle via myoendothelial gap junctions [29]. At higher rates of flow, flow-mediated vasodilation appears to reverse, resulting in a normalization of vascular diameter towards that set by the myogenic autoregulatory response [28,30]. The mechanisms governing flow-mediated vasoconstriction at higher levels of flow remain unknown.

Neurovascular Coupling

Superimposed over the intrinsic regulation of cerebral vasomotor tone is the regulatory

mechanism by which local neuronal activity in the brain is functionally coupled to changes in blood supply. Through this process, termed ‘neurovascular coupling’, the metabolic needs of active groups of neurons are met, overall cerebral blood volume is held largely constant (a necessity in an enclosed organ such as the brain), and vasomotor signals are spread from their points of origin to proximal portions of the cerebrovascular tree [1].

Neurovascular coupling occurs within an anatomical framework unique to the central nervous system and the cerebral circulation: the so-called neurovascular unit. The ‘neurovascular unit’ refers to the physical and functional interactions among the cells comprising the bulk of the central nervous system: central neurons, glial cells (astrocytes and oligodendrocytes), and vascular cells (vascular endothelium and smooth muscle) [1,31]. Within the brain parenchyma, blood vessels including arterioles, capillaries and venules, are surrounded by a layer of astrocytic endfeet, process extensions from surrounding astroglial cells [32]. The specific molecular interactions between these endfeet and vascular cells contribute to the formation and maintenance of the blood brain barrier which regulates the highly privileged access to the central nervous system [33]. Similar to the cerebral vasculature, central synapses are likewise enwrapped in astrocytic processes, which provide nourishment to the neurons and clear neurotransmitters from the synaptic cleft [31]. Importantly, it is typically the case that the same astrocyte sends processes to surround both central neuronal synapses as well as local blood vessels. Furthermore, neighboring astrocytes are extensively coupled by gap junctions, such that they form a functional electrical and molecular syncitium reaching numerous nearby synapses and spanning the lengths

of the local vasculature [34]. This astrocytic network provides a physical link between the distinct neural and vascular domains within the brain parenchyma. The cells of the neurovascular unit maintain not only close proximity to one another, but also an intricate and unique mode of multi-directional communication: vascular function is regulated by neurons and glia, neuronal function regulated by glia and vascular cells, and glial function regulated by neuronal and vascular cells [31]. This integration of neural-glial-vascular function underpins the regulatory mechanism of neurovascular coupling.

The increase in local cortical blood flow resulting from cortical neuronal activation is termed 'functional hyperemia'. The molecular mechanisms governing functional hyperemia have been the subject of intense inquiry since the 1980s, during which time a number of specific mediators of this process have been identified [1]. These include so-called 'K^+-siphoning', nitric oxide, adenosine, as well as arachidonic acid metabolites of cyclooxygenase and CYP epoxygenase enzymes. While the precise contributions of these various mediators to functional hyperemia has not been conclusively defined, each may contribute to this process, alone or in parallel, in a species-, age- and context-dependent manner.

K^+ Siphoning

During action potential generation, active neurons release high levels of K^+ from the intracellular compartment. At the same time, extracellular K^+ is a potent dilator of cerebral arterioles [35]. In 1987, Paulson and Newman [36] proposed a mechanism to account for the functional coupling of neuronal activity to increases in cortical blood flow. Terming the model 'K^+ siphoning', the authors hypothesized that cortical

astrocytes actively take up peri-neuronal K^+, transport it in a directional manner, then release it from perivascular endfeet to evoke cerebral vasodilation.

Experimental evidence supporting the K^+ siphon hypothesis accumulated slowly over the ensuing two decades. Early work demonstrated that in Mueller glial cells of the retina, the uptake of K^+ within one structural domain of the cell resulted in a proportionate efflux of K^+ from an opposing domain, thus constituting a directional K^+ siphon [37]. At a molecular level, this directional K^+ transport appeared to reflect the activity of inward-rectifier Kir4.1 channels that, given their weak rectification, permit flux of K^+ ions either in the inward or outward directions, depending upon the disposition of the electrochemical gradient [38]. Furthermore, in rat cerebral arterioles, extracellular K^+ caused vasodilation below concentrations of 10mM. These effects were sensitive to both Ba^{2+} and the drug glibenclamide, suggesting that vascular inward-rectifier as well as ATP-sensitive K^+ channels mediated the vasomotor actions of K^+ [39].

It wasn't until 2007, however, that the K^+ siphon hypothesis was directly tested. In a study utilizing Kir4.1 knockout mice, Newman's group observed that neurovascular coupling within the retina was fully intact, even in the absence of these inward-rectifier K^+ channels [40]. Based upon these findings, the authors concluded that the K+ siphoning hypothesis does not account for the coupling of neuronal activation with local changes in blood supply. Whether such a mechanism governs neurovascular coupling in other regions of the central nervous system, such as the cerebral cortex, remains unexplored.

Adenosine

Adensosine, released from both cortical neurons and astrocytes in response to activation, is the breakdown product of adenosine tri-, di- and monophosphates produced through the activity of specific *ecto*-nucleotidase enzymes [41,42]. It is also a potent vasodilator in the cerebral vasculature, acting through vascular smooth muscle adenosine A_{2A} receptors to produce vasodilation [43]. In parallel with Robert Berne's 'adenosine hypothesis' of the heart [44], it was proposed beginning in the early 1990s that adenosine participates in coupling increases in neuronal activity in the cerebral cortex to the associated functional hyperemia [45].

A number of studies conducted in rats and mice have supported the involvement of adenosine in neurovascular coupling. Rat pial arterioles dilate in response to sciatic nerve stimulation. In the presence of adenosine antagonists, including those specific to the adenosine A_{2A} receptor subtype, the functional hyperemic response is attenuated [46,47]. Furthermore, the administration of competitive adenosine uptake inhibitors had the opposite effect, potentiating sciatic nerve stimulation-evoked elevations in cerebral blood flow [45]. These findings demonstrate that the metabolic breakdown product, adenosine, participates in the process of neurovascular coupling in the rodent cerebral cortex.

Nitric Oxide

The activation of neuronal N-methyl-D-aspartate (NMDA) receptors in the central nervous system results in Ca^{2+} influx and the activation of Ca^{2+} regulated enzymes. Among these is the neuronal isoform of nitric oxide synthase (nNOS), which catalyzes the formation of the gas nitric oxide from L-arginine. Among the numerous biological

actions of nitric oxide is that of a potent vasodilator in many vascular beds, including in the cerebral circulation, where it produces vasodilation through its interaction with the enzyme soluble guanylyl cyclase [48]. Based upon the activity-dependent production of nitric oxide in cortical neurons and the high diffusibility of this gaseous transmitter, it was proposed beginning in the early 1990s that this compound functions as a mediator of neurovascular coupling [48,49].

In different models of somatosensory stimulation-evoked increases in cerebral blood flow, including sciatic nerve [49], forepaw [50] and whisker barrel field stimulation [51], inhibition of nitric oxide synthase activity blocked neurovascular coupling in the cerebral cortex. Moreover, the use of an inhibitor specific for the neuronal isoform of nitric oxide synthase, 7-nitroindazole, revealed that it was specifically nitric oxide production in neurons that participates in neurovascular coupling [51].

A detailed study by Lindauer et al. in 1999, however, demonstrated that in the cerebral vasculature, nitric oxide functioned as a permissive factor rather than as a true mediator of functional hyperemia [51]. Consistent with previous studies, the authors observed that inhibition of nitric oxide synthase activity attenuated the cerebral blood flow response to whisker stimulation by a factor of one half. However, replacement of basal levels of nitric oxide with nitric oxide donors, or the use of a cyclic guanine triphosphate analogue, restored the hyperemic response to whisker barrel stimulation even in the continued presence of nitric oxide synthase inhibition. These findings demonstrated that a certain basal level of ‘nitrergic tone’ was necessary to support the process of neurovascular coupling, however, nitric oxide *per se* was not the specific

factor accounting for the somatosensory stimulation-evoked elevations in cerebral blood flow.

Cyclooxygenase Metabolites

In addition to activating nNOS, elevations in intracellular Ca^{2+} activate phospholipase A2, which catalyzes the release of arachidonic acid from membrane phospholipids (Figure 1). In both cortical neurons and astrocytes, cyclooxygenase catalyzes the conversion of free arachidonic acid into various vasoactive prostaglandins [32,52,53]. For this reason, the cyclooxygenase signaling pathway has been proposed as a potential mediator of neurovascular coupling. Two studies from 2000 and 2001, demonstrated such a role.

In a mouse model of neurovascular coupling, whisker barrel stimulation results in increased cortical blood flow. This cortical hyperemia was attenuated both with a cyclooxygenase-2-specific pharmacological inhibitor as well as in cyclooxygenase-2 knockout mice [54]. However, treatment with a cycloxygenase-1-specific inhibitor had no effect upon neurovascular coupling, nor did cyclooxygenase-1-deficient mice demonstrate any attenuation in this response [55]. These findings demonstrate that the cyclooxygenase-2, and not the cyclooxygenase-1 isoform, participates in neurovascular coupling in the mouse.

Neurogenic Cerebral Blood Flow Regulation

Like peripheral vascular beds, the cerebral circulation is innervated by populations of perivascular vasodilator and vasoconstrictor nerves that exert control over vasomotor

tone. However, unlike peripheral vascular beds, these perivascular nerve populations do not contribute significantly to the ongoing physiological regulation of cerebral blood flow. Rather, these nerves protect the cerebral vasculature against large and potentially dangerous disturbances in cortical blood flow. Indeed, the role of cerebral perivascular nerves is most clearly highlighted under conditions wherein cerebral blood flow is acutely or chronically challenged, such as cerebral ischemia, vasospasm after subarachnoid hemorrhage, hypertension and hypotension [11,56].

Three distinct populations of perivascular nerve fibers innervate the extrinsic cerebral vasculature: parasympathetic vasodilator fibers from the otic and sphenopalatine ganglia, sympathetic vasoconstrictor fibers from the superior cervical ganglia, and primary trigeminal afferents. This innervation is largely continuous with that of the internal carotid and vertebral arteries, although the fibers surrounding the cerebral surface vasculature, including the basilar artery, communicating arteries of the Circle of Willis, conduit and resistance arteries such as the middle cerebral artery and their proximal branches, are generally considered separately from those of other cranial blood vessels. The innervation is most dense in the vessels of the greatest caliber, and ceases prior to the penetration of the surface arterioles into the Virchow-Robin space and the brain parenchyma. In this way, this innervation can be regarded as exclusively ‘extrinsic’ [11,56].

Parasympathetic Nerves

The cerebral surface vasculature is innervated by parasympathetic vasodilator nerves of primarily two origins. The posterior circulation is supplied by efferent fibers from the otic ganglia, located extracranially near the tympanic bullae. The Circle of Willis

and the anterior circulation is innervated by fibers originating in the sphenopalatine ganglia, which resides along the maxillary branch of the V cranial nerve, at the base of the orbit [57]. Within these ganglia, cell bodies generally possess a cholinergic phenotype, expressing choline acetyltransferrase. Peripheral processes surrounding the cerebral surface vasculature likewise exhibit acetylcholinesterase activity, in addition to choline acetyltransferrase immunoreactivity [56,57]. Functionally, however, the vasomotor actions of these perivascular neurons are non-cholinergic. Electrical stimulation of the sphenopalatine ganglion or its efferent nerve supply dilates cerebral surface arteries and increases cerebral blood flow in the cat and rat [58,59,60,61,62,63,64,65,66]. This effect is insensitive to atropine [60,65], demonstrating that acetylcholine is not the vasoactive transmitter at work within this system.

In addition to cholinergic markers, neuronal cell bodies of the otic and sphenopalatine ganglia and peripheral processes innervating the cerebral surface vasculature express the vasodilator neuropeptides vasoactive intestinal peptide (VIP) and pituitary adenylate cyclase activating polypeptide, as well as nNOS [62,64,67,68]. Experimental studies in the cat and the rat have demonstrated that competitive VIP and pituitary adenylate cyclase activating polypeptide receptor antagonists and nitric oxide synthase inhibition markedly reduce cerebral vasodilation resulting from stimulation of parasympathetic perivascular vasodilator nerves [61,62,63,64,66,68,69]. Thus, the vasomotor activity of these neurons is regarded as primarily peptidergic and nitrergic in nature.

The parasympathetic nerves surrounding the cerebral vasculature do not

contribute to the ongoing physiological regulation of cerebral blood flow. Lesion of the efferent nerve supply from the sphenopalatine ganglion does not alter resting cerebral blood flow [70]. Nor does inhibition of nitric oxide synthase, which is a major contributor to the vasomotor actions of these perivascular vasodilator nerves [61,66].

An important role for these parasympathetic fibers in cerebral blood flow regulation, however, is revealed under pathophysiological conditions. Under conditions of hypoperfusion, parasympathetic vasodilator nerves are activated to maintain adequate tissue perfusion. This was observed first in the context of hemorrhagic hypotension [71]. During episodes of hemorrhagic hypotension in the rat, cortical blood flow was maintained constant in intact animals. Following sectioning of the efferent nerve supply from the sphenopalatine ganglion, hemorrhagic hypotension resulted in a significant reduction in ipsilateral cortical blood flow. A similar effect is observed in the setting of experimental cerebral ischemia. Chronic lesion of the parasympathetic nerve supply to the cerebral vasculature increases the infarct volume in rats following permanent middle cerebral artery occlusion [71,72]. This suggests that under conditions of hypoperfusion, these perivascular vasodilator nerves actively increase cerebral blood flow. This conclusion was corroborated in a recent study in which stimulation of the parasympathetic and trigeminal vasodilator nerve supply to the anterior cerebral circulation reduced infarct volume in a model of transient cerebral ischemia in the rat [73]. These findings indicate that the primary function of the parasympathetic nerve supply to the cerebral surface vasculature is to safeguard cerebral perfusion, recruiting blood flow under conditions when adequate perfusion is challenged.

Sympathetic Nerves

The anterior, and to a lesser extent, the posterior cerebral surface vasculature is innervated by a dense network of sympathetic vasoconstrictor fibers. These fibers are generally regarded as adrenergic in nature, owing to their expression of markers such as tyrosine hydroxylase or dopamine β-hydroxylase [56,74,75]. In addition to norepinephrine, many cerebral sympathetic perivascular nerves also express neuropeptide Y. In immunoelectron microscopy studies, neuropeptide Y was localized to large dense-core vesicles in perivascular neuronal terminals. These dense-core vesicles co-occurred in nerve fibers with small, clear, and likely norepinephrine-containing vesicles. Based upon these findings it is assumed that norepinephrine and neuropeptide Y are both released from cerebral sympathetic perivascular nerves and contribute to the regulation of the cerebral surface vasculature by these fibers [56,76,77].

Denervation studies in several mammalian species have identified the primary source of these sympathetic fibers as the superior cervical ganglia [56,75,78]. When this ganglion is lesioned, or the efferent nerve supply is cut, norepinephrine content of the cerebral circulation is dramatically reduced, as is immunoreactivity for adrenergic markers.

Stimulation of the superior cervical ganglion results in a reduction in cerebral blood flow [79]. These vasoconstrictor fibers, however, do not appear to contribute to the regulation of cortical blood flow under physiological conditions. When the sympathetic nerve supply to the cerebral vasculature is acutely lesioned, no alteration in resting cerebral blood flow is evident [80]. This suggests that sympathetic

perivascular nerves do not contribute to those processes that set resting cerebral vasomotor tone, such as autoregulation and flow-dependent vasodilation [10,12].

Sympathetic perivascular nerves do play a key role in defining the limits of autoregulation in the cerebral circulation. Under physiological conditions, the mechanisms of cerebral autoregulation will maintain cortical blood flow nearly constant up to a certain systolic blood pressure, ~140 mmHg in rats [12,80]. At systolic blood pressures above this limit, 'autoregulatory breakthrough' occurs and cortical blood flow increases linearly with pressure. When the superior cervical ganglion is lesioned in rats, the autoregulatory limit declines to ~130 mmHg, indicating that sympathetic drive shifts the autoregulatory range upward [80]. Under conditions of chronic hypertension, the cerebral autoregulatory range shifts upwards in order to protect the cerebral circulation from the deleterious effects of chronic hyperperfusion. For example, the spontaneously hypertensive rat (mean arterial blood pressure ~165 mmHg) exhibits a right-shifted autoregulatory curve, with an upper limit of 210 mmHg. When the superior cervical ganglion is lesioned, this compensatory shift is attenuated, suggesting that sympathetic perivascular nerves participate in the compensatory autoregulatory shift during chronic hypertension.

Primary Trigeminal Afferents

The cerebral surface vasculature is innervated by a third population of perivascular nerve fibers, primary trigeminal afferents. Neurons of the trigeminal ganglia extend peripheral processes to targets throughout the head and neck, including the meningeal and cerebral blood vessels. Central processes project to the trigeminal nucleus within the brain stem [81]. The cellular phenotypes of trigeminal ganglion neurons have been

extensively characterized by immunohistochemistry and *in situ* hybridization, identifying the expression of several vasoactive neuropeptides, including calcitonin gene-related peptide (CGRP), substance P, neurokinin A and pituitary adenylate cyclase activating polypeptide [67,82,83,84,85,86]. Among these, CGRP-positive cell bodies are the most abundant, comprising 40% of human trigeminal ganglion neurons. Substance P and other neuropeptides are present in a smaller proportion (typically 20% or less) of trigeminal ganglion neurons.

This disposition of neuropeptide expression extends to the peripheral projections of trigeminal ganglion neurons surrounding the cerebral surface vasculature. Here, CGRP and the neurokinins (including substance P) are detectable in dense-core vesicles within varicosities that appear to represent pre-junctional specializations for pressure or tension reception [67,68,82,83,87,88,89]. Surgical excision of the peripheral fibers from the trigeminal ganglion results in the disappearance of nearly all CGRP and substance P immunoreactivity from the cerebral surface vasculature, suggesting that the trigeminal ganglia are the primary source of these CGRP- and neurokinin-positive fibers [86]. The sensory origin of these CGRP- and substance P-immunoreactive fibers has been confirmed using the neurotoxin capsaicin, which when administered to neonatal animals, selectively destroys sensory neurons expressing the capsaicin-gated transient receptor potential vanilloid-1 (TRPV1) cation channel. Sensory neuronal denervation with capsaicin results in the nearly complete loss of CGRP- and substance P-positive fibers from the cerebral vasculature [90].

Stimulation of the trigeminal ganglia or its peripheral nerve supply results in

the release of the neuropeptides CGRP and substance P [91,92] and marked cerebral vasodilation [63,83,87]. Although substance P and CGRP are co-released following stimulation, the vasodilator action of trigeminal afferent stimulation is almost entirely sensitive to CGRP receptor antagonists, suggesting that it is this neuropeptide that underpins these vasomotor effects [87].

The specific role of perivascular trigeminal afferents in cerebral blood flow regulation remains somewhat unclear. One proposal is that these fibers function as 'anti-constrictors', reversing the effects of various cerebral vasoconstrictors in order to maintain adequate tissue perfusion [87]. In cats, lesion of the peripheral projections of the trigeminal ganglion did not alter the magnitude of the cerebrovascular response to various vasomotor stimuli, including norepinephrine or alkaline (pH = 7.6) cerebrospinal fluid. However, nerve lesion did prolong the duration of these vasoconstrictor events. The authors conclude from these findings that trigeminal afferents contribute to the recovery of normal cerebrovascular tone following vasoconstrictor stimuli. Such a role is corroborated by studies in vasospasm patients [93,94]. In subjects following subarachnoid hemorrhage, the degree of vasospasm was correlated with the levels of sensory and parasympathetic neuropeptides in the cranial venous blood supply. The authors propose that these elevations in neuropeptide levels reflect the compensatory activity of perivascular vasodilator nerves in response to pathological vasoconstriction in the cerebral circulation.

Epoxyeicosatrienoic Acids

Arachidonic acid is liberated from membrane phospholipid pools by phospholipase A2

and subsequently metabolized by cyclooxygenase, lipoxygenase and CYP epoxygenase and hydroxylase enzymes to form a group of metabolites collectively termed 'eicosanoids' (Figure 1) [8]. EETs, epoxide metabolites of CYP epoxygenases, have garnered increasing attention since their initial identification in the liver in the early 1980s. Interest in EETs signaling has centered predominantly upon their role in the regulation of renal and cardiovascular function, particularly in their potent vasodilator actions. EETs signaling has been the subject of numerous research articles, and their effects on cellular function have been investigated in different tissues, including heart, lung, kidney, gastro-intestinal tract and brain. The vasomotor actions of EETs have been studied in the renal, coronary, pulmonary, skeletal muscle, sub-cutaneous, carotid, mesenteric, and cerebral vascular beds. These studies have yielded much valuable insight into the biochemical mechanisms of EETs synthesis, action, and metabolism [3,95].

EETs are best known for their potent vasodilator activity, including in the cerebral vasculature [96,97]. These vasomotor effects spurred the initial research into their participation in processes of cerebral blood flow regulation. Subsequent studies have expanded the role of EETs in cerebrovascular regulation beyond these well-known vasodilator actions. Indeed, their participation in processes of angiogenesis, inflammation, fibrinolysis and vascular mitogenesis suggest that EETs function as key integrators of cerebrovascular function (Table 1).

As will be described in detail below, EETs are produced both by cerebrovascular endothelial cells [5] and cortical astrocytes [96,98]. These two sources of EETs contribute to cerebral blood flow regulation: endothelium-derived EETs

participating in flow-mediated cerebral vasodilation [5], astrocyte-derived EETs contributing to neurovascular coupling in the cortex [6,7,99]. These mechanisms represent two of the three layers of cerebral blood flow regulation detailed above. Whether EETs participate in the third layer of regulation, the control of cerebral blood flow by perivascular vasomotor nerves, remains wholly unexplored.

Table 1. Cellular Effects of Epoxyeicosatrienoic Acids (EETs)

Effect	Tissue	Mechanism	References
Vasodilation	B, K, M, H, L	BK, GPCR, TRPV4	[96,100,101]
Anti-Inflammation	B, H	NF-κB	[102,103]
Anti-Smooth Muscle Migration	Ao	cAMP-PKA	[104]
Anti-Platelet Aggregation	B, HUVEC	BK, COX	[105,106,107,108]
Fibrinolysis	Ao	GPCR	[108]
Angiogenesis	B, H, L, HUVEC, Ao, Ret	MAPK, PI3 kinase-Akt, cAMP-PKA	[109,110,111,112,113,114,115,116,117]
Anti-Apoptosis	B, H, L, Ao	PI3 kinase-Akt	[118,119,120,121,122]
Anti-Oxidant	Ao		[123]

H, Heart; K, Kidney; M, Mesentery; B, Brain; L, Lung; Ao, Aorta; HUVEC, Human umbilical vein endothelial cells; Ret, Retina; BK, large-conductance Ca^{2+}-sensitive K^+ channel; GPCR, G protein-coupled receptor; TRPV4, transient receptor potential vanilloid 4 channel; cAMP-PKA, cyclic AMP – protein kinase A; COX, cyclooxygenase; MAPK, mitogen activated protein kinase; PI3 kinase, phosphatidylinositol 3-kinase.

Although at first glance the role of EETs in the brain appears to closely parallel functions described in other peripheral tissues [3,95], including a key role in the regulation of the cerebral vasculature, a more detailed review of the defined functions of EETs in the central and peripheral nervous system suggests that EETs signaling may play an important role in neuronal function. Indeed, based upon expression data, EETs

Table 2. Expression of CYP epoxygenase and sEH enzymes in neural tissue

Species	Isoform	Brain Region	Cell Type	Detection Method	EETs Profile	References
Human	CYP-4X1	W, Cb		PCR	8,9:14,15 = 1:2	[132]
Human	sEH	Co, BG, BS, Th, HTh, CP, V	N, Ast, O, EP, VSM, Endo	IHC		[133]
Mouse	CYP-2C29	W		PCR	8,9 – 6%; 11,12 – 12%; 14,15 – 82%	[134]
Mouse	CYP-2C37	W		PCR	8,9 – 24%; 11,12 – 61%; 14,15 – 15%	[134]
Mouse	CYP-2C38	W		PCR	8,9 – 9%; 11,12 – 65%; 14,15 – 26%	[134]
Mouse	CYP-2C40	W		PCR	8,9 – 16%; 11,12 – 11%; 14,15 – 40%	[134]
Mouse	CYP-4X1	Co, Hip, Cb, BS	N	WB, IHC, NB		[135]
Mouse	sEH	W, Co, BG, Hip,Th, HTh, BS, V	N, Ast	WB, IHC, MS, PCR		[136-139]
Rat	CYP-2C11	Co, OB	Ast	WB, IHC, PCR, SB, ISH	8,9 – 25%; 11,12 – 40%; 14,15 – 35%	[6,98,140-142]
Rat	CYP-2C12	W, OB		PCR		[142]
Rat	CYP-2C23	OB		PCR	8,9 – 26%; 11,12 – 51%; 14,15 – 23%	[142-143]
Rat	CYP-2C6	OB		PCR		[142]
Rat	CYP-2C7	W		WB, PCR		[141,143]
Rat	CYP-2D18	W		PCR	8,9 – 10%; 11,12 – 59%; 14,15 – 31%	[144-145]
Rat	CYP-2J3	SPG, TG	N	WB, IHC, PCR	8,9 – 29%; 11,12 – 28%; 14,15 – 43%	[146-147]
Rat	CYP-2J4	SPG, TG	N	WB, IHC, PCR		[146]
Rat	CYP-4X1	Co, Hip, Cb, BS	N	NB, ISH		[148]
Rat	sEH	W, Co, SPG, TG, V	N, Ast, VSM, O	WB, IHC, PCR		[119,138-139,146,149]

W: whole brain; Co: cerebral cortex; BG: basal ganglia; Cb: cerebellum; Hip: hippocampus; BS: brain stem; OB: olfactory bulb; Th: thalamus; HTh: hypothalamus; SPG: sphenopalatine ganglia; TG: trigeminal ganglia; V: vasculature; CP: choroid plexus. N: neurons; Ast: astrocytes; VSM: vascular smooth muscle; Endo: endothelium; EP: ependymal cells; O: oligodendrocytes. WB: Western blot; IHC: immunohistochemistry; MS: mass spectroscopy; PCR: polymerase chain reaction (RT or real time); NB: Northern blot; SB: Southern blot; ISH: in situ hybridization. 5,6: 5,6-EET; 8,9: 8,9-EET; 11,12: 11,12-EET; 14,15: 14,15-EET.

production and metabolism in the brain spans many regions and extends to peripheral and central neurons, astroglia and oligodendrocytes, vascular endothelium and vascular smooth muscle (for references, see Table 2). In terms of cellular actions, EETs signaling

is importantly involved in specific neuronal processes. EETs modulate neuronal pain processing in the brainstem [124] and the CYP epoxygenase metabolic pathway interacts with the neuro-active endocannabinoid pathway at a number of mechanistic levels [125,126,127,128]. Indeed, the long-established and often overlooked role for EETs in regulating neurohormone release from neuroendocrine regions of the brain [129,130] suggests that EETs may be key regulators of synaptic transmission. The emerging involvement of EETs signaling in these neuronal processes argues that these bioactive lipids may participate more broadly in neuronal function, and may contribute to neuroeffector roles not previously identified.

Epoxyeicosanoid Synthesis and Metabolism in Neural Tissue

Identification of EETs production in the brain followed very closely on the heels of the initial discovery of these novel CYP-derived epoxyeicosanoids [131]. In the 1990s, studies reporting the specific synthesis of EETs first by astrocytes and then by the vascular endothelium helped to secure EETs' place as key astrocyte- and endothelium-derived regulators cerebrovascular function [5,96,98]. At the time, these findings appeared to fit well with results from peripheral circulatory beds indicating that EETs functioned as an EDHF and were key regulators of vascular function [95]. More recent studies, however have characterized both the expression of CYP epoxygenases and the function of CYP-derived EETs in cell types throughout many brain regions (Table 2). The result of these studies has been the demonstration that enzymes capable of EETs synthesis and metabolism, CYP epoxygenases and soluble epoxide hydrolase (sEH), are dominantly expressed in non-vascular cells throughout the central nervous system

including both neuronal and glial cells. These findings suggest that the role of EETs signaling in the CNS may extend beyond simply that of vascular regulation and may subserve neuronal functions.

EETs Production in the Neural Tissue

Cytochrome P450 enzymes are members of the hemoprotein superfamily, important players in the cellular adaptation to stress. The CYP enzymes are membrane-bound mixed function oxidases that utilize molecular oxygen and several co-factors including P450 reductase and reduced nicotinamide adenine dinucleotide phosphate to catalyze the oxidation of substrates through the transfer of one oxygen atom to the substrate and the other to water. Two classes of CYP enzymes metabolize arachidonic acid: hydroxylases, which add a hydroxyl group to arachidonic acid to form HETEs and epoxygenases, which add an oxygen atom to a double bond of arachidonic acid to form an epoxide (Figure 1) [95,132]. Depending upon which of the four double bonds of arachidonic acid that is replaced by an epoxide, four distinct regio-isomers may be produced. As illustrated in Figure 1, arachidonic acid (5,8,11,14-Eicosatetraenoic acid) has four double bonds situated between carbon atoms 5 and 6, 8 and 9, 11 and 12, and 14 and 15, which give rise to 5,6-EET, 8,9-EET, 11,12-EET and 14,15-EET, respectively. In addition, each regio-isomer has two stereo-isomers (R,S and S,R), resulting in eight chemically distinct EETs enantiomers [95,132].

Of the many CYP enzymes, the members of the CYP-2C and CYP-2J classes are most commonly noted for their epoxygenase activity and for their role in the synthesis of EETs. This includes the human CYP-2C and CYP-2J isoforms, CYP-2C8, CYP-2C9, CYP-2C19 and CYP-2J2 [95]. In addition to members of the CYP-2C and

CYP-2J classes, however, other CYP isoforms exhibit epoxygenase activity and the ability to catalyze the synthesis of EETs, including rat CYP-2D18 [133] and the orphan isoform CYP-4X1 [134]. It is important to highlight that the synthesis of EETs from arachidonic acid is catalyzed by many different CYP isoforms and that the regio- and stereo-selectivity of these enzymes varies widely [95,132]. Human CYP-2C8 produces 11,12-EET and 14,15-EET in a 1:1.25 ratio, yet produces no 8,9-EET. By contrast, CYP-2C9 produces 8,9-EET, 11,12-EET and 14,15-EET in the ratio of 2.3:1.0:0.5. In a similar manner, the stereo-selectivity of these enzymes varies, with CYP-2C8 producing the (S,R) and (R,S) 11,12-EET stereo-isomers in a 20:80 ratio, while CYP-2C9 produces them in a 70:30 ratio [135].

CYP enzymes are conventionally associated with liver physiology where high expression levels reflect their participation in the oxidative metabolism of endogenous and xenobiotic molecules [132]. As their role in the synthesis of arachidonic acid metabolites, including those that participate in cell signaling pathways in the central nervous system, has been elucidated, the expression of CYP epoxygenase enzymes has been characterized both in the brain and the associated vasculature [3,8,95,136]. This has been done implicitly through the detection of epoxyeicosanoid production in central nervous system tissue and explicitly through molecular methods such as RT-PCR, *in situ* hybridization, and immunocytochemistry. A summary of CYP epoxygenases specifically identified in the brain is presented in Table 2.

Early studies on EETs signaling pathways centered upon their stimulatory effects upon neurohormone release from the hypothalamus and pituitary [129,130], a function that will be discussed in detail below. These first studies identified native

brain epoxygenase activity through the detection of EETs production following incubation of brain microsomes with radio-labeled arachidonic acid. As early as 1984, Capdevila et al. reported such EETs production in isolated rat pituitary microsomes [137]. The authors analyzed the relative abundance of the four EETs regio-isomers and their respective dihydroxyeicosatrienoic acid (DHET) metabolites (Figure 1) and found that 5,6-, 11,12-, and 14,15-EETs and DHETs accounted for nearly 30% of arachidonic acid metabolism in the microsomal preparation. In a later study, Junier et al. detected endogenous production of 8,9-EET, 11,12-EET, 14,15-EET in extracts from male rat hypothalamus [138]. In this study, the authors estimated the hypothalamic EETs concentration to be 120 ng/g in wet tissue. While these early studies identifying EETs as endogenous stimulators of neurohormone secretion in the hypothalamus and pituitary have been largely overshadowed by the emerging appreciation of EETs' role in cardiovascular [95] and cerebrovascular function and disease [8,136], they provided the earliest indication that epoxyeicosanoids were produced endogenously within the central nervous system and associated structures.

In the early 1990s, EETs release from forebrain structures was first reported. Utilizing gas chromatography mass spectroscopy, conversion of radio-labeled arachidonic acid into both 5,6- and 14,15-EETs was reported from mouse whole brain slices [96]. In a subsequent study, the authors reported that homogenate from primary cultured rat hippocampal astrocytes produced both 5,6-EET, 14,15-EET, and their corresponding DHET metabolites when incubated with arachidonic acid; thus identifying astrocytes as one potential site of endogenous EETs production in the central nervous system [139]. These findings were confirmed in a study by

Gebremedhin et al. in which the authors demonstrated using high pressure liquid chromatography the production of all four EETs regio-isomers in cat cerebral microsomes incubated with arachidonic acid [140]. In a subsequent study, Alkayed et al. confirmed EETs' production in cultured rat cortical astrocytes [98]. This work was later extended with the finding that EETs production by and release from cultured rat cortical astrocytes was increased in response to stimulation with the excitatory neurotransmitter glutamate [99]. This last study provided the first concrete evidence that EETs might represent a *releasable* astrocyte-derived signaling molecule in the central nervous system.

Limited experimental evidence also suggests that cerebral vascular endothelium exhibits epoxygenase activity, as demonstrated by the detection of EETs in primary cerebral vascular endothelial cells [5]. Utilizing a fluorescence-based high-performance liquid chromatography method for quantification, 5,6-, 11,12- and 14,15-EET production was identified from the cerebral endothelium. In contrast, very little endothelial production of the 8,9-EET regio-isomer was detected.

CYP Epoxygenase Expression in Neural Tissue

Despite the repeated identification of epoxygenase activity and EETs production within brain tissue, less is known concerning the expression and activity of specific CYP epoxygenases in the brain. RT-PCR screens have been conducted upon whole brain homogenate to identify the expression of CYP epoxygenase message in brain (Table 1). This has included the identification of rat CYP-2C6, CYP-2C7, CYP-2C11, CYP-2C12, CYP-2C23, CYP-2D18, mouse CYP-2C27, CYP-2C37, CYP-2C38, and CYP-2C40 in brain tissue [6,141,142,143,144]. In only two cases, rat CYP-2C11 and

CYP-2C7 [145], was protein expression confirmed by Western blot from whole brain microsomal extract. For two isoforms, rat CYP-2C11 and human, mouse and rat CYP-4X1, extensive analysis of expression and epoxygenase activity was conducted within the brain [6,99,134,141,146,147]. In cultured rat primary cortical astrocytes, Alkayed et al. demonstrated by RT-PCR, Western blot and immunocytochemistry the specific expression of the CYP-2C11 epoxygenase in cortical astrocytes, suggesting that this isoform is likely the astrocytic 'EETs-synthase' postulated by earlier work in these glial cells [99,141]. This work was later corroborated *in vivo* by the localization of CYP-2C11 to cortical astrocytes by *in situ* hybridization [6] and immunohistochemistry [148].

A second specific CYP epoxygenase isoform, CYP-4X1, was recently identified and characterized in the rat, mouse and human central nervous system. A so-called 'orphan' CYP enzyme, CYP-4X1 was initially cloned in the rat as a transcript expressed specifically in brain tissue [147]. *In situ* hybridization demonstrated widespread neuronal expression in the central nervous system, including neurons within the cerebral cortex, hippocampus, cerebellum and brain stem. Molecular cloning in the mouse later yielded the murine CYP-4X1 homologue [146], whose expression was localized to cortical, cerebellar, hippocampal and brain stem neurons by immunocytochemistry. The human CYP-4X1 homologue has likewise been cloned [134], and its mRNA has been identified in human brain tissue. In this most recent work, the metabolic profile of recombinant CYP-4X1 was characterized, including the identification of arachidonic acid epoxygenase activity.

Soluble Epoxide Hydrolase and EETs Metabolism in Neural Tissue

The biological activity of EETs *in vivo* is terminated via their metabolism through multiple pathways, including acylation and incorporation into cellular phospholipids, glutathione conjugation, further oxidation by cyclooxygenase and CYP enzymes, β-oxidation, binding to intracellular fatty acid binding protein, and sEH-catalyzed hydration to the vicinal diol DHETs (Figure 1) [132,149].

Epoxide hydrolases comprise a group of enzymes present in all living organisms that catalyze the addition of water molecules to epoxides to form corresponding diol species. Five epoxide hydrolases have been described in vertebrates: cholesterol epoxide hydrolase, hepoxilin epoxide hydrolase, leukotriene A_4 hydrolase, sEH and microsomal epoxide hydrolase. The leukotriene A_4, cholesterol and hepoxilin epoxide hydrolases have strict substrate specificity, while sEH and microsomal epoxide hydrolase exhibit a wider profile of substrate preference [150]. Despite being active in the metabolism of several chemical epoxide species, sEH has recently received the most attention for its prominent role in the conversion of bioactive EETs to DHET products that are generally regarded as having reduced biological activity (Figure 1). Of the four EETs regio-isomers, 14,15-EET possess the highest affinity for sEH [149], while increasing distance between the epoxide ring and the methyl-terminal carbon reduces the affinity for sEH, thus producing the following substrate preferences for sEH: 14,15-EET > 11,12-EET > 8,9-EET > 5,6-EET. 5,6-EET itself is metabolized poorly by sEH, and its primary route of metabolism may involve further oxidation by cyclooxygenase enzymes [100].

Soluble epoxide hydrolase is highly expressed in mouse, rat, and human brain,

as demonstrated by Western blot of whole brain homogenate from a number of studies [119,151,152,153,154]. The cell type-specific expression of sEH in the brain, however, remains the subject of some uncertainty. Results from our own group have identified dominant sEH expression within rat and mouse brain neurons. Immunohistochemical labeling of the rat and mouse cerebral cortex and striatum revealed sEH expression in neuronal soma and processes (Figure 5A,B) [119,153]. In rat brain slices, sEH immunoreactivity did not co-localize with the astrocytic marker glial fibrillary acidic protein (Figure 5C-E) although sEH labeling was apparent in striatal white matter tracks (Figure 5E), which is consistent with axonal expression of sEH. These findings were generally corroborated in a recent study by Sura et al. from human brain [155]. In that study, the authors document by immunohistochemistry the presence of sEH-immunoreactivity mainly in neurons and oligodendrocytes throughout the brain, including the cerebrum, basal ganglia, and brain stem, with only scattered astrocytes exhibiting sEH expression. The authors further noted the expression of sEH in choroid plexus ependymal cells. In contrast, one other group has recently reported sEH expression in rat astrocytes. In primary cultured rat cortical astrocytes, Rawal et al. detected sEH protein expression both by Western blot and immunofluorescence double labeling [152].

One unique feature of CYP eicosanoids, the epoxide EETs and the hydroxyl HETEs, is their ability to be re-incorporated into membrane phospholipid pools. In the case of EETs, this pathway constitutes a novel route for the clearance and regulation of bioactive EETs levels in addition to providing a latent pool of releasable EETs not dependent upon *de novo* synthesis [3,149]. Early experimental work in isolated mouse

mast cells as well as endothelial and vascular smooth muscle cells from a variety of species demonstrated that all four EETs regio-isomers were readily taken up into membrane phospholipids, including phosphatidylethanolamine, phosphatidylcholine and phosphatidylinisitol [156,157,158]. Upon stimulation with calcium ionophore, 14,15-EET was released from the phospholipid pool at rates exceeding that of arachidonic acid, suggesting that this route of EETs mobilization may be of physiological importance [156]. EETs not incorporated into the phospholipid pool were observed to be rapidly hydrolyzed into DHET species (Figure 1) and released into the media [157,158]. Subsequent work, however, demonstrated that DHETs could likewise undergo phospholipid incorporation, albeit at a lower rate than the corresponding EETs [159].

Based upon these findings, it has been hypothesized that sEH serves as a key regulator of EETs incorporation into membrane phospholipids through its hydrolysis of bioactive EETs to the more releasable DHETs species [160,161]. In porcine coronary endothelial cells, Weintraub et al. demonstrated that inhibition of sEH dramatically increased EETs incorporation into phospholipid pools. Interestingly, this effect was accompanied by an increase in overall EETs release evoked by stimulation with calcium ionophore, suggesting that through its effects on phospholipid EETs incorporation, sEH importantly regulates EETs' release and biological activity [161].

Such membrane phospholipid incorporation of EETs has likewise been observed in the central nervous system. In a study in rat primary cortical astrocyte cultures, Shivachar et al. reported the incorporation of both 8,9- and 14,15-EET into astroglial phospholipids [162]. The authors observe that 8,9-EET was incorporated

much more rapidly than 14,15-EET, a fact that they attribute the regio-selectivity of epoxide hydrolases. Indeed, pharmacological inhibition of epoxide hydrolase activity markedly increased 14,15-EET phospholipid incorporation.

The above studies describing the cell type-specific localization of CYP epoxygenases and sEH throughout the central and peripheral nervous systems, including in neurons, astroglia, oligodendrocytes, and vascular cells suggest that the epoxyeicosanoid pathway may underlie many modes of cellular signaling throughout the nervous system.

Mechanisms of EETs Action in the Central and Peripheral Nervous Systems

EETs exert a myriad of autocrine and paracrine actions upon many distinct cell types, including those within the central and peripheral nervous systems. As detailed above, cellular EETs levels are determined on the supply side by de novo synthesis by CYP epoxygenase enzymes, phospholipase A2-dependent release from the membrane phospholipids and cellular uptake from the extracellular space [3,149]. Regardless of their cellular source, EETs' immediate molecular target remains unclear and the subject of vigorous research. Available evidence suggests that EETs directly interact with a number of signaling partners, including a putative membrane-bound G protein-coupled receptor, ion channels including the transient receptor potential vanilloid-4 (TRPV4) cation channel and the peroxisome proliferator-activated receptor (PPAR) intracellular nuclear receptors [3] (Figure 2). The apparent promiscuity of epoxyeicosanoid signaling, in addition to their ability to act both via a putative G

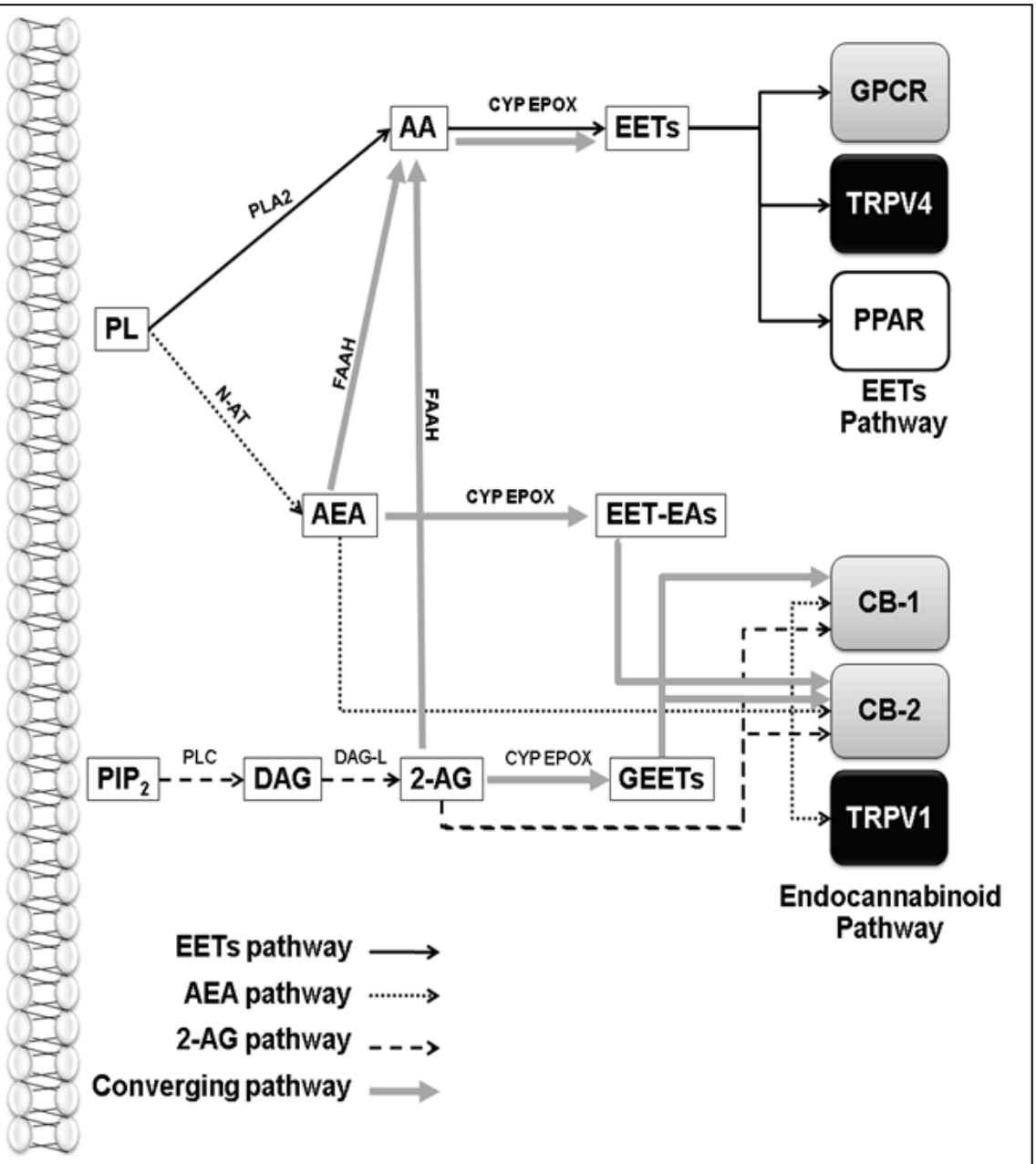

Figure 2 Routes of interaction between epoxyeicosanoid and endocannabinoid signaling pathways. In the canonical EETs signaling pathway, EETs are produced from arachidonic acid (AA) by cytochrome P450 epoxygenase (CYP EPOX) enzymes. EETs exert their cellular actions indirectly through a putative G protein-coupled receptor (GPCR) or by directly stimulating ion channels such as the transient receptor potential vanilloid-4 (TRPV4) cation channel or the peroxisome proliferator activator receptor (PPAR) nuclear receptors. The canonical endocannabinoid signaling pathway includes the synthesis of the endocannabinoids anandamide (AEA) or 2- arachidonyl (2-AG) which act as agonists at the CB-1 and CB-2 GPCRs. AEA also activates the TRPV1 cation channel. Both AEA and 2-AG can be hydrolyzed by fatty acid amido-hydroxylase or other enzymes to AA which feed directly into the CYP

EPOX – EETs signaling cascade. Both AEA and 2-AG can be epoxidized by CYP EPOX to produce EET glycerol esters (GEETs) and EET ethanolamides (EET-EAs). GEETs are high affinity CB-1 and CB-2 agonists while EET-EA activates CB2 with high affinity. PL: phospholipids; N-AT: N-acetyl transferase; PIP2: phosphatidylinositol 4,5-bisphosphate; PLC: phospholipase C; DAG: diacylglycerol; DAG-L: DAG lipase.

protein-coupled receptor and TRPV4 cation channels, is intriguing when compared to the signaling pathways employed by another lipid-based signaling pathway, the endocannabinoid system [163]. This system exerts its actions including those within the CNS via a family of G protein-coupled receptors and through the direct activation of TRPV1 cation channels. Recent functional studies suggest the provocative notion that these pathways bear more than a mere resemblance to one another, but rather interact at multiple molecular levels to regulate cellular function.

A Putative G Protein-Coupled Receptor for EETs

Evidence for a specific membrane-bound, extracellular site of action for EETs has been steadily accumulating since the early 1990s. In a series of studies in guinea pig mononuclear cells and a human monocyte cell line, Wong and colleagues identified a specific, saturable and reversible binding site for radio-labeled 14(R),15(S)-EET [164,165,166]. This site is regio- and stereo-selective, having the highest affinity for this EET enantiomer [165,166]. Ligand binding to this site was protease-sensitive, suggesting that the binding partner in question was a protein, and appeared to be under regulatory control of the protein kinase-A signaling pathway [164]. In cultured rat aortic endothelial cells, the cellular effect of a 14,15-EET analog upon aromatase activity persisted even when the molecule was chemically tethered to a silica bead [167], supporting the existence of an extracellular binding site for 14,15-EET. In a

recent study, a radio-labeled EETs agonist, 20-iodo-14,15-epoxyeicosa-8(*Z*)-enoic acid (20-I-14,15-EE8ZE) was employed to further characterize in human U937 cells this putative EETs binding partner [168]. Based upon radio-ligand displacement, the authors describe a site exhibiting relative EETs affinities of 11,12-EET > 14,15-EET >> 14,15-DHET. Further, ligand binding decreased in the presence of GTPγS, suggesting that the binding site in question is a G protein-coupled receptor. This last finding is in agreement with several previous studies that have suggested that the putative membrane-bound 'EETs receptor' is likely a G protein-coupled receptor [169,170,171].

Many of these early studies focusing on the role of EETs in the hyperpolarization and relaxation of vascular smooth muscle identified the large-conductance calcium-sensitive K^+ channel as the primary effector pathway through which EETs exert their vasomotor actions. Treatment with EETs increased the open probability of large-conductance calcium-sensitive K^+ channels in many cell types [170,172], including cerebral vascular smooth muscle, while the membrane hyperpolarizing effects of EETs were sensitive to high extracellular K^+ or K^+ channel blockade with tetraethylammonium [140]. Further experimental evidence has suggested that EETs do not interact directly with this ion channel, acting rather through a putative G protein-coupled receptor to exert their effects on large-conductance calcium-sensitive K^+ channel function. EETs are unable to activate large-conductance calcium-sensitive K^+ channel currents in inside-out detached patch recordings from vascular smooth muscle [169,170,171]. Treatment with an anti-Gsα antibody likewise blocks the effect of 11,12-EET on large-conductance calcium-

sensitive K^+ channel activity as does inhibition of ADP-ribosylation. The weight of this early data clearly suggests that EETs exert at least certain biological activities, including large-conductance calcium-sensitive K^+ channel activation, through their action at a putative Gsα-coupled G protein-coupled receptor that involves the downstream activation of ADP ribosylation.

A recent study by Behm et al. has additionally identified a novel role for EETs in regulating signaling through the thromboxane prostaglandin receptor [173]. The authors report that 14,15-EET directly antagonizes this receptor with considerable specificity and affinity. The finding that EETs are an endogenous antagonist at this receptor is intriguing, and may have important implications regarding interactions between prostaglandin and EETs signaling pathways both in vasculature and extra-vascular tissues. However, these data have not yet been reproduced and the significance of this specific binding partner in mediating the cellular actions of EETs remains undetermined.

Activation of the TRPV4 Channel

While the classical understanding of EETs signaling involves the indirect activation of large-conductance calcium-sensitive K^+ channels via a putative G protein-coupled receptor-mediated signaling pathway [95], further experimental evidence suggests that certain cellular actions of EETs may be mediated through their direct interaction with ion channels. In particular, the activation of the TRPV4 cation channel has received considerable recent attention. TRPV4 is a calcium-permeable member of the transient receptor potential vanilloid cation channel family, and closely related to the TRPV1 capsaicin receptor found on nociceptive primary afferent fibers [174]. In 2003, it was reported that 5,6- and 8,9-EET directly activate TRPV4 channels [128]. In this study,

the authors report that the activation of TRPV4 by arachidonic acid in transfected cells was sensitive to three distinct inhibitors of CYP enzymes, while direct application of 5,6- or 8,9-EET caused ruthenium red-sensitive elevations of intracellular Ca^{2+}. 5,6-EET-evoked TRPV4 currents were observed both in whole-cell and detached inside-out patch recordings, demonstrating the direct activation of TRPV4 by these EETs regio-isomers. This effect was then confirmed in mouse aortic endothelial cells, in which TRPV4 activation by osmotic cell swelling and arachidonic acid administration were sensitive to CYP epoxygenase inhibition [174]. Furthermore, 5,6-EET produced a ruthenium red-sensitive, Ca^{2+}-sensitive current that appeared to reflect the activation of native endothelial TRPV4 by this EET regio-isomer. These and other studies have established that EETs-evoked TRPV4 activation is an important regulator of calcium-dependent endothelial function, including participation in flow-induced vasodilation [4,174].

Two recent studies shed further light on the activation of TRPV4 by EETs and are more directly relevant to processes of neural function and disease. Earley et al. describe TRPV4 expression in cerebral vascular smooth muscle cells which respond to 11,12-EET treatment with the activation of whole-cell TRPV4 currents [175]. 11,12-EET administration also increases Ca^{2+} spark and large-conductance calcium-sensitive K^+ channel activity, effects that are sensitive to anti-sense oligonucleotide knockdown of TRPV4. Based upon these findings, the authors conclude that TRPV4 and the large-conductance calcium-sensitive K^+ channel form a 'novel Ca^{2+} signaling complex' in cerebral vascular smooth muscle, in which EETs activate Ca^{2+} influx via TRPV4, resulting in sarcolemmal ryanodine receptor activation, Ca^{2+} spark formation, large-

conductance calcium-sensitive K^+ channel activation, membrane hyperpolarization and consequent vasorelaxation. Based upon these findings, the activation of TRPV4 may play a key role in the vasomotor action of EETs in the cerebral circulation. A second study by Sipe et al. reports that peripheral administration of 5,6-EET activates action potential spiking in mouse colonic primary afferents [176]. These fibers expressed TRPV4 and the activation of afferent spiking activity was sensitive to ruthenium red treatment and TRPV4 gene deletion. This study suggests that EETs, through their activation of TRPV4 may stimulate neuronal action potential firing, a finding that may be relevant to the activity of trigeminal afferents which also express TRPV4 in addition to EETs-synthetic CYP epoxygenases [177,178].

Activation of PPAR Signaling

PPARs are a family of three intracellular nuclear receptors that upon ligand binding, recruit the retinoic X receptor binding partner, translocate to the nucleus, and bind to peroxisome proliferator response elements to regulate gene transcription. In particular, the PPARα receptor is known to serve as a lipid detector, being activated by fatty acids and eicosanoids and exerting regulatory control over genes involved in fatty acid metabolism and eicosanoid signaling pathways [179]. In 2002 it was initially reported that CYP ω-hydroxylase metabolites of 8,9-, 11,12- and 14,15-EET were potent trans-activators of PPARα signaling in a transfected cell line [180]. Subsequently, Ng et al. reported that in HepG2 cells, 11,12- and 14,15-EETs stimulated PPARα and PPARγ activity using a luciferase reporter assay [181]. Interestingly, the 8,9-EET regio-isomer demonstrated no activity in this assay, whereas the 14,15-DHET epoxide hydrolase metabolite exhibited robust activity. In primary rat hepatocytes, both 11,12- and 14,15-

EETs were capable of inducing the expression of known PPARα-responsive gene products, suggesting that the activation of PPAR signaling by EETs and their metabolites may be physiologically relevant [120]. The specific participation of EETs-evoked PPAR signaling in the neuronal remains unexplored. Emerging evidence suggests that PPAR signaling is a potential therapeutic target in the treatment of disease states associated with oxidative stress such as hypoxic/ischemic injury and Alzheimer's Disease [182]. The potential role for EETs signaling in these processes remains an obvious avenue for future research.

Interactions Between Epoxyeicosanoid and Endocannabinoid Signaling Pathways

Reviewing the details of the EETs signaling system as they are currently understood, it is striking how many similarities exist between this pathway and the extensively studied endocannabinoid system [163]. Both pathways are based on lipophillic signaling molecules derived from membrane phospholipids. Endocannabinoids signal through distinct G protein-coupled receptors (the CB1 and CB2 receptors) while experimental evidence supports existence of one or more putative EETs G protein-coupled receptors [3,95]. The endocannabinoid anandamide directly activates TRPV1 cation channels [163], while 5,6-, 8,9- and 11,12-EETs activate TRPV4 channels [4,128,174,175,176]. Interestingly, recent experimental evidence suggests that these pathways do not simply resemble one another, but in fact converge in the regulation of cellular function, including in the vasculature and the brain (Figure 2). In 2003, Watanabe et al. reported that both 5,6-EET and the endocannabinoid anandamide directly activate the TRPV4 channel in a transfected cell system [128]. The authors noted that the effects of anandamide were dependent first upon its hydrolysis to

arachidonic acid by the enzyme fatty acid amido-hydrolase followed by its subsequent metabolism by CYP epoxygenases. Thus, at least in the case of anandamide-evoked TRPV4 activation, the endocannabinoid signaling pathway converges with the CYP epoxygenase/EETs pathway. Similar findings have been reported in the bovine coronary endothelium, in which the endocannabinoid 2-arachidonylglycerol was produced in response to acetylcholine stimulation [126]. 2-arachidonylglycerol was then hydrolyzed to arachidonic acid, contributing to EETs-mediated endothelium-dependent vasodilation. These studies demonstrate that the endocannabinoids anandamide and 2-arachidonylglycerol, following their hydrolysis to arachidonic acid, can feed into pathways of the arachidonic acid cascade, including the CYP epoxygenase pathway.

In a second mode of interaction between the endocannabinoid and epoxyeicosanoid pathways, recent evidence also suggests the endocannabinoids anandamide and 2-arachidonylglycerol themselves may be substrates for CYP epoxygenase enzymes and that the resulting endocannabinoid epoxide metabolites may possess biological activity. In 2007, it was reported that human liver and kidney microsomes incubated with anandamide produced several CYP monoxygenase metabolites, including 20-HETE-ethanolamide, 5,6-, 8,9-, 11,12- and 14,15-EET-ethanolamide [127]. In the liver, this anandamide epoxygenase activity was attributed to the CYP-3A4 isoform, which is also expressed in activated mouse microglial cells [183]. The orphan CYP-4X1 isoform, which is expressed in human, mouse and rat brain, likewise converts anandamide to 14,15-EET-ethanolamide [134,146,147]. Interestingly, 5,6-EET-ethanolamide appears to bind to and activate the human CB2

receptor with high affinity, suggesting a role for these endocannabinoid epoxygenase metabolites in immune function [183]. The endocannabinoid 2-arachidonylglycerol can likewise serve as a substrate for CYP epoxygenases, resulting in the production of EET glycerol esters [125,184]. These endocannabinoid epoxygenase metabolites, including 11,12-EET glycerol ester and 14,15-EET glycerol ester bind with high affinity to both CB1 and CB2 receptors in rat cerebellar and spleen membranes, respectively. *In vitro*, 11,12- and 14,15-EET glycerol ester produce vasorelaxation in rat kidney arterioles and bovine coronary arteries. The former effect was sensitive to the CB1 antagonist AM251. *In vivo*, intravenous 11,12-EET glycerol ester injection in mice produced hypomotility and hypothermia, effects that were also inhibited by CB1 receptor blockade [125].

These emerging studies thus demonstrate that the epoxyeicosanoid and endocannabinoid signaling pathways may interact at a number of levels. Endocannabinoids may be hydrolyzed to free arachidonic acid which then feeds into the CYP epoxygenase pathway [126,128], or these compounds may themselves be directly converted into bioactive epoxides [125,183,184] (Figure 2). Because these interactions have only recently become apparent, their physiological and pathophysiological significance remains unclear. The presence, however, of endocannabinoid epoxygenases and epoxide metabolites [134,146,147,183] in the brain suggests that the interaction of these apparently similar signaling cascades may play an important role in neuronal function and disease.

Physiological Actions of EETs in the Neural Tissue

As has been described above, a substantial body of research identifies EETs as endogenous constituents of central and peripheral neural tissue. CYP epoxygenase expression has been reported throughout the brain, including in neurons, astrocytes and vascular endothelium (Table 2), while cell type-specific EETs release has been described from cortical astrocytes and endothelium [5,98,139]. Since the mid 1990s, investigations into the physiological role of EETs signaling in the brain have centered predominantly upon their potent activity in regulating the function of the cerebral vasculature. This includes both their well-studied participation in the process of functional hyperemia as well as their regulation of cortical angiogenesis [5,95,185]. However, it is noteworthy that the initial characterization of EETs' regulation of cellular function in the 1980s stemmed from their role as endogenous regulators of neurohormone release in the hypothalamus and anterior pituitary [129,130]. These data suggest that epoxyeicosanoids may under physiological conditions be key regulators of synaptic transmission, a cellular action that is distinct to neural function.

Vasomotor Effects of EETs in the Cerebral Circulation

Of their many cellular actions in tissues throughout the body, EETs are best known as potent vasodilators in various circulatory beds, including the heart, kidney and brain [3,95]. In the coronary and renal circulation, EETs have been identified as EDHFs, being released from the vascular endothelium in response to stimulation and acting upon adjacent vascular smooth muscle to affect hyperpolarization and relaxation [95,186]. In the cerebral circulation, several studies have documented first the direct vasoactive effects of EETs in this vascular bed and second their key role in mediating

the process of functional hyperemia.

Beginning with the work of Ellis et al., EETs were initially identified as potent vasodilators in the cerebral vasculature. Using *in vivo* rabbit and cat cranial window preparations, the authors determined the effect of topically applied EETs on cerebrocortical surface arteriolar diameter [97,100]. In this model, 5,6-EETs in micromolar concentrations produced a ~20% dilation of cerebral vessels while the 8,9-EET, 11,12-EET regio-isomers evoked less response. The dilator action of 5,6-EET was sensitive to cyclooxygenase inhibition with indomethacin, suggesting that a vasoactive cyclooxygenase metabolite of EETs was involved in this response. These findings were later extended by Gebremedhin et al. using isolated cat cerebral arteries [140]. In this study, the authors observed that 5,6-, 8,9- and 11,12-EET directly and concentration-dependently dilated cerebral arteries *in vitro*. More recent studies have confirmed EETs' vasoactivity in the cerebral circulation in rats, including the effect of 11,12-EET in isolated rat cerebral artery and 14,15-EET in the rat cranial window model [175,178]. These vasomotor actions of EETs in the cerebral vasculature are thought to be mediated by the activation of vascular smooth muscle K^+ channels, as evidenced by the sensitivity of the EETs-evoked response to the K^+ channel blocker tetraethylammonium [95,140].

More recently, the involvement of the TRPV4 cation channel in the vasomotor activity of EETs in rat cerebral arteries has been suggested. In dissociated rat cerebral vascular smooth muscle, Earley et al. reported that 11,12-EET administration produced TRPV4-like whole-cell currents that coincided with an increase in Ca^{2+} spark activity that was in turn linked to large-conductance calcium-sensitive K^+ channel activity and

membrane hyperpolarization [175]. Based upon these findings, the authors proposed the hypothesis that TRPV4 and the large-conductance calcium-sensitive K^+ channel constitute a novel Ca^{2+} signaling complex in cerebral vascular smooth muscle cells that is the molecular target of vasoactive EETs. This model was supported by the attenuation of 11,12-EET-evoked vasodilation in isolated rat cerebral arteries by antisense oligonucleotide TRPV4 gene knockdown. These studies demonstrate that as in the peripheral circulatory beds such as the coronary, renal or mesenteric vasculature [95], all EETs regio-isomers act as potent vasodilators in the cerebral circulation.

Regulation of Cortical Angiogenesis

Angiogenesis, the process through which new microvasculature is produced, occurs both in the healthy and diseased brain. In addition to the initial development of the mature cerebral vasculature, normal physiological angiogenesis may represent the vascular projection of brain plasticity [187]. The stimulation and maintenance of cortical angiogenesis is importantly regulated through interactions between astrocytes that surround the cerebral microvasculature and endothelial cells which constitute the terminal branches of the circulatory bed and sites of angiogenic growth. The interplay between cortical astrocytes and brain microcirculation was examined in earlier studies demonstrating that astrocyte-derived EETs are key regulators of cortical angiogenesis [109,110]. In the first study, the authors report that cultured cerebral microvascular endothelial cells underwent avid proliferation when treated with conditioned media from primary cortical astrocyte cultures. When the two cell types were cultured together, endothelial cells exhibited spontaneous tube formation, an *in vitro* model of angiogenesis. The endothelial cell tube formation stimulated by co-culture with

astrocytes was blocked with treatment with the CYP inhibitor 17-ODYA, suggesting that CYP metabolites mediated astrocyte-evoked angiogenic processes [109]. In the follow-up study by Zhang and Harder (2002), the authors report that inhibiting astrocytic CYP enzymes with 17-ODYA attenuated the mitogenic action of astrocyte-conditioned media on cerebral microvascular endothelial cells, demonstrating that an astrocyte-derived CYP metabolite underlies this response [110]. The authors also observe that direct treatment of endothelial cells with all four EETs regio-isomers evokes cell proliferation, with 8,9-EET being the most potent in this process. Extending these findings *in vivo,* 8,9-EET-supplemented matrigel implanted subcutaneously exhibited more robust capillary infiltration than did control matrigel implants. These studies together provide strong evidence that cortical astrocyte-derived EETs exert pro-angiogenic effects on cerebral endothelial cells and that EETs signaling may mediate angiogenesis under normal physiological conditions.

Contribution to Endothelium-Dependent Vasomotor Control

In the peripheral circulation, as in the cerebral vasculature, EETs are potent vasodilators produced by the vascular endothelium and signaling in parallel with nitric oxide as an EDHF [5,100,101,186]. This role has been investigated most extensively in the coronary circulation. In a key study by Fisslthaler et al. [186], a classical EDHF-like response was produced when isolated porcine coronary arteries were stimulated with acetylcholine in the presence of NOS and cyclooxygenase blockade. The authors then demonstrate that induction of endothelial CYP-2C8 expression with β-naphthoflavone potentiated the observed EDHF response. Conversely, oligonucleotide knockdown of CYP-2C8 expression resulted in an attenuation of the EDHF response.

These data and those from other studies demonstrate a role for endothelial EETs as putative EDHFs [101,186].

One key physiological role for EDHFs in the peripheral circulation is in flow-mediated vasodilation. As detailed above, through this process changes in mechanical endothelial shear stress are transduced by the vascular endothelium into a vasomotor dilation that coordinates changes in flow rate along the vascular tree [10,188].

Recently, endothelial EETs, through their action at the mechanosensitive TRPV4 cation channel [189], have been implicated as mediators of flow-mediated vasodilation [190,191,192]. In rat carotid artery endothelial cells, TRPV4 is expressed and can be activated by a TRPV4 agonist, arachidonic acid or hypotonic swelling. In the same vessels, flow-mediated vasodilation was inhibited by the non-specific TRPV antagonist ruthenium red, as well as by a phospholipase A2 inhibitor [190]. In a follow-up study, this group demonstrated that carotid arteries from TRPV4 knockout mice were insensitive to the TRPV4 agonist, arachidonic acid and hypotonic swelling. Furthermore, the dilation responses to changes in endothelial shear stress were completely abolished [191]. Similar findings were observed in the mesenteric vasculature [192] of TRPV4 knockout mice.

The endothelial TRPV4 cation channel is modulated by endothelial EETs [174]. In patch clamp experiments from mouse aortic endothelial cells Vriens et al. observed that hypotonic cell swelling, arachidonic acid, 5,6- and 8,9-EETs activate TRPV4 currents and Ca^{2+} signaling events. Each of these responses was absent from TPV4 knockout mouse endothelial cells. Furthermore, induction of CYP-2C expression in wild type animals with nifedepine potentiated these responses, while

CYP-2C inhibition with sulfaphenazole blocked them [174]. A recent study additionally demonstrated that the interaction of EETs and TRPV4 signaling contributes to flow-mediated vasodilation [4]. In mouse carotid arteries, EDHF-dependent flow-dependent vasodilation was observed in the presence of NOS and cyclooxygenase blockade. This flow-mediated vasodilation could be blocked either by pre-treatments with the CYP epoxygenase inhibitor N-(methylsulfonyl)-2-(2-propynyloxy)-benzenehexanamide (MS-PPOH) or with the TRPV antagonist ruthenium red. The effects of these two treatments were not additive, suggesting that they are not parallel regulatory mechanisms. TRPV4 knockout mice exhibited a reduced flow-mediated dilation response, while the residual response was insensitive to CYP epoxygenase inhibition. These data demonstrate that EETs, functioning as an EDHF and acting through the endothelial TRPV4 cation channel, contribute to flow-mediated dilation [4].

Mediators of Cortical Neurovascular Coupling

The physiological role of vasoactive EETs in the central and peripheral nervous system has been explored most extensively in the context of the phenomenon termed functional hyperemia. Functional hyperemia is the process by which local changes in brain activity are coupled both spatially and temporally with corresponding increases in local cerebral blood flow [1]. Forming the physiological basis for the functional magnetic resonance imaging technique, this process of neurovascular coupling has been the subject of intense research that has identified numerous mediators and modulators of this process, including K^+, adenosine, nitric oxide and EETs [1,185]. In 1997, Alkayed et al. reported that stimulation of cultured rat astrocytes with the

excitatory neurotransmitter glutamate increased cellular EETs production, an effect that was sensitive to CYP enzyme inhibition with miconazole [99]. The authors then demonstrated that miconazole blocked the hyperemic response to subdural glutamate infusion, supporting a role for EETs signaling in coupling excitatory neurotransmitter release with corresponding elevations in cerebral blood flow. A follow-up study produced similar results with the CYP epoxygenase inhibitor MS-PPOH in blocking the hyperemic response to subdural N-methyl-D-aspartate infusion [193]. In two further studies, MS-PPOH attenuated the cerebral blood flow response to functional activation of the rat cortex produced by whisker or electrical forepaw stimulation [6,7]. These early studies thus established a role for astrocyte-derived EETs in mediating the process of functional hyperemia in the brain [194].

More recent studies have utilized sophisticated imaging and molecular techniques to define the cellular mechanisms governing the participation of EETs in neurovascular coupling. In isolated rat retina, Metea and Newman observed that arterioles dilated both in response to light stimulation and photolysis of caged Ca^{2+} molecules loaded into perivascular astrocytic endfeet [195]. In this study, the authors reported that the vasomotor responses to both modes of stimulation were abolished by three distinct inhibitors of CYP epoxygenases. This elegant *in vitro* study extends functional activation studies carried out previously in the whole animal and confirms at the molecular level that astrocyte-derived EETs mediate neurovascular coupling in the central nervous system.

Within the field currently studying cerebral blood flow regulation, a puzzle has recently emerged concerning the occurrence of dilator versus constrictor coupling

between astrocytes and their associated microvasculature. In contrast to the findings of Matea and Newman [195] and others [32,196] utilizing both *in vitro* and *in vivo* two-photon imaging in rats and mice, Mulligan and MacVicar observed vasoconstriction of cerebral arterioles in cortical slices undergoing photolysis of astrocytic caged Ca^{2+} as well as with metabotropic glutamate receptor agonist treatment [197]. These findings suggest that differing modes of neurovascular coupling can be produced, apparently in a context-dependent manner. A study by Blanco et al. sheds some light upon this puzzle by suggesting that the resting tone of cerebral arterioles is a key determinant of the polarity of neurovascular coupling, and that changes in the vasomotor responses to EETs may underpin these shifts in polarity [198]. In this study, the authors report that in acute rat cortical slices, the vasomotor responses to stimuli such as K^+ or metabotropic glutamate receptor agonists shift in magnitude or polarity, depending on the resting tone of the vessel. Highly constricted vessels were observed to dilate avidly, while less constricted vessels responded either with less dilation (K^+) or with constriction (metabotropic glutamate receptor agonists). Interestingly, the vasomotor response to exogenous 11,12-EET exhibited this same polarity. Under constricted conditions, 11,12-EET produced monophasic vasodilation that was tetraethylammonium-sensitive. However, under conditions of reduced vascular tone, 11,12-EET produced a biphasic constriction followed by dilation. These findings, while still awaiting validation, present an intriguing mechanistic explanation for the regulation of dilator versus constrictor neurovascular coupling. Furthermore, they suggest that the vasomotor response to astrocyte-derived EETs may itself be one tunable element of this regulation.

Regulation of Neurohormone Release

Despite the more recent focus upon the role of EETs in cerebrovascular regulation, the earliest studies of EETs' function in the brain detailed a non-vascular role for EETs signaling in stimulating neurohormone release from neuroendocrine regions of the brain. In one early study in rat hypothalamus, 5,6-EET stimulated the release of somatostatin and luteinizing hormone releasing hormone [129,130]. These findings were later confirmed and extended to include the stimulation of somatostatin release from rat hypothalamus by the 8,9-EET regio-isomer. In the anterior pituitary, the four EETs regio-isomers were variously observed through the course of several studies to directly stimulate the release of luteinizing hormone, arginine vasopressin, oxytocin, prolactin and growth hormone [130,131,199,200,201]. Interestingly, in addition to these direct effects upon neurohormone release, EETs appear to mediate the actions of other neuroendocrine secretagogues. In the hypothalamus, inhibition of CYP epoxygenase activity blocks dopamine-evoked somatostatin release [129]. In the anterior pituitary, inhibition of CYP epoxygenases blocks corticotrophin-releasing factor-, β-adrenergic agonist-, and K^+-evoked corticotrophin release while thyrotropin-releasing hormone-evoked prolactin release was likewise sensitive to CYP epoxygenase inhibition [202,203]. Importantly, it was observed that stimulation of these cells with 5,6-EET resulted in intracellular Ca^{2+} mobilization, suggesting a potential mechanism through which EETs might exert these pro-secretory actions.

Analgesia and Anti-nociception

A more recent group of studies demonstrate a second manner in which EETs may participate in neural function. As a result of the observed anti-inflammatory effects of

EETs [103], experimental work in animal models of inflammatory pain have begun to explore the potential role of EETs as endogenous analgesic factors or sEH inhibition as a potential therapeutic avenue for the amelioration of inflammatory pain. In the first study on this subject, Inceoglu et al. report that both exogenous EETs and sEH inhibitor administration reduce inflammatory pain associated with hindpaw lipopolysaccharide injection in the rat [204]. In this study, topical application of either of two distinct sEH inhibitors blocked lipopolysaccharide-evoked thermal sensitization and allodynia. Topically administered methyl esther EETs produced a similar reduction in thermal sensitization. These effects of sEH inhibitors were subsequently confirmed in a second model of inflammatory pain, subplantar carrageenan-evoked thermal hyperalgesia in the rat [205]. In the most recent study from this group, Inceoglu et al. report that intra-spinal injection of two distinct sEH inhibitors block lipopolysaccharide- and carrageenan-evoked thermal hyperalgesia [124]. These functional responses coincided with a reduction in lipopolysaccharide-evoked spinal cyclooxygenase-2 mRNA induction in addition to an up-regulation of Steroidogenic Acute Regulatory Protein-1, an acute response neurosteroid-producing gene. The induction of spinal Steroidogenic Acute Regulatory Protein-1 expression could also be produced by intra-spinal injection of EETs plus cAMP, suggesting that the effects of the sEH inhibitors were the result of increased EETs signaling. Based upon these experimental findings, the authors conclude that EETs act through two distinct analgesic pathways, inhibiting cyclooxygenase-2 expression and inducing neurosteroid signaling to relieve inflammatory pain.

A recent study by Terashvili et al. added to these findings, demonstrating an

anti-nociceptive effect of 14,15-EET, but not 5,6-, 8,9- or 11,12-EET, in the rat ventrolateral periaqueductal gray [206]. In this study, Terashvili et al. report that direct microinjection of 14,15-EET into this region dose-dependently reduced tail flick latency in rats. This anti-nociceptive effect of EETs involved activation of β-endorphin and Met-enkephalin signaling via the μ and δ opioid receptors. Intriguingly, these recent studies demonstrate a potential role for EETs signaling both in peripheral and central pain processing pathways, suggesting that epoxyeicosanoids regulate physiological and pathophysiological processes in ways not related to cerebrovascular function.

A Role for EETs in the Neurogenic Regulation of the Cerebral Vasculature

As detailed above, cerebral blood flow is controlled at three overlapping mechanistic levels: intrinsic vasomotor regulation, including autoregulation and flow-mediated vasodilation; neurovascular coupling; and neurogenic regulation by parasympathetic, sympathetic and trigeminal perivascular nerve fibers [1,10,11,188].

These various modes of regulation are mediated by a diverse gathering of molecular factors. One key factor is nitric oxide, which participates at all three levels of cerebral blood flow regulation. Nitric oxide is the ‘endothelium-derived relaxing factor’ that contributes to flow-mediated cerebral vasodilation [26,28,207]. Neuronally-derived nitergic oxide likewise participates in functional hyperemia [48,51]. Lastly, nitric oxide is one of the key transmitters released from extrinsic parasympathetic vasodilator nerves surrounding the cerebral surface vasculature,

mediating the vasomotor actions of these fibers [61,63,64,66,67]. In this way, nitrergic signaling represents a common mode of cerebrovascular regulation, utilized at each of these three distinct regulatory strata.

EETs are potent vasodilators in the cerebral circulation. Emerging evidence suggests that endothelial EETs [5], signaling through the endothelial TRPV4 cation channel, contribute in parallel with nitric oxide to flow-mediated vasodilation [4,174,190,191,208]. Additionally, astrocyte-derived EETs have been implicated as key mediators of neurovascular coupling in the mouse and rat cerebral cortex [6,7,98,99]. These findings establish EETs as important regulators of cerebrovascular function at multiple levels of regulatory control. Whether EETs, like nitric oxide, contribute to the neurogenic regulation of cerebral blood flow remains unexplored.

Over the past 15 years, EETs have been primarily regarded for their potent effects upon cardiovascular function [95]. However, the earliest descriptions of the biological actions of EETs came from the hypothalamus and anterior pituitary. Here it was established that endogenous EETs contribute both to basal and stimulated release of neurohormone from this neural tissue [129,130,131,137,138,209]. Localization data demonstrates that CYP epoxygenase 'EETs-synthases' are localized to peripheral and central neurons [134,146,210,211]. More recent research has demonstrated that EETs modulate neuronal pain processing in the brainstem [124,206] and that the CYP epoxygenase metabolic pathway interacts with the neuro-active endocannabinoid pathway at a number of mechanistic levels [125,126,127,128,184]. Thus, a role for nerve-derived EETs in the neurogenic regulation of cerebral blood flow by perivascular vasomotor nerves is plausible.

Hypothesis

Experiments in this thesis test the hypothesis that nerve-derived EETs contribute to the regulation of cerebral blood flow by perivascular vasodilator nerves.

I chose to focus upon the role of EETs in the actions of vasodilator nerves rather than sympathetic fibers owing to the fact that EETs are well known as potent cerebrovasodilators [97,100]. In the succeeding four chapters, I will evaluate this hypothesis at four points. First I determine whether perivascular vasodilator nerves surrounding the cerebral surface vasculature express the biochemical machinery for the synthesis and regulation of vasodilator EETs. Second, I evaluate whether these neuronal CYP epoxygenase enzymes are constitutively active and whether EETs are endogenously present in primary trigeminal ganglion neurons. Third, I evaluate the cellular roles of neuron-derived EETs in the cellular function of primary trigeminal ganglion neurons. And fourth, I determined whether EETs contribute functionally to the *in vivo* regulation of cerebral blood flow by perivascular vasodilator nerves.

Chapter 2. Characterization of the Epoxyeicosanoid Signaling Pathway in the Cerebral Vasculature and Associated Ganglia

Data contained in this chapter appeared in the following published research articles:

Iliff JJ, Close LN, Selden NR, Alkayed NJ. A novel role for P450 eicosanoids in the neurogenic control of cerebral blood flow. *Exp Physiol*. 92(4):653-8, 2007.

Zhang W, Otsuka T, Sugo N, Ardeshiri A, Alhadid YK, Iliff JJ, Debarber AE, Koop DR, Alkayed NJ. Soluble epoxide hydrolase gene deletion is protective against experimental cerebral ischemia. *Stroke*. Jul;39(7):2073-8, 2008.

Iliff JJ, Wang R, Zeldin DC, Alkayed NJ. Epoxyeicosanoids as mediators of neurogenic vasodilation in cerebral vessels. *Am J Physiol: Heart Circ Phsyiol* May; 296(5):H1352-63, 2009.

Zhang W, Iliff JJ, Campbell C, Wang R, Hurn P, Alkayed NJ. Role of soluble epoxide hydrolase in sex-specific vascular response to cerebral ischemia. *J Cereb Blood Flow Metab*;.29(8):1475-81, 2009.

Chapter Abstract

Cerebral blood flow is regulated at multiple hierarchical levels, including intrinsic vascular regulation, neurovascular coupling, and the regulation of the cerebral surface vasculature by extrinsic perivascular nerves. EETs are potent vasodilators produced in brain by CYP epoxygenases and metabolized by sEH. Vasodilator EETs contribute both to endothelium-dependent cerebral vascular regulation in addition to being a mediator of neurovascular coupling. However, whether EETs also participate in the regulation of the cerebral vasculature by perivascular nerve fibers remains unknown. I here demonstrate that in cerebral surface arteries such as the middle cerebral artery, sEH-immunoreactivity is localized to extrinsic perivascular nerves. Double labeling studies demonstrated that sEH predominantly co-localized with neuronal nitric oxide synthase within perivascular nerve fibers. Significant co-localization for sEH was also observed with parasympathetic markers vasoactive intestinal peptide and choline actetyltransferase, in addition to the sensory fiber markers calcitonin gene-related peptide and substance P. No co-localization was observed with sympathetic fiber markers. Within both the parasympathetic sphenopalatine and trigeminal ganglia, RT-PCR identified the expression of two specific CYP epoxygenase isoforms, CYP-2J3 and CYP-2J4. Immunofluorescence double-labeling demonstrated the in the sphenopalatine and the trigeminal ganglia, CYP-2J and sEH were present in nearly all neurons. The presence of enzymes involved in EETs production and metabolism within extrinsic parasympathetic and sensory vasodilator fibers suggests a novel role for EETs in the neurogenic control of cerebral arteries.

Introduction

Cerebral blood flow is intricately regulated through multiple mechanisms that operate at different hierarchical levels to maintain adequate tissue perfusion and prevent wide fluctuations in brain blood flow. Locally, cerebral blood vessels exhibit the intrinsic capacity to respond to changes in their physical (intraluminal pressure, longitudinal shear) and chemical (pH, PO_2, PCO_2) environments, exerting an autoregulatory influence upon their own vasomotor tone. These regulatory mechanisms often involve the vascular endothelium, which acts to modulate the tone of associated vascular smooth muscle [10,12,188].

In addition, cerebral blood vessels sense and respond to changes in neuronal activity in order to fine-tune and dynamically regulate blood flow rates in accordance with local metabolic demands. This metabolism-flow coupling occurs within the so called "neurovascular unit" comprised of neurons, vascular smooth muscle, endothelium, and intervening astrocytes. These different cell types work together to match blood flow with neuronal demands, a process termed "neurovascular coupling" which forms the basis of functional magnetic resonance imaging (fMRI) [1]. Neurovascular coupling is mediated in large part by astrocytes, whose processes ensheathe both neuronal synapses and parenchymal arterioles. According to this model, astrocytes sense neuronal activity through stimulation of metabotropic glutamate receptors, leading to the release of vasoactive compounds such as K^+ [37] or cyclooxygenase and P450 eicosanoids [6,7,54,98,99] to dilate adjacent arterioles and increase nutritive blood flow.

In addition to these modes of cerebral blood flow regulation, large conduit

arteries such as the middle cerebral artery are subject to neurogenic regulation by extrinsic perivascular nerves. Three broad classes of nerve fibers innervate cerebral surface arteries: parasympathetic nitrergic vasodilator fibers, sympathetic adrenergic vasoconstrictor nerves, and trigeminal sensory vasodilator fibers [11]. These extrinsic perivascular nerves are believed to safeguard the brain against extreme fluctuations in cerebral blood flow, such as occur during transient hypoperfusion or acute hypertension, and impaired neurogenic control may contribute to the pathogenesis of neurovascular disorders such as vasospasm or cerebral ischemia.

EETs are potent vasodilators in the brain [97,100]. EETs produced in the cerebrovascular endothelium mediate vasomotor responses to changes in endothelial shear stress, while astrocyte-derived EETs have been identified as key mediators of neurovascular coupling. Though principally known for these vasodilator actions, EETs also exert anti-inflammatory, anti-thrombotic and pro-angiogenic effects [3], in addition to conferring protection against ischemic injury [119,120]. These varied protective properties have led to the targeting of EETs and their metabolic pathways as potential neuroprotective approaches against ischemic injury in the brain [120,153,154,212]. The biological effects of EETs are terminated through multiple pathways, including hydration to DHETs by sEH [132,150]. The inhibition of EETs hydration by pharmacological blockade or gene deletion of sEH is currently under investigation as a novel means of promoting EETs-mediated neuroprotection. These studies demonstrate that both sEH inhibition and gene deletion are protective against ischemic brain damage [153,154]. In the case of sEH gene deletion, marked preservation of brain blood flow during the ischemic period was observed in sEH

knockout mice compared to wild type controls, an effect that is likely ascribed to an increase in bioavailable EETs and their vasodilator action within the cerebral circulation.

The role of EETs in the regulation of cerebral blood flow both at the level of the vascular endothelium as well as their role as astrocyte-derived mediators of neurovascular coupling is well established. However, based upon the preservation of intra-ischemic cortical blood flow observed in sEH knockout mice compared to wild type controls [154], I have proposed that epoxyeicosanoid signaling similarly contributes to the regulation of the cerebral vasculature by extrinsic perivascular vasodilator nerves. To begin to test this hypothesis, I utilized Western blot and immunofluorescence double-labeling to detect and characterize the cell type-specific expression of sEH in the rat cerebral vasculature.

Preliminary findings from these studies detected prominent sEH-immunoreactivity in perivascular nerve fibers surrounding the middle cerebral and basilar arteries. As detailed above, three populations of extrinsic perivascular nerve fibers innervate the cerebral surface vasculature: parasympathetic vasodilator nerves originating in the sphenopalatine and otic ganglia, sympathetic vasoconstrictor nerves originating in the superior cervical ganglia, and sensory afferents that project to the trigeminal ganglia [11]. Based upon the expression of the EETs-regulating enzyme sEH in these perivascular nerve fibers, I further hypothesized that these neurons express one or more CYP epoxygenase isozymes. Utilizing RT-PCR, Western blot, and immunofluorescence double-labeling, I characterized sEH and CYP epoxygenase expression both in perivascular nerve fibers and in their associated ganglia.

Methods

All experiments were conducted in accordance with the National Institutes of Health guidelines for the care and use of animals in research under protocols approved by the Institutional Animal Care and Use Committee of Oregon Health and Science University.

Tissue Isolation

Cerebral Surface Vasculature

Cerebral surface vasculature was initially isolated for the quantification of sEH expression by Western blot. Adult (200-250g) male and female Wistar rats were anesthetized with isofluorane and trans-cardially perfused with ice-cold heparinzed (1 U/ml) saline. The animals were decapitated, the brain carefully removed and placed into ice-cold phosphate buffered saline. Under a dissecting microscope, the cerebral surface vasculature was dissected free from the underlying cortex. This included the basilar artery, circle of Willis, posterior, middle and anterior cerebral arteries. Isolated vessels were immediately frozen at -80°C for later fractionation.

For whole-mount cerebral artery immunofluorescence, adult male Wistar rats were anesthetized with isofluorane and trans-cardially perfused first with ice-cold heparinized (1 U/ml) saline (5 min) followed by 4% paraformaldehyde in phosphate buffered saline (5 min). Animals were decapitated, the brain carefully removed and placed in 4% paraformaldehyde for post-fixation (2 hr). Surface arteries (including

both the middle cerebral and basilar arteries) were cut proximally and distally, then peeled from the brain surface and placed in cold phosphate buffered saline for immunofluorescent analysis

Cerebral Cortex

Cerebral cortex was isolated for the quantification of sEH expression by Western blot. Adult male and female Wistar rats were anesthetized and trans-cardially perfused with ice-cold heparinized saline (1 U/ml). The brain was carefully removed and the cerebral cortex isolated and frozen at -80°C for later fractionation.

For immunofluorescent analysis of cell type-specific cortical sEH expression, paraffin-embedded 6 μm brain slices were isolated from adult male Wistar rats. Animals were anesthetized with isofluorane and trans-cardially perfused first with ice-cold heparinized (1 U/ml) saline (5 min) followed by 4% paraformaldehyde in phosphate-buffered saline (5 min). Animals were decapitated, the brain carefully removed and placed in 4% paraformaldehyde for post-fixation (2 hrs). Brains were embedded in paraffin and slices were cut on a microtome and mounted on slides for immunofluorescent analysis.

Liver

Liver samples were utilized as positive control tissues for the Western blot and RT-PCR characterization of CYP epoxygenase and sEH expression in the sphenopalatine ganglion and trigeminal ganglion. For both Western blot and RT-PCR analysis, adult male Wistar rats were anesthetized and perfused as above with ice-cold heparinized saline. Two ~5 g pieces of liver were dissected and frozen at -80°C for protein

fractionation and RNA isolation.

Sphenopalatine, Trigeminal and Superior Cervical Ganglia

Sphenopalatine and trigeminal ganglion tissue was isolated first for Western blot and RT-PCR analysis of CYP epoxygenase and sEH expression. Adult male Wistar rats were anesthetized and perfused with ice-cold heparinized saline as above. The sphenopalatine ganglion was identified as described by Suzuki et al. [60]. Briefly, a 2 cm incision was made superior to the orbit. The globe, lacrimal gland and temporalis muscle were retracted laterally. The sphenopalatine ganglion is located inferior and medial to the maxillary nerve, along the orbital wall. Once identified, the sphenopalatine ganglion was dissected clear of surrounding connective tissue with fine forceps and spring scissors, then frozen at -80°C for protein fractionation and RNA isolation. In order to isolate the trigeminal ganglion, the skull of the rat was opened and the brain was removed. The trigeminal ganglion was identified in its position within the inferior floor of the skull at the point where the trigeminal nerve divides into the V_1, V_2 and V_3 branches. The proximal trigeminal nerve and the V_{1-3} branches were cut with fine spring scissors and the trigeminal ganglion was dissected free from surrounding connective tissue, then frozen at -80°C for protein fractionation and RNA isolation.

In order to define the cell type-specific localization of CYP epoxygenases and sEH in the sphenopalatine ganglion, trigeminal ganglion and superior cervical ganglion, adult male Wistar rats were anesthetized and perfusion-fixed with 4% paraformaldehyde as described previously. The sphenopalatine ganglion and trigeminal ganglion were identified and isolated as above, then placed in 4%

paraformaldehyde for 2 hrs post-fixation. To isolate the superior cervical ganglion, a longitudinal incision was made ventrally along the trachea. The sternohyoid muscle was retracted laterally to reveal the common carotid artery and its bifurcation into the internal and external carotid arteries. The caudal portion of the artery was severed and lifted to reveal the superior cervical ganglion which was dissected free and placed in 4% paraformaldehyde for 2 hours post-fixation. All ganglia were then paraffin embedded, sliced at 6 μm thickness on a microtome and mounted on glass slides for immunofluorescent labeling.

Western Blot

The expression of CYP-2J and sEH proteins in the cerebral surface vasculature, the cortex, sphenopalatine ganglion, trigeminal ganglion and liver were interrogated by Western blot. For vascular and cortical samples, cytosolic cellular fractions were first prepared from mechanically-dissociated tissue homogenate. Tissue was homogenized in solution A (sucrose 250 mmol/L, KCl 60 mmol/L, Tris-HCl 15 mmol/L, NaCl 15 mmol/L, EDTA 5 mmol/L, EGTA 1 mmol/L, phenylmethanesulfonyl fluoride 0.5 mmol/L, and dithiothreitol 10 mmol/L) then centrifuged for 10 min at 2000 g to derive the cytoplasmic protein fraction. For sphenopalatine ganglion, trigeminal ganglion and liver samples, crude cellular extracts in solution A were utilized for Western blot analysis. Cytosolic fractions or crude cellular extracts were electrophoresed at 200 V for 105 min on SDS-10% polyacrylamide gels, then transferred to PVDF membranes for 120 min at 40 V. Membranes were washed in 0.1% Tween-20 in phosphate-

buffered saline, then blocked with 5% bovine serum albumin for 1 hr at room temperature. Following blocking, membranes were immunoblotted overnight at 4°Cwith antibodies dissolved in phosphate-buffered saline. These included a rabbit polyclonal antibody raised against the peptide sequence FNPDHFLENGQFKKRE from human CYP-2J2 (anti-CYP-2J2pep4, 1:1000; a gift from Dr. Darryl Zeldin, NIEHS), which cross-reacts with both rat CYP-2J isoforms [210], CYP-2J3 and CYP-2J4, a rabbit anti-sEH (Santa Cruz, 1:500) polyclonal antibody, a second rabbit anti-sEH antibody (1:5000; a gift from Dr. Bruce Hammock, UC Davis) and a monoclonal mouse anti-β-actin antibody (Sigma, 1:5000) that was used as a loading control for vascular and cortical blots. A general description of primary antibodies used in all studies, their characteristics and sources is given in Table 3. Secondary detection was conducted with Cy5-conjugated goat anti-rabbit and Cy3-conjugated goat anti-mouse secondary antibodies (Amersham, 1:1500) for 1 hr at room temperature. Membranes were imaged with a Typhoon® TRIO polymodal scanner (Amersham). For vascular and cortical sEH expression, replicate blots (n=3) were conducted on tissue samples from four male and four female animals. For sphenopalatine ganglion, trigeminal ganglion and liver CYP-2J and sEH expression, replicate blots (n=3) from two male animals were conducted. To ensure the specific identification of the band corresponding to sEH in cerebral cortex and cerebral surface vasculature blots, 2 ng recombinant mouse sEH was run in a neighboring well. Similarly, positive controls for CYP-2J and sEH expression included rat liver tissue that was run on sphenopalatine ganglion and trigeminal ganglion blots.

For vascular and cortical tissue samples, semi-quantitative analysis of protein

expression was conducted and expression was compared between males and females. Blots were imaged on a Typhoon® TRIO polymodal scanner (Amersham) and analyzed using ImageQuant® software (Amersham). Band intensities were measured for sEH and β-actin for each lane and sEH expression was normalized by determining the sEH:β-actin ratio. The mean and standard error of the mean (SEM) were calculated for male and female groups from each blot. Statistical analysis consisted of an unpaired Student's *t*-test with a P value < 0.05 indicating statistical significance.

Immunofluorescence

Slide-Mounted Thin Slice Immunofluorescence

In order to characterize the cell type-specific localization of CYP-2J and sEH protein in the brain, sphenopalatine ganglion, trigeminal ganglion and superior cervical ganglion, immunofluorescence labeling was conducted on slide-mounted 6 μm paraffin-embedded tissue slices. Slices were de-paraffinized, heated in 0.5 mmol/L sodium citrate buffer (pH=6.0) for antigen retrieval then blocked with 3% normal donkey serum, 0.1% Triton X-100, and 1% bovine serum albumin in phosphate-buffered saline for 30 min at room temperature. Sections were incubated at 4°C overnight with one or more primary antibodies. All primary antibodies used in these studies are listed on Table 3. After washing with phosphate-buffered saline, secondary detection was conducted with donkey anti-rabbit Alexa Fluor-488, donkey anti-mouse Alexa Fluor-594, donkey anti-sheep Alexa Fluor-594, goat anti-guinea pig Alexa Fluor-594, and donkey anti-goat Alexa Fluor-594 (1:800, Invitrogen) incubated at

room temperature for 1 hr. Sections were washed with phosphate-buffered saline,

Table 3. Primary Antibodies

Antibody	Host	Antigen	Marker For	Dilut	Source
CYP-2J Antibodies					
CYP-2J2pep4	Rabbit (P)	Human CYP-2J2 peptide (FNPDHFLENGQFKKRE)		1:1000	Dr. Darryl Zeldin, NIEHS
CYP2J2rec	Rabbit (P)	Human CYP-2J2 (recombinant)		1:100	Dr. Darryl Zeldin, NIEHS
CYP-2J6pep1	Rabbit (P)	Mouse CYP-2J6 peptide (QMEQNIMNRPLSVMQ)		1:500	Dr. Darryl Zeldin, NIEHS
CYP-2J9pep2	Rabbit (P)	Mouse CYP-2J9 peptide (GQARQPNLADRD)		1:500	Dr. Darryl Zeldin, NIEHS
sEH Antibodies					
sEH	Rabbit (P)	Human sEH (residues 340-554)		1:500	Santa Cruz
sEH	Rabbit (P)	Human sEH (recombinant)		1:5000	Dr. Bruce Hammock, UC Davis
sEH	Rabbit (P)	Human sEH peptide (DMKGYGESSAPPEIE)		1:500	Cayman Chemical
Cell Type Markers					
Substance P	Guinea Pig (P)	Substance P	Trigeminal neurons	1:500	Millipore
VIP	Sheep (P)	Synthetic peptide (1-28)	Parasympathetic neurons	1:1000	Millipore
β-actin	Mouse (M)	N-terminal peptide		1:5000	Sigma
CGRP	Goat (P)	Rat CGRP (23-37)	Trigeminal neurons	1:1000	Serotec
Choline acetyl-transferase	Sheep (P)	Porcine peptide (GLFSSYRLPGHTQDTLVAQKSS)	Parasympathetic neurons	1:1000	Millipore
Dopamine β-hydroxylase	Mouse (M)	Bovine recombinant protein	Sympathetic neurons	1:1000	Millipore
Glial fibrillary acidic protein	Mouse (M)	Porcine recombinant protein	Astrocytes	1:1000	Millipore
Myosin heavy chain I	Mouse (M)	Human peptide (DADFNGTKASE)	Vascular smooth muscle	1:1000	Abcam
NeuN	Mouse (M)	Mouse cell nuclei	All neurons	1:1000	Millipore
nNOS	Sheep (P)	Rat peptide (RSESIAFIEESKKDADEVFSS)	Parasympathetic neurons	1:1000	Millipore
Neuropeptide Y	Guinea Pig (P)	Rat recombinant preproneuropeptide Y	Sympathetic neurons	1:400	Millipore

CYP: cytochrome P450 ; sEH: soluble epoxide hydrolase; VIP: vasoactive intestinal peptide; NeuN: neuronal nuclear protein; nNOS: neuronal nitric oxide synthase; (P): polyclonal antibody; (M): monoclonal antibody.

mounted with ProLong Antifade Gold with DAPI (Invitrogen) and coverslipped. All labeling studies were conducted in at least 3 biological replicates.

In cortical slices, sEH expression was detected with a rabbit polyclonal antibody raised against recombinant human sEH (1:5000). Cell type-specific cortical sEH expression was defined using distinct markers, including mouse anti-NeuN (a neuronal marker, 1:1000; Millipore), mouse anti-glial fibrillary acidic protein (an astrocyte marker, 1:1000; Millipore) and myosin heavy chain I (a vascular smooth muscle marker, 1:1000; Abcam).

In sphenopalatine ganglion and trigeminal ganglion slices, CYP-2J expression was detected initially with a rabbit polyclonal antibody raised against recombinant human CYP-2J2 protein (CYP-2J2$_{rec}$, 1:100; a gift from Dr. Darryl Zeldin, NIEHS). The cell type-specific expression of CYP-2J and sEH proteins was determined by immunofluorescence double-labeling of trigeminal ganglion and sphenopalatine ganglion tissue. Sections were labeled as above with one or two of the following primary antibodies: rabbit anti CYP-2J2$_{rec}$ (1:100), rabbit anti-sEH (1:500, Santa Cruz), mouse anti-NeuN (1:1000, Millipore), sheep anti-neuronal nitric oxide synthase (nNOS, 1:1000, Millipore), sheep anti-vasoactive intestinal peptide (VIP, 1:1000, Millipore), guinea pig anti-substance P (1:000; Millipore); goat anti-calcitonin gene-related peptide (CGRP, 1:1000; Serotec).

In cases where co-labeling was employed between two primary antibodies from rabbit hosts, labeling was conducted sequentially: the first primary antibody was incubated as above overnight at 4°C, this primary incubated with an excess of

monovalent goat anti-rabbit Fab fragments (1:10, Jackson Immunoresearch) for 1 hr at room temperature, secondary detection of the Fab fragment conducted with donkey anti-goat Alexa Fluor-594 secondary (1:800, Invitrogen) for 1 hr at room temperature. The second primary antibody was then incubated for 1 hr at room temperature, followed by secondary detection with donkey anti-rabbit Alexa Fluor-488 antibody (1:800, Invitrogen).

Negative controls included both the omission of primary antibodies (n=1), and the pre-absorption of the rabbit anti-CYP-2J2$_{rec}$ and rabbit anti-sEH antibodies with a molar excess of recombinant human CYP-2J2 and recombinant human sEH protein, respectively (n=1). In addition, to confirm the specificity of the observed labeling, slices were incubated with separate anti-CYP-2J and anti-sEH antibodies raised against distinct antigens. These included two (both gifts from Dr. Darryl Zeldin, NIEHS) raised against synthetic peptides from the mouse CYP-2J6 (QMEQNIMNRPLSVMQ, anti-CYP-2J6pep1, n=1) and CYP-2J9 (GQARQPNLADRD, anti-CYP-2J9pep2, n=1) isoforms that cross-react with rat CYP-2J4 and CYP-2J3 isoforms, respectively. Further, an anti-sEH antibody raised against recombinant human sEH (n=1) and another raised against a distinct peptide sequence of human sEH (DMKGYGESSAPPEIE, Cayman, n=1) were employed.

In order to define sEH expression in the superior cervical ganglion, superior cervical ganglion slices were double-labeled as above with primary antibodies raised against sEH (1:5000) and dopamine β-hydroxylase (1:1000, Millipore).

Floating Whole Mount Immunofluorescence

The expression of sEH and CYP-2J protein in peripheral processes of

parasympathetic, sympathetic and sensory fibers innervating the cerebral surface vasculature was investigated through immunofluorescent double labeling of whole mount middle cerebral and basilar arteries. Paraformaldehyde-fixed arteries were prepared as detailed above. Immunofluorescence was carried out in mesh-bottom crucibles within 24-well cell culture plates. Arteries were washed three times with phosphate-buffered saline, then blocked for 1 hr at room temperature with 3% normal donkey serum, 0.1% Triton X-100, and 1% bovine serum albumin in phosphate-buffered saline. Vessels were then incubated at 4°C overnight with one or two primary antibodies. Vessels were next washed four times with phosphate-buffered saline, after which secondary detection was conducted for 1 hr at room temperature with donkey anti-rabbit Alexa Fluor-488, donkey anti-mouse Alexa Fluor-594, donkey anti-sheep Alexa Fluor-594, goat anti-guinea pig Alexa Fluor-594, and donkey anti-goat Alexa Fluor-594 (1:800, Invitrogen). Vessels were washed four times with phosphate-buffered saline, mounted on glass microscopy slides with ProLong Antifade Gold (Invitrogen) and coverslipped. All labeling studies were conducted in at least 3 biological replicates.

The expression of sEH and CYP-2J in middle cerebral artery and basilar arteries was investigated first. Vessels were probed individually with primary rabbit polyclonal antibodies raised against recombinant human sEH (1:5000) and recombinant human CYP-2J2 ($CYP\text{-}2J2_{rec}$, 1:100). In order to investigate the cerebral perivascular nerve population expressing sEH, vessels were double labeled with the antibody against recombinant human sEH (1:5000) and markers for the three specific perivascular nerve populations. To identify nitrergic parasympathetic fibers, a sheep

polyclonal antibody raised against nNOS (1:1000) was utilized. Two additional markers for parasympathetic nerve fibers were employed, including a sheep anti-VIP (1:1000) and sheep anti-choline acetyltransferase (1:1000, Millipore). Trigeminal afferents were identified by positive labeling with a goat antibody raised against CGRP (1:1000) and a guinea pig anti-substance P (1:500) antibody. Sympathetic fibers were identified by positive labeling with a mouse monoclonal antibody raised against the adrenergic marker dopamine β-hydroxylase (1:1000) as well as a guinea pig antibody directed against rat prepro-neuropeptide Y (1:400, Millipore).

Imaging

Both conventional (Leica) and laser scanning confocal (Olympus) fluorescence microscopy were utilized to observe CYP-2J and sEH localization and co-localization in cortical, sphenopalatine ganglion, trigeminal ganglion and superior cervical ganglion tissue slices, in addition whole mount cerebral arteries. In general, secondary detection of CYP-2J- and sEH-immunoreactivity utilized an ALEXA Fluor-488-conjugated antibody and was imaged using a Cy2 fluorescence filter. Secondary detection of cell type-specific counter-labels utilized an ALEXA Fluor-594-conjugated antibody and was imaged using a Texas Red fluorescence filter. Detection of nuclear staining with DAPI was accomplished with a UV emission filter. Images were acquired via a monochrome camera, then overlaid, colorized and analyzed for expression and/or co-localization using ImageJ software.

Cortical sEH expression was first imaged using single-channel conventional fluorescence microscopy at 200X and 400X magnification (10X eyepiece, 20X and 40X objective). Double labeling with cell type-specific markers was imaged using

two-channel conventional fluorescence microscopy at 200X and 400X magnification. Using the ImageJ software, red and green channels were overlaid and co-localization was assessed. For high resolution analysis of co-localization, laser scanning confocal fluorescence microscopy was utilized at 600X and 3000X (10X eyepiece, 60X objective; 5X optical zoom). Image stacks were acquired then analyzed using the Fluoview Confocal Imaging ImageJ tool (UCSD plugin set).

Expression of CYP-2J, sEH and their co-localization with cell type-specific markers in sphenopalatine ganglion and trigeminal ganglion slices was imaged using single- or multi-channel conventional fluorescence microscopy at 200X and 400X magnification. Blue, red and/or green channels were overlaid and co-localization was assessed using ImageJ software. Expression of sEH in the superior cervical ganglion was assessed using two-channel laser scanning confocal microscopy at 600X and 3000X magnification as detailed above.

Expression of sEH and CYP-2J in whole mount cerebral arteries was initially analyzed using single-channel conventional fluorescence microscopy under 200X and 400X magnification. Laser scanning confocal microscopy was then utilized to assess co-localization with markers for the three distinct perivascular nerve populations within individual fibers at high (600X and 3000X) magnification.

Quantification of Co-Localization

In order to define the cellular phenotype of CYP-2J- and sEH-expressing cells in the sphenopalatine ganglion and trigeminal ganglion, immunofluorescent double labeling and imaging of tissue sections was carried out as detailed above. In fluorescent micrographs from the sphenopalatine ganglion, immunoreactive cells labeled in the

green channel (corresponding to CYP-2J- and sEH-immunoreactivity) were counted with the ImageJ Cell Counter tool. Cells labeled in the red channel (corresponding to NeuN-, nNOS-, or VIP-immunoreactivity) were then counted, as were all cells that were labeled by both markers. Co-localization was then calculated as the percentage of green-labeled cells that were also red-labeled, and in the case of NeuN, the inverse was calculated as well. Counts were made in one randomly selected field of view (at 20X objective) from each of six bilateral ganglia slices from two separate animals. In the trigeminal ganglion, co-localization of green-labeled (corresponding to CYP-2J- and sEH-immunoreactivity) and red-labeled (corresponding to NeuN-, CGRP- and substance P-immunoreactivity) cells was calculated in the same manner from each of six bilateral ganglia slices from two separate animals. Values in Table 6 are expressed as the mean ± SEM of the percentages pooled from the six bilateral ganglia, averaged between the two biological replicates.

In whole mount middle cerebral arteries, the perivascular nerve population expressing sEH-immunoreactivity was identified through co-localization with markers for parasympathetic, sympathetic and sensory perivascular fibers. In confocal fluorescent micrographs from double-labeled middle cerebral arteries, immunoreactive fibers labeled in the green channel (corresponding to sEH-immunoreactivity) were counted as were fibers labeled in the red channel (corresponding to nNOS-, VIP-, choline acetyltransferrase-, dopamine β-hydroxylase-, neuropeptide Y-, CGRP- and substance P-immunoreactivity). Co-localization was calculated as the percentage of sEH-immunoreactive fibers that were also labeled by the population-specific marker. Counts were made from 2-5 sEH-immunoreactive fibers in one field of view (at 60X

objective, 5X optical zoom) from bilateral middle cerebral arteries isolated from three animals. Values in Table 5 are derived from the percentages pooled for the two vessels, averaged between the three biological replicates.

Table 4. PCR Primers Utilized for Detection of CYP Epoxygenase and sEH

Accession		Sequence	Pos.	Product Size (bp)
XM_001081879	→	ACTGTGACCAACCAGCTAAAGTCC	47	244
	←	GTCATGCAGCACTGATGAGAGTGA	291	
NM_017158	→	TCATTGGTGCAGGGACAGAGACAA	903	582
	←	ATGAAGCAGAGCTGGTAAGTGGGT	1485	
U33173	→	TAGCAGTGGGATGCAATGGAAGGA	362	603
	←	TTTCAGCAGCAGCAGGAGTCCATA	965	
NM_031572	→	TAGGATGTGCTCCCTGCAATGTCA	509	536
	←	TTGTGTAGGGCATGTGGATCCTGT	1045	
NM_138514	→	AAGTGCAAGAGGAAGCAAAGTGGC	442	532
	←	AGCTGTGACGTGTGGGTACTTCAT	974	
NM_031839	→	TGAACCTCAAGGACATCCCTGCAT	170	830
	←	TGGCTTGCACCTCTGGATACTTCA	1000	
NM_175766	→	ACGAGGTGCAGAGAATAGGCAACA	1109	515
	←	TCATTGCACACACTCCCTCAGTCA	1624	
NM_023025	→	TGAGGTTGCTGGATGAGGTCATGT	681	468
	←	ACCTCATGGATGACGGCATTGGTA	1149	
NM_022936	→	TCATGGGTTTCCTGAGAGCTGGTT	827	868
	←	AGGTCACCGATGGGTTCTGGATTT	1695	

Primer sequences utilized for each transcript including NCBI Accession Numbers, forward (→) and reverse (←) primer sequences, primer positions, and the predicted PCR product size (bp).

Reverse Transcriptase Polymerase Chain Reaction (RT-PCR)

To determine the specific CYP epoxygenase isoforms expressed in the trigeminal ganglion and sphenopalatine ganglion, an RT-PCR screen was conducted against 8

known rat epoxygenase isoforms from the CYP-2C and CYP-2J families, in addition to sEH, using whole tissue isolated from the trigeminal ganglion and sphenopalatine ganglion as detailed previously. Following tissue dissection, total tissue RNA was extracted per manufacturer's guidelines using an RNAqueous®-4PCR kit (Ambion). Whole tissue Poly-A RNA was reverse transcribed according to manufacturer's protocol with a RETROscript® reverse transcription kit (Ambion) using Oligo(dT) primers. PCR (30 cycles with 59°C annealing temperature) was conducted using a GeneAmp® PCR System 9700 (Applied Biosystems) with primers designed using online primer design software (Integrated DNA Technologies, Table 4), the specificity of the sequences being confirmed by BLAST search. PCR products were run on a 2% agarose gel and visualized with 0.5 μg/ml ethidium bromide read on a Typhoon® Trio multi-modal scanner (Amersham). For each transcript, replicate PCR reactions were conducted from two separate animals (n=2 biological replicates). Negative controls included the omission of PCR template material and whole cell (no reverse transcriptase) RNA in the place of cDNA. Positive controls included PCR upon liver cDNA, in which epoxygenase isoforms and sEH are abundantly expressed.

Results

Expression of Soluble Epoxide Hydrolase Protein in Rat Cerebral Vasculature

Soluble epoxide hydrolase is the enzyme chiefly responsible for EETs metabolism. [132,149]. Based upon findings from peripheral tissues [213,214], I initially hypothesized that sEH is expressed in the cerebral vasculature. In order to investigate

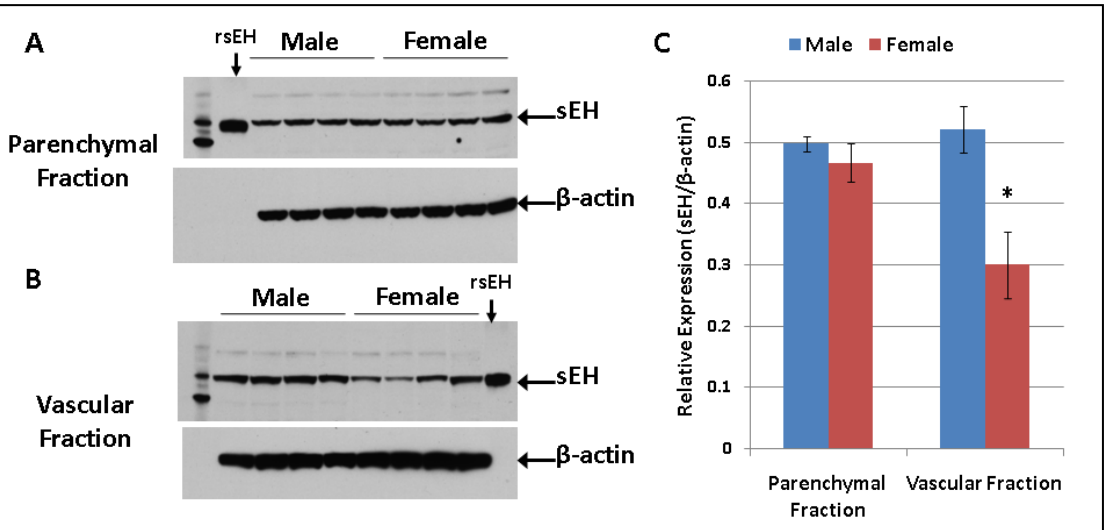

Figure 3. Western blot analysis of sEH expression in rat cerebral cortex and vasculature. Rat cerebral cortex was separated into parenchymal and vascular fractions by manual dissection. (A) Representative blot of sEH expression and β-actin loading control in parenchymal fractions. No difference in expression was observed between male and female rats. rsEH: recombinant mouse sEH. (B) Representative blot of sEH expression and β-actin loading control in vascular fractions. Male vessels exhibited greater sEH expression than did female samples. (C) Quantification of relative sEH expression in male vs. female parenchymal and vascular fraction. All values expressed as mean ± SEM. *$p < 0.01$ male vs. female (t-test).

this, I first used manual dissection to produce an enriched vascular fraction in addition to a parenchymal fraction from both male and female rats. sEH expression was then analyzed by Western blot. The cytosolic cellular fractions from the surface vasculature and the corresponding cortical parenchyma were extracted by centrifugation and analyzed by Western blot utilizing a primary polyclonal rabbit antibody raised against human sEH. Within the parenchymal and vascular fractions, a single ~60 kD band was detected that matched the positive control recombinant mouse sEH run concomitantly on the gel (Figure 3). Figure 3A and B are representative blots carried out on tissue from four age-matched male and female rats. Replicate blots (n=3) were conducted upon tissue from four male and four female animals. sEH was abundantly expressed in

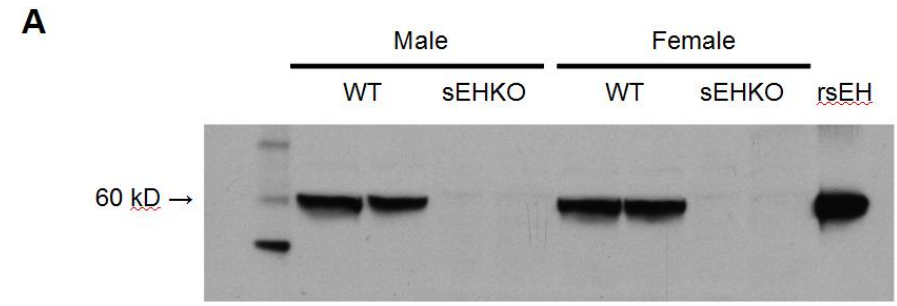

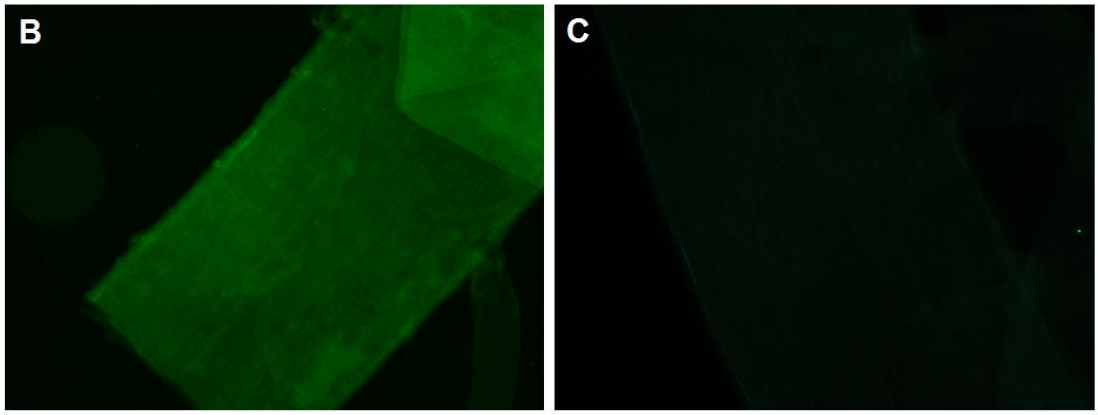

Figure 4. Evaluation of the specificity of soluble epoxide hydrolase antibody. (A) Western blot of mouse cerebral cortex from wild type (WT) and sEH knockout (sEHKO) mice probed with an antibody raised against human sEH. Robust expression of sEH is observed in WT mouse cortex, whereas sEHKO tissue is devoid of immunoreactivity. Recombinant mouse sEH (rsEH) was utilized as a positive control. (B) Whole mount rat middle cerebral artery in which primary sEH antibody is omitted from labeling protocol in depicted in Figure 6. No specific immunoreactivity is observed in perivascular nerve structures. (C) Whole mount sEHKO mouse middle cerebral artery probed with primary antibody raised against human sEH. Immunofluorescence labeling reveals no immunoreactivity in perivascular nerve structures surrounding the middle cerebral artery.

rat cortex, with no apparent gender difference when normalized to β-actin loading control (Figure 3A,C). In the cerebral surface vasculature, sEH was likewise abundantly expressed. In contrast to the parenchymal fraction, sEH expression in male animals was significantly ($P < 0.01$ Student's *t*-test, male vs. female vascular fraction) higher than that observed in females when normalized to β-actin loading control (Figure 3B,C). The specificity of this anti-sEH antibody was confirmed in blots

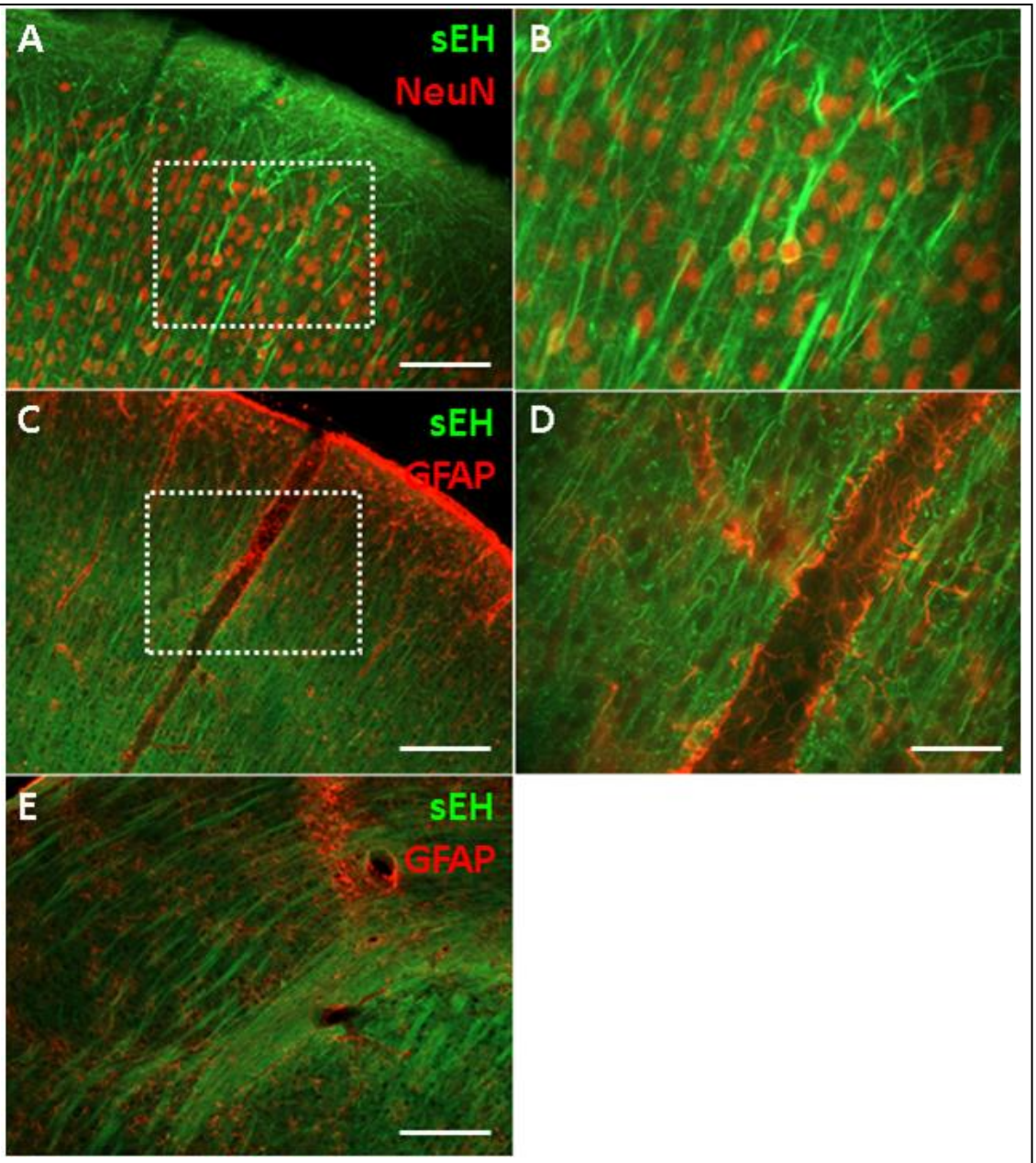

Figure 5. Expression of sEH in the rat brain. (A) sEH immunoreactivity (green) is present throughout the cortex and co-localizes with the neuronal marker NeuN. (B) Inset of A. (C) sEH-immunoreactivity does not co-localize with the astrocyte marker glial fibrillary acidic protein (red). (D) Inset of C. (E) sEH is expressed throughout the striatum, including white matter tracks.

carried out on whole brain extract from male wild type and sEH knockout mice. In these experiments, the ~60 kD band corresponding to sEH was observed in the wild type animals but was absent in sEHKO animals (Figure 4A). These findings thus

identify both the abundant expression of sEH in the rat cerebral vasculature, in addition to detecting an apparent sex difference in vascular sEH expression levels.

Having identified the expression of sEH in the cerebral surface vasculature, I next sought to define the cell type-specific localization of sEH in cortical vessels by immunofluorescent double labeling. Paraffin embedded adult male rat brain slices (6 μm) were probed with anti-sEH antibody and the cell type-specific antibodies NeuN (neuronal marker, Figure 5A,B), glial fibrillary acid protein (astrocyte marker, Figure 5C-E) and myosin heavy chain I (vascular smooth muscle marker, Figure 5A,B). Laser scanning confocal microscopy revealed that in addition to dominant neuronal expression of sEH within the rat cortex (Figure 5A,B), sEH-immunoreactivity was evident in intraparenchymal arterioles and co-localized with the vascular smooth muscle marker myosin heavy chain I (Figure 5A,B). Single-labeling studies carried out on fresh whole mount pial surface arterioles revealed that sEH-immunoreactivity in these vessels assumed a circumferential banding pattern that is characteristic of vascular smooth muscle (as opposed to longitudinal endothelial) staining (Figure 6C). Images in Figure 5 and Figure 6 are representative images of immunolabeling carried out in at least three biological replicates.

To investigate the expression of sEH in large cerebral surface conduit arteries, fresh whole mount adult male rat middle cerebral and basilar arteries were probed with anti-sEH antibody and imaged with conventional and laser scanning confocal fluorescence microscopy. Intriguingly, dominant sEH labeling was observed in perivascular nerve bundles and fibers surrounding these arteries (Figure 6D-F).

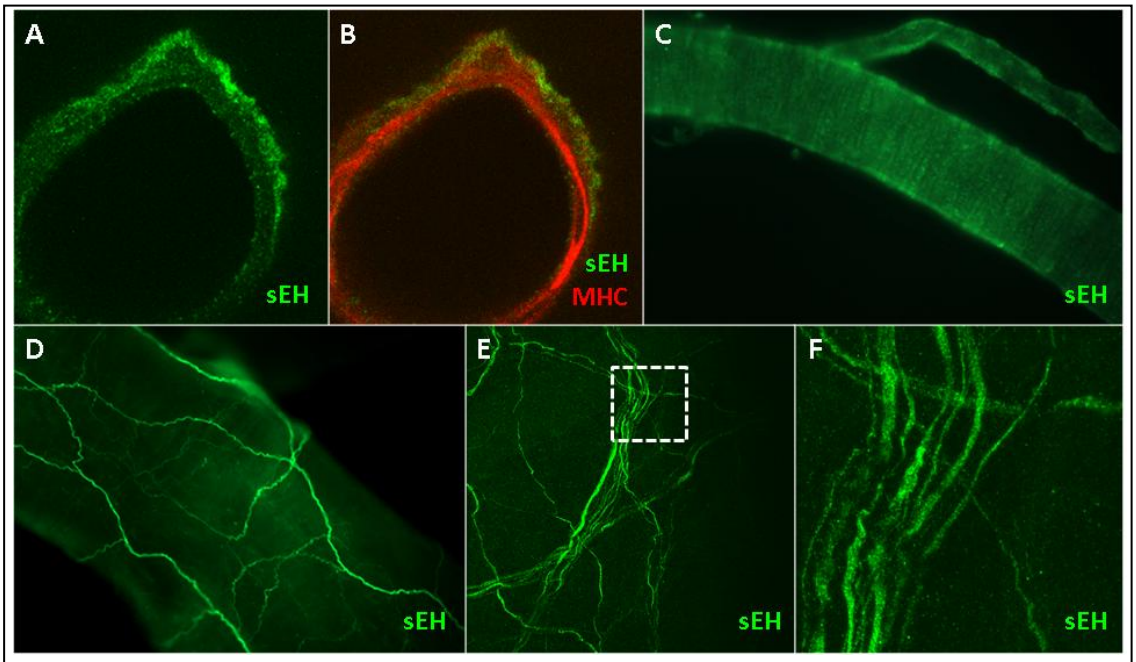

Figure 6. Immunofluorescent determination of sEH expression in cerebral vasculature. (A-B) Confocal micrographs (3000X) of intracortical arterioles in rat brain slices demonstrating sEH-immunoreactivity (green) co-localizing with the vascular smooth muscle marker myosin heavy chain I (red). (C) Fluorescence micrograph (630X) of whole-mount pial arteriole depicts sEH-immunoreactivity (green) in a circumferential banding pattern indicative of vascular smooth muscle labeling. (D) Whole-mount (200X) middle cerebral artery expresses sEH-immunoreactivity (green) dominantly in extrinsic perivascular nerve fibers. (E) High-resolution (600X) confocal micrograph of whole-mount middle cerebral artery demonstrating perivascular nerve expression of sEH, inset in (F) (3000X).

Innervation of the middle cerebral artery by sEH-positive fibers extended along the trunks of the conduit arteries and their most proximal branches, but terminated prior to distal surface branches and penetrating arterioles. This pattern of innervation matches that described for the 'extrinsic' perivascular nerve supply to the cerebral surface vasculature [11].

To ensure the specificity of the anti-sEH antibody, a number of negative controls were carried out. When anti-sEH antibody was omitted from the labeling protocol, no immunoreactivity was observed (Figure 4B, n=1). Similarly, when labeling studies were conducted on whole mount middle cerebral arteries from sEH

knockout mice, no immunoreactivity was evident in perivascular nerve structures (Figure 4C, n=2). These negative control findings argue that the perivascular immunoreactivity observed in rats was specific to the sEH protein.

Table 5. Co-localization of sEH-immunoreactivity with perivascular nerve population markers

	Parasympathetic			Sensory		Sympathetic	
	Choline Actetyltransferase	VIP	nNOS	CGRP	Substance P	Dopamine β-Hydroxylase	Neuro-peptide Y
sEH	+	+	++++	+++	+	-	-

sEH: soluble epoxide hydrolase; VIP: vasoactive intestinal peptide; nNOS: neuronal nitric oxide synthase; CGRP: calcitonin gene-related peptide. Co-localization: - : no co-localization; + : <25%; ++ : 25-50%; +++ : 50-75%; ++++ : >75%.

Characterization of sEH Expression in Perivascular Vasodilator Fibers

Immunofluorescent analysis of sEH expression in the cerebral surface vasculature identified the prominent presence of sEH-immunoreactivity in perivascular nerve bundles. This 'extrinsic' perivascular innervation of the cerebral surface vasculature is comprised of three populations of nerve fibers: parasympathetic vasodilator fibers originating in the sphenopalatine or the otic ganglia, sympathetic vasoconstrictor fibers originating in the superior cervical ganglia, and a population of trigeminal primary afferents [11]. Immunofluorescent double labeling utilizing known markers of cerebrovascular parasympathetic, sympathetic and sensory nerve populations was next undertaken to identify which of these three populations of perivascular nerves expressed sEH. Table 5 summarizes the proportions of sEH-immunoreactive fibers co-

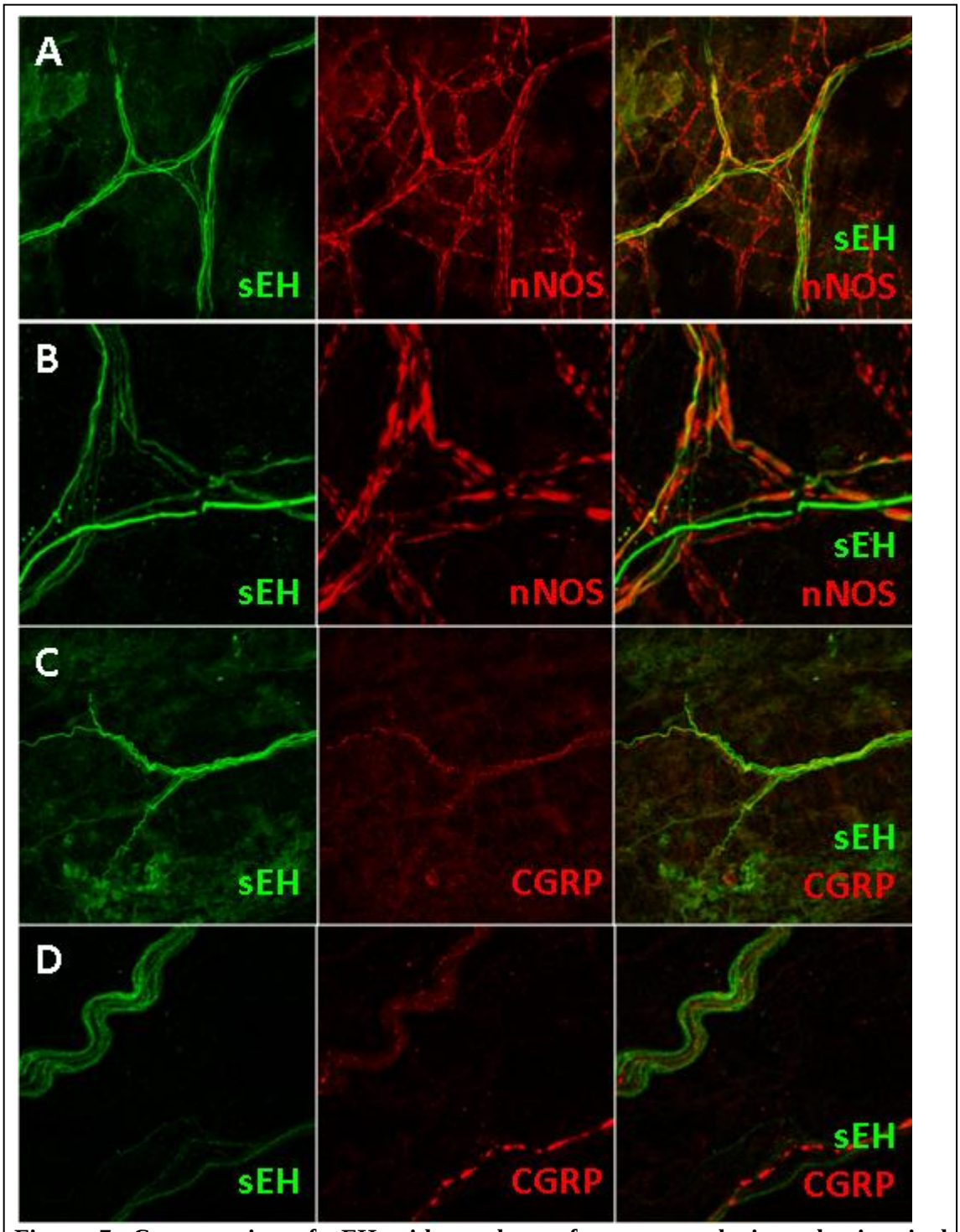

Figure 7. Co-expression of sEH with markers of parasympathetic and trigeminal perivascular vasodilator nerves. Confocal micrographs from whole mount rat middle cerebral arteries. (A) sEH-immunoreactivity (green) is present predominantly in perivascular nerve fibers and bundles, co-localizing with neuronal nitric oxide synthase (nNOS, red). (B) High resolution (3000X) images indicate that sEH-positive fibers are all nNOS-immunoreactive, whereas not all nitrergic fibers express sEH. (C) sEH- immunoreactivity (green) co-localizes with the sensory neuropeptide CGRP (red). (D) High resolution (3000X)

images demonstrate high degree of overlap between sEH- immunoreactive fibers and CGRP-positive fibers.

expressing the different nerve population markers. Co-localization was initially observed at 600X in 5-20 fibers per artery. Specific co-localization within individual fibers was confirmed at higher magnification (3000X) in 2-5 fibers per artery. Figure 7 depicts representative fibers at these magnifications.

In addition to nitric oxide, parasympathetic fibers innervating the cerebral vessels release VIP and acetylcholine [11]. Therefore, the co-localization of sEH-immunoreactivity with these parasympathetic markers was first determined (Table 5). I found that within perivascular fibers innervating the middle cerebral artery, 75% of sEH-positive fibers co-labeled for nNOS (n=6 animals, Figure 7A,B). Fibers expressing VIP or choline acetyltransferase were less numerous than nNOS-positive fibers, and represented a fraction (5-10%, n=3 each) of sEH-expressing fibers.

Perivascular sensory fibers also express nNOS, in addition to such peptidergic vasodilators as CGRP and substance P [11,81]. sEH-immunoreactivity was observed to co-localize with CGRP at a high frequency (50% of fibers; Figure 7C-D; Table 5; n=3 animals). Markedly fewer substance P- than CGRP-positive fibers were observed innervating the middle cerebral artery, and these fibers represented a correspondingly small proportion of sEH-expressing fibers (15%, Table 5, n=2).

Characterization of CYP Epoxygenase and sEH Expression in the Parasympathetic Sphenopalatine and Sensory Trigeminal Ganglia

Immunofluorescent double labeling studies revealed that the EETs-metabolizing

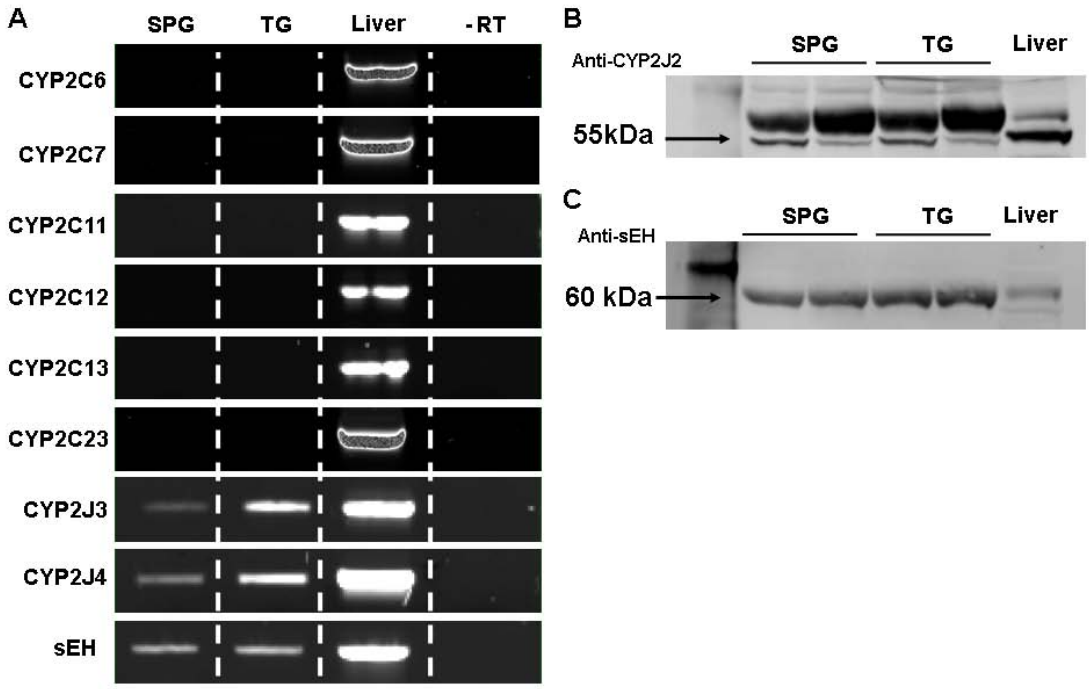

Figure 8. CYP-2J isoforms and sEH are specifically expressed in sphenopalatine and trigeminal ganglia tissue. (A) RT-PCR screen of trigeminal and sphenopalatine ganglia revealed CYP-2J3, CYP-2J4 and sEH mRNA expression. No expression of CYP-2C isoforms was detected. All transcripts were detected in positive control liver tissue while template- and reverse transcriptase (-RT)-negative controls produced no PCR products. (B) Western blot analysis of CYP-2J expression in trigeminal and sphenopalatine ganglia tissue. Immunoblot with an antibody raised against human CYP-2J2 (anti-CYP-2J2pep4) resulted in two 50-60 kDa bands, corresponding to the CYP-2J3 and CYP-2J4 isoforms. (C) Immunoblot with antibody raised against a peptide fragment of human sEH revealed a single 60 kDa band within both the trigeminal and sphenopalatine ganglia.

enzyme sEH co-localized in cerebral perivascular nerve fibers with markers for parasympathetic and sensory vasodilator nerve populations (Table 5). Cerebral parasympathetic extrinsic perivascular fibers originate in the sphenopalatine and otic ganglia, whereas the sensory afferents project to the trigeminal ganglia [11]. In order to evaluate whether neurons from these ganglia possess the biochemical machinery for EETs synthesis and regulation, a detailed characterization of CYP epoxygenase and sEH expression in the sphenopalatine and trigeminal ganglia was undertaken.

In mammalian cells, numerous CYP isoforms possess epoxygenase activity,

although these CYP epoxygenases typically fall within the CYP-2C and CYP-2J enzyme classes [95]. An RT-PCR screen using primers against 8 known rat CYP epoxygenase isoforms in addition to sEH (Table 4) identified that mRNA for 2 CYP-2J isoforms, CYP-2J3 and CYP-2J4, in addition to sEH were detectable in both sphenopalatine and trigeminal ganglia tissue (Figure 8A). Pronounced expression of all CYP epoxygenase transcripts was observed in the liver, the positive control tissue for the PCR reactions [95]. All bands were of the predicted size. No PCR products were detected in either negative control group: the RT-PCR reaction with no RNA template, and the PCR reaction with no reverse transcriptase.

RT-PCR data were confirmed with Western blot of sphenopalatine and trigeminal ganglia tissue. Utilizing a polyclonal antibody raised against a fragment of human CYP-2J2 that reacts with both rat CYP-2J3 and CYP-2J4, two distinct bands were observed in the 50-60 kDa size range in the sphenopalatine, trigeminal ganglia and positive control liver tissue (Figure 8B). These bands likely correspond to the CYP-2J3 (58 kDa) and CYP-2J4 (55 kDa) proteins identified by RT-PCR. Blotting with anti-sEH antibody revealed a single band in the 60 kDa size range in the sphenopalatine, trigeminal ganglia and positive control liver tissue (Figure 8C). Replicate blots (n=3) were conducted on tissue from two male animals. These data corroborate the immunofluorescence findings in the cerebral vasculature (Figure 7) and identify a specific class of CYP epoxygenases (CYP-2Js) expressed within the neuronal tissue of the sphenopalatine and trigeminal ganglia.

RT-PCR and Western blot identified the expression of CYP-2J epoxygenases and sEH in sphenopalatine and trigeminal ganglia tissue. To determine the cell type-

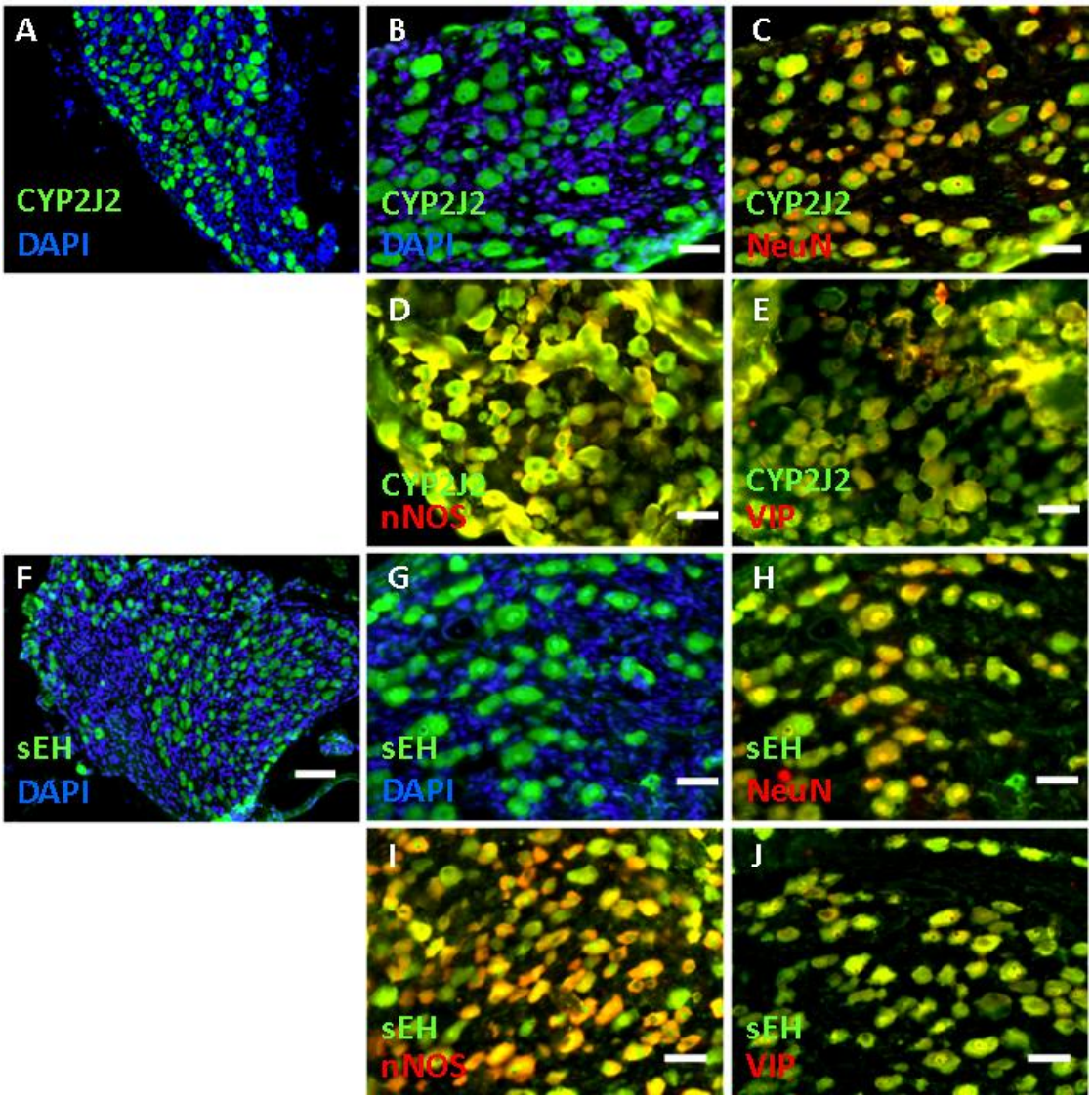

Figure 9. Localization of CYP-2J- and sEH-immunoreactivity in parasympathetic sphenopalatine ganglion neurons. (A) CYP-2J2-immunoreactivity (green) was distributed throughout the sphenopalatine ganglion. (B-C) Double labeling against the neuronal marker NeuN (red) indicated that CYP-2J2-immunoreactivity (green) was restricted primarily to sphenopalatine ganglion neurons. (D-E) Most CYP-2J2-immunoreactive (green) neurons co-localized with nNOS (red, D) while only a fraction of CYP-2J2- immunoreactive (green) neurons were VIP-positive (red, E). (F) sEH-immunoreactivity (green) in the sphenopalatine ganglion was widely distributed throughout the ganglion. (G-H) Double labeling against NeuN (red) revealed sEH-immunoreactivity in most neurons. Less intense sEH-immunoreactivity (green) was also apparent in glial cells. (I-J) Most CYP-2J2-immunoreactive (green) neurons co-localized with nNOS (red, I) whereas only a fraction were VIP-positive (red, J). Scale bars: A, F – 60 μm; B-E, G-J – 30 μm.

specific expression of CYP-2J and sEH in these ganglia, immunofluorescence double-labeling of sphenopalatine and trigeminal ganglia slices was conducted with

antibodies raised against recombinant human CYP-2J2 (which cross-reacts with rat CYP-2J3 and CYP-2J4 [210]) and sEH.

Table 6. Co-Localization of CYP-2J- and sEH-Immunoreactivity with Markers for Parasympathetic and Sensory Neuron Populations

Sphenopalatine Ganglia (Parasympathetic)			
	NeuN	**nNOS**	**VIP**
CYP-2J2	96.6 ± 3.2 (90.7 ± 2.9)	81.8 ± 8.3	25.2 ± 1.7
sEH	92.4 ± 7.7 (69.8 ± 20.4)	87.4 ± 4.4	19.5 ± 3.2

Trigeminal Ganglia (Sensory)			
	NeuN	**CGRP**	**Substance P**
CYP-2J2	97.4 ± 2.6 (94.0 ± 0.2)	22.4 ± 0.2	16.2 ± 0.5
sEH	90.7 ± 6.0 (74.2 ± 3.9)	55.8 ± 7.2	33.2 ± 13.2

Quantification of co-localization between CYP-2J2- and sEH-immunoreactivity, the neuronal marker NeuN, or neuronal nitric oxide synthase (nNOS), the neuropeptides vasoactive intestinal peptide (VIP), calcitonin gene-related peptide (CGRP) or substance P. Values represent the percentage of CYP-2J2- or sEH-immunoreactive cells also expressing NeuN, CGRP or substance P. Values in parentheses represent the percentage of labeled neurons (NeuN-positive cells) also expressing CYP-2J2- or sEH-immunoreactivity.

The expression of CYP-2J and sEH was examined in 6 µm paraffin-embedded sphenopalatine ganglion slices by conventional fluorescence microcopy. Probing the sphenopalatine ganglion with the anti-CYP-2J2rec antibody labeled primarily cells of neuronal morphology (Figure 9A). Co-labeling with the neuronal marker NeuN revealed that virtually all CYP-2J2-immunoreactivity (97%) was restricted to neuronal cell bodies while most neurons (91%) were CYP-2J2-immunoreactivity (Figure 9B-C, Table 6). Co-labeling with antibodies against nNOS or VIP revealed that most (82%) CYP-2J2-immunoreactive cells were also nNOS-positive (Figure 9D, Table 6), whereas only a portion of them (25%) appeared to express the neuropeptide VIP

(Figure 9E, Table 6).

Immunofluorescence labeling of sEH in the sphenopalatine ganglion revealed that sEH was expressed throughout the sphenopalatine ganglion, including dominant localization in cells with neuronal morphology as well as less intense immunoreactivity in apparent glial cells (Figure 9F). Double labeling studies with the neuronal marker NeuN revealed that most (92%) sEH-immunoreactive cell bodies were labeled as neurons while a smaller portion of the overall NeuN-positive neuronal pool (70%) were sEH-positive (Figure 9G,H, Table 6). As with CYP-2J2-immunoreactivity in the sphenopalatine ganglion, most (87%) sEH-immunoreactive cells were nNOS-positive (Figure 9I, Table 6) while only a fraction (20%) appeared to express VIP (Figure 9J, Table 6).

Within the trigeminal ganglion, CYP-2J2-immunoreactivity was broadly expressed in cell bodies with neuronal morphology; including those of small, medium, and large diameters (Figure 10A). Co-labeling with the neuron-specific marker NeuN demonstrated near complete overlap between CYP-2J2- and NeuN-immunoreactivity (Figure 10D-E; Table 6). Virtually every CYP-2J2-positive cell was NeuN-positive (97%), and conversely, nearly all NeuN-positive cells were CYP-2J2-positive (94%). Little CYP-2J2-immunoreactivity was observed outside NeuN-labeled cell bodies, suggesting that CYP-2J proteins are not significantly expressed in either Schwann or satellite cells. To determine the cellular phenotype of trigeminal ganglion neurons expressing CYP-2J proteins, double-labeling with antibodies against CGRP and substance P was carried out. Expression of CGRP and substance P was observed in a fraction of trigeminal neurons, of which virtually all were CYP-2J2-positive (Figure

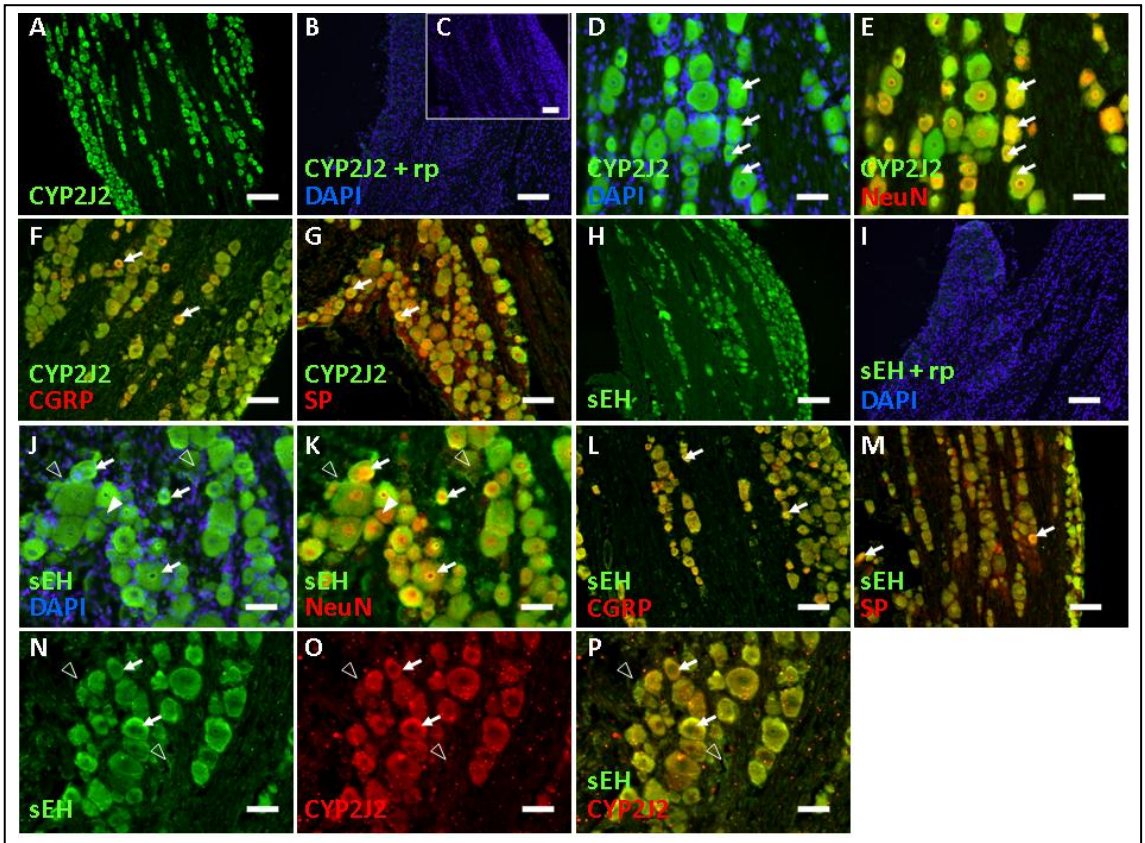

Figure 10. Localization of CYP-2J- and sEH-immunoreactivity to sensory trigeminal ganglion neurons. (A) CYP-2J2-immunoreactivity (green) was widely distributed throughout the trigeminal ganglion. (B) Labeling with the anti-CYP-2J2rec antibody following pre-absorption with recombinant human CYP-2J2rec protein (+rp) revealed no apparent CYP-2J2-immunoreactivity (green). (C) Omission of primary antibodies from labeling protocol resulted in no non-specific labeling. (D-E) Double labeling against the neuronal marker NeuN (red) indicated that CYP-2J2-immunoreactivity (green) was restricted primarily to trigeminal ganglion neurons (arrows). (F-G) A fraction of CYP-2J2-immunoreactive (green) neurons in the trigeminal ganglion were immunoreactive for the neuropeptides CGRP (red, F) and substance P (red, G) (arrows), whereas virtually all CGRP- and substance P-positive cells were CYP-2J2-immunoreactive. (H) sEH-immunoreactivity (green) was widely distributed in the trigeminal ganglion. (I) Labeling with the anti-sEH antibody following pre-absorption with recombinant human sEH protein (+rp) resulted in no sEH-immunoreactivity (green). (J-K) Double labeling against NeuN (red) revealed sEH-immunoreactivity (green) in most (arrows), but not all (filled arrowheads) neurons. sEH-immunoreactivity was also apparent in non-neuronal cells of satellite (outline arrowheads) and Schwann cell morphology (not shown). (L-M) A fraction of sEH-immunoreactive (green) neurons in the trigeminal ganglion were immunoreactive for the neuropeptides CGRP (red, L) and substance P (red, M) (arrows), whereas virtually all CGRP- and substance P-positive cells were sEH-immunoreactive. (N-P) Double labeling with antibodies against sEH and CYP-2J2 demonstrated that sEH-immunoreactivity (green) and CYP-2J2-immunoreactivity (red) co-localize within the same trigeminal ganglion neurons (arrows), while sEH-immunoreactivity appeared to be additionally present in satellite (outline arrowheads) and Schwann cells. Scale bars: A, D-H, K-M – 60 μm; B, C, I, J, N-P – 30 μm.

10F, G). Of the CYP-2J2-positive trigeminal ganglion cells, a corresponding fraction (22% and 16%) were immunoreactive for CGRP or substance P, respectively (Table 6).

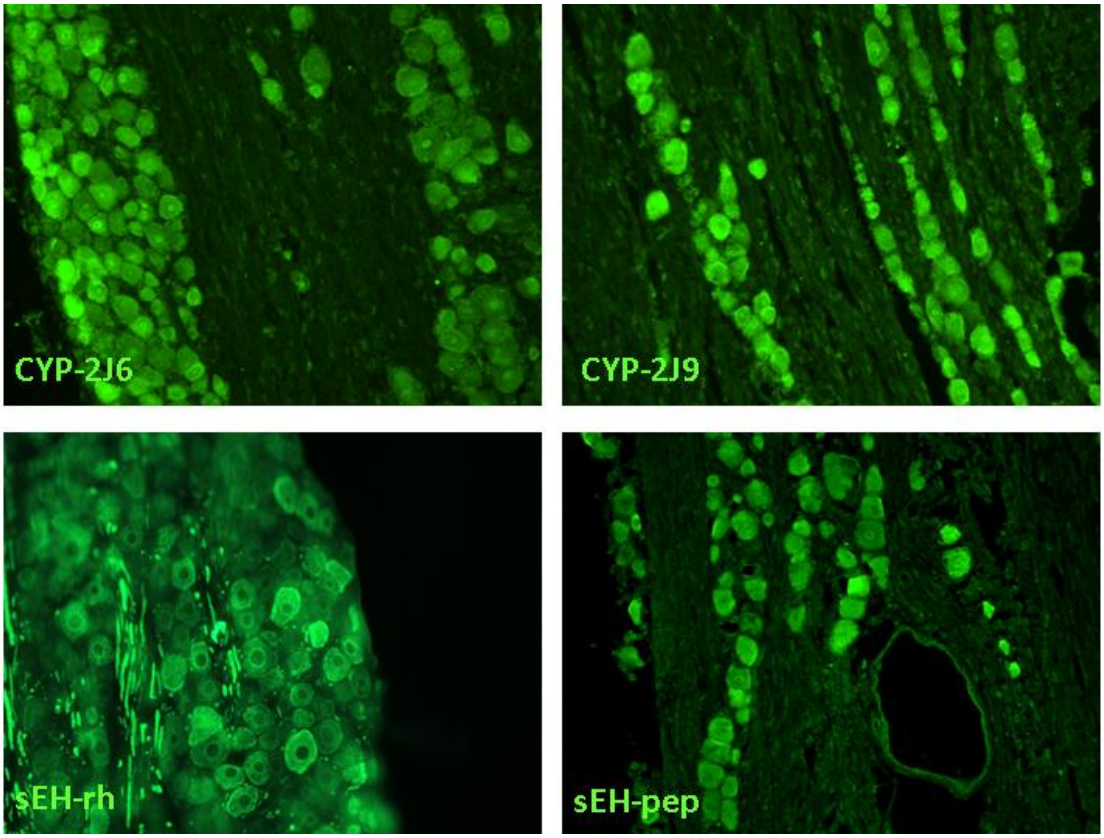

Figure 11. Evaluation of CYP-2J- and sEH-immunoreactivity in the trigeminal ganglion with distinct primary antibodies. Conventional fluorescence micrographs from rat trigeminal ganglia slices utilizing primary rabbit antibodies raised against distinct CYP-2J and sEH antigens. (A) Labeling with an antibody raised against a polypeptide sequence of mouse CYP-2J6 that cross-reacts with rat CYP-2J4. (B) Labeling with an antibody raised against a polypeptide sequence of mouse CYP-2J9 that cross-reacts with rat CYP-2J3. (C) Labeling with a rabbit polyclonal against recombinant human sEH (sEH-rh). (D) Labeling with a rabbit polyclonal against a distinct polypeptide sequence of human sEH (sEH-pep, Cayman Chemical).

Trigeminal ganglion expression of sEH was likewise interrogated by

immunofluorescence double labeling. sEH-immunoreactivity was observed throughout the ganglia, localizing to cell bodies of neuronal morphology (Figure 10H). Compared to CYP-2J2, sEH-immunoreactivity was of a lower intensity, was less universally neuronal, and appeared to include cells of both Schwann and satellite cell morphology (Figure 10J-K; Table 6). Localization of sEH-immunoreactivity in CGRP- and substance P-positive neurons also displayed a similar pattern to CYP-2J2-immunoreactivity (Figure 10L-M); most CGRP- and substance P-positive neurons were sEH-positive while only a portion of sEH-positive cell bodies exhibited immunoreactivity for these two neuropeptides (Table 6).

To determine whether CYP-2J and sEH proteins are expressed within the same individual neurons, co-labeling of trigeminal ganglion slices with antibodies against both CYP-2J2 and sEH was conducted (Figure 10N-P). It was generally observed that CYP-2J2- and sEH-immunoreactivity were present in the same neurons. However, as noted above, expression of sEH appeared more irregular and not solely restricted to neuronal cell bodies.

When primary antibodies were omitted from the double labeling protocol, no labeling of the trigeminal ganglion was observed (Figure 10C). Likewise, when the anti-CYP-2J2$_{rec}$ and anti-sEH antibodies were pre-absorbed with a molar excess of recombinant human CYP-2J2 or sEH, no CYP-2J2- or sEH-immunoreactivity was observed within the trigeminal ganglion (Figure 10B,I). To further confirm the specificity of the anti-CYP-2J2$_{rec}$ antibody, trigeminal ganglion slices were labeled with two additional antibodies against distinct CYP-2J antigens: one against a polypeptide sequence of mouse CYP-2J6 that cross-reacts with rat CYP-2J4 (CYP-

2J6$_{pep1}$), and another against a polypeptide sequence of mouse CYP-2J9 (CYP-2J9$_{pep2}$) that cross-reacts with rat CYP-2J3. Both of these antibodies displayed similar labeling patterns to the anti-CYP-2J2$_{rec}$ antibody (Figure 11A,B), although minor differences in cellular and sub-cellular distribution of CYP-2J6- and CYP-2J9-immunoreactivity were observed. To confirm the specificity of the anti-sEH antibody, labeling of trigeminal ganglion slices was carried out with two additional anti-sEH antibodies raised against distinct antigens. Labeling with a rabbit polyclonal against recombinant human sEH or a rabbit polyclonal against a distinct polypeptide sequence of human sEH (Cayman Chemical) resulted in immunoreactivity very similar to that of the Santa Cruz antibody (Figure 11C,D). Based upon these findings, the CYP-2J2-immunoreactivity and sEH-immunoreactivity observed in trigeminal ganglion neurons appears to be specific.

These data in total argue that both the EETs-synthetic CYP-2J (likely both CYP-2J3 and CYP-2J4 isoforms) and EETs-regulatory sEH proteins are present in neurons of the sensory trigeminal ganglion and the parasympathetic sphenopalatine ganglion.

Characterization of CYP-2J Expression in Perivascular Nerve Fibers

Having identified the expression of CYP-2J in neurons throughout both the sphenopalatine and the trigeminal ganglia, the expression of CYP-2J protein in peripheral perivascular processes surrounding the rat middle cerebral artery was interrogated by immunofluorescent double-labeling. Probing with a rabbit polyclonal antibody raised against recombinant human CYP-2J2 (CYP-2J2$_{rec}$), conventional

fluorescence microscopy revealed that CYP-2J-immunoreactivity was detectable in perivascular structures surrounding the middle cerebral artery. The intensity of labeling, however, was markedly reduced compared to that of sEH-immunoreactivity. Further, double labeling against nNOS demonstrated that CYP-2J-immunoreactivity was detectable only in large nerve bundles, not extending to individual nerve fibers (Figure 12A-B). Figure 12 consists of representative images from four biological replicates.

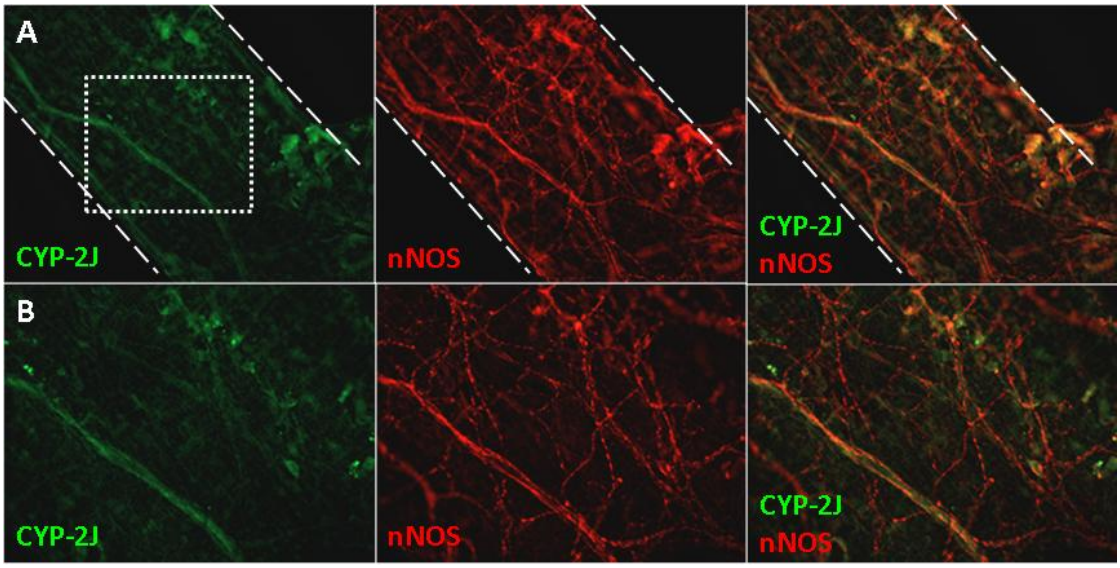

Figure 12. Immunofluorescent determination of CYP-2J expression in cerebral vasculature. Conventional fluorescence micrographs from whole mount rat middle cerebral artery. (A) CYP-2J immunoreactivity (green) is present only at low levels in perivascular nerve bundles surrounding the middle cerebral artery. CYP-2J-immunoreactivity is not seen in individual fibers, including those that co-label with nNOS (red). (B) 400X view of inset.

Characterization of sEH Expression in Sympathetic Perivascular Nerve Fibers and the Superior Cervical Ganglia

In addition to parasympathetic and sensory fibers, the cerebral surface vasculature is innervated by a third population of sympathetic vasoconstrictor fibers that are

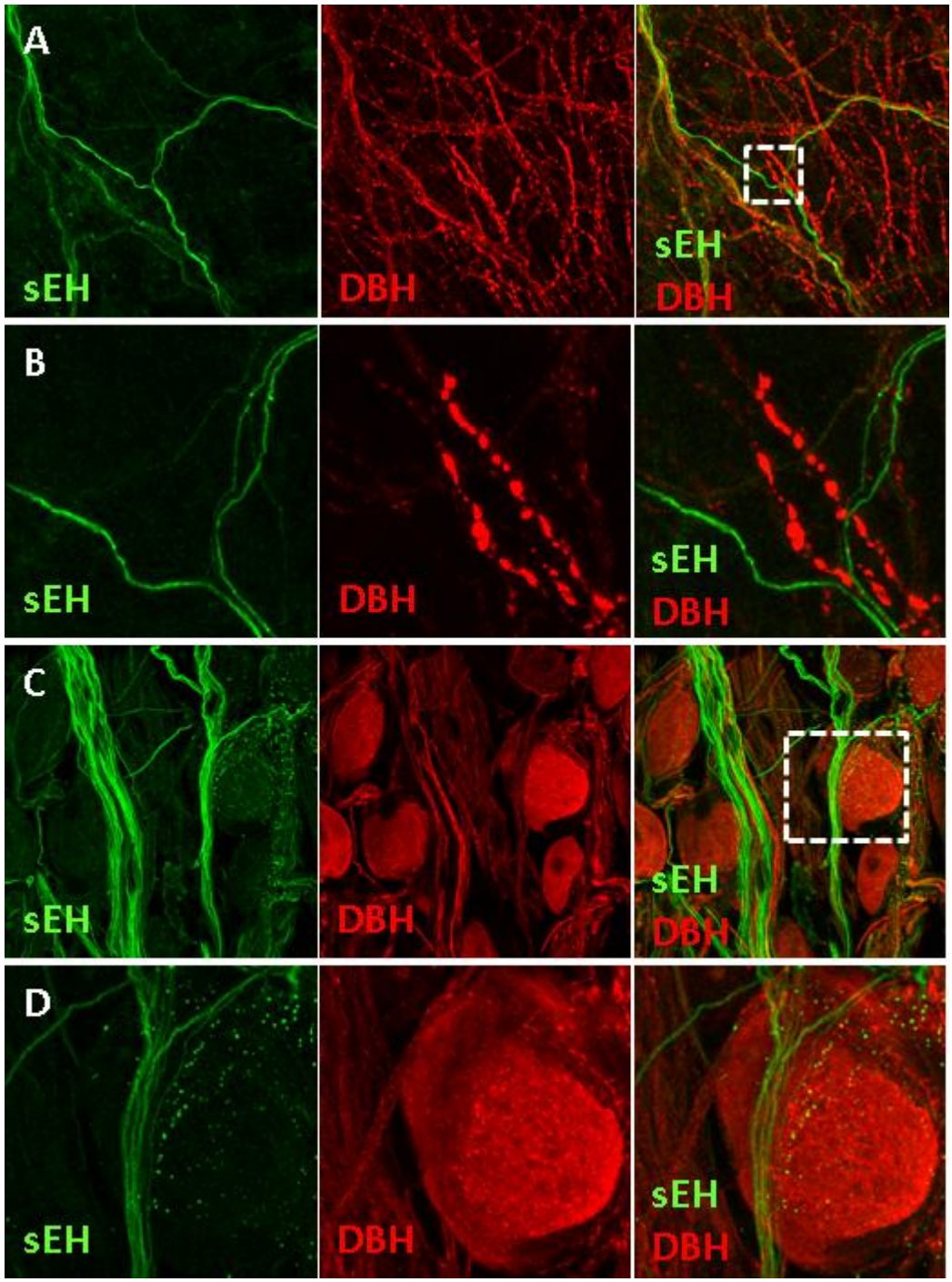

Figure 13. Localization of sEH-immunoreactivity in sympathetic perivascular fibers and superior cervical ganglia. Confocal fluorescence micrograph from rat whole mount middle cerebral arteries (A-B) and superior cervical ganglia (C-D). (A) Perivascular fibers exhibiting sEH-immunoreactivity (green) do not typically express the sympathetic marker fiber dopamine β-hydroxylase (red). Though nerve bundles appear to contain both sEH- and dopamine β-hydroxylase-positive fibers, these markers do not generally co-localize in individual fibers seen at high resolution (B, 3000X). (C-D) In the superior cervical ganglia,

sEH-immunoreactive (green) fibers are evident. These are not dopamine β-hydroxylase-positive (red) and may represent pre-ganglion fibers. In contrast, sEH-immunoreactivity is absent from superior cervical ganglion neuronal cell bodies.

primarily adrenergic, although many fibers also express neuropeptide Y [11]. Double labeling studies conducted in whole-mount middle cerebral artery demonstrated that sEH expression in perivascular fibers was observed in a small portion of those expressing the adrenergic marker dopamine β-hydroxylase (Figure 13A-B; Table 6). Similarly, sEH expression was observed in a minority of neuropeptide Y-immunoreactive fibers (Table 6). The observed co-expression with dopamine β-hydroxylase and neuropeptide-Y, however, was infrequent and was observed only in those fibers exhibiting the weakest sEH-immunoreactivity.

The sympathetic innervation of the cerebral surface vasculature originates predominantly in the superior cervical ganglia [11]. sEH immunofluorescence double labeling was conducted in paraffin-embedded adult male superior cervical ganglion slices (6 µm) probed with anti-sEH and anti- dopamine β-hydroxylase antibodies and co-localization was assessed by confocal microscopy. Within the superior cervical ganglion, sEH-immunoreactivity was observed in many neuronal processes, but not in cell bodies (that C). Interestingly, sEH-immunoreactive fibers were generally not dopamine β-hydroxylase-positive (that D). The abundance of sEH-immunoreactive processes within the superior cervical ganglion in combin*a*tion with the complete lack of sEH-positive soma suggests that these sEH-expressing processes are pre-ganglion fibers. Such a conclusion is supported by the general lack of co-localization between sEH and dopamine β-hydroxylase in cerebral extrinsic perivascular fibers (that A-B). that consists of representative images taken from three biological replicates.

Discussion

I have proposed that just as endothelium- and astrocyte-derived EETs contribute to the regulation of cerebral blood flow, EETs likewise participate in the regulation of cerebral blood flow by extrinsic perivascular nerves. The expression of both EETs-synthetic CYP epoxygenase and EETs-regulatory sEH enzymes was evaluated both peripherally in perivascular nerve fibers surrounding the middle cerebral artery, as well as in the ganglia that house the cell bodies of these neurons. In this study, I document for the first time the expression of the epoxyeicosanoid-regulatory enzyme sEH both in cerebral vascular smooth muscle and in parasympathetic and sensory perivascular vasodilator nerve fibers innervating the cerebral surface vasculature. Further, I identify a specific family of CYP epoxygenases, the CYP-2J isozymes, expressed with sEH in neurons of the parasympathetic sphenopalatine and sensory trigeminal ganglia. These findings demonstrate that parasympathetic and trigeminal perivascular nerves possess the biochemical machinery necessary for EETs synthesis and regulation.

The role of epoxyeicosanoid signaling in the regulation of cerebral blood flow is well known and has been the subject of vigorous study since the initial identification of EETs as astrocyte-derived vasodilators of cerebral vessels [96,97,98,100]. Current understanding of the epoxyeicosanoid signaling axis in the neurovascular unit is that cortical neuronal activity causes the activation of astrocytic metabotropic glutamate receptors, followed by the Ca^{2+}-dependent release of EETs from astrocytes to act upon neighboring microvasculature. Here the EETs act upon the vascular smooth muscle, producing hyperpolarization and vasodilation [185]. In the present study, I identify the

expression of sEH in the vascular smooth muscle of both intraparenchymal and surface arterioles of the cerebral vasculature (Figure 6A-C). This finding is in agreement with observations from peripheral vascular beds including the kidney and the liver, in which sEH-IR is observed in the vascular smooth muscle layer [213,214]. Previous reports have described the release of vasodilator EETs from both cerebrovascular endothelium and cortical astrocytes [5,98]. The obvious function of sEH in cerebral vascular smooth muscle is to terminate the vasoactive effects of these EETs within their target cell type. Expression of sEH in the vascular smooth muscle thus completes the epoxyeicosanoid signaling system within the neurovascular unit, and suggests a functional role for sEH in regulating the vasoactive effects of endothelium- and astrocyte-derived EETs in the cerebral circulation.

A major finding of the present study is the identification of dominant expression of sEH in the cerebral surface vasculature within perivascular vasodilator nerve fibers (Figure 6D-F). These initial findings were extended with analysis of the sphenopalatine and trigeminal ganglia, which house the cell bodies of the parasympathetic and sensory fiber populations in question [11]. RT-PCR and Western blot demonstrated the expression of sEH mRNA and protein within these tissues (Figure 8), while immunofluorescence double labeling confirmed that sEH-immunoreactivity is present almost exclusively in neuronal cell bodies within these ganglia (Figure 9F-J, 10J-K; Table 6). Although the dominant expression of sEH in perivascular nerve fibers was unexpected, it is consistent with the observed expression of sEH in neurons throughout the mammalian central nervous system [119,153,155]. Indeed, work from our own group has documented expression of sEH in both mouse

and rat cortical neurons (Figure 5) [119,153]. Similarly, immunohistochemical analysis of human brain samples has demonstrated that sEH- immunoreactivity is expressed in neurons throughout many brain regions including the cerebral cortex and basal ganglia [155]. It is noteworthy that while the expression of sEH has been well documented previously in central neurons, and now for the first time in peripheral neurons, the role of sEH in neuronal function remains almost completely undefined. In vivo work from our group demonstrated that inhibition of sEH or genetic deletion of the EPHX2 gene resulted in marked protection against experimental stroke in mice [102,153,154]. In the latter case of EPHX2 gene deletion, this protection appeared to result from a preservation of cerebral blood flow during the intra-ischemic period [154]. Intriguingly, a functional genomics study from our group demonstrated that neurons in culture could be protected from simulated ischemic insult through inhibition of sEH or the introduction of non-functional sEH protein variants [119]. Because these experiments were carried out in rat primary cortical neuronal culture, the effects of sEH protein function upon post-ischemic neuronal viability suggest that neuronal sEH contributes to neuronal vulnerability to ischemic insult.

Having detected the prominent expression of the EETs-regulatory enzyme sEH in parasympathetic and sensory nerve populations surrounding the cerebral surface vasculature, I hypothesized that these neurons may express enzymes capable of synthesizing EETs, CYP epoxygenases. Conducting an RT-PCR screen against known rat CYP-2C and CYP-2J epoxygenase isoforms, I detected the specific expression of two CYP-2J isoforms, CYP-2J3 and CYP-2J4, in both the sphenopalatine and trigeminal ganglia (Figure 8A). These findings were confirmed by Western blot

(Figure 8B) and the neuronal expression of CYP-2J in these tissues determined by immunofluorescence double labeling (Figure 9, 10). Such neuronal expression of CYP epoxygenase is in agreement with previous studies describing neuronal localization of CYP epoxygenases in brain. Furthermore, my finding that CYP-2J is expressed in peripheral neurons is consistent with a previous study demonstrating CYP-2J expression in autonomic ganglia in human and rat gut [215]. Despite these previous reports of neuronal epoxygenase expression, no study to date has proposed or provided evidence for a functional role of neurogenic EETs either in central or peripheral neuronal function.

In the present study, I identify by RT-PCR, Western blot and immunofluorescence the expression of sEH and CYP-2J enzymes in neurons of the sphenopalatine and trigeminal ganglia. In the case of both enzymes, immunoreactivity was observed primarily within neuronal cell bodies throughout the ganglia (Figure 9, 10; Table 6). As detailed above, when peripheral neuronal processes surrounding the cerebral surface vasculature were scrutinized, sEH-immunoreactivity was plainly evident both in perivascular nerve bundles and in individual fibers (Figure 6D-F). In contrast, when whole mount middle cerebral arteries were probed with an antibody raised against CYP-2J enzymes, very little CYP-2J-immunoreactivity was evident (Figure 12). Low level labeling was observed in some perivascular nerve structures, including primarily large nerve bundles but was not evident in individual nerve fibers. In contrast to the co-localization observed between sEH and nNOS (Figure 7A-B) in perivascular nerve fibers, very little overlap was detected between nNOS- and CYP-2J-immunoreactivity (Figure 12). Thus while both CYP-2J and sEH are clearly

detectable in sphenopalatine and trigeminal ganglia neuronal cell bodies, only sEH can be detected in peripheral processes surrounding the cerebral surface vasculature. One explanation for these findings is the fact that sEH is a soluble cytosolic enzyme while CYP enzymes localize to the endoplasmic reticulum [132]. The paucity of CYP-2J-immunoreactivity in peripheral neuronal processes may reflect the limited presence of endoplasmic reticulum and its associated proteins in peripheral processes compared to the soma.

Immunofluorescence double labeling demonstrated that sEH-immunoreactivity in perivascular nerve fibers surrounding the cerebral surface vasculature exhibited high levels of co-expression with nNOS and CGRP (Figure 7, Table 5), markers for the parasympathetic and trigeminal vasodilator nerve populations [11]. Similarly, though fewer fibers overall were positively labeled for the parasympathetic markers choline acetyltransferrase and VIP or the sensory neuropeptide substance P, these fibers reliably exhibited sEH-immunoreactivity. When surface arteries were probed with antibodies against the sympathetic markers dopamine β-hydroxylase or neuropeptide Y, very little co-labeling was observed (Figure 13A-B, Table 5). Similarly, when sEH-expression in the sympathetic superior cervical ganglia was interrogated by immunofluorescence double labeling, virtually no co-localization was observed either in dopamine β-hydroxylase-positive nerve fibers or cell bodies (Figure 13C-D). Intriguingly, considerable sEH-immunoreactivity was detectable in the superior cervical ganglia, however, it was restricted only to dopamine β-hydroxylase-negative fibers (Figure 13C-D). Based upon this observation, I surmise that these sEH-positive processes represent cholinergic pre-ganglionic fibers.

As noted above, the neuronal expression of EETs-synthetic CYP epoxygenase and EETs-regulatory sEH enzymes has been reported previously; including within cortical and peripheral autonomic neurons [119,153,215]. As of yet, no definitive role for these enzymes in neuronal function has been identified. In the present study, considerable specificity in the expression profiles of these enzymes is observed. sEH expression both in peripheral neuronal processes innervating the cerebral surface vasculature (Figure 7, Table 5), as well as in associated ganglia (Figure 9, 10), is restricted primarily to populations of parasympathetic and trigeminal vasodilator fibers, and is apparently absent from sympathetic vasoconstrictor fibers (Figure 13, Table 5). Within the parasympathetic SPG and the sensory TG, two isozymes from a specific CYP family (the CYP-2Js) are expressed to the exclusion of any from the CYP-2C family (Figure 8A). In both the sphenopalatine and trigeminal ganglia, the expression of both CYP-2J and sEH is generally neuron-specific (Figure 9, 10; Table 6). Hence, it is evident that both parasympathetic sphenopalatine ganglia neurons and sensory trigeminal afferents specifically possess the biochemical machinery for the synthesis (CYP-2J) and regulation (sEH) of vasodilator EETs.

Based upon these findings, neuronal CYP-2J and sEH expression may represent a second, novel axis of EETs signaling in the cerebral circulation, reflecting the participation of epoxyeicosanoids in the regulation of the cerebral vasculature by these extrinsic perivascular vasodilator nerve fibers. Within this conceptual framework, activation of perivascular vasodilator nerves results in CYP-2J-dependent EETs mobilization, which are in turn regulated through metabolism by neuronal sEH. One potential action of these neurogenic EETs is that of a nerve-derived relaxing

factor, released from perivascular nerves to act upon associated vascular smooth muscle to affect hyperpolarization and vasorelaxation, actions that are terminated by vascular smooth muscle-localized sEH. In order to evaluate such a proposed role for perivascular nerve-derived EETs, I next sought to determine whether CYP epoxygenase activity is detectable in these nerve populations, and whether EETs represent an endogenous constituent of these cells.

Chapter 3. Evaluation of CYP Epoxygenase Activity in Primary Trigeminal Ganglion Neurons

Data contained in this chapter appeared in the following research article that is under review:

Iliff JJ, Balkowiec A, Alkayed NJ. The regulation of trigeminal ganglion neuroeffector function by epoxyeicosanoid signaling. *J Neurochem* (under review) 2009.

Chapter Abstract

The cerebral surface vasculature is innervated by two populations of extrinsic perivascular vasodilator nerves: parasympathetic fibers from the sphenopalatine ganglia and trigeminal primary afferents. I previously reported that neurons within these ganglia, including those projecting to the cerebral surface vasculature, express CYP epoxygenase and sEH enzymes which synthesize and regulate bioactive EETs, respectively. Based upon this expression, I have proposed that EETs contribute to the regulation of the cerebral surface vasculature by perivascular vasodilator neurons. Herein I utilize a primary rat trigeminal ganglion neuronal culture model to evaluate whether these CYP epoxygenases are constitutively functional and whether EETs are endogenously present within these neurons. The expression of both CYP-2J epoxygenases and sEH in primary trigeminal ganglion neurons cultures was evaluated by immunocytochemistry. Next, cells were subjected to a sensitive LC-MS/MS analysis for the presence of EETs within cellular extracts. LC-MS/MS revealed the presence of substantial quantities of 8,9-EETs (17% of cellular EETs), 11,12-EETs (34%) and 14,15-EETs (45%) within cell extracts. Additionally, the 5,6-DHETs hydrolysis product of 5,6-EETs was detected (4%). This profile of EETs production matches very closely that described for recombinant rat CYP-2J3. These data demonstrate that CYP-2J epoxygenases are constitutively active in primary rat trigeminal ganglion neurons, and that EETs are endogenously present within these cells.

Introduction

The cerebral surface vasculature is innervated by three populations of 'extrinsic' perivascular nerves: parasympathetic vasodilator fibers originating in the sphenopalatine and the otic ganglia, sympathetic vasoconstrictor fibers originating in the superior cervical ganglia, and a third population of primary trigeminal afferents that exert local efferent vasodilator actions in the cerebral circulation [11]. In the previous chapter, I report that EETs-synthetic CYP-2J epoxygenase and EETs-metabolizing sEH enzymes are expressed in neurons of the sphenopalatine and the trigeminal ganglia (Figure 9, 10), including peripheral perivascular fibers innervating the cerebral surface vasculature (Figure 7). Importantly, it was observed that both CYP-2J and sEH expression was specifically localized to these two populations of perivascular vasodilator fibers, and did not extend to either cell bodies within the sympathetic superior cervical ganglia or peripheral sympathetic fibers innervating the cerebral surface vasculature (Figure 13).

In the cerebral circulation, EETs function as potent vasodilators [97,100,175]. Previous studies have demonstrated that cerebrovascular endothelium-derived EETs contribute to flow-mediated vasodilation [4,5,174,190,191,208] while astrocyte-derived EETs are mediators of neurovascular coupling [6,7,98,99]. I have proposed that EETs contribute in a similar manner to the regulation of the cerebral vasculature by the abovementioned perivascular vasodilator nerves, although such a role has not been previously investigated. Consistent with this central hypothesis, the expression of the EETs-synthetic CYP-2J epoxygenase and EETs-regulatory sEH enzymes within these neuronal populations demonstrates that these vasodilator neurons possess the

biochemical machinery necessary for the synthesis and regulation of vasodilator EETs. Whether these enzymes are constitutively active under basal conditions and whether EETs are produced within these neurons remains unknown.

In the present study, I utilize a purified primary trigeminal ganglion neuronal culture model to evaluate basal epoxygenase activity *in vitro.* In intact rat trigeminal and sphenopalatine ganglia tissue, both CYP-2J3 and CYP-2J4 enzymes were identified by RT-PCR, Western blot and immunofluorescence (Figure 6, 8). Herein I confirm the expression of CYP-2J epoxygenase and sEH within primary trigeminal ganglion neurons. Further, I utilize a sensitive liquid chromatography tandem mass spectroscopy technique to detect the presence of EETs, and hence native epoxygenase activity, within these neurons under resting conditions. The profile of respective EETs regio-isomers detected within these primary trigeminal ganglion neurons is then compared to the experimentally-derived catalytic profiles for CYP-2J3 and CYP-2J4 in order to ascertain whether the actions of one or both of these epoxygenase isozymes accounts for the production of EETs *in vitro*.

Methods

Primary Trigeminal Ganglion Neuron Culture

Postnatal day 2-3 (P2-3) Sprague-Dawley rat pups were deeply anesthetized with isofluorane and rapidly decapitated. Trigeminal ganglia were rapidly dissected bilaterally from each animal and placed in ice-cold Ca^{2+}/Mg^{2+}-free Dulbecco's phosphate-buffered saline (Invitrogen). The ganglia were digested first with 0.15% trypsin (Sigma) in Ca^{2+}/Mg^{2+}-free Hanks Balanced Salt Solution (Invitrogen) for 30

min at 37 ºC, then with 0.2% collagenase (Sigma) in Ca^{2+}/Mg^{2+}-free Hanks Balanced Salt Solution for 30 min at 37 ºC. Following digestion, ganglia were washed with 0.1% soybean trypsin inhibitor (Sigma) in Ca^{2+}/Mg^{2+}-containing phosphate-buffered saline (Invitrogen) followed by a rinse in the plating medium. Ganglia were dissociated by trituration within a 1 ml plastic serological pipette. Trigeminal ganglion neurons were purified on a 35%-60% Percoll (GE Healthcare) gradient as described by Buldyrev et al. [216], washed with plating media, then plated onto poly-D-lysine (Sigma) and laminin (Sigma)-coated 6 or 24 well cell culture plates (Falcon) at a density of 8 and 2 ganglia per well, respectively. Cultures were grown for four days in Neurobasal-A medium (Invitrogen) supplemented with B-27 (Invitrogen), 0.5 mmol/L glutamine (Invitrogen), 2.5% fetal bovine serum (HyClone), penicillin-streptomycin (Invitrogen) and 50 ng/ml nerve growth factor (Invitrogen).

Immunocytochemistry

For immunocytochemistry, trigeminal ganglion neurons were plated at a low density (0.5 ganglion/well) on poly-D-lysine and laminin-coated glass coverslips within 24-well cell culture plates. After four days, coverslips were washed three times with warm PBS, fixed with 4% paraformaldehyde in phosphate-buffered saline for 10 min, washed three times with phosphate-buffered saline, then blocked for 1 hr at room temperature with 5% normal donkey serum (Jackson Immunoresearch), 1% bovine serum albumin (Sigma) and 0.5% Triton-X (Sigma) in phosphate-buffered saline. Coverslips were incubated with primary antibodies in 1% bovine serum albumin and 0.5% Triton-X in phosphate-buffered saline overnight at 4 ºC, then washed four times

with phosphate-buffered saline, and incubated with secondary antibodies in 1% bovine serum albumin and 0.5% Triton-X in phosphate-buffered saline for 1 hr at room temperature. Coverslips were last washed four times with phosphate-buffered saline, then mounted on glass slides with Prolong Gold Antifade (Invitrogen).

To evaluate the localization of CYP-2J and sEH enzymes in primary trigeminal ganglion neurons, primary rabbit polyclonal antibodies raised against recombinant human CYP-2J2 ($CYP\text{-}2J2_{rec}$, 1:500, a gift from Dr. Darryl Zeldin, NIEHS [210]) and against residues 340-554 from human sEH (1:100, Santa Cruz) were utilized. To determine CYP-2J or sEH co-localization with the neuropeptides CGRP or substance P, double labeling was conducted with a primary goat polyclonal antibody raised against rat CGRP (1:500, Serotec) and a primary guinea pig polyclonal antibody raised against residues 1-11 of rat substance P (1:500, Millipore). Localization of CYP-2J and sEH in capsaicin-responsive trigeminal nociceptors was evaluated by double labeling with an primary guinea pig polyclonal antibody raised against residues 817-838 of the rat transient receptor potential vanilloid-1 (TRPV1) channel (1:1000, Abcam). Secondary detection utilized donkey anti-rabbit ALEXA Fluor-488, donkey anti-goat ALEXA Fluor-594 and donkey anti-guinea pig ALEXA Fluor-594 secondary antibodies (1:800, Invitrogen). Imaging was conducted on a conventional fluorescence microscope (Leica) with image analysis conducted with ImageJ software (NIH). All immunocytochemical localization studies were carried out in at least three independent cell culture runs (n=3 biological replicates) while representative images were selected to demonstrate CYP-2J and sEH immunoreactivity.

Liquid Chromatography-Tandem Mass Spectrometry

The presence of EETs within primary trigeminal ganglion neurons was assayed. Un-stimulated neurons from one well from three cell culture runs (n=3 biological replicates) were first washed three times with HEPES-buffered saline, then scraped and collected from 6 well plates (8 ganglia/well) in phosphate-buffered saline. Cell suspensions were centrifuged at 14,000xg for 10 min at 4 ºC to pellet the cells, and the phosphate-buffered saline was aspirated. Pellets were re-suspended in 200 µL phosphate-buffered saline then frozen at -80°C until the time of processing. Cell pellets were thawed on ice and spiked with 200 pg of d8-14,15-EET and d8-15-HETE internal standard, and 5 µl 1%BHT in methanol was added per ml of sample. 1 ml of KOH (1 mol/L) was added to each sample, after which the samples were hydrolyzed for 30 min at 40°C, cooled for 5 min at room temperature, then neutralized with 1 ml HCl (1 mol/L). The pH of the samples was checked and they were further acidified with 88% formic acid to pH=3.0. Samples were extracted 2 times with 2 ml ethyl acetate. The combined organic layers were dried in the SpeedVac, brought up in 1 ml hexane, re-dried, brought up in start solvent (45:55 Acetonitrile:H_20), and subjected liquid chromatography-tandem mass spectrometry (LC-MS/MS) analysis.

DHETs, HETEs and EETs levels were analyzed using the 4000 Q-TRAP hybrid/linear mass spectrometer (Applied Biosystems) with electrospray ionization in negative mode. The instrument was interfaced with a Prominence High-Performance Liquid Chromatography unit (Shimadzu). Resolution was obtained with a 2.1x250mm, 5µ BetaBasic C18 High-Performance Liquid Chromatography column with guard and gradient elution with water (A) and acetonitrile (B); both with 0.002% acetic acid

Table 7. Quadrupole Mass Spectrometer Parameters for EETs, DHETs and HETEs Analysis

Compound	Q1mass	Q3mass	Time (msec)	DP (volts)	EP (volts)	CE (volts)	CXP (volts)
D8-14,15-EET	327	182	180	-70	-10	-18	-13
14,15-DHET	337	237	180	-80	-10	-22	-3
11,12-DHET	337	197	180	-70	-10	-26	-13
8,9-DHET	337	185	180	-80	-10	-24	-15
5,6-DHET	337	145	180	-85	-10	-24	-1
11-HETE	319	167	180	-65	-10	-22	-17
12-HETE	319	179	180	-70	-10	-20	-15
15-HETE	319	219	180	-65	-10	-18	-21
20-HETE	319	245	180	-70	-10	-22	-1
14,15-EET	319	175	180	-70	-10	-18	-9
11,12-EET	319	208	180	-70	-10	-16	-13
8,9-EET	319	155	180	-70	-10	-18	-1
5,6-EET	319	191	180	-70	-10	-18	-13

EET: epoxyeicosatrienoic acid; DHET: dihydroxyeicosatrienoic acid; HETE: hydroxyeicosatetraenoic acid.

under the following conditions: 45-60% B over 1 min, linear to 65% B over 15 min, linear to 95% B over 0.10 min, isocratic at 95% B for 4 min, linear to 45% B over 0.1 min, isocratic at 45% B for 10 min. Flow rate was 0.5 ml/min and column temperature was 40°C. Electrospray ionization source parameters included curtain gas 50, ion spray voltage -4000, temperature 550 °C with ion source gas 1 and gas 2 at 50 and an entrance potential of -10 V. Samples were infused individually and instrument parameters were optimized for multiple reaction monitoring with selective transitions as summarized in Table 7. The amount of DHETs, EETs or HETEs compounds in the sample was calculated by comparison of the area ratio of the compound with d8-

14,15-EET or d8-15-HETE internal standard, then compared to a standard curve generated from blank phosphate-buffered saline spiked with known amounts of DHETs, EETs and HETEs. Quantification of cell extract analyte levels represents the mass of analyte detected in reconstituted cell extract (8 ganglia cell pellet re-suspended in 200 µl phosphate-buffered saline).

Chemicals

HEPES-buffered saline consisted of 25 mmol/L HEPES, 140 mmol/L NaCl, 3.5 mmol/L KCl, 2.5 mmol/L $CaCl_2$, 1 mmol/L $MgCl_2$, 3.3 mmol/L D-glucose, and 1% bovine serum albumin (pH 7.4).

Statistics

All values are expressed as the mean ± standard error of the mean (SEM).

Results

Expression of CYP-2J and sEH in Primary Trigeminal Ganglion Neurons

In the previous chapter, I reported the expression of two EETs-synthetic CYP-epoxygenases CYP-2J3 and CYP-2J4 and the EETs-metabolizing sEH enzymes in rat trigeminal ganglion neurons (Figure 10). In the current study, the expression of CYP-2J and sEH in primary cultured trigeminal ganglion neurons was first assessed by immunocytochemistry. After four days in culture, primary trigeminal ganglion neurons exhibited avid process extension and dendritic arborization. Labeling of trigeminal

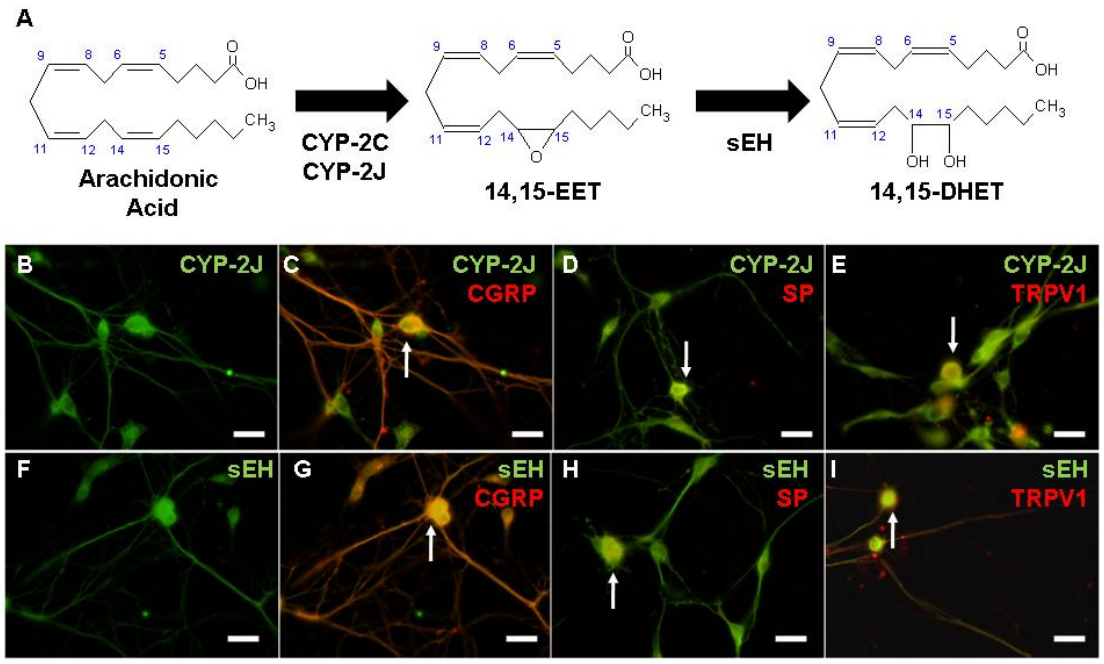

Figure 14. Expression of CYP epoxygenase and soluble epoxide hydrolase in primary trigeminal ganglion neurons. (A) Cytochrome P450 epoxygenase enzymes of the CYP-2C and CYP-2J families convert arachidonic acid to four epoxyeicosatrienoic acid (EET) regio-isomers: 5,6-EET, 8,9-EET, 11,12-EET and 14,15-EET (shown). EETs are degraded by soluble epoxide hydrolase (sEH) to produce dihydroxyeicosatrienoic acids (DHETs). (B-I) Immunocytochemistry of rat primary trigeminal ganglion neurons, day 4 in culture. CYP-2J epoxygenase is broadly expressed in primary trigeminal ganglion neurons (B), including those expressing the neuropeptides calcitonin gene-related peptide (CGRP, C) and substance P (D), in addition to the transient receptor potential vanilloid-1 (TRPV1) cation channel (E). (F) Soluble epoxide hydrolase is expressed in trigeminal ganglion neurons. sEH-immunoreactivity co-localizes with the neuropeptides CGRP (G) and substance P (H), in addition to the TRPV1 cation channel (I). All images are representative of at least three biological replicates.

ganglion neurons with an antibody against human CYP-2J2, which cross-reacts with both rat CYP-2J3 and CYP-2J4 isoforms [210], resulted in strong immunoreactivity throughout virtually all primary neurons. Labeling was most pronounced in the cell soma, although weaker immunoreactivity was evident in neuronal processes (Figure 14B, n=3 replicates). Labeling with an antibody raised against a peptide fragment of human sEH revealed similarly broad expression of this enzyme throughout virtually

all primary trigeminal ganglion neurons (Figure 14F, n=3). Co-labeling with an antibody raised against rat CGRP revealed that nearly all CGRP-positive neurons exhibited CYP-2J- and sEH-immunoreactivity (Figure 14B-C, n=3; Figure 14F-G, n=3). Probing for the expression of the neuropeptide substance P revealed a small number of trigeminal ganglion neurons expressing substance P. Of these substance P-positive neurons, all expressed CYP-2J (Figure 14D, n=3) and sEH (Figure 14H, n=3). Co-localization was also observed between CYP-2J and the capsaicin-activated cation channel TRPV1 in trigeminal ganglion neurons (Figure 14E, n=3; Figure 14I, n=3). These data thus confirm my previous findings in vivo (Figure 10) and demonstrate that primary trigeminal ganglion neurons generally express both the EETs-synthetic CYP-2J and the EETs-metabolizing sEH enzymes.

Detection of Epoxyeicosanoids in Primary Trigeminal Ganglion Neuronal Cell Extract

Having identified the expression of CYP epoxygenase enzymes in primary trigeminal ganglion neurons, I next evaluated whether these enzymes were functionally active and whether EETs are endogenously present within these cells. After four days in culture, trigeminal ganglion neuron cellular extracts were assayed for EETs, DHETs and HETEs products by LC-MS/MS in three independent cell culture sets. 8,9-EET (90.8 ± 17.8 pg/ml), 11,12-EET (177.9 ± 51.6 pg/ml) and 14,15-EET (236.2 ± 56.9 pg/ml) were readily detectable in cellular extracts (Table 8, n=3). While 5,6-EET itself was not detected, 5,6-DHET was detected at low levels (18.2 ± 3.0 pg/ml). The lipoxygenase metabolites 11-HETE (45.6 ± 12.0 pg/ml), 12-HETE (40.7 ± 5.1 pg/ml) and 15-HETE (111.2 ± 5.0 pg/ml) were present within the trigeminal ganglion neuron

cellular extract, whereas the CYP hydroxylase metabolite 20-HETE was not detectable. These findings demonstrate that EETs are endogenous constituents of primary trigeminal ganglion neurons.

Table 8. Identification of EETs as Endogenous Constituents of Primary Trigeminal Ganglion Neurons.

Analyte	Levels (pg)	Analyte	Levels (pg)	Analyte	Levels (pg)
11-HETE	45.6 ± 12.0	**5,6-EET**	ND	**5,6-DHET**	18.2 ± 3.0
12-HETE	40.7 ± 5.1	**8,9-EET**	90.8 ± 17.8	**8,9-DHET**	ND
15-HETE	111.2 ± 5.0	**11,12-EET**	177.9 ± 51.6	**11,12-DHET**	ND
20-HETE	ND	**14,15-EET**	236.2 ± 56.9	**14,15-DHET**	ND

Profile of HETEs, EETs and DHETs detected in trigeminal ganglion neuron cell extract. Data represents values from 3 replicate cell culture runs. Values in cell extract reflect the analyte present in reconstituted cell suspension derived from one culture well, and consisting of 8 ganglia. ND: not detectable.

Discussion

In the present study, I demonstrate that within primary cultured trigeminal ganglion neurons, CYP epoxygenase enzymes exhibit constitutive activity and that EETs are present endogenously within these neurons. I first confirmed the expression of the EETs-synthetic CYP-2J epoxygenase enzymes within primary trigeminal ganglion neurons by immunocytochemistry. I then utilized a sensitive LC-MS/MS methodology to detect the presence of all four EETs regio-isomers in cellular extracts from these neurons.

In the previous chapter, I detailed the expression of two distinct CYP

epoxygenase isozymes, CYP-2J3 and CYP-2J4, as well as the EETs-metabolizing enzyme sEH in the rat sphenopalatine and trigeminal ganglia neurons (Figure 9, 10). Herein I confirm that these enzymes are also expressed in primary trigeminal ganglion neurons (Figure 14). Probing for the expression of CYP-2J by immunocytochemistry and utilizing an antibody raised against recombinant human CYP-2J2 that cross-reacts with both rat CYP-2J3 and CYP-2J4, pronounced expression was detected in all primary neurons observed. These findings confirm those from immunofluorescence studies previously conducted in native rat ganglionic tissue. Extending the earlier findings, it was observed that *in vitro*, the localization of CYP-2J-immunoreactivity was unevenly distributed to the neuronal cell bodies, with less abundant labeling extending throughout the peripheral neuronal processes. These observations likely reflect the sub-cellular localization of CYP enzymes to the endoplasmic reticulum [132]. Thus, the relative paucity of CYP-2J labeling in peripheral processes compared to that observed in the soma may result from the relative scarcity of endoplasmic reticulum within these processes. Such a finding is consistent with the immunofluorescence labeling conducted in native rat tissue. Within the sphenopalatine and trigeminal ganglion, neuronal cell bodies exhibited pronounced and universal labeling with the same anti-human CYP-2J2 primary antibody (Figure 9, 10). However, in the peripheral cerebral vasculature to which fibers from these ganglia project, very little CYP-2J-immunoreactivity was observed in perivascular nerve fibers (Figure 12).

The present results similarly confirm the expression of the EETs-metabolizing enzyme sEH in trigeminal ganglion neurons (Figure 10). Immunocytochemistry

revealed sEH expression in virtually all of the neurons present in primary culture. In contrast to the sub-cellular localization of CYP-2J (Figure 14), sEH expression extended throughout both the cell soma and the peripheral processes. This pattern is likely attributable to the cytosolic localization of sEH, in contrast to the microsomal localization of CYP-2J [132]. Indeed, these data corroborate the results stemming from native rat sphenopalatine and trigeminal ganglia tissue. Here, sEH immunoreactivity was observed in both the central soma within the ganglia (Figure 10), as well as in peripheral nerve fibers innervating the cerebral surface vasculature (Figure 7).

CYP-2J expression was identified in primary trigeminal ganglion neurons utilizing an antibody that cross-reacts with all known mammalian CYP-2J enzymes [210]. RT-PCR and Western blot conducted in native rat trigeminal ganglia, however, demonstrated that it is specifically the CYP-2J3 and CYP-2J4 isoforms that are expressed in these tissues (Figure 8). Both of these enzymes exhibit epoxygenase activity [95,210,217]. When recombinant CYP-2J3 is incubated with arachidonic acid, it produces all four EETs regio-isomers in the following proportions: 14,15-EETs (41%), 11,12-EETs (27%), 8,9-EETs (28%) and 5,6-EETs (4%) [210]. CYP-2J4, on the other hand, produces only small amounts of the four EETs regio-isomers in addition to the arachidonic acid hydroxylase metabolite 20-HETE [217]. In order to determine whether either of these CYP epoxygenase enzymes are active under basal conditions and whether EETs are constitutively present in primary trigeminal ganglion neurons, a sensitive LC-MS/MS method was utilized. Whole cell extract was isolated, hydrolyzed under acidic conditions to liberate esterified lipids, and assayed for the

presence of all four EETs regio-isomers, the four corresponding DHETs metabolites, and a number of HETEs metabolites of arachidonic acid. Because of the hydrolysis step, the values obtained represent the 'total' cellular content of these eicosanoids; including both the free intracellular pool as well as the phospholipid membrane-bound pool.

LC-MS/MS readily identified the presence of the 14,15-EETs, 11,12-EETs and 8,9-EETs regio-isomers within the cellular extract (Table 8). 5,6-EETs was not directly detected in the cells. However, the hydrolysis product 5,6-DHETs was detected at low levels and likely represents the spontaneous oxidative breakdown product of endogenous 5,6-EET [3,132]. Among the four EETs regio-isomers, the relative abundance was as follows: 14,15-EET (45%) > 11,12-EET (34%) > 8,9-EET (17%) > 5,6-DHET (4%). In addition to these EETs and DHETs, the 11-, 12- and 15-HETE metabolites of arachidonic acid were readily detected in trigeminal ganglion cellular extract while the 20-HETE metabolite was not detectable under the present conditions. It is noteworthy that the profile of EETs regio-isomers detected within primary trigeminal ganglion neurons matches almost exactly the distribution of regio-isomers produced by recombinant CYP-2J3 in a biochemical assay [210]. This profile does not match that of CYP-2J4, which produces 20-HETE in addition to small amounts of the EETs regio-isomers [217]. This suggests that the CYP-2J3 isozyme is constitutively active in primary trigeminal ganglion neurons, and that it is this epoxygenase isoform that constitutes the pool of total cellular EETs present under basal conditions.

In the present chapter, I provide expression data that confirm the presence of the EETs-synthetic CYP-2J and EETs-metabolizing sEH enzymes in primary

trigeminal ganglion neurons. Further, liquid chromatography-tandem mass spectrometry revealed the presence of all four EETs regio-isomers within these cells under basal conditions. The constitutive activity of these epoxygenase enzymes and the endogenous presence of EETs within these cells suggests that neurogenic EETs may regulate the cellular function or effector actions of these neurons and is consistent with the broader hypothesis that neurogenic EETs contribute to the regulation of cerebral blood flow by perivascular vasodilator nerves. However, whether these endogenous EETs contribute in any meaningful way to trigeminal neuronal function remains unknown.

Chapter 4. The Regulation of Neuropeptide Release from Primary Trigeminal Ganglion Neurons by Epoxyeicosanoids

Data contained in this chapter appeared in the following research article that is under review:

Iliff JJ, Balkowiec A, Alkayed NJ. The regulation of trigeminal ganglion neuroeffector function by epoxyeicosanoid signaling. *J Neurochem* (under review) 2009.

Chapter Abstract

EETs are biologically active endogenous eicosanoids produced from arachidonic acid by CYP epoxygenases and metabolized by sEH. I previously described the expression of CYP-2J epoxygenase and sEH in rat trigeminal ganglion neurons, including those innervating the cerebral surface vasculature. CYP epoxygenases in primary trigeminal ganglion neurons were observed to be constitutively active, and EETs endogenously present within these cells. However the cellular role of these neuronal EETs is unknown. I determined the effect of trigeminal ganglion neuronal stimulation on EETs formation and the role of EETs in modulating the release of CGRP, a well-established cerebral vasodilator, by trigeminal ganglion neurons. Stimulation of trigeminal ganglion neurons for one hour with the TRPV1 channel agonist capsaicin (100 nmol/L) or depolarizing K^+ (60 mmol/L) increased CGRP release as measured by ELISA. Using LC-MS/MS, no EETs were detectable in media after stimulation. However, stimulation-evoked CGRP release was attenuated by 30 min pre-treatment with the EETs antagonist 14,15-EEZE (10 μmol/L). K^+ stimulation elevated CGRP release 2.9 ± 0.3-fold above control levels, while in the presence of 14,15-EEZE this K^+-evoked CGRP release was significantly reduced to 1.1 ± 0.2-fold above control release ($p<0.01$ ANOVA, n=6). 14,15-EEZE likewise attenuated capsaicin-evoked CGRP release from trigeminal ganglion neurons ($p<0.05$ ANOVA, n=6 cell culture experiments). Similarly, pre-treatment with the CYP epoxygenase inhibitor MS-PPOH (10 μmol/L) for 48 hrs attenuated stimulation-evoked CGRP release. These data demonstrate that neuron-derived EETs act as an intracellular regulator of neuropeptide release from rat trigeminal ganglion neurons, which may have important clinical

implications for treatment of migraine, stroke and vasospasm after subarachnoid hemorrhage.

Introduction

Neurons of the trigeminal ganglia provide the sensory innervation of the head and face, in addition to contributing to the perivascular nerve supply of the meningeal and cerebral surface vasculature [81]. Stimulation of these perivascular trigeminal afferents results in both peripheral and central release of neuropeptide transmitters, including CGRP and substance P that mediate peripheral vasodilation and inflammation as well as central pain transmission. In the cerebral vasculature, stimulation of primary trigeminal afferents or the trigeminal ganglia results in cerebral vasodilation that is mediated almost exclusively by the vasoactive neuropeptide CGRP [63,83]. Under physiological conditions, this peripheral vasodilator action functions to normalize cerebral blood flow following vasoconstriction. Lesion of these neurons inhibits recovery of blood flow following the application of vasoconstrictor stimuli, while aberrant activation of these fibers produces both dural and pial neurogenic inflammation [83].

In the previous two chapters, I demonstrated that rat trigeminal ganglion neurons, including those that innervate the cerebral surface vasculature, express CYP-2J epoxygenase and sEH enzymes, which function as synthetic and regulatory enzymes for the vasoactive eicosanoids, EETs (Figure 7, 8, 10). LC-MS/MS revealed that EETs were endogenously present within primary trigeminal ganglion neurons, likely resulting from the constitutive activity of the CYP-2J3 isozyme (Table 8). The presence of these bioactive eicosanoids under basal conditions suggests that they may participate in the cellular function or effector actions of these trigeminal afferents. However the nature and scope of this participation remains unexplored.

Given the established vasodilator effects of EETs in the cerebral circulation [97,100], one possibility is that EETs represent a releasable lipid-based vasoactive paracrine factor, synthesized in and released from trigeminal ganglion neurons in parallel with other transmitters such as the vasoactive neuropeptides CGRP or substance P. A second possibility is that EETs function as intracellular signaling molecules, regulating the release of other neurotransmitters from trigeminal ganglion neurons. In the present study, I evaluate these potential roles of EETs signaling in the effector function of trigeminal ganglion neurons using an *in vitro* primary cell culture model. Utilizing LC-MS/MS, I first assess the potential release of EETs species from trigeminal ganglion neurons. I then examine pharmacologically EETs' participation in the regulation of neuropeptide release from trigeminal ganglion neurons, by investigating the contribution of EETs signaling to basal and stimulation-evoked CGRP and substance P release from primary trigeminal ganglion neurons.

Methods

Liquid Chromatography-Tandem Mass Spectrometry

The release of EETs from primary trigeminal ganglion neurons following stimulation was determined by LC-MS/MS. Primary trigeminal ganglion neurons were grown in 6 well cell culture dishes (8 ganglia/well) for four days. The cells were washed three times with HEPES-buffered saline then stimulated for 1 hr at 37 ºC with 100 nmol/L capsaicin or 60 mmol/L KCl in HEPES-buffered saline. Following stimulation, the conditioned buffer was collected and subjected to LC-MS/MS analysis of DHETs,

EETs and HETEs content. For these data, buffer from one well from three distinct cell culture runs was collected (n=3 biological replicates) and frozen at -80°C until the time of processing. Conditioned buffer was thawed on ice, spiked with 200 pg d8-14,15-EET and d8-15-HETE internal standard, and 5 µl 1% BHT in methanol was added per ml of sample. The sample was acidified with 88% formic acid to pH=3.0, determined using pH paper. The media samples were extracted 2 times with 2 ml ethyl acetate and the organic layers were combined and dried under vacuum in a Speed Vac. Sample was brought up in 1 ml of hexane and then re-dried before being brought up in start solvent, then subjected to LC-MS/MS analysis as detailed above.

Neuropeptide Release Assay

The release of the neuropeptides CGRP and substance P from primary trigeminal ganglia neurons was assayed using commercially available enzyme-linked immunosorbent assays (ELISA). Trigeminal ganglia neuron cultures were grown for four days on 24-well cell culture plates (2 ganglia/well). To determine basal levels of neuropeptide release, cells were washed three times with warm HEPES-buffered saline, then incubated for 1hr at 37ºC with fresh HEPES-buffered saline. The conditioned buffer was then collected and assayed for neuropeptide content by ELISA. To evaluate evoked neuropeptide release from primary trigeminal ganglion neurons, cells were washed 3 times with HEPES-buffered saline, then treated for 30 min at 37ºC with pharmacological agents or vehicle in HEPES-buffered saline. Cells were then stimulated with either the TRPV1 agonist capsaicin (100 nmol/L) or depolarizing

K^+ (60 mmol/L) in HEPES-buffered saline, with the continued presence of pharmacological agents or vehicle for 1 hr at 37ºC. Following stimulation, the conditioned buffer was collected and assayed for neuropeptide content by ELISA. For each cell culture run, two sister culture wells represented each experimental condition. Neuropeptide release was measured independently from each, then averaged to produce a single biological replicate (n=1). On each cell culture plate, the evoked neuropeptide release was normalized to the average basal release measured from an HEPES-buffered saline-treated un-stimulated control wells subjected to the same washes and buffer changes as stimulated wells, in order to reduce experimental variability among biological replicates.

Basal and evoked CGRP release was measured using a commercially available rat CGRP ELISA kit (SPIBio) according to the manufacturer's recommended protocol. Briefly, duplicate 100 µL undiluted conditioned HEPES-buffered saline samples from each trigeminal ganglion neuron culture well were assayed. CGRP content was determined photometrically by measuring absorbance at 405 nm on an automated plate reader (Molecular Devices). Absorbance values were corrected by blank subtraction, averaged and converted to CGRP concentration using a 7 point CGRP standard curve. All measured experimental values fell within the linear range of the standard curve.

Stimulation-evoked substance P release was likewise measured using a commercially available rat substance P ELISA kit (Cayman). Briefly, duplicate 50 µL conditioned HEPES-buffered saline samples from each trigeminal ganglion neuronal culture well were assayed. Samples were diluted 1:100 in ELISA buffer and substance P content was determined photometrically by measuring absorbance at 405 nm.

Absorbance values were corrected by blank subtraction, averaged and converted to substance P concentration using an 8 point substance P standard curve. All measured experimental values fell within the linear range of the standard curve.

Chemicals

Capsaicin (Sigma) was initially dissolved in 100% ethyl alcohol, then diluted in HEPES-buffered saline to a 1 µmol/L 10X stock solution (1% ethanol) and stored at 4 °C until use. Fresh stock was prepared bi-weekly. 100 nmol/L capsaicin stimulation buffer (0.1% ethanol) was prepared fresh for each experiment. 14,15-Epoxyeicosa-5(Z)-enoic acid (14,15-EEZE), 14,15-EET, 11,12-EET, 8,9-EET and 5,6-EET (Cayman) were dried using a SpeedVac, dissolved in dimethylsulfoxide to form a 1000X stock solutions. N-(methylsulfonyl)-2-(2-propynyloxy)-benzenehexanamide (MS-PPOH, Cayman Chemical) and 12-[[(tricyclo[3.3.1.13,7]dec-1-ylamino)carbonyl]amino]-dodecanoic acid (AUDA, Cayman Chemical) were dissolved in dimethylsulfoxide to form a 1000X stock solution, and stored at -20 °C until use. Compounds were then diluted 1:1000 in HEPES-buffered saline (0.1% dimethylsulfoxide) fresh for each experiment.

Statistics

All values are expressed as the mean ± SEM. To account for variability in experimental conditions, trigeminal ganglion neuron density and neuropeptide release between cell culture biological replicates, evoked neuropeptide release was

normalized to the average release within two un-stimulated HEPES-buffered saline-treated control wells on each cell culture plate (Normalized Neuropeptide Release = Stimulated Release/Control Release). The effect of pharmacological blockade on evoked neuropeptide release was analyzed by one-way analysis of variance (ANOVA) with a *post hoc* Tukey's test to evaluate individual group differences. Single treatments were compared to control responses using Student's *t*-test. A p value < 0.05 was considered significant.

Results

Stimulated EETs Release from Primary Trigeminal Ganglion Neurons

EETs release from primary trigeminal ganglion neurons in response to 1 hr stimulation with either depolarizing K^+ (60 mmol/L) or the TRPV1 agonist capsaicin (100 nmol/L) was evaluated by LC-MS/MS in three independent cell culture sets. Conditioned buffer was collected after 1 hr, and analyzed for the four EETs regio-isomers: 5,6-EET; 8,9-EET; 11,12-EET and 14,15-EET; their corresponding DHET epoxide hydrolase metabolites, and CYP hydroxylase and lipoxygenase metabolite HETEs. In the conditioned buffer, none of the four EETs regio-isomers, their respective DHET metabolites, nor the CYP hydroxylase metabolite 20-HETE, were detectable after stimulation with either K^+ or capsaicin (Table 9, n=3 for each stimulation). In contrast, the lipoxygenase metabolite HETEs were readily detected in buffer from K^+-stimulated trigeminal ganglion neurons (11-HETE: 86.1 ± 7.9 pg/ml; 12-HETE: 147.3 ± 22.2 pg/ml; 15-HETE: 118.0 ± 6.1 pg/ml). Similarly, 11-HETE (79.3 ± 7.9 pg/ml), 12-HETE (122.3 ± 20.4 pg/ml) and 15-HETE (111.4 ± 12.9 pg/ml)

Table 9. Epoxyeicosatrienoic Acids (EETs) are not Released from Primary Trigeminal Ganglion Neurons in Response to Stimulation.

Analyte	K^+-Stimulated (pg/ml)	Capsaicin-Stimulated (pg/ml)
11-HETE	86.1 ± 7.9	79.3 ± 7.9
12-HETE	147.3 ± 22.2	122.3 ± 20.4
15-HETE	118.0 ± 6.1	111.2 ± 12.9
20-HETE	ND	ND
5,6-EET	ND	ND
8,9-EET	ND	ND
11,12-EET	ND	ND
14,15-EET	ND	ND
5,6-DHET	ND	ND
8,9-DHET	ND	ND
11,12-DHET	ND	ND
14,15-DHET	ND	ND

Profile of HETEs, EETs and DHETs detected in K^+- and capsaicin-conditioned buffer from trigeminal ganglion neurons. Data represents values from 3 replicate cell culture runs. Concentrations in media represent absolute analyte concentration derived from single cell culture wells consisting of 8 ganglia. ND: Not detectable.

were detected in buffer from capsaicin-stimulated trigeminal ganglion neurons. These findings suggest that while certain lipoxygenase metabolite HETEs are released by primary trigeminal ganglion neurons during K^+ and capsaicin stimulation, CYP epoxygenase metabolite EETs are not.

Direct Action of EETs upon Neuropeptide Release from Trigeminal Ganglion Neurons

I next sought to determine whether the administration of exogenous EETs directly stimulated CGRP release from primary trigeminal ganglion neurons. After four days in

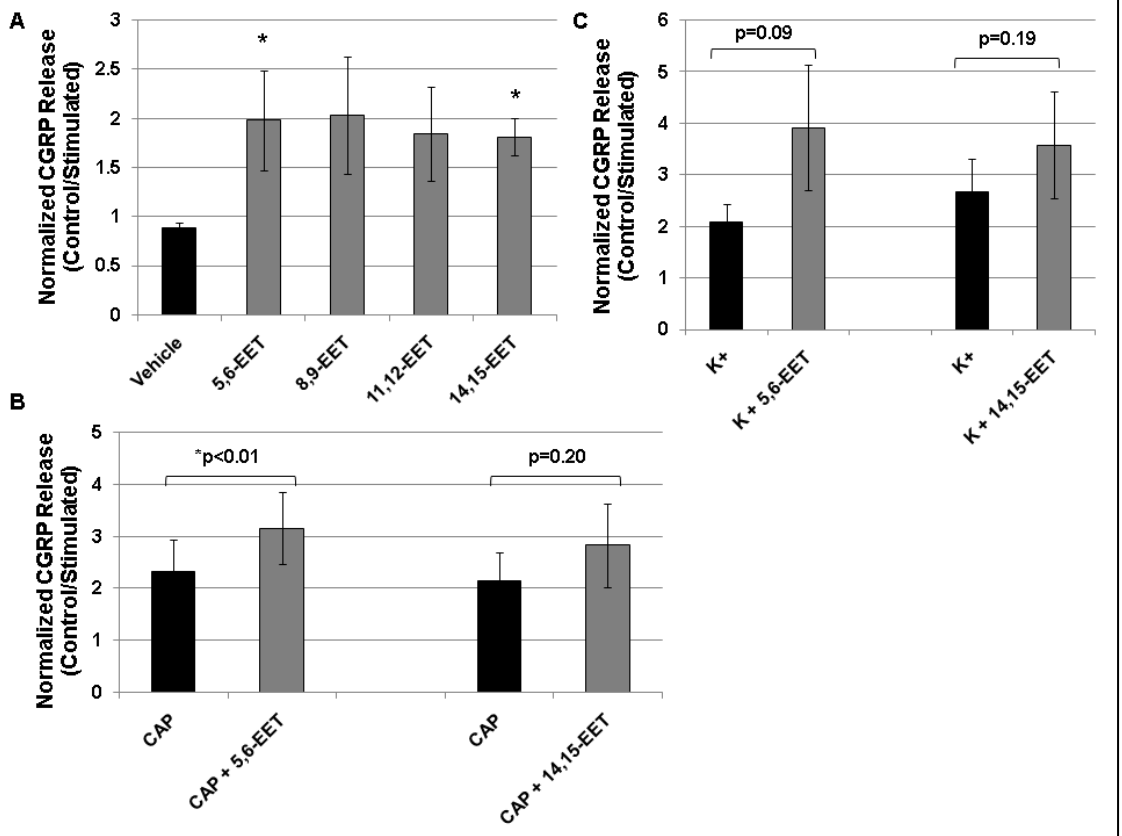

Figure 15. Direct effects of EETs upon basal and evoked release of CGRP from primary trigeminal ganglion neurons. (A) Rat primary trigeminal ganglion neurons (day 4 in culture) were treated for 1 hr with each of the four EETs regio-isomers (1 μmol/L), then the media were assayed for CGRP release by ELISA. EETs treatment stimulated CGRP release from trigeminal ganglion neurons ($p<0.05$, ANOVA n=6), while the specific effects of 5,6-EET and 14,15-EET were determined to be significant by post hoc analysis. (B) 30 min pre-treatment with the 5,6-EET regio-isomer significantly potentiated capsaicin (CAP, 100 nmol/L)-evoked CGRP release (*$p<0.01$,t-test; n=5). There was as similar trend with the effect of pre-treatment with the 14,15-EET regio-isomer upon capsaicin-stimulated CGRP release, however this did not achieve statistical significance ($p=0.20$, t-test; n=5). (C) 30 min pre-treatment of primary trigeminal ganglion neurons with either 5,6-EET or 14,15-EET tended to increase K+ (60 mmol/L)-evoked CGRP release, although this effect likewise did not achieve statistical significance ($p=0.09$ and 0.19; t-test; n= 5 and 4, respectively).

culture, cells were treated for 1 hr with either one of the four EETs regio-isomers: 5,6-EET; 8,9-EET; 11,12-EET; 14,15-EET (1 μmol/L) or vehicle. The conditioned buffer was collected and assayed for CGRP release by ELISA. ANOVA revealed that EETs treatment significantly altered CGRP release ($p<0.05$, n=6). *Post hoc* Tukey's analysis

for between-group comparison demonstrated that both the 14,15-EET and 5,6-EET regio-isomers significantly increased CGRP release compared to vehicle control. In the presence of vehicle alone, CGRP release was 0.9 ± 0.1-times that of the untreated control wells. Treatment with 14,15-EET and 5,6-EET increased CGRP release 2.0 ± 0.5- and 1.8 ± 0.2-fold over basal release, respectively (Figure 15A, n=6). The 8,9-EET and 11,12-EET regio-isomers tended to stimulate trigeminal ganglion neuron CGRP release (2.0 ± 0.6 and 1.8 ± 0.5-fold increase in CGRP release compared to un-stimulated control, respectively; Figure 15A, n=6) as well, however these effects did not achieve statistical significance in *post hoc* analysis. These findings demonstrate that exogenous EETs directly stimulate neuropeptide release from primary trigeminal ganglion neurons.

In addition to directly stimulating neuropeptide release from primary trigeminal ganglion neurons, EETs might also act as modulators of evoked neuropeptide release from these cells. Thus, the ability of exogenous EETs to potentiate evoked neuropeptide release from primary trigeminal ganglion neurons was next examined. trigeminal ganglion neurons were co-stimulated for 1 hr with the TRPV1 agonist capsaicin (100 nmol/L) or depolarizing K^+ (60 mmol/L) and either the 5,6-EET or the 14,15-EET regio-isomer (1 μmol/L). The conditioned buffer was collected and analyzed for CGRP release by ELISA. Co-administration of capsaicin and 5,6-EET significantly ($p<0.01$, t-test; n=6) increased neuropeptide release from a 2.3 ± 0.6-fold increase over basal release with capsaicin plus vehicle to a 3.2 ± 0.7-fold stimulated release in the presence of 5,6-EET (Figure 15B). For the 14,15-EET

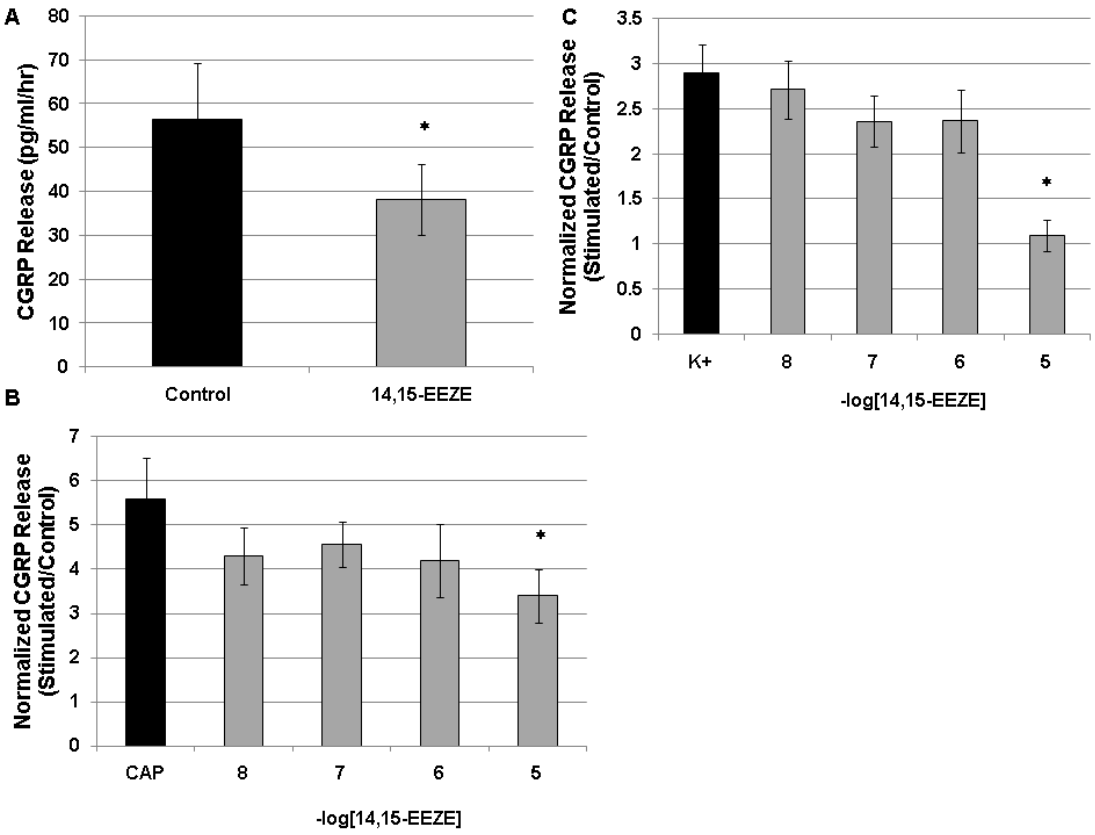

Figure 16. Inhibition of CGRP release from primary trigeminal ganglion neurons by 14,15-EEZE. (A) Rat primary trigeminal ganglion neurons (day 4 in culture) were incubated for 1 hr in blank buffer, then buffer was assayed for CGRP release by ELISA. Treatment with the EETs antagonist 14,15-EEZE (10 μmol/L) significantly reduced basal CGRP release ($p<0.01$, t-test, control vs. 14,15-EEZE; n=14). (B-C) Trigeminal ganglion neurons were stimulated for 1 hr with capsaicin (CAP, 100 nmol/L) or K+ (60 mmol/L), then the buffer was assayed for CGRP release. (B) 30 min pre-treatment with the EETs antagonist 14,15-EEZE attenuated capsaicin-evoked CGRP release (*$p<0.05$, ANOVA, treatment vs. capsaicin alone; n=6). (C) 30 min pre-treatment with 14,15-EEZE attenuated K+ -evoked CGRP release (*$p<0.01$, ANOVA, treatment vs. K^+ alone; n=6).

regio-isomer, there was a trend towards a similar effect upon capsaicin-evoked neuropeptide release, elevating it from a 2.1 ± 0.6-fold increase over basal release with capsaicin and vehicle alone, to a 2.8 ± 0.8-fold increase in the presence of 14,15-EET ($p=0.20$, t-test; n=6). Similar trends were observed for both the effects of 5,6-EET (n=5) and 14,15-EET (n=4) upon K^+-induced CGRP release (Figure 15C, t-test:

p=0.09 and 0.19, respectively). These findings suggest that in addition to directly stimulating neuropeptide release from primary trigeminal ganglion neurons, exogenous EETs also enhance release of neuropeptides from these neurons that is evoked by other stimuli.

Role of EETs in Neuropeptide Release from Trigeminal Ganglion Neurons

I next sought to determine whether endogenous EETs regulate the release of other neurotransmitters, such as the neuropeptides CGRP or substance P, from primary trigeminal ganglion neurons. Under un-stimulated conditions after four days in culture, primary trigeminal ganglion neurons released CGRP at a basal rate of 56.6 ± 12.7 $pg*ml^{-1}*hr^{-1}$. When EETs' action was inhibited with the EETs antagonist 14,15-EEZE (10 µmol/L), basal CGRP release was significantly reduced to 38.3 ± 8.1 $pg*ml^{-1}*hr^{-1}$ (Figure 16A, $p<0.01$, *t*-test, control vs. 14,15-EEZE, n=14 culture wells per condition), suggesting that endogenous EETs up-regulate basal CGRP release from primary trigeminal ganglion neurons.

I then determined the effect of EETs on stimulated neuropeptide release from trigeminal ganglion neurons in response to membrane depolarization or activation of the Ca^{2+}-permeable capsaicin-gated TRPV1 channel. After four days in culture, primary trigeminal ganglion neurons were stimulated for 1 hr with the TRPV1 agonist capsaicin (100 nmol/L) or depolarizing K^+ (60 mmol/L), and the conditioned buffer was collected and assayed for the release of the neuropeptide CGRP by ELISA. Following stimulation with capsaicin or depolarizing K^+, CGRP release increased approximately 5- and 3-fold, respectively, above basal levels measured in sister un-stimulated wells (Figure 16B-C). In order to evaluate the contribution of EETs

signaling to CGRP release from trigeminal ganglion neurons evoked by these two stimuli, cells were pre-treated for 30 min with vehicle or the putative EETs antagonist 14,15-EEZE (10 nmol/L–10 μmol/L), then stimulated with either capsaicin or K^+, as above. In the presence of vehicle, capsaicin stimulation increased CGRP release 5.6 ± 1.0-fold over basal levels. Pre-treatment with 14,15-EEZE attenuated capsaicin-evoked CGRP release, reducing release to 3.4 ± 0.6-fold over basal levels at a concentration of 10 μmol/L (Figure 16B; $p<0.05$, ANOVA vehicle vs. 14,15-EEZE treatment; n=6 experiments). Tukey's *post hoc* analysis identified a significant individual effect of 14,15-EEZE at 10 μmol/L. In the presence of vehicle, depolarizing K^+ elevated CGRP release 2.9 ± 0.3-fold over basal levels. Pre-treatment with 14,15-EEZE significantly reduced K^+-evoked CGRP release to 1.1 ± 0.2-fold over basal levels (Figure 16C; $p<0.01$, ANOVA vehicle vs. 14,15-EEZE treatment; n=6 experiments). *Post hoc* analysis identified specific treatment differences at 10 μmol/L 14,15-EEZE. In total, inhibition of EETs' actions with the putative EETs antagonist 14,15-EEZE significantly attenuated evoked CGRP release from primary trigeminal ganglion neurons. This demonstrates that endogenous EETs signaling is a positive regulator of evoked neuropeptide release from these cells.

In order to further evaluate the contribution of endogenous EETs signaling to evoked neuropeptide release from primary trigeminal ganglion neurons, the effect of pharmacological inhibition of CYP epoxygenase (EETs 'synthase') with MS-PPOH was next examined. EETs and their DHET metabolites are capable of being re-esterified and incorporated into the phospholipid bilayer [149,161]. These membrane-

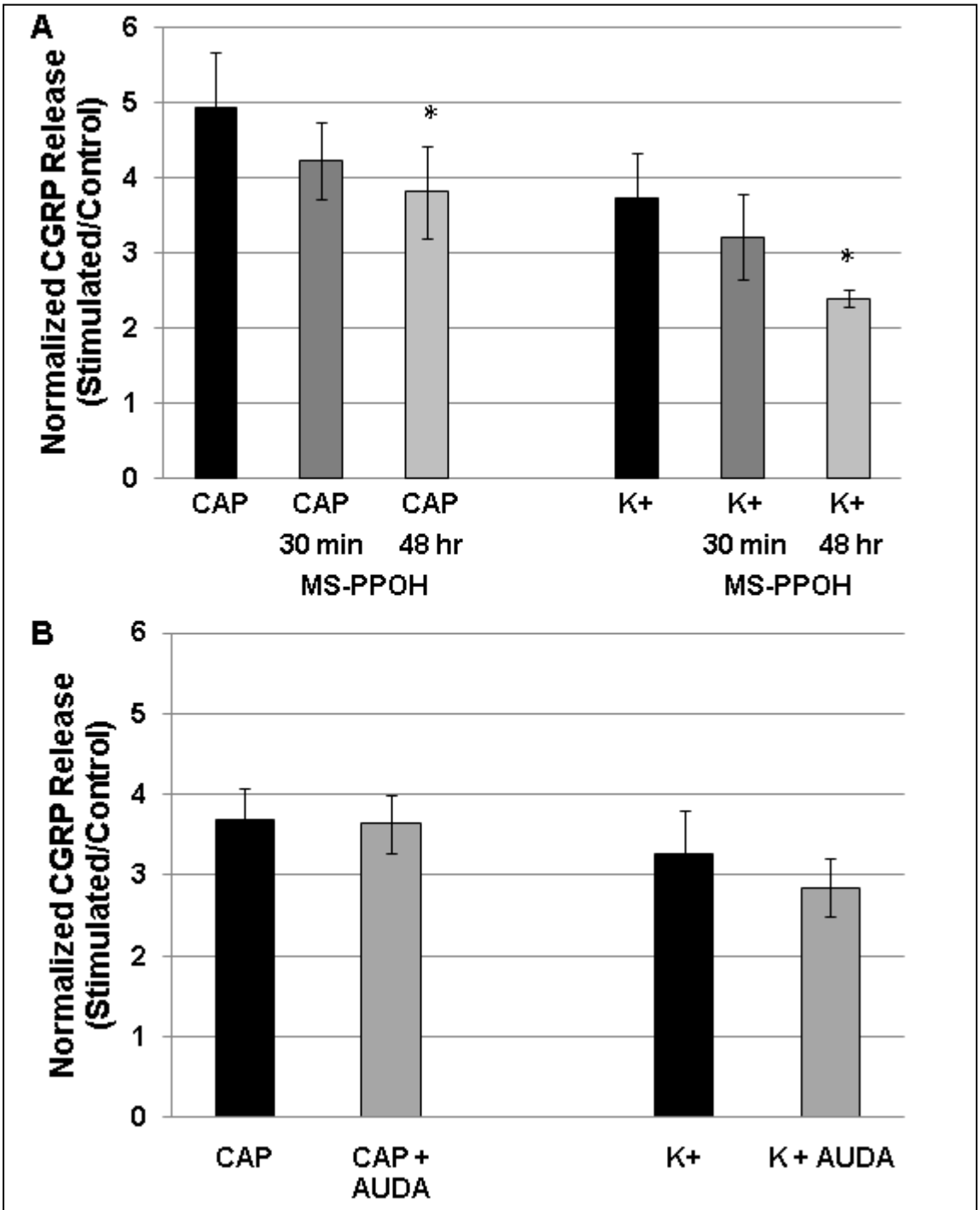

Figure 17. Inhibition of evoked CGRP release by MS-PPOH. Rat primary trigeminal ganglion neurons (day 4 in culture) were stimulated for 1 hr with capsaicin (CAP, 100 nmol/L) or K^+ (60 mmol/L), then the media were assayed for CGRP release by ELISA. (A) 30 min pre-treatment with the CYP epoxygenase inhibitor MS-PPOH (20 µmol/L) did not significantly alter capsaicin- or K^+-evoked CGRP release. Long-term (48 hr) treatment with MS-PPOH significantly attenuated both capsaicin- and K^+-stimulated CGRP release (*$p<0.05$, ANOVA,

treatment vs. capsaicin or K^+ alone; n=6 and 5, respectively). (B) 30 min pre-treatment with the sEH inhibitor AUDA (1 μmol/L) did not significantly alter the release of CGRP from trigeminal ganglion neurons following stimulation with either capsaicin or K^+ (t-test, n=11 and 6, respectively).

bound EETs constitute a releasable pool that does not require *de novo* synthesis by CYP epoxygenases. To inhibit *de novo* EETs synthesis, primary neurons were pre-treated for 30 min with MS-PPOH. Additionally, an extended 48 hr pre-treatment with this CYP epoxygenase inhibitor was utilized to deplete the latent pool of esterified EETs present in the phospholipid membrane. Analysis of variance revealed that treatment with MS-PPOH significantly altered stimulated CGRP release in response to both 100 nmol/L capsaicin ($p<0.05$, n=6) and 60 mmol/L K^+ ($p<0.01$, n=5). Specifically, pre-treatment with MS-PPOH for 30 min did not significantly alter the stimulated release of CGRP in response to either capsaicin or K^+ compared to vehicle (Figure 17A, n=6). However, 48 hr pre-treatment with MS-PPOH significantly reduced capsaicin-evoked CGRP release from 4.9 ± 0.7-fold increase over basal release with vehicle to a 3.8 ± 0.6-fold increase over basal release with MS-PPOH. Similarly, 48 hr pre-treatment with MS-PPOH reduced K^+-evoked neuropeptide release from trigeminal ganglion neurons, from a 3.7 ± 0.6-fold increase over basal release with vehicle treatment to a 2.4 ± 0.1-fold increase over basal release with drug (Figure 17A). These data corroborate the effects of the EETs antagonist 14,15-EEZE upon evoked neuropeptide release from trigeminal ganglion neurons and thus support the contribution of endogenous EETs signaling to this process. Further, these findings suggest that the bioactive EETs in primary trigeminal ganglion neurons are not derived

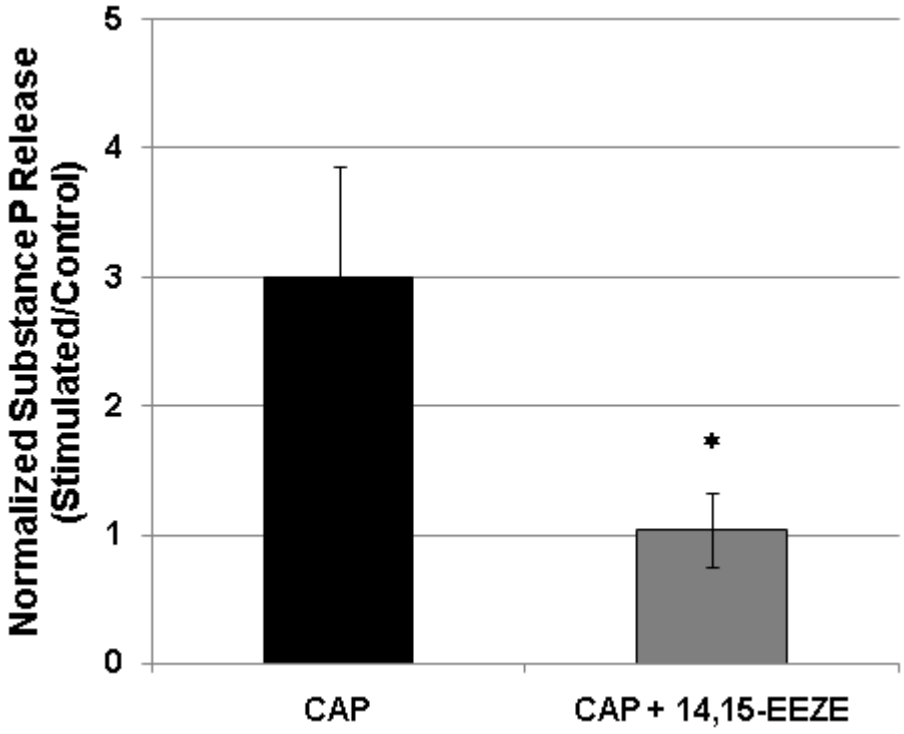

Figure 18. The EETs antagonist 14,15-EEZE blocks evoked substance P release from trigeminal ganglion neurons. Rat primary trigeminal ganglion neurons (day 4 in culture) were stimulated for 1 hr with capsaicin (CAP, 100 nmol/L), then the media were assayed for substance P release by ELISA. 30 min pre-treatment with the EETs antagonist 14,15-EEZE (10 µmol/L) blocked capsaicin-stimulated substance P release (*P < 0.05, t-test, treatment vs. capsaicin alone; n=4).

from *de novo* synthesis, but rather are released from a pre-formed pool.

EETs are principally metabolized by the enzyme sEH, which in vascular cells is a key determinant of bioavailable EETs levels [149,160]. I next evaluated the effect of the sEH inhibitor AUDA upon evoked CGRP release from trigeminal ganglion neurons. After four days in culture, primary trigeminal ganglion neurons were pre-treated for 30 min with either vehicle or AUDA (1 µmol/L), and then stimulated for 1 hr with either capsaicin (100 nmol/L) or depolarizing K^+ (60 mmol/L). The conditioned buffers were removed and assayed for CGRP content by ELISA.

Interestingly, 30 min pre-treatment with AUDA did not alter either capsaicin- or K^+-evoked CGRP release from primary trigeminal ganglion neurons (Figure 17B; n=11and 6; p=0.48 and 0.32; respectively).

In order to evaluate whether EETs' role in the regulation of neuropeptide release is specific to CGRP or rather extends more generally to other trigeminal neuropeptides, I assessed the sensitivity of stimulation-evoked release of substance P from trigeminal ganglion neurons to inhibition of the EETs pathway. After four days in culture, primary trigeminal ganglion neurons were stimulated for 1 hr with the TRPV1 agonist capsaicin (100 nmol/L) and substance P release into the media was measured by ELISA. When pre-treated with the EETs antagonist 14,15-EEZE (10 μmol/L) for 30 min, capsaicin-evoked substance P release was significantly ($p<0.05$, *t*-test, n=4 independent cultures) reduced from a 3.0 ± 0.9-fold increase with vehicle treatment to a 1.0 ± 0.3-fold increase with 14,15-EEZE treatment (Figure 18). This finding supports the contribution of EETs signaling to evoked neuropeptide release from trigeminal ganglion neurons and suggests that this action is general, and not limited to CGRP release.

Discussion

In the present study, I demonstrate that EETs are endogenous regulators of neuropeptide release from rat trigeminal ganglion neurons. I first establish that administration of exogenous EETs directly stimulates the release the neuropeptide CGRP from these neurons. Furthermore, I demonstrate that inhibition of endogenous

EETs signaling in trigeminal ganglion neurons attenuates both basal and evoked neuropeptide release from these cells.

I have proposed that neurogenic EETs contribute to the regulation of the cerebral vasculature by perivascular vasodilator nerves. In the previous chapter, I establish that EETs-synthetic CYP-2J epoxygenase enzymes expressed in trigeminal ganglion neurons are constitutively active, and that EETs are endogenously present in these cells under basal conditions (Table 8). In the present study, I sought to define the specific role of these endogenous EETs in trigeminal ganglion neuronal function. I initially hypothesized that in response to activation, trigeminal ganglion neurons release EETs to act post-junctionally on innervated vascular smooth muscle and regulate the vasomotor tone of the associated vasculature. To evaluate this hypothesis, I utilized a primary rat trigeminal ganglion neuronal culture model to determine if EETs are released from these cells. Despite the use of a sensitive LC-MS/MS methodology for the detection of EETs, none of the four EETs regio-isomers, or their DHET hydrolysis products were detected in conditioned trigeminal ganglion neuronal media following a 1hr stimulation with either depolarizing concentrations of K^+ (60 mmol/L) or the TRPV1 agonist capsaicin (100 nmol/L). Importantly, under the same experimental conditions, the release of the neuropeptides CGRP (50-500 pg/ml) and substance P (1-10 pg/ml) were readily detectable by ELISA both in un-stimulated and stimulated cultures. Moreover, the 11-, 12- and 15-HETE lipoxygenase metabolites of arachidonic acid were also detectable in conditioned media by LC-MS/MS under both basal and stimulated conditions, despite being present in lower relative concentrations than most of the EETs regio-isomers in the neuronal cell extracts (Table 8). These

findings indicate that EETs are likely not released in significant quantities from primary trigeminal ganglion neurons either under basal conditions or following stimulation. It must be noted, however, that the release of EETs at concentrations below the limit of detection of the LC-MS/MS method (<5 pg/ml) or the rapid re-uptake of released EETs into the cells cannot be formally excluded.

I next investigated a second proposed role of endogenous EETs in trigeminal ganglion function: that of a regulator of neuropeptide release. Although most recent research has focused upon EETs' contribution to cardiovascular regulation [95], the earliest studies describing biological actions of epoxide metabolites of arachidonic acid focused on their role in the regulation of neurohormone release from the hypothalamus and anterior pituitary. Early studies demonstrated that all four EETs regio-isomers, which were constitutively present in both hypothalamic and pituitary tissue, were capable of directly stimulating the release of somatostatin, luteinizing hormone-releasing hormone, luteinizing hormone, arginine vasopressin, oxytocin, prolactin and growth hormone from this neuroendocrine tissue. Inhibition of EETs synthesis additionally blocked neuroendocrine secretagogue-stimulated hormone release from these tissues, demonstrating that endogenous hypothalamic and pituitary EETs are positive regulators of neurohormone release [129,130,131,137,138,200,201,202,209].

In light of this established role of EETs signaling in this neural cell function, I proposed that endogenous EETs likewise positively regulate neuropeptide release from trigeminal ganglion neurons. In the hypothalamic and pituitary tissue, it was observed that exogenous EETs directly stimulate neurohormone release

[129,130,131,199,200,201,202,209]. In the present study, I sought to determine whether EETs are sufficient to directly stimulate neuropeptide release from trigeminal ganglion neurons. Under un-stimulated conditions, inhibition of endogenous EETs signaling with the EETs antagonist 14,15-EEZE significantly reduced basal release of CGRP from trigeminal ganglion neurons. This suggests that endogenous EETs contribute to neuropeptide release independent of TPV1 channel activation or membrane depolarization. Similarly, when trigeminal ganglion neurons were directly stimulated with exogenous EETs (in the absence of capsaicin or depolarizing K^+), CGRP release was increased approximately 2-fold above basal levels of release. When exogenous EETs were co-administered with either capsaicin or K^+, the result was an additive increase in neuropeptide release compared to the individual stimuli alone. Thus, EETs are sufficient to directly stimulate neuropeptide release from primary trigeminal ganglion neurons independent of TRPV1 activation with capsaicin or membrane depolarization with K^+.

Pre-treatment with the EETs antagonist 14,15-EEZE generally inhibited neuropeptide release from primary trigeminal ganglion neurons. This included basal CGRP release, capsaicin- and K^+-stimulated CGRP release and capsaicin-evoked substance P release. Importantly, long-term inhibition of EETs synthesis with the CYP epoxygenase inhibitor MS-PPOH attenuated capsaicin- and K^+-evoked CGRP release, demonstrating that the effect of 14,15-EEZE upon neuropeptide release from primary trigeminal ganglion neurons was mediated by the EETs signaling pathway. The differential effect of short-term (30 min) versus long-term (48 hr) CYP epoxygenase inhibition upon evoked neuropeptide release may shed light upon the cellular source

of bioactive EETs in trigeminal ganglion neurons. EETs and their DHET hydrolysis products can be re-esterified and stored within the phospholipid bilayer. In both vascular endothelium and brain astrocytes, these membrane-bound esterified EETs form a ready pool from which EETs are released in response to stimulation, a process that is not dependent upon *de novo* synthesis and is thus resistant to short-term CYP epoxygenase inhibition [149,161]. The observation that 30 min treatment with MS-PPOH did not significantly alter the evoked neuropeptide release from trigeminal ganglion neurons while long-term CYP epoxygenase inhibition reduced neuropeptide release in a similar manner to 14,15-EEZE, suggests that a similar esterified pool may be the source of bioactive EETs in primary trigeminal ganglion neurons *in vivo*. The effects of the EETs antagonist 14,15-EEZE and the CYP epoxygenase inhibitor MS-PPOH upon neuropeptide release demonstrate that just as endogenous EETs regulate stimulated release of neurohormones from hypothalamic or pituitary tissue [129,200,201], endogenous EETs signaling contributes to evoked neuropeptide release from trigeminal ganglion neurons.

One surprising finding of the present study was the absence of an effect of sEH inhibition upon evoked neuropeptide release. sEH is a key regulator of EETs metabolism and inhibition of sEH activity elevates bioactive EETs levels and potentiates EETs-mediated effects in several cell systems [205,218,219]. Thus, my expectation was that sEH inhibition would exert the opposite effect of EETs antagonism with 14,15-EEZE or CYP epoxygenase inhibition with MS-PPOH, elevating evoked CGRP release from primary trigeminal ganglion neurons. It is noteworthy that although the 8,9-EET, 11,12-EET and 14,15-EET regio-isomers were

readily detected in primary trigeminal ganglion neuronal extract, only the DHET hydrolysis product of 5,6-EET, which is a poor substrate for sEH, was detected. This absence of cellular DHETs suggests that although sEH is expressed throughout trigeminal ganglion neurons and their processes both in vivo (Figure 7, 10) and *in* vitro (Figure 14), it may not exhibit sufficient catalytic activity under basal conditions to affect EETs function following acute inhibition. It is possible that sEH regulates EETs incorporation into the phospholipid membrane pools, as has been described in the vascular endothelium [160,161]. Such activity may be sequestered functionally and/or spatially from a prospective membrane-delimited lipid signaling domain and its inhibition may not acutely alter EETs activity.

To interrogate the contribution of the EETs signaling pathway to neuropeptide release from trigeminal ganglion neurons, I utilized the putative EETs antagonist 14,15-EEZE. One major factor currently hampering the study of the biological activities of EETs is the lack of an identified EETs receptor and the resulting absence of specific pharmacological tools. While considerable experimental evidence points to the existence of one or more putative G protein-coupled receptors through which EETs exert their biological actions, a number of other molecular targets are directly activated by EETs, including the TRPV4 cation channel [3,128,174,175]. In the study initially describing the 14,15-EEZE antagonist and characterizing its activity in isolated bovine coronary arteries, the compound competitively antagonized the dilation response to all four EETs regio-isomers [220]. Many subsequent studies have demonstrated the efficacy and specificity of 14,15-EEZE in blocking EETs-mediated processes in a number of cell systems [168,221,222,223,224], however, none have

defined which of the putative EETs binding partners are specifically antagonized by this analogue. Because the structure of 14,15-EEZE and 14,15-EET are identical save for the saturation of the 8,9 and 11,12 olefins [220], it is conceivable that this compound competes nonspecifically, antagonizing the binding of all four EETs regio-isomers at all such binding partners.

In summary, the present study identifies a novel role for endogenous EETs in regulating both basal and evoked neuropeptide release from primary rat trigeminal ganglion neurons. Parallel to EETs' regulation of neurohormone release in the hypothalamus and anterior pituitary described in early studies [129,130,131,200,201,202,209], exogenous EETs directly stimulate neuropeptide release from primary trigeminal ganglion neurons while blockade of the EETs signaling pathway attenuates evoked neuropeptide release. The identification of a signaling pathway that regulates the release of both CGRP and substance P improves our understanding of these key effector pathways, and may provide a novel therapeutic target in the treatment of disorders associated with aberrant activation of trigeminal neuronal function.

Chapter 5. Evaluation of the Role of Epoxyeicosanoids in the Regulation of Cerebral Blood Flow by Extrinsic Perivascular Vasodilator Nerves

Data contained in this chapter appeared in the following published research article:

Iliff JJ, Wang R, Zeldin DC, Alkayed NJ. Epoxyeicosanoids as mediators of neurogenic vasodilation in cerebral vessels. *Am J Physiol: Heart Circ Phsyiol* May; 296(5):H1352-63, 2009.

Chapter Abstract

The cerebral surface vasculature is innervated by three populations of extrinsic perivascular nerve fibers, including parasympathetic vasodilator fibers originating in the sphenopalatine ganglia and primary trigeminal afferents. EETs are potent vasodilators produced from arachidonic acid by CYP epoxygenases and metabolized by sEH. I demonstrated the expression of active CYP-2J epoxygenases in both sphenopalatine and trigeminal ganglia neurons, with EETs being endogenously present within these cells. Further, EETs were observed to regulate the release of vasoactive neuropeptides from these neurons. Herein I evaluate whether neurogenic EETs signaling is functionally involved in the regulation of cerebral blood flow by perivascular vasodilator nerves. Cerebral blood flow responses were monitored by laser Doppler flowmetry in adult male rats via closed cranial windows. Neurogenic cortical hyperemia was elicited by electrical stimulation of the efferent extrinsic perivascular nerve supply in the ethmoidal nerve and by chemically stimulating oral trigeminal fibers with capsaicin. Peripheral administration to the cortical surface of the putative EETs antagonist 14,15-EEZE (10 μmol/L) attenuated the neurogenic Cerebral blood flow response to electrical (from a peak of 23 ± 4% at 20 Hz with vehicle to 7 ± 1% following treatment, $p<0.05$ ANOVA, n=6) and chemical stimulation (from a peak value of 33 ± 8% with 1 mmol/L capsaicin to 16 ± 3% with treatment, $p<0.05$ ANOVA, n=8). These results demonstrate that epoxyeicosanoid signaling plays a functional role in the regulation of cerebral blood flow by perivascular vasodilator fibers.

Introduction

The cerebral surface vasculature is innervated by three populations of 'extrinsic' perivascular nerves: parasympathetic vasodilator fibers originating in the sphenopalatine and otic ganglia, sympathetic vasoconstrictor fibers originating in the superior cervical ganglia and a third population of primary trigeminal afferents that exert local efferent vasodilator actions in the cerebral circulation. Under physiological conditions, the extrinsic perivascular nerve supply to the cerebral vasculature does not appear exert ongoing regulatory control over regional cerebral blood flow [11]. However, these perivascular nerve fibers contribute to the normalization of vascular caliber following other vasomotor stimuli; for example reducing cerebrovascular tone following the cessation of pial arteriolar vasoconstriction by norepinephrine [83]. Additionally, these fibers participate in the response of the cerebral circulation to potentially damaging deviations of blood flow, such as occur during acute or chronic hypertension, hypotension or under ischemic conditions [71,72,73].

In the previous chapters, I reported first that the EETs-synthetic CYP-2J epoxygenase enzymes are expressed in neurons of the parasympathetic sphenopalatine and sensory trigeminal ganglia (Figure 9, 10). I then demonstrated that these enzymes are constitutively functional in primary trigeminal ganglion neuronal culture, and that EETs are endogenously present within these cells (Table 8). Lastly, I reported that these endogenous EETs positively regulate the release of the vasoactive neuropeptides CGRP and substance P, both under basal conditions and following neuronal stimulation (Figure 16). However, whether these neurogenic EETs contribute in any

way to the vasomotor function of these perivascular fibers is unknown. In the present study I evaluate the functional role of EETs signaling in the regulation of cerebral blood flow by extrinsic perivascular vasodilator fibers. Utilizing two distinct *in vivo* models of neurogenic cerebral vasodilation, I evaluate whether the vasodilator function of these fibers is sensitive to pharmacological blockade of the EETs signaling system.

Methods

Closed Cranial Window Preparation

All experiments were conducted upon 250-300g adult male Wistar rats (Charles River). Animals were initially anesthetized with 2-2.5% isofluorane. A closed cranial window was constructed as described in detail by Morii et al. [225] (Figure 19). The femoral artery and vein were cannulated for the measurement of blood pressure, blood gas values, and the delivery of drugs. An intraperitoneal catheter was implanted and α-chloralose and urethane (50 and 500 mg/kg i.p., respectively) anesthesia replaced isofluorane. Animals were tracheotomized, paralyzed with D-tubocurarine (1 mg/kg) and mechanically ventilated to control arterial blood gas values. The animal's head was fixed in a stereotaxic frame, the skull over the left parietal cortex in the middle cerebral artery territory was exposed, a craniotomy performed and the dura incised and reflected to provide direct pharmacological access to the cortical surface vasculature. The cranial window was constructed, covered with a glass coverslip and perfused with a perfusion pump with artificial cerebral spinal fluid through PE-50 inflow and

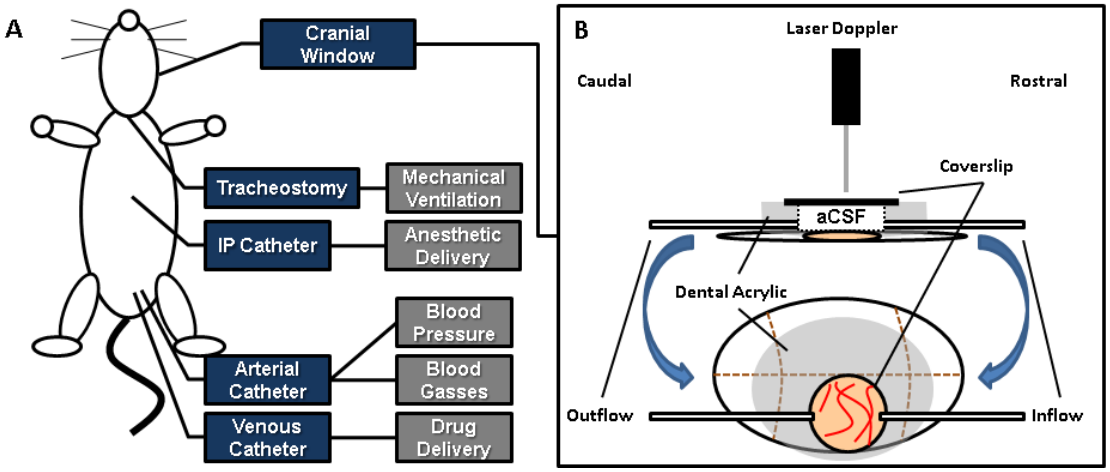

Figure 19. Schematic of rat closed cranial window preparation. (A) Adult male rats were anesthetized, mechanically ventilated, and surgically instrumented with femoral arterial and venous catheters for the measurement of arterial blood pressure, blood gas values and for the delivery of intravenous drugs. An intraperitoneal (IP) catheter was used to deliver anesthetics. (B) Side-on (top) and top-down (bottom) view of a closed cranial window installed over the right somatosensory cortex. The overlying bone and dura were removed to provide direct access to the cerebral surface vasculature. The window and the cortical surface were perfused with artificial cerebrospinal fluid (aCSF) and cortical blood flow was monitored with laser Doppler flowmetry.

outflow tubes. Cortical blood flow was monitored by laser Doppler flowmetry (Moor Instruments), the probe being positioned over a cortical surface artery in the middle cerebral artery territory.

Determination of the Role of EETs in Neurogenic Vasodilation in the Cerebral Circulation

To define the role of EETs in the regulation of the cerebral surface vasculature by perivascular vasodilator nerves, I utilized as a model of neurogenic vasodilation the electrical stimulation of efferent nerve fibers entering the ethmoidal foramen as described by Ayajiki et al. [63] (Figure 20). Briefly, the cerebral surface vasculature

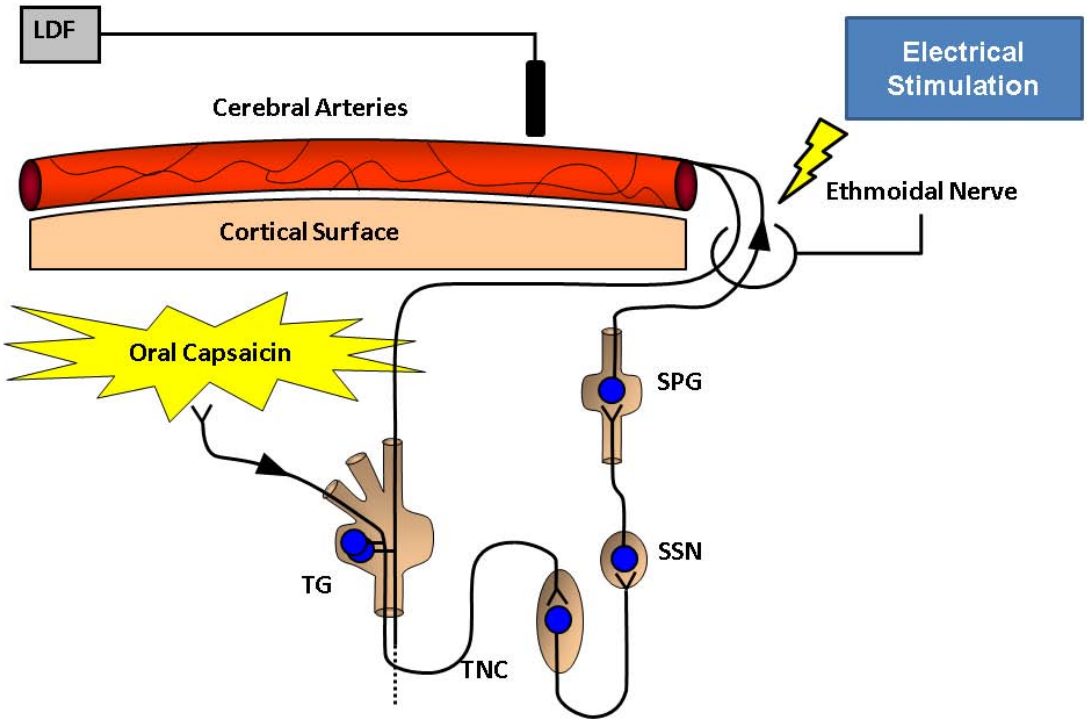

Figure 20. Cerebral neurogenic vasodilation paradigm. Cerebral blood flow was monitored by laser Doppler flowmetry (LDF) via a closed cranial window. CSF and drugs was administered within the window, directly to the cortical surface. Electrical stimulation of the efferent parasympathetic and afferent trigeminal nerve supply to the anterior cerebral vasculature in the ethmoidal nerve produces neurogenic cerebral vasodilation. Oral capsaicin administration activates TRPV1-expressing trigeminal afferents, which recruits trigeminovascular reflex hyperemia via brain stem connections with the parasympathetic sphenopalatine ganglia (SPG). Trigeminal ganglia, TG; trigeminal nucleus caudalis, TNC; superior salivary nucleus, SSN.

was exposed using a closed cranial window over the middle cerebral artery territory of the parietal cortex. The ethmoidal nerve bundle containing parasympathetic efferent fibers from the sphenopalatine ganglion and sensory afferents projecting to the trigeminal ganglion was isolated and stimulated with a fine bipolar stimulating electrode (1 ms pulse at 10 V) for 30 s. The resulting changes in cerebral blood flow and mean arterial blood pressure were monitored. A frequency-response curve (5, 10, 20 Hz) was constructed and the effect of the putative EETs antagonist 14,15-EEZE (10

µmol/L n=8) [220], administered to the cortical surface 30 min prior to stimulation, upon the neurogenic hyperemic response was determined.

To confirm the specificity of the putative EETs antagonist 14,15-EEZE in blocking EETs-mediated signaling, I directly administered increasing concentrations of 14,15-EET (10 nmol/L-10 µmol/L) to the cortical surface and recorded the resulting increase in cerebral blood flow both in the presence and absence of 14,15-EEZE (10 µmol/L, n=4). In these experiments, the effect of 14,15-EEZE upon the cerebral blood flow response to transient hypercapnia was likewise determined both prior to and following drug treatment. Mild transient hypercapnia was induced by ventilating the rat with a 5% CO2/30% O2/65% N2 gas mixture for 3 min, during which the cerebral blood flow response was monitored.

Chemical Stimulation of Oral Trigeminal Fibers

A second, more 'physiological' model of neurogenic cerebrovasodilation was evoked through stimulation of oral trigeminal nociceptor fibers as previously described by Gottselig and Messlinger [69]. Cumulative doses of the TRPV1 agonist capsaicin (300 µl, 10 µmol/L–1 mmol/L) were instilled orally at 10 min intervals, the resulting cortical hyperemia was measured by laser Doppler flowmetry (Figure 20).

To determine the role of EETs signaling in the neurogenic regulation of the cortical vasculature, pharmacological inhibition of portions of the EETs signaling system was employed. The putative EETs antagonist 14,15-EEZE (10 µmol/L, n=8), or the CYP epoxygenase inhibitor MS-PPOH (20 µmol/L, n=8) were perfused in the

closed cranial window for 45 min individually for each of two groups of animals. In each case, capsaicin dose-response trials were repeated within the same animal, both in the absence and presence of the pharmacological agent. In order to control for sensitization or desensitization of the capsaicin-evoked hyperemic response, half of the trials from each group began with the vehicle treatment arm followed by the drug treatment arm. In the other half, the order was reversed. The two treatment arms were separated by a 1 hr period during which the mouth was liberally irrigated with saline. Additionally, in a separate group of animals the capsaicin dose-response trials were repeated with the same 1 hr period between arms in order to detect any measurable sensitization or desensitization of this response (n=4).

To confirm that the capsaicin-evoked cerebral blood flow response was in fact mediated by cortical perivascular vasodilator nerves originating in the parasympathetic sphenopalatine ganglion or the sensory trigeminal ganglion, the efferent parasympathetic and afferent sensory nerve supply to the anterior circle of Willis was surgically cut as it entered the ethmoidal foramen. Following 1 hr of recovery time, the effect of nerve lesion upon the hyperemic response to oral trigeminal fiber stimulation was measured (n=4).

Optical Microangiography

To confirm that the cortical hyperemic response to oral capsaicin administration was in fact the result of cerebral vasodilation, rather than an associated elevation in perfusion pressure, in a limited study (n = 1) I employed a novel optical coherence

tomography-based imaging technique termed optical microangiography [226,227] which is capable of resolving 3D distribution of dynamic blood perfusion at the capillary level *in vivo*. Briefly, the cortex was illuminated at 1310 nm, the resulting backscattered and reference light being detected to produce spectral interferograms within the imaging system. Volumetric imaging data was collected by scanning the probe beam through a 1000 x 500 x 512 voxel cube, representing 2.5 x 2.5 x 2 mm^3 (x-y-z) of tissue. For high temporal resolution scans, continuous x-z plane scans were performed at a selected segment of the middle cerebral artery. Imaging of the left middle cerebral artery was conducted through a thinned skull. Capsaicin (10 μmol/L) was administered orally as above and the resulting hyperemic response was imaged through a thinned skull, including changes in middle cerebral artery diameter, middle cerebral artery blood velocity, and middle cerebral artery volume rate (flow).

Chemicals

The composition of artificial cerebrospinal fluid was as follows (in meq/l): 156.5 Na^+, 2.95 K^+, 2.50 Ca^{2+}, 1.33 Mg^{2+} and 24.6 HCO_3^-, and (in mg/dl) 66.5 dextrose and 40.2 urea. Capsaicin (vehicle: 0.1% ethanol in saline), D-Tubocurarine, α-chloralose and urethane were purchased from Sigma. 14,15-EET (vehicle: 0.1% ethanol in artificial cerebrospinal fluid), 14,15-EEZE (vehicle: 0.1% ethanol in artificial cerebrospinal fluid) and MS-PPOH (vehicle: 0.1% ethanol in artificial cerebrospinal fluid) were purchased from Cayman Chemical.

Statistics

All data are expressed as means ± SEM. Variations among animals in mean arterial blood pressure and laser Doppler flowmetry were normalized by reporting them as the percentage change from the baseline value (100% x (final value-baseline value)/baseline value). Comparisons of data were made with paired or un-paired Student's *t*-test or with ANOVA, followed by a *post hoc* Tukey's test. A value of $p < 0.05$ was considered significant.

Results

No treatment (excepting transient hypercapnia) had any significant effect upon mean arterial blood pressure, blood gas values, or the cerebrovascular reactivity to mild hypercapnic ventilation (Table 10).

EETs Signaling in the Cerebral Blood Flow Response to Ethmoidal Nerve Stimulation

In order to investigate the role of EETs signaling in the regulation of cerebral blood flow by perivascular vasodilator nerves, electrical stimulation of the ethmoidal nerve was utilized to produce neurogenic cerebral vasodilation which was assessed by laser Doppler flowmetry within a closed cranial window preparation. The ethmoidal nerve is comprised of both the efferent parasympathetic and afferent trigeminal nerve supply

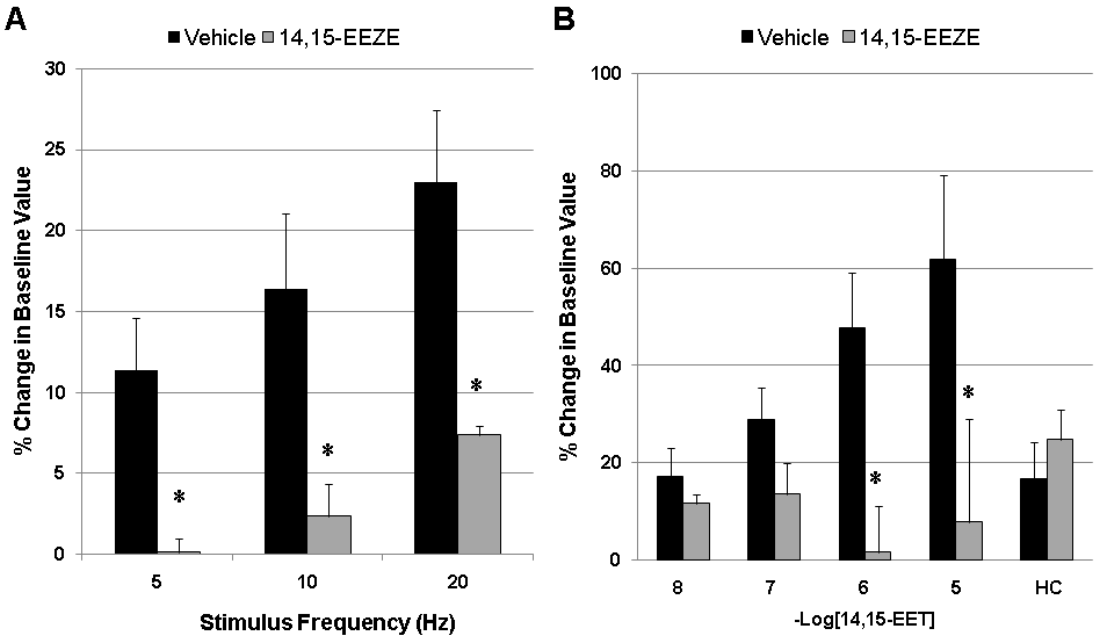

Figure 21. Effect of 14,15-EEZE upon neurogenic vasodilation evoked by electrical ethmoidal nerve stimulation. (A) Electrical stimulation of ethmoidal nerve (30 s, 5-20 Hz) produced a frequency-dependent increase in cortical blood flow. This response was significantly attenuated by pre-treatment with the putative EETs antagonist 14,15-EEZE (*P < 0.05 ANOVA vehicle treated vs. 14,15-EEZE-treated, n=6). (B) Direct administration of 14,15-EET to the cortical surface produced a dose-dependent increase in cerebral blood flow. This effect was blocked by the putative EETs antagonist 14,15-EEZE (*P < 0.05 ANOVA vehicle treated vs. 14,15-EEZE-treated, n=4), while the cerebral blood flow response to transient hypercapnia was not altered by treatment with 14,15-EEZE.

to the anterior cerebral surface vasculature. Electrical stimulation of the ethmoidal nerve resulted in a frequency-dependent increase in cortical blood flow (Figure 21A). This hyperemia began immediately upon the initiation of the stimulus train, peaking within 20 s and returning immediately to baseline cerebral blood flow values upon termination. Importantly, the stimulus-evoked increase in cortical blood flow was not accompanied by any changes in mean arterial blood pressure or other physiological parameter (Table 10). Pharmacological blockade of the EETs signaling pathway with

Table 10. Effect of Drug Treatment Upon Physiological and Cerebrovascular Variables

Treatment Group	MABP (mmHg)	pH	$PaCO_2$	PaO_2	DCBF (%)	HC_I	HC_F
None	94 ± 6	7.40 ± .08	35.8 ± 4.6	154 ± 22	3.5 ± 1.1	18.0 ± 4.3	30.3 ± 13.4
Hypercapnia	90 ± 6	7.36 ± .12	49.6 ± 8.7	127 ± 15	18.0 ± 4.3	NA	NA
14,15-EET	107 ± 10	7.38 ± .09	32.5 ± 5.1	117 ± 12	61.8 ± 17.5	38.1 ± 9.6	26.1 ± 12.0
14,15-EEZE	103 ± 9	7.39 ± .06	29.7 ± 8.3	150 ± 19	-7.8 ± 3.3	19.7 ± 8.3	26.1 ± 10.4
MS-PPOH	98 ± 12	7.40 ± .07	34.9 ± 6.1	145 ± 14	-5.4 ± 10.1	19.6 ± 1.7	22.6 ± 2.5
Electrical Stimulation	102 ± 12	7.38 ± .02	31.6 ± 4.5	138 ± 9	23.4 ± 4.2	36.8 ± 5.9	69.2 ± 18.7
Capsaicin	98 ± 14	7.41 ± .05	31.1 ± 6.4	161 ± 36	25.2 ± 4.1	18.6 ± 9.4	30.3 ± 7.2
Nerve Lesion	95 ± 7	7.41 ± .04	34.1 ± 9.2	114 ± 7	1.5 ± 7.7	25.9 ± 11.2	37.1 ± 10.1

All values are means ± SE. MABP, mean arterial blood pressure; Pa_{CO2}, arterial P_{CO2}; Pa_{O2}, arterial P_{O2}; DCBF, % change (100% x (final value – initial value)/initial value) in LDF value; HC_I, initial % change in LDF to transient hypercapnia; HC_F, post-treatment % change in LDF to transient hypercapnia.

the putative EETs antagonist 14,15-EEZE (10 μmol/L, n=6) significantly attenuated the hyperemic response to ethmoidal nerve stimulation, from a peak of 23 ± 4% at 20 Hz with vehicle treatment to 7 ± 1% following antagonist administration (Figure 21A, *P < 0.05 ANOVA vehicle vs. 14,15-EEZE treatment).

In order to confirm that 14,15-EEZE effectively inhibited EETs-mediated actions in the cerebral circulation, the effect of the antagonist on EETs-evoked increases in cerebral blood flow was assessed. Direct administration of 14,15-EETs (10 nmol/L-10 μmol/L) to the cortical surface produced a concentration-dependent increase in cerebral blood flow (Figure 21, peak value 62% at 10 μmol/L 14,15-EETs). The increase in cerebral blood flow resulting from 14,15-EETs administration was

blocked by pre-treatment of the cortical surface vasculature with 10 µmol/L 14,15-EEZE (8% at 10 µmol/L 14,15-EETs; *$p < 0.05$ ANOVA 14,15-EETs vs. 14,15-EETs + 14,15-EEZE; n = 4).

An unrelated vasomotor stimuli, transient mild hypercapnic ventilation, was utilized to demonstrate that the action of 14,15-EEZE was specific to EETs-mediated effects. Animals were ventilated for 3 min with a 5% CO_2, 30% O_2, 65% N_2 gas mixture to induce transient and mild hypercapnia ($PaCO_2$ ~ 45 mmHg vs. baseline value of ~30 mmHg). As has been described previously, such a stimulus produces cortical hyperemia that is independent of the EETs signaling pathway. Importantly, pre-treatment of the cortical surface with 14,15-EEZE (10 µmol/L, n=4) had no effect on the hyperemic response to transient hypercapnia (Figure 21B), thus indicating that the effects of 14,15-EEZE upon cerebral blood flow are specific to EETs signaling pathways.

Characterization of Neurogenic Vasodilation Resulting from Oral Trigeminal Fiber Stimulation

A second mode of stimulation was used to further evaluate the role of EETs signaling in the regulation of cerebral blood flow by cerebral perivascular vasodilator nerves. Stimulation of TRPV1-expressing trigeminal nociceptors with the neurotoxin capsaicin results in a reflex cortical hyperemia that is believed to involve the ‘trigeminovascular’ recruitment of efferent parasympathetic vasodilation of the

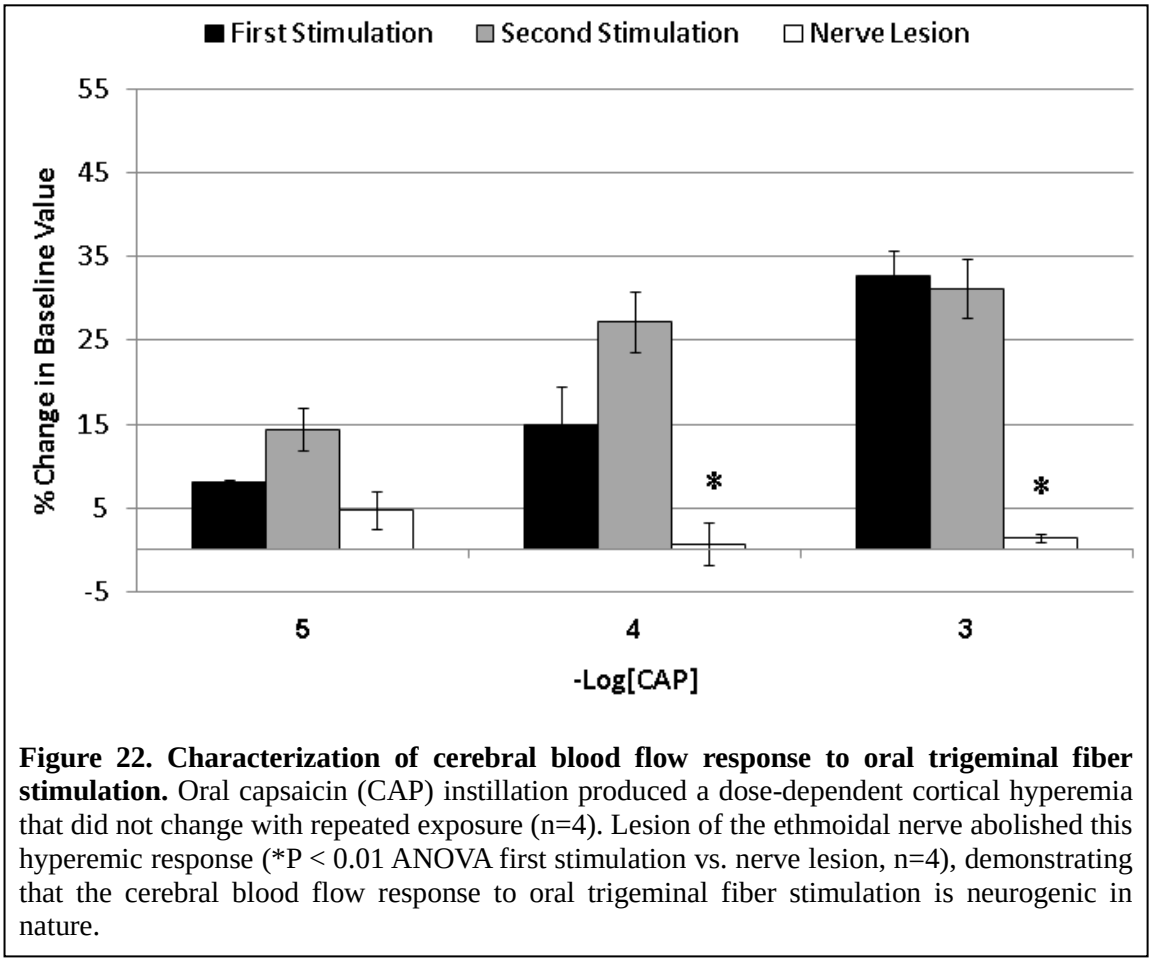

Figure 22. Characterization of cerebral blood flow response to oral trigeminal fiber stimulation. Oral capsaicin (CAP) instillation produced a dose-dependent cortical hyperemia that did not change with repeated exposure (n=4). Lesion of the ethmoidal nerve abolished this hyperemic response (*P < 0.01 ANOVA first stimulation vs. nerve lesion, n=4), demonstrating that the cerebral blood flow response to oral trigeminal fiber stimulation is neurogenic in nature.

cerebral surface vasculature [69]. Accordingly, oral instillation of capsaicin (10 µmol/L–1 mmol/L) produced a concentration-dependent cortical hyperemia peaking at 33 ± 3% at the highest concentration of 1 mmol/L (Figure 22). This response was slow to develop, peaking 4-8 min following capsaicin instillation and persisting for the 10 min duration of exposure. The capsaicin-evoked hyperemia was reversible, cerebral blood flow returning to basal levels after oral irrigation with saline and a one-hour recovery period. Repeated instillation of capsaicin following recovery resulted in an unchanged hemodynamic response (Figure 22), ruling out sensitization or desensitization of this effector pathway under the present experimental conditions.

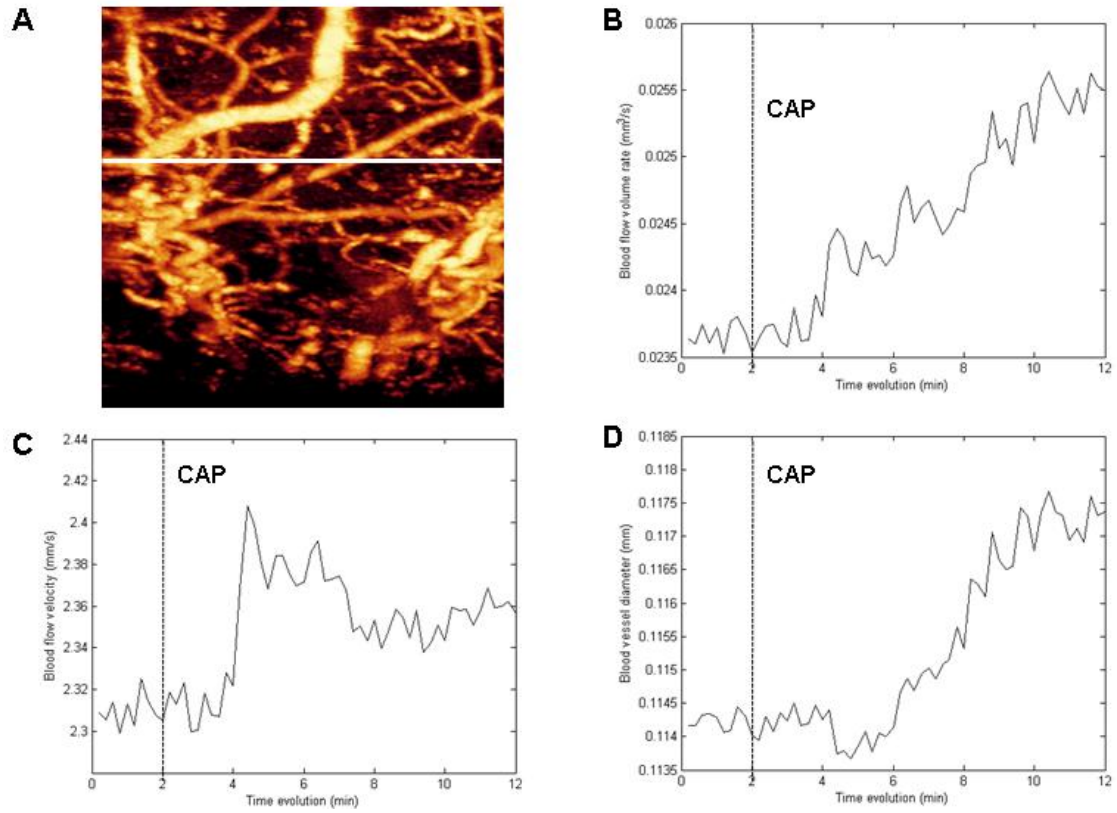

Figure 23. Evaluation of cerebral hemodynamic response to oral capsaicin administration by optical microangiography. (A) Optical microangiography image of the rat cortical vasculature. The middle cerebral artery was imaged through cross-section 2-D (x-z plane) line scan (white line). (B) Oral nociceptor stimulation (10 μmol/L capsaicin (CAP)) produced a long-lasting increase in middle cerebral artery blood flow beginning 2 minutes following the onset of stimulation and peaking at 108.5% of baseline value. (C) An immediate, small (2.6%) and static elevation in middle cerebral artery blood velocity accompanied the onset of capsaicin instillation. This effect does not account for the middle cerebral artery blood flow response. (D) Oral capsaicin stimulation produced a gradual and long-lasting increase in middle cerebral artery diameter to 102.8% of baseline that corresponds both temporally and in terms of magnitude to the flow effect observed in A.

In some cases, a mild (<10 mmHg) pressor effect was observed in response to oral capsaicin instillation. This effect was transient, resolving within the first minute following oral trigeminal fiber stimulation, in contrast to the observed hyperemia which peaked minutes later and persisted for an extended period of time. Optical

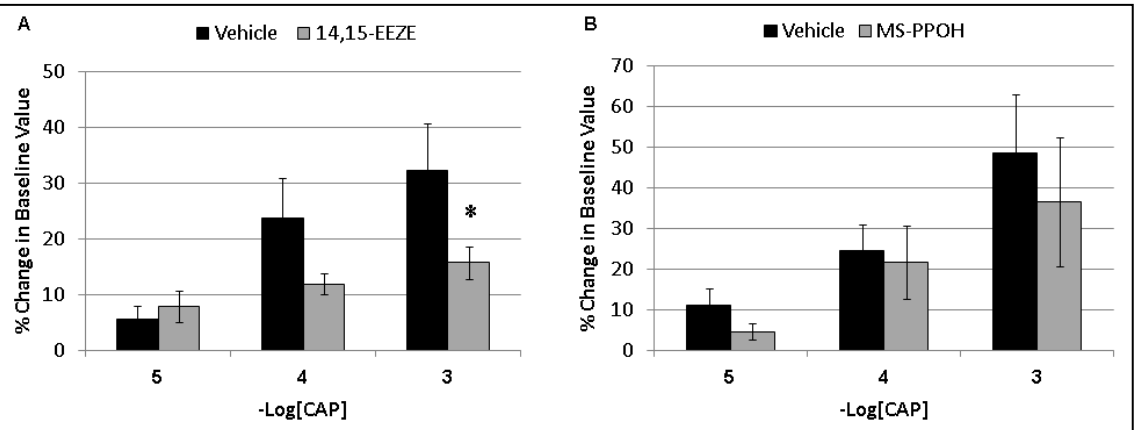

Figure 24. Role of EETs signaling in the cerebral blood flow response to oral trigeminal fiber stimulation. (A) Local application of the putative EETs antagonist 14,15-EEZE attenuated the hyperemic response to oral trigeminal fiber stimulation ($p<0.05$ ANOVA vehicle treated vs. 14,15-EEZE treated, n=8). (B) Local administration of the CYP epoxygenase inhibitor MS-PPOH did not significantly alter the vascular response to oral capsaicin (CAP) administration (n = 8).

microangiography imaging of the rat middle cerebral artery revealed that oral capsaicin (10 μmol/L) administration resulted in a persistent increase in volume rate (flow), increasing to 108.5% of baseline levels within 8 min of stimulation (Figure 23B). At the onset of nociceptor stimulation, a small (2.6%) and static elevation in blood velocity was recorded that accounted for the immediate component of the middle cerebral artery blood flow response (Figure 23C). A 2.8% dilation of the middle cerebral artery was then observed that accounted for the majority of the stimulation-evoked blood flow response (Figure 23D), following the 4^{th} power relationship between diameter and flow predicted by Poiseuille's Law. These findings confirm that the increase in middle cerebral artery flow rate is attributable primarily to direct vasodilation rather than a change in perfusion pressure resulting from nociceptor activation.

In order to confirm that the cerebral blood flow response to oral trigeminal

fiber stimulation was 'neurogenic' in nature, the parasympathetic and trigeminal nerve supply to the anterior cortical surface vasculature in the ethmoidal nerve was lesioned. Nerve lesion did not alter mean arterial blood pressure, blood gas values, resting cerebral blood flow or the reactivity of the cortical vasculature to transient hypercapnia (Table 10). The cerebral blood flow response to oral trigeminal fiber stimulation with capsaicin was abolished by nerve transection (Figure 22, $P<0.01$ ANOVA intact vs. nerve lesion, $n = 4$), demonstrating that this response required intact peripheral transmission to the cerebral vasculature. These findings establish that the cortical hyperemia resulting from oral trigeminal fiber stimulation is due to the *bona fide* neurogenic dilation of cortical surface arteries.

EETs Signaling in the Cerebral Blood Flow Response to Oral Trigeminal Fiber Stimulation

The participation of EETs signaling in the regulation of cerebral blood flow by perivascular vasodilator nerves was evaluated by examining the effect of the putative EETs receptor antagonist 14,15-EEZE on the cortical hyperemia produced by oral trigeminal fiber stimulation. Pre-treatment of the cortical surface vasculature with 14,15-EEZE (10 µmol/L, n=8) attenuated the hyperemic response to oral capsaicin instillation, from a peak value of 33 ± 8% with 1 mmol/L capsaicin in the absence of inhibitor to 16 ± 3% in the presence of 14,15-EEZE (Figure 24A, $P < 0.05$ ANOVA vehicle vs. 14,15-EEZE treatment). In contrast, inhibition of CYP epoxygenase activity with MS-PPOH (n=8) did not significantly alter the cortical hyperemic

response oral trigeminal fiber stimulation (Figure 24B). These pharmacological data provide evidence for the functional involvement of EETs signaling in the regulation of cerebral blood flow by extrinsic perivascular vasodilator fibers.

Discussion

In the present study, I demonstrate a functional role for EETs in the regulation of cerebral blood flow by perivascular vasodilator nerves. These findings support a novel role for perivascular nerve-derived EETs in the regulation of cerebral blood flow by extrinsic perivascular vasodilator fibers.

Cerebral blood flow is controlled in part by extrinsic perivascular nerve fibers innervating conduit arteries of the cerebral surface vasculature, including the middle cerebral artery. This extrinsic innervation is composed of three populations of perivascular fibers: sympathetic vasoconstrictor fibers from the superior cervical ganglia, parasympathetic vasodilator fibers from the sphenopalatine or otic ganglia, and vasodilator sensory afferents that project to trigeminal ganglia [11]. In previous chapters, I document the presence of the EETs-synthetic CYP-2J and EETs-metabolizing sEH enzymes in both parasympathetic sphenopalatine and trigeminal neurons (Figure 9, 10), including those innervating the cerebral vasculature (Figure 7). These CYP epoxygenase enzymes were found to be constitutively functional in primary trigeminal ganglion neurons, with endogenous EETs being detected within these cells by LC-MS/MS (Table 8). Lastly, I demonstrated that these neurogenic EETs positively regulate the release of the vasoactive neuropeptides CGRP and substance P from these neurons (Figure 16). These findings raise the possibility that

these lipids may contribute to neurogenic vasodilation by these fibers.

To determine if EETs play a functional role in the neurogenic control of cerebral blood flow, I stimulated vasodilation using two methods. The first method entailed direct electrical stimulation of efferent nerve fibers innervating the middle cerebral artery [63], whereas the second method involved chemical stimulation of oral nociceptors with the TRPV1 agonist capsaicin, as previously described by Gottselig and Messlinger [69]. This latter method involves the activation of a neuronal reflex pathway including the trigeminal ganglia, the trigeminal and superior salivary nuclei in the brain stem, and the recruitment of efferent parasympathetic fibers from the sphenopalatine ganglia. While this method involves the indirect stimulation of parasympathetic vasodilator fibers, it may be considered more physiological than direct nerve stimulation.

To confirm that chemical stimulation-evoked dilation is specifically mediated through nerve activation, I demonstrated that lesion of the ethmoidal nerve, which is composed of trigeminal afferents and efferent parasympathetic sphenopalatine ganglia fibers innervating the anterior circle of Willis, abolished the cerebral blood flow response to oral capsaicin administration. I further confirmed that the hyperemic response to oral nociceptor stimulation was attributable to cerebrovasodilation rather than any effect of capsaicin administration on perfusion pressure and blood velocity.

I found that 14,15-EEZE alone slightly reduced basal cerebral blood flow, suggesting that EET signaling contributes to the maintenance of resting cerebral blood flow. Such a finding is in agreement with a previous study [141] in rats demonstrating that inhibition of CYP enzymes with miconazole reduced resting cerebral blood flow.

It is inconsistent with other recent findings in which 14,15-EEZE had no discernible effect on resting cerebral blood flow [228]. These disparate responses, in light of the mild effects of 14,15-EEZE on resting cerebral blood flow in the present study, suggest that the contribution of EET signaling to resting cerebral blood flow may be small in magnitude and sensitive to differences in experimental methodology.

Within both models of neurogenic vasodilation, pretreatment of the cortical surface vasculature with the putative EETs antagonist 14,15-EEZE markedly attenuated the hyperemic response to chemical or electrical stimulation. Because the cerebral blood flow response to transient hypercapnia was not altered by 14,15-EEZE, it is unlikely that the small shift in basal vascular tone or a nonspecific effect on vascular reactivity accounts for the ability of 14,15-EEZE to inhibit neurogenic hyperemia. Rather, these findings suggest that EET signaling participates in the regulation of cerebral blood flow by extrinsic perivascular vasodilator nerves.

In contrast to the present results with the putative EETs antagonist 14,15-EEZE, administration of the CYP epoxygenase inhibitor MS-PPOH to the cortical surface did not alter cerebral blood flow responses to oral trigeminal fiber stimulation. This result is consistent with those from the above primary trigeminal ganglion neuronal cultures in which short-term inhibition of CYP epoxygenase did not alter stimulus-evoked neuropeptide release, whereas long term CYP epoxygenase inhibition mimicked the effect of the EETs antagonist 14,15-EEZE (Figure 16, 17). This suggests that *de novo* synthesis of EETs is not required for the present neurogenic vasodilation and may reflect the existence of a latent membrane phospholipid-bound pool of EETs not depleted within the 45-min treatment window. Such a releasable

pool of EETs has been described in the vascular endothelium [159] and brain astrocytes [162]. Interestingly, although I reported robust CYP-2J immunoreactivity in trigeminal and sphenopalatine neuronal soma (Figure 9, 10), I did not detect CYP-2J immunoreactivity in individual perivascular neurons surrounding whole mount cerebral surface arteries (Figure 12). One explanation for these findings is that in perivascular nerves, EETs may be synthesized centrally, whereas release of these vasoactive compounds may occur peripherally from a latent membrane-bound pool.

The present findings support my initial hypothesis that vasodilator EETs represent novel nerve-derived relaxing factors in the cerebral circulation. It is important to note that the cellular mechanisms underpinning the regulation of cerebral arteries by parasympathetic and sensory perivascular fibers have been studied in detail, and the vasomotor actions of these nerves have been largely attributed to such factors as nitric oxide and the neuropeptides VIP and CGRP [11]. In a study [69] characterizing the cerebral blood flow response to oral capsaicin administration, the hyperemic response to capsaicin was abolished by the administration of a VIP receptor antagonist to the dural surface. In other studies [62,63,83] investigating cerebral blood flow responses to electrical stimulation of parasympathetic and sensory perivascular fibers, major contributions have been reported for nitric oxide and CGRP. Given the pronounced effect of 14,15-EEZE upon neurogenic hyperemia reported in the present study, it is likely that the EETs signaling pathway interacts in some manner with these other vasomotor pathways.

In my own *in vitro* studies, I was unable to detect the release of EETs from primary trigeminal ganglion neurons by a sensitive LC-MS/MS method, either basally

or in response to two different modes of neuronal stimulation (Table 9). In contrast, the release from these neurons of the vasoactive neuropeptides CGRP and substance P was readily detectable (Figure 16), as was that of three different arachidonic acid metabolite HETEs (Table 9). These data suggest that EETs may not act as a releasable nerve-derived relaxing factor as I initially hypothesized. In primary trigeminal ganglion neuronal cultures, it was observed that neuronal EETs regulated stimulus-evoked release of both CGRP and substance P. In light of these findings, the current *in vivo* data demonstrating a role for EETs signaling in the regulation of cerebral blood flow by perivascular vasodilator nerves may be attributable to EETs' role in regulating the release of vasodilator neuropeptides such as CGRP or VIP. Such a role was recently observed for prostaglandin E2 in the modulation of nitric oxide release from sphenopalatine ganglia neurons [229] and for cannabidiol in the modulation of CGRP release from dorsal root ganglia neurons [230].

In summary, I identify for the first time the functional involvement of EETs signaling in the neurogenic regulation of cerebral blood flow by these vasodilator fibers. These findings suggest that the role of EETs in regulating vasoactive neuropeptide release from primary trigeminal ganglion neurons is functionally relevant *in* vivo. Such a role for neurogenic EETs will have significant implications upon our understanding of the role that these important vasoactive lipids play in cardiovascular regulation. Their specific presence in the cerebral vasculature may have important clinical significance relative to neurovascular disorders such as migraine, vasospasm after subarachnoid hemorrhage, and stroke.

Chapter 6. Summary and Conclusions

Cerebral blood flow is regulated across a wide range of physiological conditions, matching the high metabolic demands of this extremely sensitive organ. This regulation is accomplished through three overlapping modes of vasomotor control. First, cerebral blood vessels intrinsically regulate their own vasomotor tone in response to changes in their physical and chemical environments [10,188]. This includes endothelium-dependent flow-mediated vasodilation, a process through which changes in endothelial shear stress are transduced by the endothelium to produce vasodilation, coordinating vasomotor tone along the cerebrovascular tree. Next, local cerebral blood flow is matched to changes in local neuronal activation, and thus metabolic demand, through the process of neurovascular coupling [1]. Through this mechanism, neuronal activity results in the neuronal or astrocytic production of vasoactive factors that dilate local cortical arterioles to increase local blood supply. Lastly, the cerebral surface vasculature is innervated by three populations of vasomotor perivascular nerves [11,56]. These peripheral vasodilator and vasoconstrictor nerves exert a 'top-down' regulation of regional cerebral blood flow and function to safeguard the cerebral circulation from damaging hypoperfusion or hyperperfusion.

EETs are potent vasodilators in the cerebral vasculature where they exert numerous regulatory influences upon vascular function [96,97]. In addition to being pro-angiogenic, anti-inflammatory and anti-thrombotic (Table 1), EETs contribute to the vasomotor regulation of the cerebral circulation at multiple levels. Endothelium-derived EETs participate in the intrinsic regulation of vasomotor tone, contributing to

flow-mediated vasodilation [4,5,174,190,191,192]. In a second mode of vasomotor regulation, astrocyte-derived EETs are mediators of neurovascular coupling in the cerebral cortex [6,7,99,193,194]. Whether EETs similarly participate in the third level of vasomotor control, the regulation of the cerebral surface vasculature by perivascular nerves, has not previously been investigated.

Although most recent attention has focused upon EETs' myriad cardiovascular effects, early and emerging experimental evidence suggested that EETs may also participate in elements of neural function as well. The earliest described biological function for these 'epoxide metabolites of arachidonic acid' came from the neural tissue of the hypothalamus and anterior pituitary. Here EETs were identified as endogenous constituents of this neural tissue, and as regulators of neurohormone release [129,130,131,199,200,201,202,203]. In more recent work, the neuron-specific expression of EETs-synthetic CYP-4X1 epoxygenases has been reported in human, rat and mouse brain [134,146,147]. In primary cortical neuronal culture, inhibition of the EETs-metabolizing enzyme sEH (which is thought to elevate endogenous EETs levels) protects neurons against simulated ischemic cell death [119]. This suggests a direct cytoprotective action of endogenous neuronal EETs in cortical neurons. These and other emerging studies suggest that in addition to their well-known cardiovascular effects, EETs may participate in the regulation of neuronal function.

In the present series of studies, I have tested the broad hypothesis that EETs contribute to the regulation of the cerebral surface vasculature by perivascular vasodilator nerves. To evaluate this hypothesis, I addressed four research questions. First, do cerebral perivascular vasodilator nerves express the biochemical machinery

for the synthesis and regulation of vasodilator EETs? Next, are CYP epoxygenases constitutively active in trigeminal ganglion neurons, and are EETs endogenously present within these neurons? Third, are EETs released from trigeminal ganglion neurons, and if not, what role do they play in neuronal cell function? Last, I evaluated whether EETs signaling participated functionally in the *in vivo* regulation of the cerebral surface vasculature by perivascular vasodilator nerves.

CYP Epoxygenase Enzymes are Specifically Expressed in Sphenopalatine and Trigeminal Ganglion Neurons

In Chapter 2, I evaluated whether perivascular vasodilator nerves express the enzymes necessary for the activity of the EETs signaling pathway. Prior data from our lab group had identified the expression of the EETs-metabolizing enzyme sEH in mouse cortical neurons by immunohistochemistry and in cerebral blood vessels by Western blot [153,154]. In my own preliminary data, I confirmed these findings in the rat (Figure 3, 5). Seeking to define the cell type-specific expression of sEH in cerebral arteries, I identified the expression of sEH in perivascular nerve fibers innervating the cerebral surface vasculature (Figure 6). While the neuronal expression of sEH was not necessarily novel, its expression in perivascular nerves was intriguing. Two questions emerged from these observations: which of the three populations of cerebral perivascular nerves express sEH, and does sEH expression reflect the presence of the EETs signaling pathway within these neurons? I addressed these questions experimentally in the order posed here.

Immunofluorescence double labeling studies revealed strong co-localization of sEH with nNOS and CGRP, moderate co-localization with VIP, choline acetyltransferrase, and substance P, and only very limited co-localization with dopamine β-hydroxylase and neuropeptide Y (Figure 7, 13, Table 5). Although the somewhat promiscuous expression of nNOS, VIP and CGRP between parasympathetic and trigeminal perivascular neurons prevented the specific identification of sEH expression in either population, the absence of sEH labeling in neuropeptide Y- or dopamine β-hydroxylase-positive neurons suggested that sEH was specifically expressed in the two vasodilator nerve populations, and not the vasoconstrictor nerve population. Immunofluorescence labeling within the sphenopalatine, trigeminal and superior cervical ganglia, which house the parasympathetic, sensory and sympathetic neuronal cell bodies [11], respectively, confirmed this finding. sEH expression was present in neurons throughout the sphenopalatine and trigeminal ganglia (Figure 9, 10). In contrast, cell bodies within the sympathetic superior cervical ganglia were devoid of sEH-immunoreactivity (Figure 13). This expression was corroborated at the mRNA level by RT-PCR which demonstrated sEH expression in both the sphenopalatine and trigeminal ganglia (Figure 8). These findings provide conclusive evidence that sEH, an enzyme importantly involved in EETs metabolism and regulation, is expressed specifically in perivascular vasodilator nerves, but not vasoconstrictor nerves, within the cerebral circulation. Given the potent vasodilator activity of EETs in the cerebral circulation [97,100], these findings provided the impetus for the broad hypothesis that neurogenic EETs contribute to the regulation of cerebral blood flow by perivascular vasodilator, as opposed to constrictor, nerves.

In light of these findings, I next sought to evaluate whether EETs-synthetic CYP epoxygenase enzymes were likewise expressed in these neurons. In mammalian systems, numerous CYP enzymes exhibit varying degrees of epoxygenase activity [95,132]. Thus, to test the hypothesis that perivascular vasodilator nerves express enzymes capable of EETs synthesis, I conducted an RT-PCR screen probing for the expression of eight known CYP epoxygenases of the CYP-2C and CYP-2J families (Figure 8). The specificity of the result was striking. While no CYP-2C expression was detected in the sphenopalatine and trigeminal ganglia, both rat CYP-2J isoforms, CYP-2J3 and CYP-2J4 were detected. The expression of these CYP-2J enzymes within these ganglia was confirmed by Western blot (Figure 8), while the specific expression of these enzymes in neuronal cell bodies within these ganglia was demonstrated by immunofluorescence double labeling (Figure 9, 10). These findings were conclusive, and suggested that CYP-2J exhibits neuron-specific expression within the parasympathetic sphenopalatine and trigeminal ganglia.

One obvious omission from the above studies was the orphan CYP epoxygenase CYP-4X1, which exhibits neuron-specific expression in the human, rat and mouse brain [134,146,147]. Using the same experimental approach, it would be useful to evaluate the expression of this neuronal CYP epoxygenase in the sphenopalatine and trigeminal ganglia. Conversely, it would be of interest whether CYP-2J likewise exhibits neuron-specific expression in the central nervous system. A previous report in the rat and human gut [215], in addition to the present findings detail CYP-2J expression in peripheral neurons while CYP-4X1 expression has been observed only in central neurons. One intriguing possibility is that different CYP

epoxygenases are expressed in peripheral versus central neurons. Because CYP-2J3, CYP2J4 and CYP-4X1 all produce a different distribution of the four EETs regio-isomers [134,146,147,210], and these four EETs regio-isomers may exhibit different biological activities [3,95], their segregation into peripheral versus central neurons might suggest distinct roles for EETs in these broad classes of neurons.

Given the universal expression of CYP-2J in neurons of the sphenopalatine and trigeminal ganglia (Table 6), CYP-2J and sEH must be co-expressed in most neurons within these parasympathetic and sensory ganglia. Immunofluorescent double labeling within the trigeminal ganglia confirmed this proposition (Figure 10N-P), however the lack of CYP-2J immunoreactivity in processes surrounding the cerebral surface vasculature (Figure 12) precluded the same analysis peripherally. Whether the expression of CYP-2J is exclusive to the parasympathetic and sensory neurons and does not extend to sympathetic neurons cannot yet be definitively stated. sEH expression was not observed in either cell bodies of the sympathetic superior cervical ganglia or peripheral sympathetic fibers innervating the cerebral surface vasculature (Figure 13). The corresponding analysis of CYP-2J expression in the superior cervical ganglia was not conducted. Thus, the expression of CYP-2J enzymes in sEH-negative sympathetic neurons cannot be excluded. While the present studies have focused upon the actions of EETs in perivascular vasodilator nerve populations, the production of EETs in sympathetic vasoconstrictor nerves likewise cannot be ruled out. This possibility complicates the interpretation of the current *in vivo* data evaluated below. For this reason, a detailed study of the expression of CYP epoxygenases within the sympathetic superior cervical ganglia would be of significant future interest.

CYP Epoxygenase is Constitutively Active and EETs Endogenously Present in Primary Cultured Trigeminal Ganglion Neurons

The experimental findings reported in Chapter 2 demonstrate conclusively that a specific family of CYP epoxygenases, the CYP-2Js, is expressed in neurons of the parasympathetic sphenopalatine and sensory trigeminal ganglia in rats. In Chapter 3, I sought to determine whether these enzymes were constitutively functional and whether EETs were endogenously present in these neuronal populations. For this work, a primary trigeminal ganglion neuronal culture model was adopted in order to evaluate the presence and functional contributions of EETs exclusively in neurons. Trigeminal ganglia were selected for study owing to their greater size (in dimensions and number of neurons) compared to the sphenopalatine ganglia. Utilizing a sensitive LC-MS/MS methodology, I assayed the presence of different arachidonic acid metabolites, including EETs and the hydrolysis product DHETs, in whole cell extracts from these neurons.

LC-MS/MS analysis detected the presence of 3 out of 4 EETs regio-isomers: 8,9-, 11,12- and 14,15-EET in trigeminal ganglion neurons. It also detected the 5,6-DHET metabolite. Because 5,6-EET is a poor substrate for sEH [3,149,150], the 5,6-DHET analyte likely represents the spontaneous hydrolysis produce of the unstable 5,6-EET regio-isomer. In this way, it appears that all four EETs regio-isomers are present within primary trigeminal ganglion neurons. As detailed in Chapter 3, the distribution of these EETs regio-isomers matches almost perfectly that of recombinant CYP-2J3 as characterized in a cell free biochemical assay [210]. These findings thus

demonstrate that the CYP epoxygenase enzymes detected in trigeminal ganglia in Chapter 2 are functional under basal conditions and that EETs are endogenous constituents of these neurons.

The expression of CYP-2J4 was also detected in trigeminal ganglion tissue (Figure 8). Because the CYP-2J4 isoform is known to produce significant quantities of the hydroxyl metabolite 20-HETE [231], the absence of this analyte from the LC-MS/MS results argues that CYP-2J4 is not active under basal conditions.

One perplexing finding from these studies was the absence of detectable DHETs within these cells despite the pronounced expression of sEH both *in vivo* and *in vitro* (Figure 10, 14). sEH rapidly hydrolyzes the EET regio-isomers into corresponding DHET species, with a substrate preference following the epoxide's proximity to the ω–carbon [3,149,150]. Although 14,15-EET was detected in considerable abundance within trigeminal ganglion neurons (Table 8) and represents the preferred substrate for sEH, no 14,15-DHET was detected. I can think of two explanations for this surprising finding. The first is that despite the expression of sEH within these neurons, this enzyme is catalytically inactive under the present experimental conditions. sEH activity is regulated both transcriptionally and by its sub-cellular sequestration into peroxisomes [232,233,234,235]. Such 'silent' sEH expression would be considered exceedingly unusual, however, as such modification of sEH is reported to produce a graded, rather than complete inhibition of EETs hydrolysis. Given the recent advent of commercially-available epoxide hydrolase assays [236], this possibility could be evaluated by determining whether epoxide hydrolase activity is present within these cells under basal conditions. This could be

done from both freshly-isolated trigeminal ganglion neurons, as well as from neurons subjected to primary culture conditions.

A second possibility centers upon the biochemical preparation used in the current LC-MS/MS analysis. In the present experiments, trigeminal ganglion extracts were subjected to acid hydrolysis in order to chemically liberate esterified EETs from the membrane phospholipids. In this way, the measures reported herein can be regarded as 'total cellular EETs'. EETs within cells typically exist in two compartments: membrane EETs (esterified) and 'free' EETs within the cytosol [237,238,239,240]. Although DHET re-incorporation into membrane phospholipids has been reported [241], it occurs at a much reduced rate compared to that of the corresponding EET regio-isomer. Thus, DHETs are typically restricted to the free cytosolic compartment. It is possible that our lipid extraction protocol 'lost' the free cytosolic fraction of EETs and DHETs, retaining only the membrane bound EETs. This would explain the presence of all four EETs regio-isomers (liberated from the membrane phospholipids) and the absence of any of the DHETs species (trapped in the cytosolic fraction with other free EETs). This possibility could be evaluated by conducting lipid extractions in parallel, with one sample undergoing acid hydrolysis to derive the total EETs fraction, and the other foregoing acid hydrolysis and representing the free EETs fraction. I would expect the free EETs fraction to have at least a low level of analyte detectable by LC-MS/MS. If EETs are detected in the free fraction, then the possibility that sEH is catalytically silent under basal conditions in trigeminal ganglion neurons is supported. If no EETs are detected in the free fraction, this may suggest a potential flaw in our lipid extraction protocol, and would require

the revisitation of this subject before the question of cellular EETs and DHETs levels could be conclusively decided.

No Evidence for the Release of EETs from Primary Trigeminal Ganglion Neurons

In the present series of studies, I proposed that EETs contribute to the regulation of cerebral blood flow by perivascular vasodilator nerves. Implicit within this broad hypothesis was the fact that EETs are potent cerebral vasodilators [97,100], and hence, my initial proposal that EETs are released by these vasodilator nerves to mediate their vasomotor action upon the associated cerebral vasculature. The finding in Chapter 3 that CYP epoxygenases are constitutively functional and that EETs are endogenously present within primary cultured trigeminal ganglion neurons (Table 8) suggests the possibility that these lipids may be released from these neurons, either basally or in response to activation. In Chapter 4 I sought to determine whether evidence of EETs release from trigeminal ganglion neurons could be detected by LC-MS/MS. However, despite plating neurons at a high density (10 ganglia/well) to maximize signal, I was not able to detect the presence of any of the four EETs regio-isomers or their corresponding DHET metabolites in the conditioned media from these cells (Table 9). This included either under basal conditions (1 hr incubation with buffer alone) or following a strong stimulus with depolarizing K^+ (60 mmol/L) or the TRPV1 agonist capsaicin (100 nmol/L). As discussed in Chapter 4, this failure to detect EETs or DHETs in the conditioned media does not likely represent a failure of either the lipid extraction methodology or the stimulus paradigm. Several HETE metabolites of arachidonic acid were detectable in significant quantities in the conditioned media,

indicating a successful lipid extraction. Under basal conditions, neuropeptide release into the conditioned media was readily detectable by ELISA, and under the same stimulation paradigm, the release of neuropeptide increased by up to 5-fold.

Although these findings suggest that EETs are not released from trigeminal ganglion neurons either under basal conditions or following stimulation, alternate explanations must also be considered. It is possible that EETs are released from these neurons, but in a manner that results in media concentrations below the limit of detection for this LC-MS/MS method (<5 pg/ml). Such low concentrations in the media might result either from the rapid sequestration of these lipophillic molecules from the aqueous media compartment and back into the lipid membrane, or from an active re-uptake processes. Either of these scenarios could conceivably result in undetectable levels of EETs within the media despite their release in physiologically relevant quantities. To evaluate these possibilities, it would be necessary to significantly improve the signal-to-noise ratio of the current LC-MS/MS protocol for the detection of EETs. One possible way to improve the sensitivity of the LC-MS/MS methodology would be to incubate the neurons with radiolabeled arachidonic acid and then assay the media for the release of radiolabeled EETs. A second approach could be to utilize a ‘trapping’ scheme to bind and preserve released EETs before they could be taken back up. Such a methodology that employs culturing and stimulating sensory neurons directly on antibody-coated ELISA plates has been used to detect the release of neurotrophins [242]. ELISA kits for the detection of 14,15-DHET are currently commercially available based upon an antibody that recognizes the DHET metabolite of 14,15-EET. If a similar antibody could be generated that binds one of the EETs

regio-isomers, a similar 'ELISA-*in situ*' technique could be used to detect low-level EETs release from trigeminal ganglion or other neurons. In light of these considerations, the present conclusion that EETs are not released from trigeminal ganglion neurons must remain a qualified one.

EETs are Regulators of Neuropeptide Release from Primary Trigeminal Ganglion Neurons

Having found no evidence for the release of EETs from primary trigeminal ganglion neurons, I modified my hypothesis to propose a second potential role for the EETs detected in these cells in Chapter 3. Early evidence in the EETs research field identified these 'novel epoxide metabolites of arachidonic acid' as regulators of hypothalamic and pituitary neurohormone release [129,130,131,199,200,201,202,203]. In these studies, three general experimental findings were made: EETs were present in rat hypothalamic and pituitary tissue extracts, exogenous administration of the various EETs regio-isomers stimulated neurohormone release from these tissues, and inhibition of CYP epoxygenase activity inhibited evoked neurohormone release in these cells. Based upon these studies, I surmised that the role of EETs in regulating the release of neurohormones in neuroendocrine tissue might be generalizable to other neuronal populations. Thus I next proposed that EETs regulate neuropeptide release from primary trigeminal ganglion neurons. Methodologically, I sought to follow the route of the earlier studies in neuroendocrine tissue. I had already identified the endogenous presence of the four EETs regio-isomers or their metabolites in primary trigeminal ganglion neurons (Table 8). I therefore set out to evaluate whether EETs

could directly stimulate neuropeptide release from these cells, and whether inhibition of EETs signaling reduced the release of neuropeptides evoked by other stimuli.

The finding that exogenous EETs directly stimulate CGRP release (Figure 15) is consistent with their pro-secretory effects in neuroendocrine tissue [129,199,200,201]. Compared to vehicle control, both 5,6-EETs and 14,15-EETs increased CGRP release approximately 2-fold. The other regio-isomers appeared to exert effects similar in magnitude, however, these were not statistically significant. In light of these data, it is reasonable to conclude that at least certain EETs (5,6- and 14,15-EETs) can directly stimulate neuropeptide release from primary trigeminal ganglion neurons. It is possible that the other EETs regio-isomers do exert an effect upon neuropeptide release, but with differing affinities. Such regio-selectivity has been reported for a number of EETs-mediated responses [3], including their vasomotor actions in the cerebral circulation [97,100]. In light of the present data, it would be useful to conduct more detailed concentration-response curves with larger sample sizes for the effects of the EETs regio-isomers upon neuropeptide release from primary trigeminal ganglion neurons. In this way, EETs-evoked neuropeptide release could be evaluated more definitively.

A key finding in the evaluation of EETs' role in neuropeptide release from primary trigeminal ganglion neurons was the observation that the putative EETs antagonist 14,15-EEZE attenuated stimulus-evoked CGRP and substance P release in response to stimulation with either capsaicin (100 nmol/L) or depolarizing K^+ (60 mmol/L, Figure 16). These findings are consistent with those from the hypothalamus and anterior pituitary, where inhibition of the EETs synthesis inhibited secretagogue-

evoked release of neurohormones [130,138,203], and suggest that EETs signaling contributes to this stimulus-evoked neuropeptide release. There are, however, some considerations that undermine the certainty of this conclusion.

First, the concentration-dependence of 14,15-EEZE-inhibition of CGRP release is weak (Figure 16B-C), dropping off mainly at the 10 μmol/L concentration. Such a steep concentration-response relationship runs contrary to 14,15-EEZE's established role as a non-specific competitive antagonist of EETs' effects [220] and may suggest a non-specific action of this antagonist upon trigeminal ganglion neuronal health or release capacity. Two further studies would help rule out such non-specific actions of this antagonist. The first is to determine whether 14,15-EEZE is directly toxic to these neurons, evaluating cell death in culture by the standard lactate dehydrogenase or other method following capsaicin or K^+ stimulation in the presence of absence of 14,15-EEZE or vehicle. In this way, the contribution of an interaction between stimulation, 14,15-EEZE and vehicle to neuronal toxicity could be evaluated and separated from the reported effect of 14,15-EEZE on evoked neuropeptide release.

A second possibility is that 14,15-EEZE is non-specifically interfering with primary trigeminal ganglion neuronal function at concentrations above 1 μmol/L. Such an effect would account for the steep concentration-response relationship observed for 14,15-EEZE inhibition of evoked neuropeptide release. One possible way to rule out such an effect would be to determine whether 14,15-EEZE blocks the stimulus-evoked release of other non-peptide transmitters from these neurons. In the present studies, I report that EETs contribute to the release of neuropeptides while in neuroendocrine tissue, EETs contribute to neurohormone release [130,138,203]. These

transmitters are all released from large dense-core vesicles [243,244]. It is possible that EETs contribute only to transmitter release from this type of large vesicle and not from smaller vesicles containing small molecule transmitters such as glutamate. Similar experiments could be conducted evaluating the effect of 14,15-EEZE upon glutamate or other transmitter release from primary trigeminal ganglion neurons [245]. The preservation of evoked release of these transmitters in the presence of inhibition of neuropeptide transmitter release would argue strongly for the specific action of EETs in facilitating neuropeptide transmitter release from primary trigeminal ganglion neurons.

One finding that does suggest that the effect of 14,15-EEZE upon evoked neuropeptide release is specific to the action of the EETs signaling pathway is the similar inhibition of capsaicin- and K^+-evoked CGRP release by long-term inhibition of CYP epoxygenase activity by MS-PPOH (Figure 16, 17). The ability of two distinct pharmacological agents, acting on two different targets, to inhibit evoked release strongly supports the involvement of EETs signaling in this process. That being said, there are some important caveats to the interpretation of the MS-PPOH data as well.

The primary caveat centers upon the observation that long term (48 hr) but not acute (30 min) inhibition of CYP epoxygenase with MS-PPOH reduced stimulus-evoked CGRP release from primary trigeminal ganglion neurons. This finding was not entirely unexpected, as EETs are known to be released from pre-formed pools in phospholipid membranes in both endothelial cells and cortical astrocytes [139,160,161]. EETs release from these esteriefied pools is insensitive to acute CYP epoxygenase inhibition, but can be blocked when cellular EETs levels are depleted by

long-term CYP epoxygenase inhibition. Thus, the present experimental findings are consistent with the release of EETs from a pre-formed pool, perhaps residing in membrane phospholipids. This conclusion was not directly tested, however.

Two important experiments could be conducted to confirm this mode of EETs mobilization in primary trigeminal ganglion cells. The first is to determine if inhibition of phospholipase A2 has the same effect as 14,15-EEZE upon evoked neuropeptide release. As this is the enzyme responsible for cleavage of esterified EETs from membrane phospholipids [237], its inhibition should result in a similar effect as 14,15-EEZE or long-term CYP epoxygenase inhibition. A second important experiment would be to confirm that long-term CYP epoxygenase inhibition does in fact deplete cellular EETs levels. This could be done in a straightforward manner, treating primary trigeminal ganglion neurons for 48 hours with MS-PPOH or vehicle, then subjecting cell extracts to LC-MS/MS analysis of EETs content. If EETs are being released from a stored pool in the phospholipid membrane, long-term inhibition of CYP epoxygenase should result in a reduction in cellular EETs levels.

A second caveat regarding the present findings with MS-PPOH is similar to the issues arising from 14,15-EEZE treatment. Does long-term treatment with MS-PPOH non-specifically kill primary trigeminal ganglion neurons or render them in some way non-functional? Evaluation of whether 48 hr treatment with MS-PPOH causes cell death, as measured by lactate dehydrogenase or other assays, would help to rule out toxicity of this drug at this time point. Furthermore, determining whether small-molecule neurotransmitter release (such as glutamate) remains intact following long-term CYP epoxygenase inhibition would confirm that this drug is not non-specifically

rendering general neuronal function inoperable.

As with the LC/MS-MS studies, the present neuropeptide release studies produced one particularly surprising result. Despite the abundant expression of sEH in both trigeminal ganglion neurons *in situ* (Figure 10) and in primary culture (Figure 14), pharmacological inhibition with the sEH inhibitor AUDA had no discernable effect upon evoked neuropeptide release (Figure 17B). Because sEH is the enzyme chiefly responsible for cellular EETs breakdown [3,95], inhibition of sEH is commonly used experimentally to potentiate EETs mediated effects. In the present experiments, I expected that AUDA treatment would elevate capsaicin- and K^+-evoked neuropeptide release above control levels. As discussed in Chapter 4, the absence of an effect of sEH inhibition upon evoked neuropeptide release suggests that basal sEH activity does not impinge upon the EETs pool contributing to evoked neuropeptide release. One possible explanation for this finding is that sEH is inactive in primary trigeminal ganglion neurons under basal conditions. This notion is supported by the absence of detectable DHETs metabolites in cellular extracts despite the presence of significant quantities of the preferred substrates of sEH: 14,15-EET, 11,12-EET, and 8,9-EET (Table 8-9). A second possibility is that EETs function within membrane-localized microdomains, released from membrane phospholipids and acting to facilitate neuropeptide release within small spatial domains, from which sEH activity is spatially segregated.

In either case, the question arises as to what role, if any, the sEH expressed in trigeminal ganglion neurons plays in neuronal function or the regulation of the EETs signaling pathway. One possibility stems from a second established role for sEH in

cellular EETs regulation: the regulation of membrane incorporation of free cellular EETs [239]. Experimental work in the vascular endothelium demonstrated that one cellular function of sEH is to regulate the rate and extent of EETs re-esterification into membrane phospholipids by shunting free EETs which are readily re-incorporated down the DHETs (which are relatively poorly re-esterified [241]) metabolic pathway. Thus sEH inhibition was observed to increase the amount of EETs present within membrane phospholipids [161]. In this context, sEH within trigeminal ganglion neurons may function in the maintenance and regulation of the membrane-bound EETs pool, rather than in the regulation of the free EETs pool contributing to neuropeptide release. One way to test such a role of sEH activity would be to examine the effects of long-term sEH inhibition. In the above scenario long-term sEH inhibition, like long-term CYP epoxygenase inhibition, would be expected to shift the composition of the membrane phospholipid EETs pool. It would be useful to determine whether 48 hour inhibition of sEH resulted in elevated EETs levels detectable within the membrane phospholipid pool by LC-MS/MS. Furthermore, such an enrichment of membrane phospholipid EETs would be expected to impact the acute effects of cellular EETs. Therefore it would be useful to determine whether chronic sEH inhibition potentiates evoked neuropeptide release owing to an expansion of the membrane-releasable EETs pool. Such a functional effect ought to be sensitive both to acute inhibition by 14,15-EEZE, but also to concurrent long-term inhibition of CYP epoxygenase by MS-PPOH.

In total, the present pharmacological data with 14,15-EEZE and MS-PPOH offer strong support for the involvement of EETs signaling in the stimulus-evoked release of neuropeptides from primary trigeminal ganglion neurons. This conclusion,

however, is tentative and requires further experimental confirmation to ensure that the effects of these agents are indeed specific and to elucidate the role of sEH in regulating trigeminal ganglion neuronal EETs levels and cellular function.

EETs Contribute to the *In Vivo* Regulation of Cerebral Blood Flow by Perivascular Vasodilator Nerves

In Chapter 4 I evaluated two potential roles of endogenous EETs in trigeminal ganglion neuronal function. I found no evidence for their release from these neurons, either under basal conditions or following stimulation. I did find, however, that the evoked release of neuropeptides was positively regulated by endogenous EETs signaling. This included the release of the vasoactive neuropeptides CGRP and substance P. In chapter 5, I sought to extend these findings to determine whether EETs signaling contributes to the regulation of the cerebral vasculature by perivascular vasodilator nerve populations, including perivascular trigeminal afferents.

The primary finding from the *in vivo* experiments was that the EETs antagonist 14,15-EEZE, administered peripherally to the cortical surface where the junctions between these peripheral vasodilator nerves and their target vascular smooth muscle reside, blocked the cerebral blood flow response in two distinct models of neurogenic cerebral vasodilation (Figure 21, 24). Importantly, in the same preparation, 14,15-EEZE did not alter the vasodilator response to mild hypercapnia but did antagonize the dilator response to exogenous 14,15-EETs. These findings suggest that the effect of 14,15-EEZE within the cranial window model was specific to the EETs signaling pathway.

In interpreting the findings of these *in vivo* studies, two matters must be taken into account. The first of these has been raised already in my discussion of the *in vitro* neuropeptide release data. In the current studies, the EETs antagonist 14,15-EEZE blocked the cerebral blood flow response to perivascular vasodilator nerve stimulation, while the CYP epoxygenase inhibitor MS-PPOH had no effect when administered acutely for 45 min (Figure 24). These results are fully consistent with my findings for *in vitro* neuropeptide release (Figure 16, 17). However, they raise many of the same questions. First, does the absence of an acute effect of MS-PPOH *in vivo* reflect the fact that neurogenic EETs are released from a pre-formed pool, such as from membrane phospholipids, that is insensitive to acute CYP epoxygenase blockade? This proposition is supported by my *in vitro* data demonstrating that long-term (48 hr), but not acute (30 min) treatment of trigeminal ganglion neurons inhibited evoked neuropeptide release from these neurons.

Testing this hypothesis *in vivo* becomes somewhat more difficult than in primary cultures. One key test of this hypothesis is whether peripheral (in the cranial window) inhibition of phospholipase A2, the enzyme that liberates esterified EETs from membrane phospholipids [237], exerts the same effect as 14,15-EEZE when acutely administered. Given the inherent non-specificity of this enzyme, however, this experiment would not be fully conclusive. Long-term inhibition of CYP epoxygenase in the cranial window is not necessarily practicable. Should inhibition of CYP epoxygenase of longer than 4-6 hours be necessary to deplete this putative EETs pool, this *in vivo* preparation would cease to be a viable experimental option. A more involved, but also more definitive experiment would be to effect long-term

knockdown of the two EETs synthases in trigeminal or sphenopalatine ganglia by siRNA approaches. Because I have identified the specific expression of two CYP epoxygenases in these ganglia (Figure 8), CYP-2J3 and CYP-2J4, and because they are closely related in terms of sequence [210,231], it would be feasible to produce an shRNA construct to silence these genes. Utilizing lentiviral vectors, shRNA virus could be injected into the small trigeminal or sphenopalatine ganglia with a reasonable expectation of a high level of infection throughout the ganglia. Following long-term shRNA treatment (days to weeks), the effect of trigeminal and parasympathetic neuron-specific CYP-2J gene knockdown on EETs levels in the ganglia could be evaluated by LC-MS/MS. Similarly, the effect of ganglionic CYP-2J knockdown upon the *in vivo* cerebral blood flow responses to perivascular vasodilator nerve stimulation could be determined. If successful, this experiment would provide definitive confirmation that neurogenic EETs are contributing to this process.

The second matter that must be considered is alluded to in the preceding discussion. The cerebral blood flow response to perivascular vasodilator nerve stimulation was sensitive to the EETs antagonist 14,15-EEZE. While this finding implicates the EETs signaling pathway in the action of these neurons, it does not definitively demonstrate that the EETs in question are *neurogenic* in nature. Although the present expression of CYP epoxygenase and the presence of EETs in trigeminal and sphenopalatine ganglion neurons, in addition to the functional role of EETs in evoked vasoactive neuropeptide release from these neurons support this proposition, the involvement of EETs from another cellular source cannot be ruled out. In the cerebral circulation, both vascular endothelium [5] and perivascular astrocytes [98]

produce EETs that contribute to the regulation of vasomotor tone. It is formally possible that other factors released from these neurons, such as the neuropeptide CGRP could act upon either of these nearby cell types, evoking EETs mobilization and their subsequent action on cerebral vasomotor tone. The viral shRNA approach outlined above may provide a powerful means to confirm that neurogenic EETs are participating in the regulation of cerebral blood flow by perivascular vasodilator nerves.

In light of these two considerations, the present *in vivo* findings provide strong evidence for participation of EETs signaling in the regulation of cerebral blood flow by perivascular vasodilator nerves. Whether the EETs involved are derived from a pre-formed pool and are neurogenic in nature remains to be definitively assessed.

A Model for the Role of EETs in Perivascular Vasodilator Nerve Function

In the present series of experiments, I provide evidence supporting my central hypothesis that perivascular vasodilator nerve-derived EETs contribute to the regulation of cerebral blood flow by these neurons. I demonstrate that both parasympathetic neurons within the sphenopalatine ganglia and primary sensory afferents within the trigeminal ganglia express EETs-synthetic CYP-2J epoxygenase enzymes. I confirm that these CYP epoxygenase enzymes are constitutively active in primary cultured trigeminal ganglion neurons and that EETs are endogenously present within these cells. I identify a role for these lipid signaling molecules as regulators of neuropeptide release from trigeminal ganglion neurons, including the vasoactive

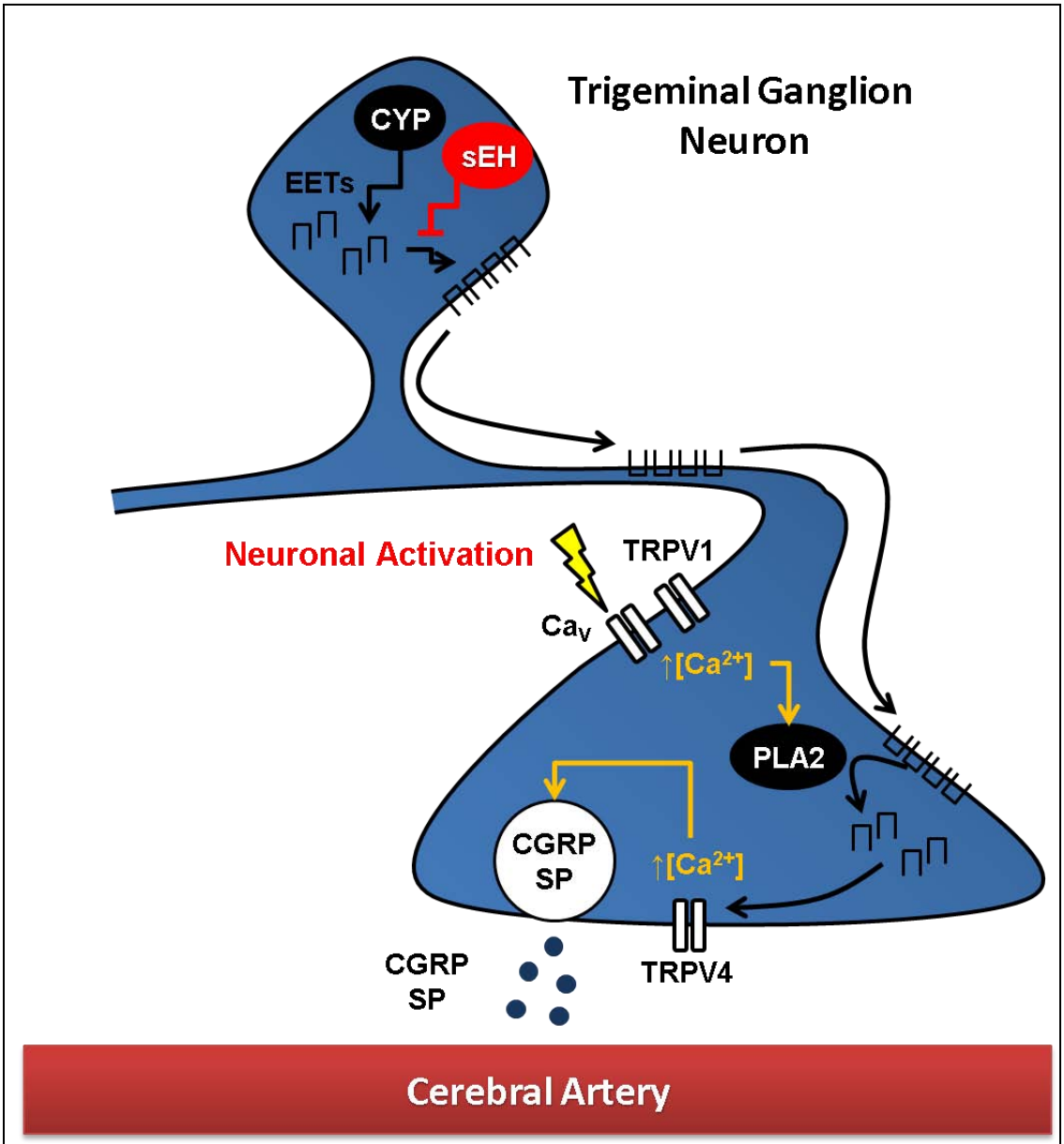

Figure 25. Model for the role of EETs in perivascular vasodilator nerve function. EETs are synthesized centrally in parasympathetic sphenopalatine and sensory trigeminal ganglion neurons through the action of CYP-2J epoxygenase enzymes (CYP) localized to the neuronal cell body. sEH regulates that re-incorporation of EETs into membrane phospholipids. Esterified EETs are trafficked to peripheral processes, where they are liberated by the activity of phosholipase A2 (PLA2) enzymes, which are activated in a Ca^{2+}-dependent manner in response to neuronal activation. Free EETs act on TRPV4 cation channel to increase Ca^{2+} influx into the cell, resulting in exocytotic release of vasoactive neuropeptides such as CGRP or substance P (SP). Neuropeptides act upon adjacent cerebral arteries to evoke vasodilation.

neuropeptides CGRP and substance P. Lastly, I provide *in vivo* data demonstrating that

EETs contribute to the regulation of the cerebral arteries by these perivascular vasodilator nerves. While these findings support a role for EETs signaling in neurogenic cerebral blood flow regulation, the molecular basis for this involvement remains unresolved. Below, I propose a unifying model that accounts for and extends the present experimental findings (Figure 25), speculating on the molecular details of EETs' participation in perivascular vasodilator nerve function, and suggesting experimental approaches to test these propositions.

EETs are Stored in Membrane Phospholipids

Parasympathetic neurons of the sphenopalatine ganglia and sensory neurons of the trigeminal ganglia specifically express CYP-2J epoxygenase enzymes (Figure 8-10). These enzymes are functional, given the detection of all four EETs regio-isomers within cell extracts from primary cultured trigeminal ganglion neurons (Table 8). *In vitro* studies demonstrated that long-term (48 hr) but not acute (45 min) inhibition of CYP epoxygenase blocked the cellular actions of EETs upon neuropeptide release (Figure 17), while the EETs antagonist 14,15-EEZE exhibited efficacy within the acute treatment window (Figure 16). These findings were corroborated *in vivo* where 14,15-EEZE acutely attenuated the dilator response to perivascular vasodilator nerve stimulation (Figure 21, 24) while MS-PPOH had no effect in the acute treatment window. Based upon these findings, I propose that EETs in trigeminal ganglion neurons are stored in a releasable pool, esterified in membrane phospholipids.

Immunofluorescence data suggested that the EETs-synthetic CYP-2J enzyme

was abundantly expressed in neuronal cell bodies of the trigeminal and sphenopalatine ganglia (Figure 9-10), while CYP-2J-immunoreactivity was not readily detected in peripheral processes surrounding the middle cerebral artery (Figure 12). Based upon this pattern of localization, I propose that initial synthesis and membrane incorporation of EETs occurs within the neuronal cell body. These membrane-stored EETs may then be trafficked either as part of secretory vesicles or other membrane-bound organelles to peripheral processes where EETs may participate in the regulation of neuropeptide release. Such a trafficking event is consistent with the efficacy of long-term (48 hrs) but not acute (45 min) inhibition of CYP epoxygenase in blocking neuropeptide release (Figure 17).

In *in vitro* neuropeptide release studies, sEH inhibition had no effect upon neuropeptide release (Figure 17), despite apparently abundant expression of this protein in trigeminal and sphenopalatine ganglion neurons (Figure 8-10). Based upon these findings, I propose that sEH functions primarily in the regulation of EETs membrane incorporation. If EETs synthesis and membrane phospholipid esterification occurs centrally rather than peripherally as I propose, then sEH function may be both spatially and functionally segregated from the direct regulation of EETs levels involved in neuropeptide release or evoked vasodilation.

Four experiments described above would begin to test this proposed model of EETs incorporation into the phospholipid pool. If EETs are liberated from membrane phospholipids, then the proposed biological actions of EETs, including the regulation of evoked neuropeptide release and of neurogenic cerebral vasodilation, should be sensitive to acute phospholipase A2 inhibition. Further, long-term inhibition of CYP

epoxygenase or sEH should have opposing effects upon esterified EETs levels as detected by LC-MS/MS.

EETs are Released from Membrane Phospholipids Following Neuronal Activation by Calcium-Dependent Phospholipase A2

The EETs antagonist 14,15-EEZE inhibited neuropeptide release resulting from trigeminal ganglion neuronal activation by both depolarizing concentrations of K^+ and the TRPV1 agonist capsaicin (Figure 16, 18). Similarly, peripheral administration of 14,15-EEZE within a cranial window blocked the cerebral blood flow response to perivascular vasodilator nerve stimulation (Figure 21, 24). These findings suggest that bioactive EETs are mobilized in perivascular vasodilator nerves in response to neuronal activation. Based upon these findings I propose that Ca^{2+} influx, resulting from voltage-sensitive Ca^{2+} channel activation following membrane depolarization or TRPV1 activation following capsaicin stimulation, causes Ca^{2+}-dependent phospholipase A2 activation and EETs release from membrane phospholipids. Although the upstream source of Ca^{2+} differs in different cell types, such a Ca^{2+}-dependent mechanism has been implicated in astrocytic (following metabotropic glutamate receptor activation) and endothelial (following muscarinic acetylcholine receptor activation) EETs mobilization [3,95].

The liberation of phospholipid-bound EETs into the free EETs pool could be assayed by conducting parallel LC-MS/MS analysis in cell extracts subjected to acid hydrolysis (total cell EETs) or to no hydrolysis (free EETs). If EETs mobilization from the phospholipid pool occurs in a Ca^{2+}-dependent phospholipase A2-mediated manner,

then either K^+- or capsaicin-evoked EETs mobilization should be sensitive to either removal of extracellular Ca^{2+}, treatment with calcium chelators or pharmacological inhibition of phospholipase A2. Furthermore, to confirm that these EETs are liberated from a releasable pool rather than by *de novo* synthesis, this mobilization of EETs into the free pool should be insensitive to acute CYP epoxygenase inhibition with MS-PPOH.

EETs Activate TRPV4 to Stimulate Neuronal Neuropeptide Release

In primary trigeminal ganglion neuronal cultures, EETs directly stimulated neuropeptide release while the EETs antagonist 14,15-EEZE and the CYP epoxygenase inhibitor MS-PPOH attenuated evoked neuropeptide release. Although these findings suggest the endogenous EETs regulate neuropeptide release in trigeminal ganglion neurons, the molecular target for EETs in this process remains unknown. In this context, the TRPV4 cation channel is an intriguing candidate to consider. TRPV4 is a Ca^{2+}-permeable cation channel that is activated by a number of different EETs regio-isomers [128,174,175]. Functional evidence from rat primary trigeminal ganglion neurons suggests that TRPV4 is expressed and functional in these neurons [246,247]. In the rat spinal cord dorsal horn, activation of TRPV4 causes the Ca^{2+}-dependent release of both CGRP and substance P [248]. Furthermore, activation of TRPV4 in primary colonic afferents with 5,6-EET triggers the discharge of action potentials and mechanical hyperalgesia [176]. Based upon these data, I propose that endogenous EETs bind to and activate TRPV4 to mediate evoked neuropeptide release

from trigeminal ganglion neurons.

Three experimental approaches could be used to evaluate such a role for TRPV4. First, it would be helpful to determine if the neuropeptide release resulting from exogenous EETs administration is sensitive to TRPV4 inhibition. While this approach is hampered by the lack of TRPV4-specific inhibitors, EETs-evoked neuropeptide release from primary trigeminal ganglion neurons could be evaluated in neurons from TRPV4 knockout mice, and also from wild type neurons subjected siRNA knockdown of TRPV4 expression. These approaches have been recently utilized to demonstrate a role for TRPV4 activity in flow-mediated vasodilation vascular organ culture models [190,192,249]. Using a similar methodology *in vitro*, the sensitivity of K^+- and capsaicin-evoked neuropeptide release to TRPV4 inhibition could also be evaluated. If TRPV4 mediates the effects of endogenous EETs in regulated neuropeptide release, then I would expect that cells from TRPV4 knockout mice or those subjected to TRPV4 gene knockdown would exhibit reduced EETs-, K^+ and capsaicin-evoked neuropeptide release. Finally, these results could be extended *in vivo*, and the effect of TRPV4 gene knockout or knockdown upon the cerebral blood flow response to perivascular vasodilator nerve stimulation could be evaluated.

Conclusions and Implications

In summary, the present series of studies detail the novel regulation of vasoactive neuropeptide release from perivascular vasodilator nerves by epoxyeicosanoids. The expression of enzymes capable of EETs synthesis is demonstrated in both neurons of the parasympathetic sphenopalatine and sensory trigeminal ganglia. EETs are

specifically identified within primary trigeminal ganglion neurons while endogenous EETs signaling is functionally implicated in the regulation of neuropeptide release from these neurons. This regulation of vasoactive neuropeptide release appears to account for the observed contribution of endogenous EETs signaling to the regulation of cerebral blood flow by perivascular vasodilator nerves *in vivo.*

The findings of the present series of studies may have implications beyond the proposed role for epoxyeicosanoids in neurogenic cerebral blood flow regulation. In these studies, a novel role for epoxyeicosanoids in a non-vascular cell type is identified. Specifically, neurogenic EETs are identified as positive regulators of neuropeptide release from primary trigeminal ganglion neurons. The similarities between the present findings and those of previous studies in the neuroendocrine hypothalamus and anterior pituitary are striking [129,130,131,199,200,201,202,203]. In both cases, EETs are identified as endogenous regulators of peptide transmitter release from neural cells. Additionally, this regulation extended to neuropeptide and neurohormone release resulting from distinct pathways of cell stimulation. These findings suggest that EETs may exert their regulatory effects upon neuropeptide or neurohormone release well downstream of the proximal pathways activated by capsaicin, K^+, dopamine, or β-adrenergic agonists in these studies. Moreover, the convergence of these findings suggests that EETs may participate more broadly in neural processes such as peptidergic neurotransmission than has been previously appreciated. Most directly, this may extend to other populations of primary sensory afferents, such as those of the dorsal root ganglia, but may include other elements of the peripheral nervous system and perhaps the central nervous system as well. Though

the early studies have been largely overshadowed over the past 15 years by an increasing appreciation of the cardiovascular effects of EETs [3,95], it may be an opportune time to begin to revisit and expand consideration of the role of EETs in neural function, particularly in regards to its regulation of peptidergic neurotransmission.

References

1. Girouard H, Iadecola C (2006) Neurovascular coupling in the normal brain and in hypertension, stroke, and Alzheimer disease. J Appl Physiol 100: 328-335.

2. Kulik T, Kusano Y, Aronhime S, Sandler AL, Winn HR (2008) Regulation of cerebral vasculature in normal and ischemic brain. Neuropharmacology 55: 281-288.

3. Spector AA, Norris AW (2007) Action of epoxyeicosatrienoic acids on cellular function. Am J Physiol Cell Physiol 292: C996-1012.

4. Loot AE, Popp R, Fisslthaler B, Vriens J, Nilius B, et al. (2008) Role of cytochrome P450-dependent transient receptor potential V4 activation in flow-induced vasodilatation. Cardiovascular Research 80: 445-452.

5. Medhora M, Narayanan J, Harder D (2001) Dual regulation of the cerebral microvasculature by epoxyeicosatrienoic acids. Trends Cardiovasc Med 11: 38-42.

6. Peng X, Zhang C, Alkayed NJ, Harder DR, Koehler RC (2004) Dependency of cortical functional hyperemia to forepaw stimulation on epoxygenase and nitric oxide synthase activities in rats. J Cereb Blood Flow Metab 24: 509-517.

7. Peng X, Carhuapoma JR, Bhardwaj A, Alkayed NJ, Falck JR, et al. (2002) Suppression of cortical functional hyperemia to vibrissal stimulation in the rat by epoxygenase inhibitors. Am J Physiol Heart Circ Physiol 283: H2029-2037.

8. Phillis JW, Horrocks LA, Farooqui AA (2006) Cyclooxygenases, lipoxygenases, and epoxygenases in CNS: their role and involvement in neurological disorders. Brain Res Rev 52: 201-243.

9. Iliff JJ, Jia J, Nelson J, Goyagi T, Klaus J, et al. (2009) Epoxyeicosanoid signaling in CNS function and disease. Prostaglandins Other Lipid Mediat.

10. Faraci FM, Heistad DD (1998) Regulation of the Cerebral Circulation: Role of Endothelium and Potassium Channels. Physiol Rev 78: 53-97.

11. Hamel E (2006) Perivascular nerves and the regulation of cerebrovascular tone. Journal of Applied Physiology (Bethesda, Md: 1985) 100: 1059-1064.

12. Paulson OB, Strandgaard S, Edvinsson L (1990) Cerebral autoregulation. Cerebrovascular and Brain Metabolism Reviews 2: 161-192.

13. Pelligrino DA, Wang Q, Koenig HM, Albrecht RF (1995) Role of nitric oxide, adenosine, N-methyl-D-aspartate receptors, and neuronal activation in hypoxia-induced pial arteriolar dilation in rats. Brain Research 704: 61-70.

14. Faraci FM, Breese KR, Heistad DD (1994) Cerebral vasodilation during hypercapnia. Role of glibenclamide- sensitive potassium channels and nitric oxide. Stroke 25: 1679-1683.

15. Bryan RM, Marrelli SP, Steenberg ML, Schildmeyer LA, Johnson TD (2001) Effects of luminal shear stress on cerebral arteries and arterioles. American Journal of Physiology Heart and Circulatory Physiology 280: H2011-2022-H2011-2022.

16. Gebremedhin D, Lange AR, Lowry TF, Taheri MR, Birks EK, et al. (2000) Production of 20-HETE and its role in autoregulation of cerebral blood flow. Circulation Research 87: 60-65.

17. Harder DR, Roman RJ, Gebremedhin D, Birks EK, Lange AR (1998) A common pathway for regulation of nutritive blood flow to the brain: arterial muscle

membrane potential and cytochrome P450 metabolites. Acta Physiologica Scandinavica 164: 527-532.

18. Reid JM, Davies AG, Ashcroft FM, Paterson DJ (1995) Effect of L-NMMA, cromakalim, and glibenclamide on cerebral blood flow in hypercapnia and hypoxia. Am J Physiol Heart Circ Physiol 269: H916-922-H916-922.

19. Fredricks KT, Liu Y, Rusch NJ, Lombard JH (1994) Role of endothelium and arterial K+ channels in mediating hypoxic dilation of middle cerebral arteries. Am J Physiol Heart Circ Physiol 267: H580-586-H580-586.

20. Taguchi H, Heistad DD, Kitazono T, Faraci FM (1994) ATP-sensitive K+ channels mediate dilatation of cerebral arterioles during hypoxia. Circ Res 74: 1005-1008.

21. Armstead WM (1997) Role of nitric oxide, cyclic nucleotides, and the activation of ATP-sensitive K+ channels in the contribution of adenosine to hypoxia-induced pial artery dilation. Journal of Cerebral Blood Flow and Metabolism: Official Journal of the International Society of Cerebral Blood Flow and Metabolism 17: 100-108.

22. Fabricius M, Lauritzen M (1994) Examination of the role of nitric oxide for the hypercapnic rise of cerebral blood flow in rats. Am J Physiol Heart Circ Physiol 266: H1457-1464-H1457-1464.

23. Iadecola C, Xu X (1994) Nitro-L-arginine attenuates hypercapnic cerebrovasodilation without affecting cerebral metabolism. Am J Physiol Regul Integr Comp Physiol 266: R518-525-R518-525.

24. Iadecola C, Zhang F (1994) Nitric oxide-dependent and -independent components

of cerebrovasodilation elicited by hypercapnia. Am J Physiol Regul Integr Comp Physiol 266: R546-552-R546-552.

25. Wang Q, Pelligrino DA, Baughman VL, Koenig HM, Albrecht RF (1995) The role of neuronal nitric oxide synthase in regulation of cerebral blood flow in normocapnia and hypercapnia in rats. Journal of Cerebral Blood Flow and Metabolism: Official Journal of the International Society of Cerebral Blood Flow and Metabolism 15: 774-778.
26. Fujii K, Heistad DD, Faraci FM (1991) Flow-mediated dilatation of the basilar artery in vivo. Circulation Research 69: 697-705.
27. Gaw AJ, Bevan JA (1993) Flow-induced relaxation of the rabbit middle cerebral artery is composed of both endothelium-dependent and -independent components. Stroke 24: 105-109.
28. Ngai AC, Winn HR (1995) Modulation of Cerebral Arteriolar Diameter by Intraluminal Flow and Pressure. Circ Res 77: 832-840.
29. Busse R, Edwards G, Félétou M, Fleming I, Vanhoutte PM, et al. (2002) EDHF: bringing the concepts together. Trends in Pharmacological Sciences 23: 374-380.
30. Garcia-Roldan JL, Bevan JA (1990) Flow-induced constriction and dilation of cerebral resistance arteries. Circ Res 66: 1445-1448.
31. Giaume C, Koulakoff A, Roux L, Holcman D, Rouach N (2010) Astroglial networks: a step further in neuroglial and gliovascular interactions. Nat Rev Neurosci 11: 87-99.
32. Takano T, Tian G-F, Peng W, Lou N, Libionka W, et al. (2006) Astrocyte-mediated

control of cerebral blood flow. Nature Neuroscience 9: 260-267.

33. Ballabh P, Braun A, Nedergaard M (2004) The blood-brain barrier: an overview: structure, regulation, and clinical implications. Neurobiology of Disease 16: 1-13.

34. Oberheim NA, Tian G-F, Han X, Peng W, Takano T, et al. (2008) Loss of astrocytic domain organization in the epileptic brain. The Journal of Neuroscience: The Official Journal of the Society for Neuroscience 28: 3264-3276.

35. Kuschinsky W, Wahl M, Bosse O, Thurau K (1972) Perivascular Potassium and pH as Determinants of Local Pial Arterial Diameter in Cats: A MICROAPPLICATION STUDY. Circ Res 31: 240-247.

36. Paulson OB, Newman EA (1987) Does the release of potassium from astrocyte endfeet regulate cerebral blood flow? Science 237: 896-898.

37. Newman EA, Frambach DA, Odette LL (1984) Control of extracellular potassium levels by retinal glial cell K+ siphoning. Science 225: 1174-1175.

38. Kofuji P, Ceelen P, Zahs KR, Surbeck LW, Lester HA, et al. (2000) Genetic Inactivation of an Inwardly Rectifying Potassium Channel (Kir4.1 Subunit) in Mice: Phenotypic Impact in Retina. J Neurosci 20: 5733-5740.

39. Nguyen T-S, Winn HR, Janigro D (2000) ATP-sensitive potassium channels may participate in the coupling of neuronal activity and cerebrovascular tone. Am J Physiol Heart Circ Physiol 278: H878-885-H878-885.

40. Metea MR, Kofuji P, Newman EA (2007) Neurovascular coupling is not mediated by potassium siphoning from glial cells. The Journal of Neuroscience: The

Official Journal of the Society for Neuroscience 27: 2468-2471.

41. Dunwiddie TV, Masino SA (2001) The role and regulation of adenosine in the central nervous system. Annual Review of Neuroscience 24: 31-55.

42. Xu H-L, Pelligrino DA (2007) ATP release and hydrolysis contribute to rat pial arteriolar dilatation elicited by neuronal activation. Experimental Physiology 92: 647-651.

43. Ngai AC, Coyne EF, Meno JR, West GA, Winn HR (2001) Receptor subtypes mediating adenosine-induced dilation of cerebral arterioles. American Journal of Physiology Heart and Circulatory Physiology 280: H2329-2335-H2329-2335.

44. Rubio R, Berne RM (1969) Release of adenosine by the normal myocardium in dogs and its relationship to the regulation of coronary resistance. Circ Res 25: 407-415.

45. Ko KR, Ngai AC, Winn HR (1990) Role of adenosine in regulation of regional cerebral blood flow in sensory cortex. Am J Physiol Heart Circ Physiol 259: H1703-1708-H1703-1708.

46. Iliff JJ, D'Ambrosio R, Ngai AC, Winn HR (2003) Adenosine receptors mediate glutamate-evoked arteriolar dilation in the rat cerebral cortex. American Journal of Physiology Heart and Circulatory Physiology 284: H1631-1637-H1631-1637.

47. Meno JR, Nguyen T-sK, Jensen EM, Alexander West G, Groysman L, et al. (2005) Effect of caffeine on cerebral blood flow response to somatosensory stimulation. Journal of Cerebral Blood Flow and Metabolism: Official Journal

of the International Society of Cerebral Blood Flow and Metabolism 25: 775-784.

48. Faraci FM, Breese KR (1993) Nitric oxide mediates vasodilatation in response to activation of N- methyl-D-aspartate receptors in brain. Circ Res 72: 476-480.

49. Northington FJ, Matherne GP, Berne RM (1992) Competitive inhibition of nitric oxide synthase prevents the cortical hyperemia associated with peripheral nerve stimulation. Proceedings of the National Academy of Sciences of the United States of America 89: 6649-6652.

50. Buerk DG, Ances BM, Greenberg JH, Detre JA (2003) Temporal Dynamics of Brain Tissue Nitric Oxide during Functional Forepaw Stimulation in Rats. NeuroImage 18: 1-9.

51. Lindauer U, Megow D, Matsuda H, Dirnagl U (1999) Nitric oxide: a modulator, but not a mediator, of neurovascular coupling in rat somatosensory cortex. Am J Physiol Heart Circ Physiol 277: H799-811-H799-811.

52. Garavito RM, Mulichak AM (2003) The structure of mammalian cyclooxygenases. Annual Review of Biophysics and Biomolecular Structure 32: 183-206.

53. Wang H, Hitron IM, Iadecola C, Pickel VM (2005) Synaptic and Vascular Associations of Neurons Containing Cyclooxygenase-2 and Nitric Oxide Synthase in Rat Somatosensory Cortex. Cereb Cortex 15: 1250-1260.

54. Niwa K, Araki E, Morham SG, Ross ME, Iadecola C (2000) Cyclooxygenase-2 Contributes to Functional Hyperemia in Whisker-Barrel Cortex. J Neurosci 20: 763-770.

55. Niwa K, Haensel C, Ross ME, Iadecola C (2001) Cyclooxygenase-1 Participates

in Selected Vasodilator Responses of the Cerebral Circulation. Circ Res 88: 600-608.

56. Gulbenkian S, Uddman R, Edvinsson L (2001) Neuronal messengers in the human cerebral circulation. Peptides 22: 995-1007.

57. Suzuki N, Hardebo JE, Owman C (1990) Origins and pathways of choline acetyltransferase-positive parasympathetic nerve fibers to cerebral vessels in rat. Journal of Cerebral Blood Flow and Metabolism: Official Journal of the International Society of Cerebral Blood Flow and Metabolism 10: 399-408.

58. Seylaz J, Hara H, Pinard E, Mraovitch S, MacKenzie ET, et al. (1988) Effect of stimulation of the sphenopalatine ganglion on cortical blood flow in the rat. Journal of Cerebral Blood Flow and Metabolism: Official Journal of the International Society of Cerebral Blood Flow and Metabolism 8: 875-878.

59. Suzuki N, Gotoh F, Gotoh J, Koto A (1991) Evidence for in vivo cerebrovascular neurogenic vasodilatation in the rat. Clinical Autonomic Research: Official Journal of the Clinical Autonomic Research Society 1: 23-26.

60. Suzuki N, Hardebo JE, Kåhrström J, Owman C (1990) Selective electrical stimulation of postganglionic cerebrovascular parasympathetic nerve fibers originating from the sphenopalatine ganglion enhances cortical blood flow in the rat. Journal of Cerebral Blood Flow and Metabolism: Official Journal of the International Society of Cerebral Blood Flow and Metabolism 10: 383-391.

61. Morita-Tsuzuki Y, Hardebo JE, Bouskela E (1993) Inhibition of nitric oxide synthase attenuates the cerebral blood flow response to stimulation of postganglionic parasympathetic nerves in the rat. Journal of Cerebral Blood

Flow and Metabolism: Official Journal of the International Society of Cerebral Blood Flow and Metabolism 13: 993-997.

62. Ignacio CS, Curling PE, Childres WF, Bryan RM (1997) Nitric oxide-synthesizing perivascular nerves in the rat middle cerebral artery. The American Journal of Physiology 273: R661-668-R661-668.

63. Ayajiki K, Fujioka H, Shinozaki K, Okamura T (2005) Effects of capsaicin and nitric oxide synthase inhibitor on increase in cerebral blood flow induced by sensory and parasympathetic nerve stimulation in the rat. J Appl Physiol 98: 1792-1798.

64. Goadsby PJ, Uddman R, Edvinsson L (1996) Cerebral vasodilatation in the cat involves nitric oxide from parasympathetic nerves. Brain Research 707: 110-118.

65. Lee TJF (1980) Direct evidence against acetylcholine as the dilator transmitter in the cat cerebral artery. European Journal of Pharmacology 68: 393-394.

66. Morita Y, Hardebo JE, Bouskela E (1994) The role of nitric oxide in the cerebrovascular flow response to stimulation of postganglionic parasympathetic nerves in the rat. Journal of the Autonomic Nervous System 49 Suppl: S77-81-S77-81.

67. Edvinsson L, Elsås T, Suzuki N, Shimizu T, Lee TJ (2001) Origin and Co-localization of nitric oxide synthase, CGRP, PACAP, and VIP in the cerebral circulation of the rat. Microscopy Research and Technique 53: 221-228.

68. Uddman R, Goadsby PJ, Jansen I, Edvinsson L (1993) PACAP, a VIP-like peptide: immunohistochemical localization and effect upon cat pial arteries and cerebral

blood flow. Journal of Cerebral Blood Flow and Metabolism: Official Journal of the International Society of Cerebral Blood Flow and Metabolism 13: 291-297.

69. Gottselig R, Messlinger K (2004) Noxious chemical stimulation of rat facial mucosa increases intracranial blood flow through a trigemino-parasympathetic reflex--an experimental model for vascular dysfunctions in cluster headache. Cephalalgia 24: 206-214.

70. Tanaka K, Fukuuchi Y, Shirai T, Nogawa S, Nozaki H, et al. (1995) Chronic transection of post-ganglionic parasympathetic and nasociliary nerves does not affect local cerebral blood flow in the rat. Journal of the Autonomic Nervous System 53: 95-102.

71. Koketsu N, Moskowitz MA, Kontos HA, Yokota M, Shimizu T (1992) Chronic parasympathetic sectioning decreases regional cerebral blood flow during hemorrhagic hypotension and increases infarct size after middle cerebral artery occlusion in spontaneously hypertensive rats. J Cereb Blood Flow Metab 12: 613-620.

72. Kano M, Moskowitz MA, Yokota M (1991) Parasympathetic denervation of rat pial vessels significantly increases infarction volume following middle cerebral artery occlusion. Journal of Cerebral Blood Flow and Metabolism: Official Journal of the International Society of Cerebral Blood Flow and Metabolism 11: 628-637.

73. Henninger N, Fisher M (2007) Stimulating circle of Willis nerve fibers preserves the diffusion-perfusion mismatch in experimental stroke. Stroke 38: 2779-

2786.

74. Lincoln J (1995) Innervation of cerebral arteries by nerves containing 5-hydroxytryptamine and noradrenaline. Pharmacology & Therapeutics 68: 473-501.

75. Nielsen KC, Owman C (1967) Adrenergic innervation of pial arteries related to the circle of Willis in the cat. Brain Research 6: 773-776.

76. Kapadia SE, de Lanerolle NC (1984) Immunohistochemical and electron microscopic demonstration of vascular innervation in the mammalian brainstem. Brain Research 292: 33-39.

77. Uddman R, Ekblad E, Edvinsson R, Håkanson R, Sundler F (1985) Neuropeptide Y-like immunoreactivity in perivascular nerve fibres of the guinea-pig. Regulatory Peptides 10: 243-257.

78. Edvinsson L, Owman C, Rosengren E, West KA (1972) Concentration of Noradrenaline in Pial Vessels, Choroid Plexus, and Iris during Two Weeks after Sympathetic Ganglionectomy or Decentralization. Acta Physiologica Scandinavica 85: 201-206.

79. Busija DW (1986) Unilateral and bilateral sympathetic effects on cerebral blood flow during normocapnia. The American Journal of Physiology 250: H498-502-H498-502.

80. Sadoshima S, Fujii K, Yao H, Kusuda K, Ibayashi S, et al. (1986) Regional cerebral blood flow autoregulation in normotensive and spontaneously hypertensive rats--effects of sympathetic denervation. Stroke; a Journal of Cerebral Circulation 17: 981-984.

81. Edvinsson L, Uddman R (2005) Neurobiology in primary headaches. Brain Res Brain Res Rev 48: 438-456.

82. Edvinsson L, Brodin E, Jansen I, Uddman R (1988) Neurokinin A in cerebral vessels: characterization, localization and effects in vitro. Regulatory Peptides 20: 181-197.

83. Edvinsson L, Ekman R, Jansen I, McCulloch J, Uddman R (1987) Calcitonin gene-related peptide and cerebral blood vessels: distribution and vasomotor effects. Journal of Cerebral Blood Flow and Metabolism: Official Journal of the International Society of Cerebral Blood Flow and Metabolism 7: 720-728.

84. Edvinsson L, Hara H, Uddman R (1989) Retrograde tracing of nerve fibers to the rat middle cerebral artery with true blue: colocalization with different peptides. Journal of Cerebral Blood Flow and Metabolism: Official Journal of the International Society of Cerebral Blood Flow and Metabolism 9: 212-218.

85. Quartu M, Diaz G, Floris A, Lai ML, Priestley JV, et al. (1992) Calcitonin gene-related peptide in the human trigeminal sensory system at developmental and adult life stages: immunohistochemistry, neuronal morphometry and coexistence with substance P. Journal of Chemical Neuroanatomy 5: 143-157.

86. Tajti J, Uddman R, Möller S, Sundler F, Edvinsson L (1999) Messenger molecules and receptor mRNA in the human trigeminal ganglion. Journal of the Autonomic Nervous System 76: 176-183.

87. McCulloch J, Uddman R, Kingman TA, Edvinsson L (1986) Calcitonin gene-related peptide: functional role in cerebrovascular regulation. Proceedings of the National Academy of Sciences of the United States of America 83: 5731-

5735.

88. Uddman R, Edvinsson L, Ekman R, Kingman T, McCulloch J (1985) Innervation of the feline cerebral vasculature by nerve fibers containing calcitonin gene-related peptide: Trigeminal origin and co-existence with substance P. Neuroscience Letters 62: 131-136.

89. Gulbenkian S, Merighi A, Wharton J, Varndell IM, Polak JM (1986) Ultrastructural evidence for the coexistence of calcitonin gene-related peptide and substance P in secretory vesicles of peripheral nerves in the guinea pig. Journal of Neurocytology 15: 535-542.

90. Duckles SP, Levitt B (1984) Specificity of capsaicin treatment in the cerebral vasculature. Brain Research 308: 141-144.

91. Buzzi MG, Carter WB, Shimizu T, Heath H, Moskowitz MA (1991) Dihydroergotamine and sumatriptan attenuate levels of CGRP in plasma in rat superior sagittal sinus during electrical stimulation of the trigeminal ganglion. Neuropharmacology 30: 1193-1200.

92. Goadsby PJ, Edvinsson L, Ekman R (1988) Release of vasoactive peptides in the extracerebral circulation of humans and the cat during activation of the trigeminovascular system. Annals of Neurology 23: 193-196.

93. Juul R, Hara H, Gisvold SE, Brubakk AO, Fredriksen TA, et al. (1995) Alterations in perivascular dilatory neuropeptides (CGRP, SP, VIP) in the external jugular vein and in the cerebrospinal fluid following subarachnoid haemorrhage in man. Acta Neurochirurgica 132: 32-41.

94. Juul R, Edvinsson L, Gisvold SE, Ekman R, Brubakk AO, et al. (1990) Calcitonin

gene-related peptide-LI in subarachnoid haemorrhage in man. Signs of activation of the trigemino-cerebrovascular system? British Journal of Neurosurgery 4: 171-179.

95. Roman RJ (2002) P-450 metabolites of arachidonic acid in the control of cardiovascular function. Physiol Rev 82: 131-185.

96. Amruthesh SC, Falck JR, Ellis EF (1992) Brain synthesis and cerebrovascular action of epoxygenase metabolites of arachidonic acid. J Neurochem 58: 503-510.

97. Ellis EF, Amruthesh SC, Police RJ, Yancey LM (1991) Brain synthesis and cerebrovascular action of cytochrome P-450/monooxygenase metabolites of arachidonic acid. Advances in Prostaglandin, Thromboxane, and Leukotriene Research 21A: 201-204.

98. Alkayed NJ, Narayanan J, Gebremedhin D, Medhora M, Roman RJ, et al. (1996) Molecular characterization of an arachidonic acid epoxygenase in rat brain astrocytes. Stroke 27: 971-979.

99. Alkayed NJ, Birks EK, Narayanan J, Petrie KA, Kohler-Cabot AE, et al. (1997) Role of P-450 arachidonic acid epoxygenase in the response of cerebral blood flow to glutamate in rats. Stroke 28: 1066-1072.

100. Ellis EF, Police RJ, Yancey L, McKinney JS, Amruthesh SC (1990) Dilation of cerebral arterioles by cytochrome P-450 metabolites of arachidonic acid. The American Journal of Physiology 259: H1171-1177-H1171-1177.

101. Campbell WB, Gebremedhin D, Pratt PF, Harder DR (1996) Identification of epoxyeicosatrienoic acids as endothelium-derived hyperpolarizing factors.

Circulation Research 78: 415-423.

102. Koerner IP, Zhang W, Cheng J, Parker S, Hurn PD, et al. (2008) Soluble epoxide hydrolase: regulation by estrogen and role in the inflammatory response to cerebral ischemia. Frontiers in Bioscience: A Journal and Virtual Library 13: 2833-2841.

103. Node K, Huo Y, Ruan X, Yang B, Spiecker M, et al. (1999) Anti-inflammatory properties of cytochrome P450 epoxygenase-derived eicosanoids. Science (New York, NY) 285: 1276-1279.

104. Sun J, Sui X, Bradbury JA, Zeldin DC, Conte MS, et al. (2002) Inhibition of vascular smooth muscle cell migration by cytochrome p450 epoxygenase-derived eicosanoids. Circulation Research 90: 1020-1027.

105. Fitzpatrick FA, Ennis MD, Baze ME, Wynalda MA, McGee JE, et al. (1986) Inhibition of cyclooxygenase activity and platelet aggregation by epoxyeicosatrienoic acids. Influence of stereochemistry. The Journal of Biological Chemistry 261: 15334-15338.

106. Heizer ML, McKinney JS, Ellis EF (1991) 14,15-Epoxyeicosatrienoic acid inhibits platelet aggregation in mouse cerebral arterioles. Stroke; a Journal of Cerebral Circulation 22: 1389-1393.

107. Krötz F, Riexinger T, Buerkle MA, Nithipatikom K, Gloe T, et al. (2004) Membrane-potential-dependent inhibition of platelet adhesion to endothelial cells by epoxyeicosatrienoic acids. Arteriosclerosis, Thrombosis, and Vascular Biology 24: 595-600.

108. Node K, Ruan XL, Dai J, Yang SX, Graham L, et al. (2001) Activation of Galpha

s mediates induction of tissue-type plasminogen activator gene transcription by epoxyeicosatrienoic acids. The Journal of Biological Chemistry 276: 15983-15989.

109. Munzenmaier DH, Harder DR (2000) Cerebral microvascular endothelial cell tube formation: role of astrocytic epoxyeicosatrienoic acid release. American Journal of Physiology Heart and Circulatory Physiology 278: H1163-1167-H1163-1167.

110. Zhang C, Harder DR (2002) Cerebral capillary endothelial cell mitogenesis and morphogenesis induced by astrocytic epoxyeicosatrienoic Acid. Stroke; a Journal of Cerebral Circulation 33: 2957-2964.

111. Michaelis UR, Fisslthaler B, Medhora M, Harder D, Fleming I, et al. (2003) Cytochrome P450 2C9-derived epoxyeicosatrienoic acids induce angiogenesis via cross-talk with the epidermal growth factor receptor (EGFR). The FASEB Journal: Official Publication of the Federation of American Societies for Experimental Biology 17: 770-772.

112. Potente M, Fisslthaler B, Busse R, Fleming I (2003) 11,12-Epoxyeicosatrienoic acid-induced inhibition of FOXO factors promotes endothelial proliferation by down-regulating p27Kip1. The Journal of Biological Chemistry 278: 29619-29625.

113. Pozzi A, Macias-Perez I, Abair T, Wei S, Su Y, et al. (2005) Characterization of 5,6- and 8,9-epoxyeicosatrienoic acids (5,6- and 8,9-EET) as potent in vivo angiogenic lipids. The Journal of Biological Chemistry 280: 27138-27146.

114. Wang Y, Wei X, Xiao X, Hui R, Card JW, et al. (2005) Arachidonic acid

epoxygenase metabolites stimulate endothelial cell growth and angiogenesis via mitogen-activated protein kinase and phosphatidylinositol 3-kinase/Akt signaling pathways. The Journal of Pharmacology and Experimental Therapeutics 314: 522-532.

115. Fleming I (2007) Epoxyeicosatrienoic acids, cell signaling and angiogenesis. Prostaglandins & Other Lipid Mediators 82: 60-67.

116. Michaelis UR, Fisslthaler B, Barbosa-Sicard E, Falck JR, Fleming I, et al. (2005) Cytochrome P450 epoxygenases 2C8 and 2C9 are implicated in hypoxia-induced endothelial cell migration and angiogenesis. Journal of Cell Science 118: 5489-5498.

117. Michaelis UR, Xia N, Barbosa-Sicard E, Falck JR, Fleming I (2008) Role of cytochrome P450 2C epoxygenases in hypoxia-induced cell migration and angiogenesis in retinal endothelial cells. Investigative Ophthalmology & Visual Science 49: 1242-1247.

118. Dhanasekaran A, Al-Saghir R, Lopez B, Zhu D, Gutterman DD, et al. (2006) Protective effects of epoxyeicosatrienoic acids on human endothelial cells from the pulmonary and coronary vasculature. American Journal of Physiology Heart and Circulatory Physiology 291: H517-531-H517-531.

119. Koerner IP, Jacks R, DeBarber AE, Koop D, Mao P, et al. (2007) Polymorphisms in the human soluble epoxide hydrolase gene EPHX2 linked to neuronal survival after ischemic injury. The Journal of Neuroscience: The Official Journal of the Society for Neuroscience 27: 4642-4649.

120. Liu M, Alkayed NJ (2005) Hypoxic preconditioning and tolerance via hypoxia

inducible factor (HIF) 1alpha-linked induction of P450 2C11 epoxygenase in astrocytes. Journal of Cerebral Blood Flow and Metabolism: Official Journal of the International Society of Cerebral Blood Flow and Metabolism 25: 939-948.

121. Medhora M, Dhanasekaran A, Gruenloh SK, Dunn LK, Gabrilovich M, et al. (2007) Emerging mechanisms for growth and protection of the vasculature by cytochrome P450-derived products of arachidonic acid and other eicosanoids. Prostaglandins & Other Lipid Mediators 82: 19-29.

122. Yang W, Holmes BB, Gopal VR, Kishore RVK, Sangras B, et al. (2007) Characterization of 14,15-epoxyeicosatrienoyl-sulfonamides as 14,15-epoxyeicosatrienoic acid agonists: use for studies of metabolism and ligand binding. The Journal of Pharmacology and Experimental Therapeutics 321: 1023-1031.

123. Yang B, Graham L, Dikalov S, Mason RP, Falck JR, et al. (2001) Overexpression of cytochrome P450 CYP2J2 protects against hypoxia-reoxygenation injury in cultured bovine aortic endothelial cells. Molecular Pharmacology 60: 310-320.

124. Inceoglu B, Jinks SL, Ulu A, Hegedus CM, Georgi K, et al. (2008) Soluble epoxide hydrolase and epoxyeicosatrienoic acids modulate two distinct analgesic pathways. Proceedings of the National Academy of Sciences of the United States of America 105: 18901-18906.

125. Chen J-K, Chen J, Imig JD, Wei S, Hachey DL, et al. (2008) Identification of novel endogenous cytochrome p450 arachidonate metabolites with high affinity for cannabinoid receptors. The Journal of Biological Chemistry 283:

24514-24524.

126. Gauthier KM, Baewer DV, Hittner S, Hillard CJ, Nithipatikom K, et al. (2005) Endothelium-derived 2-arachidonylglycerol: an intermediate in vasodilatory eicosanoid release in bovine coronary arteries. American Journal of Physiology Heart and Circulatory Physiology 288: H1344-1351-H1344-1351.

127. Snider NT, Kornilov AM, Kent UM, Hollenberg PF (2007) Anandamide metabolism by human liver and kidney microsomal cytochrome p450 enzymes to form hydroxyeicosatetraenoic and epoxyeicosatrienoic acid ethanolamides. The Journal of Pharmacology and Experimental Therapeutics 321: 590-597.

128. Watanabe H, Vriens J, Prenen J, Droogmans G, Voets T, et al. (2003) Anandamide and arachidonic acid use epoxyeicosatrienoic acids to activate TRPV4 channels. Nature 424: 434-438.

129. Capdevila J, Chacos N, Falck JR, Manna S, Negro-Vilar A, et al. (1983) Novel hypothalamic arachidonate products stimulate somatostatin release from the median eminence. Endocrinology 113: 421-423.

130. Negro-Vilar A, Snyder GD, Falck JR, Manna S, Chacos N, et al. (1985) Involvement of eicosanoids in release of oxytocin and vasopressin from the neural lobe of the rat pituitary. Endocrinology 116: 2663-2668.

131. Snyder GD, Capdevila J, Chacos N, Manna S, Falck JR (1983) Action of luteinizing hormone-releasing hormone: involvement of novel arachidonic acid metabolites. Proceedings of the National Academy of Sciences of the United States of America 80: 3504-3507.

132. Zeldin DC (2001) Epoxygenase pathways of arachidonic acid metabolism. The

Journal of Biological Chemistry 276: 36059-36062.

133. Thompson CM, Capdevila JH, Strobel HW (2000) Recombinant cytochrome P450 2D18 metabolism of dopamine and arachidonic acid. The Journal of Pharmacology and Experimental Therapeutics 294: 1120-1130.

134. Stark K, Dostalek M, Guengerich FP (2008) Expression and purification of orphan cytochrome P450 4X1 and oxidation of anandamide. The FEBS Journal 275: 3706-3717.

135. Daikh BE, Lasker JM, Raucy JL, Koop DR (1994) Regio- and stereoselective epoxidation of arachidonic acid by human cytochromes P450 2C8 and 2C9. The Journal of Pharmacology and Experimental Therapeutics 271: 1427-1433.

136. Liu M, Hurn PD, Alkayed NJ (2004) Cytochrome P450 in neurological disease. Current Drug Metabolism 5: 225-234.

137. Capdevila J, Snijder GD, Falck JR (1984) Epoxygenation of arachidonic acid by rat anterior pituitary microsomal fractions. FEBS Letters 178: 319-322.

138. Junier MP, Dray F, Blair I, Capdevila J, Dishman E, et al. (1990) Epoxygenase products of arachidonic acid are endogenous constituents of the hypothalamus involved in D2 receptor-mediated, dopamine-induced release of somatostatin. Endocrinology 126: 1534-1540.

139. Amruthesh SC, Boerschel MF, McKinney JS, Willoughby KA, Ellis EF (1993) Metabolism of arachidonic acid to epoxyeicosatrienoic acids, hydroxyeicosatetraenoic acids, and prostaglandins in cultured rat hippocampal astrocytes. J Neurochem 61: 150-159.

140. Gebremedhin D, Ma YH, Falck JR, Roman RJ, VanRollins M, et al. (1992)

Mechanism of action of cerebral epoxyeicosatrienoic acids on cerebral arterial smooth muscle. The American Journal of Physiology 263: H519-525-H519-525.

141. Alkayed NJ, Birks EK, Hudetz AG, Roman RJ, Henderson L, et al. (1996) Inhibition of brain P-450 arachidonic acid epoxygenase decreases baseline cerebral blood flow. Am J Physiol 271: H1541-1546.

142. Kawashima H, Strobel HW (1995) cDNA cloning of a novel rat brain cytochrome P450 belonging to the CYP2D subfamily. Biochemical and Biophysical Research Communications 209: 535-540.

143. Luo G, Zeldin DC, Blaisdell JA, Hodgson E, Goldstein JA (1998) Cloning and expression of murine CYP2Cs and their ability to metabolize arachidonic acid. Archives of Biochemistry and Biophysics 357: 45-57.

144. Zaphiropoulos PG, Wood T (1993) Identification of the major cytochrome P450s of subfamily 2C that are expressed in brain of female rats and in olfactory lobes of ethanol treated male rats. Biochemical and Biophysical Research Communications 193: 1006-1013.

145. Warner M, Gustafsson JA (1994) Effect of ethanol on cytochrome P450 in the rat brain. Proceedings of the National Academy of Sciences of the United States of America 91: 1019-1023.

146. Al-Anizy M, Horley NJ, Kuo CWS, Gillett LC, Laughton CA, et al. (2006) Cytochrome P450 Cyp4x1 is a major P450 protein in mouse brain. FEBS J 273: 936-947.

147. Bylund J, Ericsson J, Oliw EH (1998) Analysis of cytochrome P450 metabolites

of arachidonic and linoleic acids by liquid chromatography-mass spectrometry with ion trap MS. Analytical Biochemistry 265: 55-68.

148. Iliff JJ, Close LN, Selden NR, Alkayed NJ (2007) A novel role for P450 eicosanoids in the neurogenic control of cerebral blood flow in the rat. Exp Physiol 92: 653-658.

149. Spector AA, Fang X, Snyder GD, Weintraub NL (2004) Epoxyeicosatrienoic acids (EETs): metabolism and biochemical function. Progress in Lipid Research 43: 55-90.

150. Newman JW, Morisseau C, Hammock BD (2005) Epoxide hydrolases: their roles and interactions with lipid metabolism. Progress in Lipid Research 44: 1-51.

151. Johansson C, Stark A, Sandberg M, Ek B, Rask L, et al. (1995) Tissue specific basal expression of soluble murine epoxide hydrolase and effects of clofibrate on the mRNA levels in extrahepatic tissues and liver. Archives of Toxicology 70: 61-63.

152. Rawal S, Morisseau C, Hammock BD, Shivachar AC (2009) Differential subcellular distribution and colocalization of the microsomal and soluble epoxide hydrolases in cultured neonatal rat brain cortical astrocytes. Journal of Neuroscience Research 87: 218-227.

153. Zhang W, Koerner IP, Noppens R, Grafe M, Tsai H-J, et al. (2007) Soluble epoxide hydrolase: a novel therapeutic target in stroke. Journal of Cerebral Blood Flow and Metabolism: Official Journal of the International Society of Cerebral Blood Flow and Metabolism 27: 1931-1940.

154. Zhang W, Otsuka T, Sugo N, Ardeshiri A, Alhadid YK, et al. (2008) Soluble

epoxide hydrolase gene deletion is protective against experimental cerebral ischemia. Stroke 39: 2073-2078.

155. Sura P, Sura R, Enayetallah AE, Grant DF (2008) Distribution and expression of soluble epoxide hydrolase in human brain. The Journal of Histochemistry and Cytochemistry: Official Journal of the Histochemistry Society 56: 551-559.

156. Bernstrom K, Kayganich K, Murphy RC, Fitzpatrick FA (1992) Incorporation and distribution of epoxyeicosatrienoic acids into cellular phospholipids. The Journal of Biological Chemistry 267: 3686-3690.

157. Fang X, VanRollins M, Kaduce TL, Spector AA (1995) Epoxyeicosatrienoic acid metabolism in arterial smooth muscle cells. Journal of Lipid Research 36: 1236-1246.

158. VanRollins M, Kaduce TL, Knapp HR, Spector AA (1993) 14,15-Epoxyeicosatrienoic acid metabolism in endothelial cells. Journal of Lipid Research 34: 1931-1942.

159. VanRollins M, Kaduce TL, Fang X, Knapp HR, Spector AA (1996) Arachidonic acid diols produced by cytochrome P-450 monooxygenases are incorporated into phospholipids of vascular endothelial cells. The Journal of Biological Chemistry 271: 14001-14009.

160. Fang X, Kaduce TL, Weintraub NL, Harmon S, Teesch LM, et al. (2001) Pathways of epoxyeicosatrienoic acid metabolism in endothelial cells. Implications for the vascular effects of soluble epoxide hydrolase inhibition. The Journal of Biological Chemistry 276: 14867-14874.

161. Weintraub NL, Fang X, Kaduce TL, VanRollins M, Chatterjee P, et al. (1999)

Epoxide hydrolases regulate epoxyeicosatrienoic acid incorporation into coronary endothelial phospholipids. The American Journal of Physiology 277: H2098-2108-H2098-2108.

162. Shivachar AC, Willoughby KA, Ellis EF (1995) Effect of protein kinase C modulators on 14,15-epoxyeicosatrienoic acid incorporation into astroglial phospholipids. Journal of Neurochemistry 65: 338-346.

163. Kano M, Ohno-Shosaku T, Hashimotodani Y, Uchigashima M, Watanabe M (2009) Endocannabinoid-mediated control of synaptic transmission. Physiological Reviews 89: 309-380.

164. Wong PY, Lai PS, Falck JR (2000) Mechanism and signal transduction of 14 (R), 15 (S)-epoxyeicosatrienoic acid (14,15-EET) binding in guinea pig monocytes. Prostaglandins & Other Lipid Mediators 62: 321-333.

165. Wong PY, Lai PS, Shen SY, Belosludtsev YY, Falck JR (1997) Post-receptor signal transduction and regulation of 14(R),15(S)-epoxyeicosatrienoic acid (14,15-EET) binding in U-937 cells. Journal of Lipid Mediators and Cell Signalling 16: 155-169.

166. Wong PY, Lin KT, Yan YT, Ahern D, Iles J, et al. (1993) 14(R),15(S)-epoxyeicosatrienoic acid (14(R),15(S)-EET) receptor in guinea pig mononuclear cell membranes. Journal of Lipid Mediators 6: 199-208.

167. Snyder GD, Krishna UM, Falck JR, Spector AA (2002) Evidence for a membrane site of action for 14,15-EET on expression of aromatase in vascular smooth muscle. American Journal of Physiology Heart and Circulatory Physiology 283: H1936-1942-H1936-1942.

168. Yang C, Kwan YW, Seto SW, Leung GPH (2008) Inhibitory effects of epoxyeicosatrienoic acids on volume-activated chloride channels in rat mesenteric arterial smooth muscle. Prostaglandins & Other Lipid Mediators 87: 62-67.

169. Fukao M, Mason HS, Kenyon JL, Horowitz B, Keef KD (2001) Regulation of BK(Ca) channels expressed in human embryonic kidney 293 cells by epoxyeicosatrienoic acid. Molecular Pharmacology 59: 16-23.

170. Li PL, Campbell WB (1997) Epoxyeicosatrienoic acids activate K+ channels in coronary smooth muscle through a guanine nucleotide binding protein. Circulation Research 80: 877-884.

171. Li PL, Chen CL, Bortell R, Campbell WB (1999) 11,12-Epoxyeicosatrienoic acid stimulates endogenous mono-ADP-ribosylation in bovine coronary arterial smooth muscle. Circulation Research 85: 349-356.

172. Zou AP, Fleming JT, Falck JR, Jacobs ER, Gebremedhin D, et al. (1996) Stereospecific effects of epoxyeicosatrienoic acids on renal vascular tone and K(+)-channel activity. The American Journal of Physiology 270: F822-832-F822-832.

173. Behm DJ, Ogbonna A, Wu C, Burns-Kurtis CL, Douglas SA (2009) Epoxyeicosatrienoic acids function as selective, endogenous antagonists of native thromboxane receptors: identification of a novel mechanism of vasodilation. The Journal of Pharmacology and Experimental Therapeutics 328: 231-239.

174. Vriens J, Owsianik G, Fisslthaler B, Suzuki M, Janssens A, et al. (2005)

Modulation of the Ca2 permeable cation channel TRPV4 by cytochrome P450 epoxygenases in vascular endothelium. Circulation Research 97: 908-915.

175. Earley S, Heppner TJ, Nelson MT, Brayden JE (2005) TRPV4 forms a novel Ca2+ signaling complex with ryanodine receptors and BKCa channels. Circulation Research 97: 1270-1279.

176. Sipe WEB, Brierley SM, Martin CM, Phillis BD, Cruz FB, et al. (2008) Transient receptor potential vanilloid 4 mediates protease activated receptor 2-induced sensitization of colonic afferent nerves and visceral hyperalgesia. American Journal of Physiology Gastrointestinal and Liver Physiology 294: G1288-1298-G1288-1298.

177. Hermanstyne TO, Markowitz K, Fan L, Gold MS (2008) Mechanotransducers in rat pulpal afferents. Journal of Dental Research 87: 834-838.

178. Iliff JJ, Wang R, Zeldin DC, Alkayed NJ (2009) Epoxyeicosanoids as mediators of neurogenic vasodilation in cerebral vessels. Am J Physiol Heart Circ Physiol 296: H1352-1363.

179. Wray J, Bishop-Bailey D (2008) Epoxygenases and peroxisome proliferator-activated receptors in mammalian vascular biology. Experimental Physiology 93: 148-154.

180. Cowart LA, Wei S, Hsu M-H, Johnson EF, Krishna MU, et al. (2002) The CYP4A isoforms hydroxylate epoxyeicosatrienoic acids to form high affinity peroxisome proliferator-activated receptor ligands. The Journal of Biological Chemistry 277: 35105-35112.

181. Ng VY, Huang Y, Reddy LM, Falck JR, Lin ET, et al. (2007) Cytochrome P450

eicosanoids are activators of peroxisome proliferator-activated receptor alpha. Drug Metabolism and Disposition: The Biological Fate of Chemicals 35: 1126-1134.

182. Sudhahar V, Shaw S, Imig JD (2010) Epoxyeicosatrienoic Acid Analogs and Vascular Function. Current Medicinal Chemistry.

183. Snider NT, Nast JA, Tesmer LA, Hollenberg PF (2009) A cytochrome P450-derived epoxygenated metabolite of anandamide is a potent cannabinoid receptor 2-selective agonist. Molecular Pharmacology 75: 965-972.

184. Awumey EM, Hill SK, Diz DI, Bukoski RD (2008) Cytochrome P-450 metabolites of 2-arachidonoylglycerol play a role in Ca2+-induced relaxation of rat mesenteric arteries. Am J Physiol Heart Circ Physiol 294: H2363-2370.

185. Koehler RC, Gebremedhin D, Harder DR (2006) Role of astrocytes in cerebrovascular regulation. Journal of Applied Physiology (Bethesda, Md: 1985) 100: 307-317.

186. Fisslthaler B, Popp R, Kiss L, Potente M, Harder DR, et al. (1999) Cytochrome P450 2C is an EDHF synthase in coronary arteries. Nature 401: 493-497.

187. Isaacs KR, Anderson BJ, Alcantara AA, Black JE, Greenough WT (1992) Exercise and the brain: angiogenesis in the adult rat cerebellum after vigorous physical activity and motor skill learning. J Cereb Blood Flow Metab 12: 110-119.

188. Faraci FM, Sobey CG (1998) Role of Potassium Channels in Regulation of Cerebral Vascular Tone. J Cereb Blood Flow Metab 18: 1047-1063.

189. Plant TD, Strotmann R (2007) TRPV4. Handbook of Experimental

Pharmacology: 189-205.

190. Köhler R, Heyken W-T, Heinau P, Schubert R, Si H, et al. (2006) Evidence for a functional role of endothelial transient receptor potential V4 in shear stress-induced vasodilatation. Arteriosclerosis, Thrombosis, and Vascular Biology 26: 1495-1502.

191. Hartmannsgruber V, Heyken W-T, Kacik M, Kaistha A, Grgic I, et al. (2007) Arterial response to shear stress critically depends on endothelial TRPV4 expression. PloS One 2: e827-e827.

192. Mendoza SA, Fang J, Gutterman DD, Wilcox DA, Bubolz AH, et al. (2010) TRPV4-mediated endothelial Ca2+ influx and vasodilation in response to shear stress. Am J Physiol Heart Circ Physiol 298: H466-476-H466-476.

193. Bhardwaj A, Northington FJ, Carhuapoma JR, Falck JR, Harder DR, et al. (2000) P-450 epoxygenase and NO synthase inhibitors reduce cerebral blood flow response to N-methyl-D-aspartate. American Journal of Physiology Heart and Circulatory Physiology 279: H1616-1624-H1616-1624.

194. Harder DR, Alkayed NJ, Lange AR, Gebremedhin D, Roman RJ (1998) Functional hyperemia in the brain: hypothesis for astrocyte-derived vasodilator metabolites. Stroke 29: 229-234.

195. Metea MR, Newman EA (2006) Glial cells dilate and constrict blood vessels: a mechanism of neurovascular coupling. The Journal of Neuroscience: The Official Journal of the Society for Neuroscience 26: 2862-2870.

196. Simard M, Arcuino G, Takano T, Liu QS, Nedergaard M (2003) Signaling at the gliovascular interface. The Journal of Neuroscience: The Official Journal of the

Society for Neuroscience 23: 9254-9262.

197. Mulligan SJ, MacVicar BA (2004) Calcium transients in astrocyte endfeet cause cerebrovascular constrictions. Nature 431: 195-199.

198. Blanco VM, Stern JE, Filosa JA (2008) Tone-dependent vascular responses to astrocyte-derived signals. Am J Physiol Heart Circ Physiol 294: H2855-2863.

199. Canonico PL, Judd AM, Koike K, Valdenegro CA, MacLeod RM (1985) Arachidonate stimulates prolactin release in vitro: a role for the fatty acid and its metabolites as intracellular regulator(s) in mammotrophs. Endocrinology 116: 218-225.

200. Cashman JR (1989) 5,6-Epoxyeicosatrienoic acid stimulates growth hormone release in rat anterior pituitary cells. Life Sciences 44: 1387-1393.

201. Cashman JR, Hanks D, Weiner RI (1987) Epoxy derivatives of arachidonic acid are potent stimulators of prolactin secretion. Neuroendocrinology 46: 246-251.

202. Cashman JR, Snowdowne KW (1992) Prolactin secretion in anterior pituitary cells: effect of eicosanoids. Eicosanoids 5: 153-161.

203. Luini AG, Axelrod J (1985) Inhibitors of the cytochrome P-450 enzymes block the secretagogue-induced release of corticotropin in mouse pituitary tumor cells. Proceedings of the National Academy of Sciences of the United States of America 82: 1012-1014.

204. Inceoglu B, Jinks SL, Schmelzer KR, Waite T, Kim IH, et al. (2006) Inhibition of soluble epoxide hydrolase reduces LPS-induced thermal hyperalgesia and mechanical allodynia in a rat model of inflammatory pain. Life Sciences 79: 2311-2319.

205. Inceoglu B, Schmelzer KR, Morisseau C, Jinks SL, Hammock BD (2007) Soluble epoxide hydrolase inhibition reveals novel biological functions of epoxyeicosatrienoic acids (EETs). Prostaglandins & Other Lipid Mediators 82: 42-49.

206. Terashvili M, Tseng LF, Wu H-E, Narayanan J, Hart LM, et al. (2008) Antinociception produced by 14,15-epoxyeicosatrienoic acid is mediated by the activation of beta-endorphin and met-enkephalin in the rat ventrolateral periaqueductal gray. The Journal of Pharmacology and Experimental Therapeutics 326: 614-622.

207. Paravicini TM, Miller AA, Drummond GR, Sobey CG (2006) Flow-induced cerebral vasodilatation in vivo involves activation of phosphatidylinositol-3 kinase, NADPH-oxidase, and nitric oxide synthase. Journal of Cerebral Blood Flow and Metabolism: Official Journal of the International Society of Cerebral Blood Flow and Metabolism 26: 836-845.

208. Mendoza SA, Fang J, Gutterman DD, Wilcox DA, Bubolz AH, et al. (2009) TRPV4-mediated endothelial Ca2+ influx and vasodilation in response to shear stress. American Journal of Physiology Heart and Circulatory Physiology.

209. Snyder G, Lattanzio F, Yadagiri P, Falck JR, Capdevila J (1986) 5,6-Epoxyeicosatrienoic acid mobilizes Ca2+ in anterior pituitary cells. Biochemical and Biophysical Research Communications 139: 1188-1194.

210. Wu S, Chen W, Murphy E, Gabel S, Tomer KB, et al. (1997) Molecular cloning, expression, and functional significance of a cytochrome P450 highly expressed

in rat heart myocytes. The Journal of Biological Chemistry 272: 12551-12559.

211. Snider NT, Walker VJ, Hollenberg PF (2010) Oxidation of the Endogenous Cannabinoid Arachidonoyl Ethanolamide by the Cytochrome P450 Monooxygenases: Physiological and Pharmacological Implications. Pharmacological Reviews.

212. Iliff JJ, Alkayed NJ (2009) Soluble Epoxide Hydrolase Inhibition: Targeting Multiple Mechanisms of Ischemic Brain Injury with a Single Agent. Future Neurology 4: 179-199.

213. Enayetallah AE, French RA, Barber M, Grant DF (2006) Cell-specific subcellular localization of soluble epoxide hydrolase in human tissues. The Journal of Histochemistry and Cytochemistry: Official Journal of the Histochemistry Society 54: 329-335.

214. Enayetallah AE, French RA, Thibodeau MS, Grant DF (2004) Distribution of soluble epoxide hydrolase and of cytochrome P450 2C8, 2C9, and 2J2 in human tissues. The Journal of Histochemistry and Cytochemistry: Official Journal of the Histochemistry Society 52: 447-454.

215. Zeldin DC, Foley J, Goldsworthy SM, Cook ME, Boyle JE, et al. (1997) CYP2J subfamily cytochrome P450s in the gastrointestinal tract: expression, localization, and potential functional significance. Molecular Pharmacology 51: 931-943.

216. Buldyrev I, Tanner NM, Hsieh H-y, Dodd EG, Nguyen LT, et al. (2006) Calcitonin gene-related peptide enhances release of native brain-derived neurotrophic factor from trigeminal ganglion neurons. Journal of

Neurochemistry 99: 1338-1350.

217. Zeldin DC, Foley J, Ma J, Boyle JE, Pascual JM, et al. (1996) CYP2J subfamily P450s in the lung: expression, localization, and potential functional significance. Molecular Pharmacology 50: 1111-1117.

218. Larsen BT, Miura H, Hatoum OA, Campbell WB, Hammock BD, et al. (2006) Epoxyeicosatrienoic and dihydroxyeicosatrienoic acids dilate human coronary arterioles via BK(Ca) channels: implications for soluble epoxide hydrolase inhibition. American Journal of Physiology Heart and Circulatory Physiology 290: H491-499-H491-499.

219. Seubert JM, Sinal CJ, Graves J, DeGraff LM, Bradbury JA, et al. (2006) Role of soluble epoxide hydrolase in postischemic recovery of heart contractile function. Circulation Research 99: 442-450.

220. Gauthier KM, Deeter C, Krishna UM, Reddy YK, Bondlela M, et al. (2002) 14,15-Epoxyeicosa-5(Z)-enoic acid: a selective epoxyeicosatrienoic acid antagonist that inhibits endothelium-dependent hyperpolarization and relaxation in coronary arteries. Circulation Research 90: 1028-1036.

221. Gross GJ, Gauthier KM, Moore J, Campbell WB, Falck JR, et al. (2009) Evidence for role of epoxyeicosatrienoic acids in mediating ischemic preconditioning and postconditioning in dog. American Journal of Physiology Heart and Circulatory Physiology 297: H47-52-H47-52.

222. Keserü B, Barbosa-Sicard E, Popp R, Fisslthaler B, Dietrich A, et al. (2008) Epoxyeicosatrienoic acids and the soluble epoxide hydrolase are determinants of pulmonary artery pressure and the acute hypoxic pulmonary vasoconstrictor

response. The FASEB Journal: Official Publication of the Federation of American Societies for Experimental Biology 22: 4306-4315.

223. Liu X, Li C, Falck JR, Roman RJ, Harder DR, et al. (2008) Interaction of nitric oxide, 20-HETE, and EETs during functional hyperemia in whisker barrel cortex. American Journal of Physiology Heart and Circulatory Physiology 295: H619-631-H619-631.

224. Webler AC, Michaelis UR, Popp R, Barbosa-Sicard E, Murugan A, et al. (2008) Epoxyeicosatrienoic acids are part of the VEGF-activated signaling cascade leading to angiogenesis. American Journal of Physiology Cell Physiology 295: C1292-1301-C1292-1301.

225. Morii S, Ngai AC, Winn HR (1986) Reactivity of rat pial arterioles and venules to adenosine and carbon dioxide: with detailed description of the closed cranial window technique in rats. Journal of Cerebral Blood Flow and Metabolism: Official Journal of the International Society of Cerebral Blood Flow and Metabolism 6: 34-41.

226. Wang RK, Hurst S (2007) Mapping of cerebro-vascular blood perfusion in mice with skin and skull intact by Optical Micro-AngioGraphy at 1.3 mum wavelength. Optics Express 15: 11402-11412.

227. Wang RK, Jacques SL, Ma Z, Hurst S, Hanson SR, et al. (2007) Three dimensional optical angiography. Optics Express 15: 4083-4097.

228. Shi Y, Liu X, Gebremedhin D, Falck JR, Harder DR, et al. (2008) Interaction of mechanisms involving epoxyeicosatrienoic acids, adenosine receptors, and metabotropic glutamate receptors in neurovascular coupling in rat whisker

barrel cortex. Journal of Cerebral Blood Flow and Metabolism: Official Journal of the International Society of Cerebral Blood Flow and Metabolism 28: 111-125.

229. Jadhav V, Jabre A, Chen M-F, Lee TJ-F (2009) Presynaptic prostaglandin E2 EP1-receptor facilitation of cerebral nitrergic neurogenic vasodilation. Stroke; a Journal of Cerebral Circulation 40: 261-269.

230. Qin N, Neeper MP, Liu Y, Hutchinson TL, Lubin ML, et al. (2008) TRPV2 is activated by cannabidiol and mediates CGRP release in cultured rat dorsal root ganglion neurons. The Journal of Neuroscience: The Official Journal of the Society for Neuroscience 28: 6231-6238.

231. Zhang QY, Ding X, Kaminsky LS (1997) CDNA cloning, heterologous expression, and characterization of rat intestinal CYP2J4. Arch Biochem Biophys 340: 270-278.

232. Tanaka H, Kamita SG, Wolf NM, Harris TR, Wu Z, et al. (2008) Transcriptional regulation of the human soluble epoxide hydrolase gene EPHX2. Biochim Biophys Acta 1779: 17-27.

233. Ai D, Fu Y, Guo D, Tanaka H, Wang N, et al. (2007) Angiotensin II up-regulates soluble epoxide hydrolase in vascular endothelium in vitro and in vivo. Proc Natl Acad Sci U S A 104: 9018-9023.

234. Chang C, Gill SS (1991) Purification and characterization of an epoxide hydrolase from the peroxisomal fraction of mouse liver. Arch Biochem Biophys 285: 276-284.

235. Patel BN, Mackness MI, Nwosu V, Connock MJ (1986) Subcellular localization

of epoxide hydrolase in mouse liver and kidney. Biochem Pharmacol 35: 231-235.

236. Jones PD, Wolf NM, Morisseau C, Whetstone P, Hock B, et al. (2005) Fluorescent substrates for soluble epoxide hydrolase and application to inhibition studies. Anal Biochem 343: 66-75.

237. Fang X, Weintraub NL, Spector AA (2003) Differences in positional esterification of 14,15-epoxyeicosatrienoic acid in phosphatidylcholine of porcine coronary artery endothelial and smooth muscle cells. Prostaglandins Other Lipid Mediat 71: 33-42.

238. Fang X, Kaduce TL, Weintraub NL, Harmon S, Teesch LM, et al. (2001) Pathways of epoxyeicosatrienoic acid metabolism in endothelial cells. Implications for the vascular effects of soluble epoxide hydrolase inhibition. J Biol Chem 276: 14867-14874.

239. Weintraub NL, Fang X, Kaduce TL, VanRollins M, Chatterjee P, et al. (1999) Epoxide hydrolases regulate epoxyeicosatrienoic acid incorporation into coronary endothelial phospholipids. Am J Physiol 277: H2098-2108.

240. Fang X, VanRollins M, Kaduce TL, Spector AA (1995) Epoxyeicosatrienoic acid metabolism in arterial smooth muscle cells. J Lipid Res 36: 1236-1246.

241. VanRollins M, Kaduce TL, Fang X, Knapp HR, Spector AA (1996) Arachidonic acid diols produced by cytochrome P-450 monooxygenases are incorporated into phospholipids of vascular endothelial cells. J Biol Chem 271: 14001-14009.

242. Balkowiec A, Katz DM (2000) Activity-dependent release of endogenous brain-

derived neurotrophic factor from primary sensory neurons detected by ELISA in situ. J Neurosci 20: 7417-7423.

243. Gulbenkian S, Merighi A, Wharton J, Varndell IM, Polak JM (1986) Ultrastructural evidence for the coexistence of calcitonin gene-related peptide and substance P in secretory vesicles of peripheral nerves in the guinea pig. J Neurocytol 15: 535-542.

244. Saermark T, Andersen NM, Atke A, Jones PM, Vilhardt H (1986) Processing and secretion in the neurohypophysis. Stability of isolated secretory vesicles and role of internal pH. Biochem J 236: 77-84.

245. Xiao Y, Richter JA, Hurley JH (2008) Release of glutamate and CGRP from trigeminal ganglion neurons: Role of calcium channels and 5-HT1 receptor signaling. Mol Pain 4: 12.

246. Chen L, Liu C, Liu L, Cao X (2009) Changes in osmolality modulate voltage-gated sodium channels in trigeminal ganglion neurons. Neurosci Res 64: 199-207.

247. Chen L, Liu C, Liu L (2008) The modulation of voltage-gated potassium channels by anisotonicity in trigeminal ganglion neurons. Neuroscience 154: 482-495.

248. Grant AD, Cottrell GS, Amadesi S, Trevisani M, Nicoletti P, et al. (2007) Protease-activated receptor 2 sensitizes the transient receptor potential vanilloid 4 ion channel to cause mechanical hyperalgesia in mice. J Physiol 578: 715-733.

249. Loot AE, Popp R, Fisslthaler B, Vriens J, Nilius B, et al. (2008) Role of

cytochrome P450-dependent transient receptor potential V4 activation in flow-induced vasodilatation. Cardiovasc Res 80: 445-452.